C76-320.3/501

CHEMICAL VAPOR DEPOSITION GROWTH

ANNUAL REPORT

Contract No. 954372

"This work was performed for the Jet Propulsion Laboratory, California Institute of Technology, under NASA Contract NAS7-100 for the U. S. Energy Research and Development Administration, Division of Solar Energy.

The JPL Low-Cost Silicon Solar Array Project is funded by ERDA and forms part of the ERDA Photovoltaic Conversion Program to initiate a major effort toward the development of low-cost solar arrays."

Rockwell International

Page intentionally left blank

ABSTRACT

The activities of the first nine months of the contract are described. A laboratory-type CVD reactor system with a vertical deposition chamber and sample pedestal heated by an external rf coil is used for these investigations. The reactor system has been extensively modified by installation of mass flow controllers, automatic process sequence timers, and special bellows-sealed air-operated valves for overall improved performance.

Many potential suppliers of candidate substrate materials for the CVD Si sheet growth have been contacted, and numerous samples of materials have been obtained from them for evaluation — including glasses, glass-ceramics, polycrystalline ceramics (especially aluminas), and some glazed metals and ceramics. Many of these have been characterized for their surface and/or structural properties important to Si film growth, and these results are given. Two special glasses (Corning Code 1715 and Owens-Illinois GS211) and several large-grained polycrystalline aluminas (≥ 99.5 percent purity) have appeared most promising of the materials investigated to date. Cost data for some of the aluminas corresponding to purchases in large quantities at present-day prices are given, and some of the factors involved in these costs are discussed.

CVD experiments were carried out to establish baseline performance data for the reactor system, including temperature distributions on the sample pedestal, effects of carrier gas flow rate on temperature, effects of carrier gas flow rate on film thickness uniformity in H_2 and in He (with H_2 producing more uniform results), and Si film growth rate by SiH_4 pyrolysis as a function of temperature for H_2 and for He. An activation energy for the deposition process in the temperature range up to 850–900°C of ~1.8 eV was found for either carrier gas. Above that temperature range the growth rate still increases with temperature in H_2 but with a much lower activation energy (~0.14 eV). For He the rate passes through a maximum at 850–900°C, decreasing rapidly for further increases in temperature, indicating a difference in the deposition process at high temperatures (>850°C) in the two gases.

The results of Si CVD experiments with various candidate substrate materials in H_2 or in He atmospheres have been varied. Encouraging results have been achieved for Si deposition in He atmospheres on several of the glasses; deposition on Corning Code 1715 glass resulted in polycrystalline films with {100} and/or {110} preferred orientations, depending upon the deposition temperature in the 850–1000°C range, and with apparent grain sizes of about 4 μm. Fired polycrystalline alumina with enlarged grains resulting from supplementary high-temperature firing procedures beyond the normal commercial processing has been found very promising for growth of Si sheet with enhanced grain sizes. Films with epitaxial regions in individual grains well over 200 μm across have been prepared on recrystallized Vistal alumina substrates, and predominantly {110} preferred orientations result, although the film orientation is dependent on deposition temperature and other parameters.

Polycrystalline boron-doped (p-type) CVD Si films have been prepared on various substrates, with measured carrier concentrations in the range from 5×10^{14} to over 5×10^{19} cm^{-3}. Epitaxial films grown simultaneously on single-crystal sapphire substrates have been used as the baseline reference material in evaluating the electrical properties of the polycrystalline films. Experiments with SiH_4–$HC\ell$ mixtures have been undertaken, as the first step in developing a two-step deposition process intended to result in enhanced grain growth in the Si sheet. Results of this work, which is continuing, are discussed.

Various film characterization procedures — including classical metallography, SEM analyses, X-ray diffraction analyses, surface profilometry, and electrical measurements (resistivity, carrier concentration, mobility, spreading resistance profiles, and minority-carrier lifetime by the C-V-t method) — have been used to correlate Si sheet properties with CVD parameters and substrate properties. These evaluation procedures and measurements are given in considerable detail.

Experimental solar cell structures have been made at OCLI both in epitaxial Si sheet (on sapphire substrates) and in polycrystalline material on alumina substrates, the former to provide an indication of what might be an upper limit on performance of the latter. Preliminary results are given, as obtained in cell structures not specially designed to allow for the unique properties of the sheet material — and fabricated in material known to be far from optimum for photovoltaic performance. Low power conversion efficiencies have been obtained in the epitaxial as well as the polycrystalline Si sheet, probably because of short minority carrier diffusion lengths in both cases; other factors involved are also discussed.

Tentative conclusions and recommendations based on the work to date are outlined, and plans for the next six months are given. Manpower and funding expenditures are summarized, and the updated technical program plan is included.

CONTENTS

CONTENTS (Cont)

ILLUSTRATIONS

ILLUSTRATIONS (Cont)

ILLUSTRATIONS (Cont)

ILLUSTRATIONS (Cont)

TABLES

1. INTRODUCTION

This contract began 29 December 1975, and is of 18-month duration. This Annual Report covers the first nine months of the program, through 30 September 1976.

The purpose of the contract is to explore the chemical vapor deposition (CVD) method for the growth of Si sheet on inexpensive substrate materials. The work is carried out at the Rockwell Electronics Research Division in Anaheim, and also involves some experimental solar cell fabrication and evaluation by the Photoelectronics Group of Optical Coating Laboratory, Inc. (OCLI), in City of Industry, California.

The formal objective of the contract is development of CVD techniques for producing large areas of Si sheet on inexpensive substrate materials, with sheet properties suitable for fabricating solar cells meeting the technical goals of the Low Cost Silicon Solar Array Project (LCSSAP). The techniques developed are to be directed toward (1) minimum-cost processing, (2) production of sheet having properties adequate to result in cells with terrestrial array efficiency of 10 percent or more, and (3) eventual scale-up to large-quantity production.

The CVD method as applied to Si sheet growth involves pyrolysis or reduction of a suitable Si compound at elevated temperature and (approximately) atmospheric pressure in a flow-through (open-tube) system. A carrier gas is used to transport the reactants to the deposition chamber, in which the substrate is mounted on a SiC-coated carbon pedestal heated by rf from outside the chamber. The properties of the Si sheet are determined by deposition temperature, reactant concentrations, the nature of the carrier gas, the Si source compound used, growth rate, doping impurities (added by introduction of appropriate compounds into the carrier gas stream), and the properties of the substrate.

The specific technical goals established for the contract include the following:

Si sheet area (per sample)	30 cm^2
Si sheet deposition rate	5 μm per min
Si sheet thickness	20 to 100 μm
Si sheet crystal structure	100 μm average grain size
Intragrain dislocation density	$<10^4$ per cm^2

The principal technical problems to be solved are (1) establishing preferred CVD process parameters (temperature, reactant concentrations, carrier gas composition, doping impurities, growth rate) for optimized intragrain properties for the Si sheet grown on various substrate materials; (2) identifying suitable substrate materials that will survive the environment of the CVD process and be potentially inexpensive and available in large areas, yet be as favorable as possible to Si grain growth; and (3) achieving adequate grain size in the Si sheet to provide satisfactory solar cell properties.

Many characteristics of the CVD method indicate that it has considerable promise for achieving the 1985 technical and cost goals of the LCSSAP: (1) it produces only that amount of Si that is actually required for the photovoltaic effect, without the requirement of additional Si for purely structural reasons; (2) it is a relatively low-temperature process and thus is energy-conservative, not requiring melting of Si at any stage;

(3) it does not require refined/purified polycrystalline Si starting material, using instead a high-purity compound of Si that is actually a product of one of the early steps in the preparation of polycrystalline semiconductor-grade Si; (4) it is inherently a large-area process, capable of potential scale-up to areas that are practical for large array fabrication in the LCSSAP; (5) impurity doping for junction formation can be carried out during CVD growth of the Si sheet; (6) thicknesses are closely controllable by reactant flow-rate adjustments; and (7) it has the capability for eventual development of a continuous fabrication process, in which the Si material, the junction or barrier, and the required contacts are all fabricated in a single integrated series of operations in one apparatus.

Si sheet growth by CVD on inexpensive substrates will almost certainly be polycrystalline, because such substrates will be either amorphous or microcrystalline and will thus provide little or no ordering influence on the growth mechanism. However, the prospects of at least closely approaching the project goal of 10 percent terrestrial array efficiency are considered good. The chances of obtaining sufficient cost reduction per unit area of active cell surface appear strong enough that a cost-per-watt figure within the project goals should be achievable with this process.

The contract program is composed of six main technical tasks, as follows: (1) modification and test of an existing CVD reactor system; (2) identification and/or development of suitable inexpensive substrate materials; (3) experimental investigation of CVD process parameters using various candidate substrate materials; (4) preparation of Si sheet samples for various special studies, including solar cell fabrication; (5) evaluation of the properties of the Si sheet material produced by the CVD process; and (6) fabrication and evaluation of experimental solar cell structures by OCLI, using standard and near-standard processing techniques.

The progress achieved during the first nine months is described by task in the following section, followed by a summary of conclusions and recommendations and an outline of the work planned for the next six months. This is followed by the New Technology statement and a listing of references used in this report.

The manpower and funding expenditures to date are summarized in Appendix A, and the Updated Technical Program Plan is included as Appendix B.

2. TECHNICAL DISCUSSION

This section contains a summary of the results obtained during the first nine months in performance of the Statement of Work of this contract, with interpretation of the results where appropriate. This discussion is arranged by task, although the interlocking of the tasks is such that this distinction is not always successfully made.

2.1 TASK 1. MODIFICATION AND TEST OF EXISTING CVD REACTOR SYSTEM

The apparatus used for the chemical vapor deposition of Si films has been highly developed in recent years. The experimental system used at Rockwell consists of six main components: (1) deposition chamber (reactor); with provision for supporting the heated substrates on which Si is deposited; (2) reactant gas manifold and distribution line system, with appropriate metering, valving, and controls; (3) reservoirs or tanks of the required reactant and carrier gases, with associated purifiers and/or filters; (4) vacuum system for evacuating selected portions of the reactor and gas manifold, as needed; (5) provision for burning, reprocessing, or otherwise discharging the exhaust gases exiting from the reactor system; and (6) power supply for heating the substrates in the reactor chamber - usually an rf generator with an external coil which couples to a susceptor, which also serves as the substrate support.

Throughout the first quarter of this program an existing laboratory-type CVD reactor system with a vertical deposition chamber was used. This system is similar to that used extensively at Rockwell in previous studies of semiconductor epitaxial growth by CVD, and is shown schematically in simplified form in Figure 2-1.

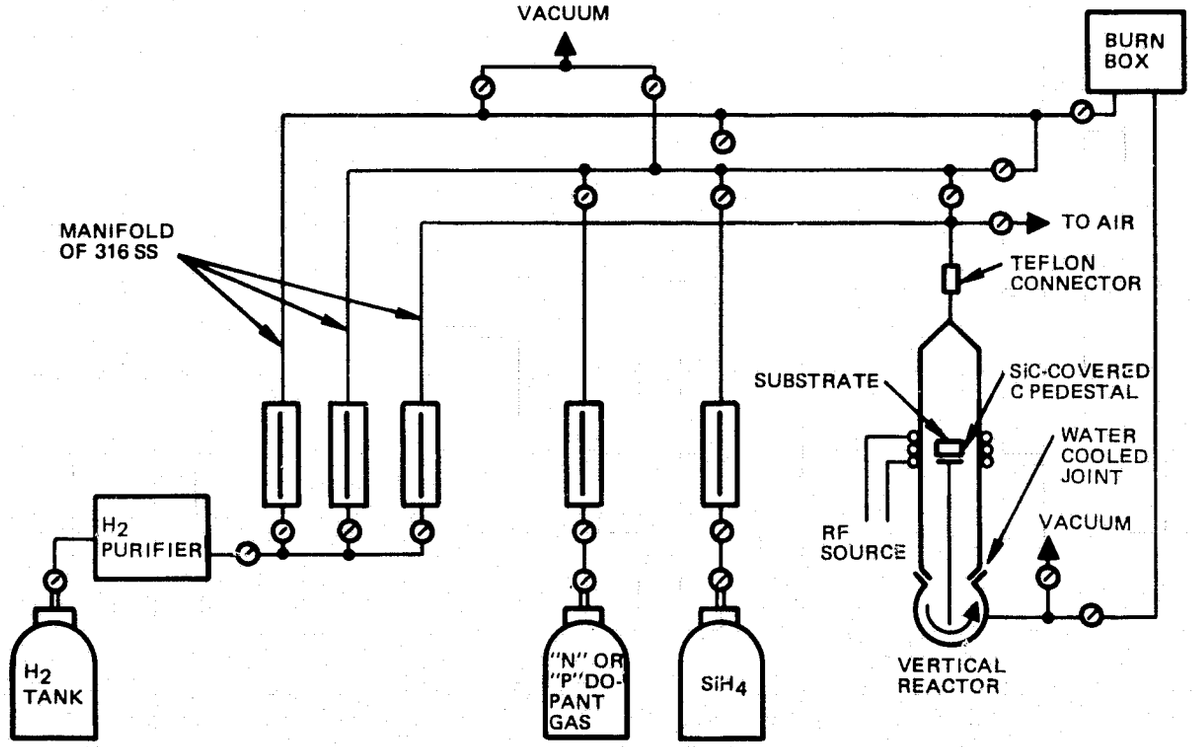

Figure 2-1. Simplified Schematic Diagram of Vertical-chamber CVD Apparatus for Si Sheet Growth

Even in its simplest form a system of this type provides the following capabilities:

1. Growth of undoped or doped Si films on any substrate that will withstand the growth temperature, using several different sources of Si, including SiH_4, or a Si halide, or mixtures of SiH_4 and $HC\ell$

2. Etching of Si on the substrate or removal of solid reaction products from the walls between deposition experiments, using $HC\ell$

3. Use of one or more carrier gases to establish a desired growth atmosphere

4. Evacuation of sections of the apparatus, including the reactor chamber, while gas flows are continued in other sections

5. "Homogenization" of gas flows prior to introduction of the gases into the reactor

6. Trapping of moisture and other condensables that are typical of the impurities present in "electronic grade" gases.

To improve the control of the Si CVD process for this program a number of modifications were planned for the reactor system shown in Figure 2-1. These changes were intended to provide a more versatile system that would offer greater reproducibility and reliability than previously available.

The modifications were originally scheduled for completion by the end of the first quarter, but because of vendor delays in delivery of some of the key components to be used in the system it was necessary to reschedule completion of the modifications to early in the second quarter.

Modifications in the Si CVD reactor system were completed in mid-April and the contractually-required Design and Performance Review of the modified system was conducted for JPL personnel on 15 April 1976, as scheduled (see Updated Technical Program Plan, Appendix B). The Standard Operation Procedure for the modified reactor system was also completed and delivered to JPL personnel at the time of the review.

A schematic diagram of the reactor system incorporating the modifications is given in Figure 2-2. The modifications include the following main items:

1. Thirteen Tylan Model FC-260 Mass Flow Controllers (MFC). All gas lines involved directly in the CVD process are controlled by this means. The only lines not so controlled are the carrier gas bypass and reactant "dump-out" line leading to the burn-box at the top of the reactor-system hood enclosure, and a separate H_2 line to admit that gas to the chamber for pre-deposition "etching" when carrier gases other than H_2 are being used. The controller locations are as follows:

   2 in parallel main gas flow lines, one leading into the reactor chamber and the other provided for mixing reactants in desired proportions and at constant total flow prior to introduction into the chamber;

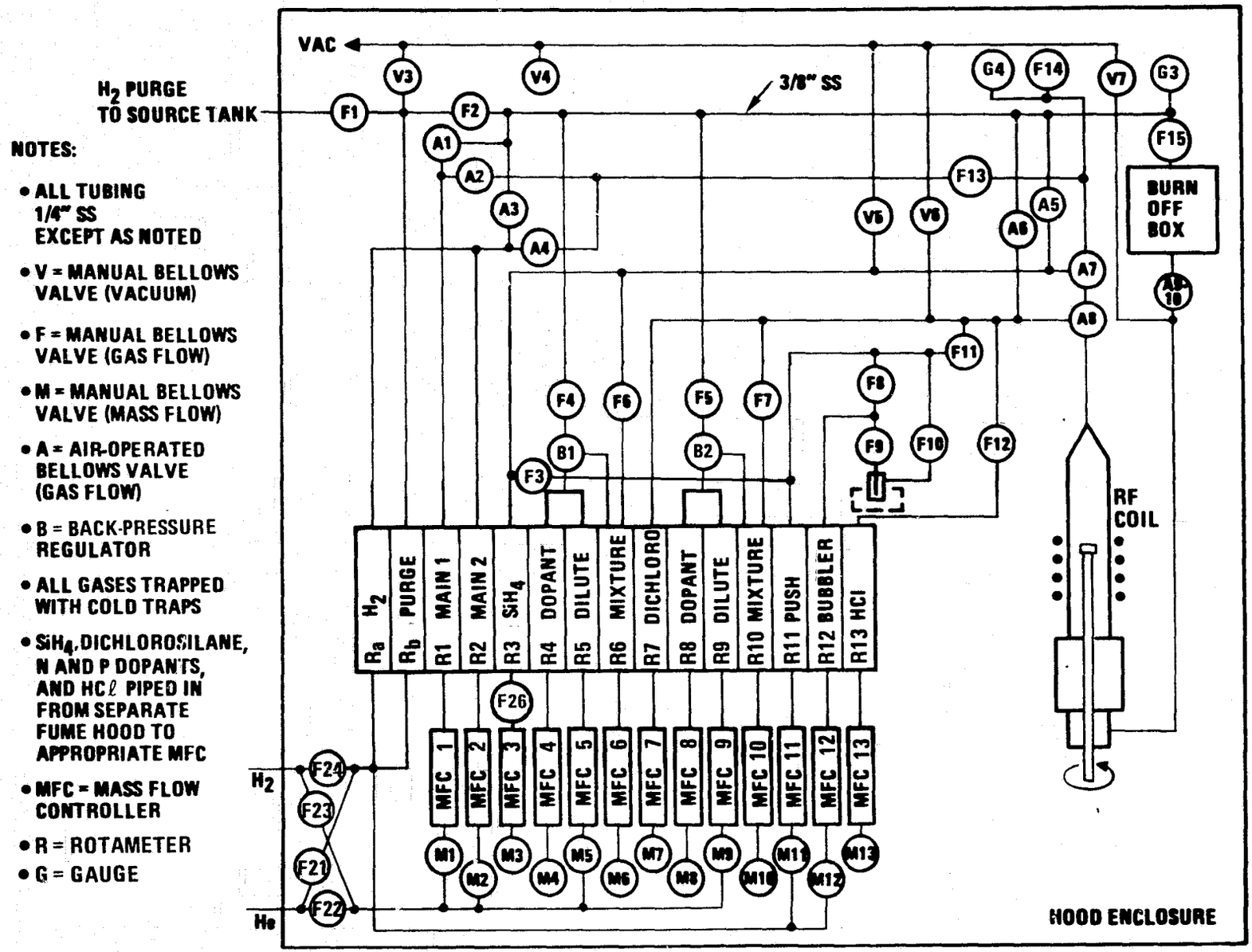

Figure 2-2. Schematic Diagram of Modified Si CVD Reactor System

3 in Si source compound supply lines (SiH_4, $SiH_2C\ell_2$, and a bubbler for $SiHC\ell_3$ or $SiC\ell_4$);

1 in bubbler-source carrier gas line;

1 in $HC\ell$ line;

2 in dopant lines (n- and p-type impurity source compounds);

2 in gas lines for dilution of doping compounds; and

2 in diluted dopant lines (n and p type).

2. One Tylan Model GPT-104 Automatic Sequence Timer associated with the controllers. The timer is capable of providing automatically-timed control of flow intervals in 10 different lines (i.e., 10 signal channels), with up to four different events (such as on and off) per channel programmable in each cycle of the sequencer.

3. Four Tylan Model RO-14 Control and Readout Units. These are included in the centralized control panel to handle the outputs of the 13 mass flow controllers. Each readout unit has a maximum capacity of four input channels.

4. Two Model 5150A Hewlett-Packard Thermal Printers. Each of these is capable of sequential printing of 20 channels of digital information per cycle of the printer (printing time ~ 1/3 sec per line, data input acceptance interval adjustable down to one second). These can be used to provide permanent records of experimental parameters when desired. These printers each includesa timer, so that all data are related to printed digital time recordings.

5. Ten Nupro Model 4BK air-operated valves. These are triggered by switch-activated solenoids, and are installed on the reactor system to improve control over film thickness, nucleation phenomena, and impurity concentration and distribution. Two of these valves are Nupro Model SS-4BK-S2 zero-dead-space valves, to further reduce the amount of uncontrolled and/or unwanted reactant flow in the system.

6. Onc Alcatel Model ZM2012C Vacuum Pump. This pump serves both as the forepump for the trapped mercury-vapor diffusion pump and as the roughing pump for the reactor system. This type of pump has improved pumping speed over conventional oil-immersed mechanical vane pumps, provides essentially zero backstreaming of hydrocarbon vapors because of its "dry" construction, and is relatively quiet in operation.

In addition to the reactor system itself, which is enclosed in a separate high-flow-rate fume hood, an external control center is housed in a separate floormounted cabinet at the side of the hood. This cabinet accommodates the sequence timer, the four readout units, two recorder-printers, and the master valve control panel.

The entire CVD reactor system is shown in the photograph in Figure 2-3; the external control cabinet can be seen at the left, the bank of mass flow controllers in the lower center, and the vertical reactor chamber at the right. A close-up view of the mass flow controllers is shown in Figure 2-4. The conventional rotameters can be seen above the mass flow controllers; these were left in the system to provide convenient visual indication of gas flow and, incidentally, a continuing check on the functioning of the controllers. Later developments indicated this to have been a fortunate decision.

Following completion of the reactor modifications and after two deposition experiments were carried out with the modified system, it was observed that there were significant discrepancies between the reactant gas flow rates as read (and controlled) by the mass flow controllers and the rates indicated by the conventional rotameters that had been left in the lines in series with the controllers. Upon careful investigation of the problem in collaboration with the manufacturer (Tylan Corporation, Torrance, CA), it was determined that faulty temperature sensors had inadvertently been used in the mass flow control units, rendering their calibrations inaccurate and/or unstable. Each of the units was returned to the manufacturer for replacement of the sensor, after which proper performance of the devices appeared to be obtained on the Si CVD system.

However, further problems of inaccurate and/or unstable performance of several of the mass flow controllers appeared, and it was subsequently determined by the manufacturer that faulty insulating cement had been used in assembling the temperature sensors into the units. This problem was also very promptly corrected by the manufacturer.

Several other minor difficulties were encountered during the second quarter in achieving full operational capability of the reactor system, and a few minor changes have been made in the system since the Design and Performance Review. For example, a four-way ball valve was found to allow He from the input gas line to leak into the input H_2 line. In its place, separate stainless steel lines for each gas and connecting manual bellows-sealed valves were installed. In addition, a manual bellows-sealed valve was added between the SiH_4 mass flow controller and the glass rotameter to help minimize contamination of the SiH_4 mass flow controller by possible entry of water vapor or air through any minute leaks in the system. These changes are included in the diagram of Figure 2-2.

The bellows-sealed valve was added during the HCℓ addition experiments (see Para 2. 3), when it was noted that the SiH_4 flow-rate readings on the MFC readouts were not consistent from run to run with the readings on the glass rotameter that is in series with the MFC calibrated for SiH_4. Several experiments done with MFC readouts at the same value (25 ccpm) indicated quite large growth rate differences (as great as 1 μm/min), in terms of the rotameter readings. As a temporary expedient in subsequent experiments the rotameter readings, rather than the MFC readings, were used until the problem was corrected.

When the SiH_4 was finally disassembled, a white coating--presumably SiO_2--was observed on the interior surfaces, indicative of air and/or moisture contamination of the SiH_4. For the entire month of July the Si CVD experiments were carried out with the MFC used merely as a valve; flow-rate readings were obtained from the glass rotameter kept in series with the MFC. Following completion of the last CVD experiments planned for that series (in July), the MFC from the SiH_4 line was removed and returned to the manufacturer for cleaning, adjustment, and recalibration. For the CVD experiments done in August the MFC position in the line was bypassed and the rotameter was again used for flow-rate readings.

The MFC was returned by the vendor in time for use in the CVD experiments planned for September. Although a discrepancy still exists between the MFC readout and the SiH_4 flow rate as obtained from the rotameter reading, for the present - at least - the readings are reproducible and film growth rates can be produced as desired.

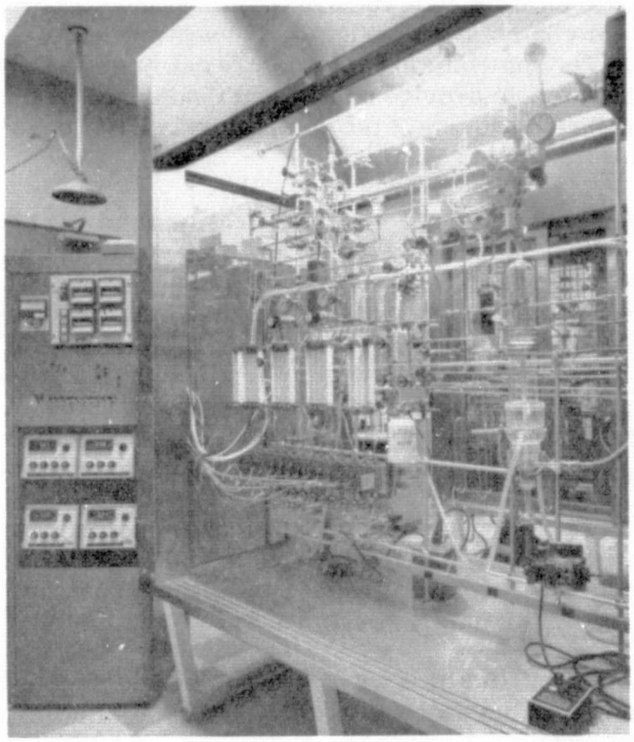

Figure 2-3. Overall View of Modified Si CVD Reactor System, Showing Control Center in Separate Cabinet, Bank of Mass Flow Controllers in Lower Center, and Vertical Reactor Chamber at Right

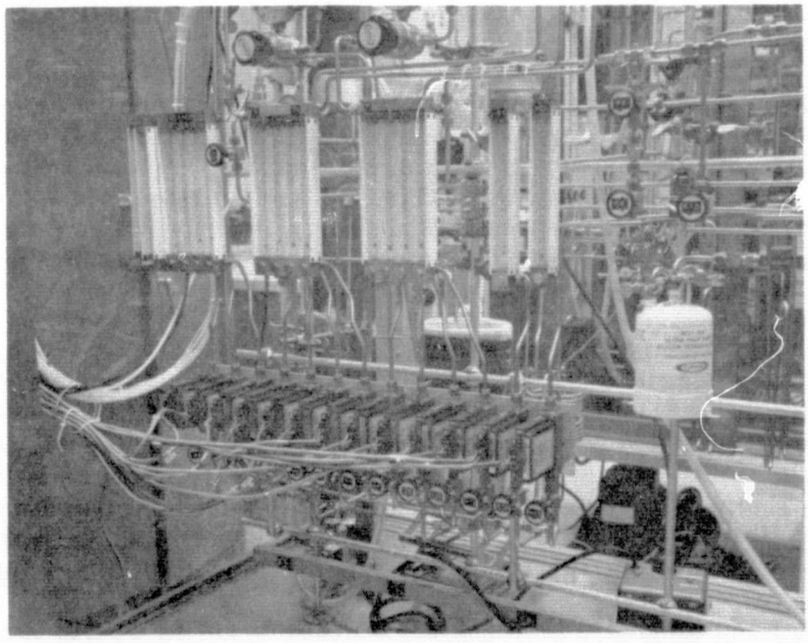

Figure 2-4. Close-Up View of Bank of 13 Mass Flow Controllers

2.2 TASK 2. IDENTIFICATION/DEVELOPMENT OF SUITABLE SUBSTRATE MATERIALS

The 1985 cost goals of the LCSSAP are such that it seems almost certain that no single-crystal material (other than perhaps Si itself) could be used as the substrate for low-cost large-area Si solar arrays meeting the technical performance goals of the project. Future developments could alter this outlook, but for the requirements of this contract other materials far less favorable to Si crystal growth must be considered and evaluated. This is the starting premise in the search for candidate substrate materials.

2.2.1 Rationale and Procedure for Material Selection

In attempting to identify candidate substrate materials for CVD growth of Si sheet which will meet the technical goals of this contract, several considerations are necessary. First of all, the material must be potentially inexpensive. This means that as an absolute upper limit, in today's market as well as in 1985, it must be less expensive than Si itself for comparable sizes and shapes.

Next, it must be - now or potentially - available in relatively large areas. Present technology should already have produced similar material in sizes larger than those in which commercially available Si is now produced.

In addition, the properties of the substrate material should be compatible with those of Si. Its linear thermal expansion behavior should parallel that of Si as closely as possible, from at least the Si sheet deposition temperature down to room temperature. The Si film must also be chemically stable with respect to the substrate surface, so that the transition layer at the interface does not cause separation or other interaction of the two components. Also, the substrate surface must be stable relative to the carrier gas and the products of Si formation—notably, H_2 when SiH_4 is the source of Si, and $HC\ell$ when the Si-containing halides are used to produce the Si.

Only a few classes of materials now available commercially could be considered initially as candidate substrate materials, based on cost, availability, and reported properties. These include the amorphous glasses, glass-ceramics, and polycrystalline ceramics. Many glasses are available in very large sheet form, and others are potentially susceptible to fabrication into large sheets. Some glass-ceramics are also produced in large sheets (the order of square meters), and many polycrystalline ceramic materials are now available in areas up to about 300 cm^2.

In contemplating the use of an amorphous glass as a substrate, it is necessary to consider the effect of temperature on certain glass properties, notably the thermal expansion coefficient and the viscosity. Convention has identified certain viscosity values with some of the physical characteristics that are important in this program: strain point, $\sim 3 \times 10^{14}$ poises; annealing point, $\sim 10^{13}$ poises; softening point, $\sim 10^{7.6}$ poises; and working point, $\sim 10^{4}$ poises.

From room temperature to just below the strain point, which is generally regarded as the upper limit for use of an annealed glass, thermal expansion coefficients (TEC) for glasses tend to remain nearly constant, increasing only slightly with temperature. However, with further increase in temperature into the annealing range the viscosity decreases and a large and rapid increase in TEC occurs. Although the

reduction in viscosity at temperatures above the annealing point might seem to eliminate a glass from consideration for possible use as a substrate for Si sheet growth in that temperature range, there have been studies of Si layer growth on such surfaces in the past (Ref 1), and such a system might have some promise in the present work.

The importance of the TEC of the substrate material relative to that of Si in the range between room temperature and the Si deposition temperature is emphasized by the data given in Figure 2-5. This shows the TEC as a function of temperature for several glasses and other possible substrate materials, as well as for some other familiar materials for comparison, throughout the range from below room temperature up to Si CVD temperatures. These data provide guidance in the selection of candidate materials for further experimental evaluation.

Although many of the glasses produced commercially are not normally available in plate or flat substrate form, it is considered that flat substrates could be produced by techniques well-known in the glass industry if the need were demonstrated. Only two readily available commercial glasses have strain points above the lowest temperatures at which Si growth is considered technically possible by CVD techniques; these are the aluminosilicates Corning Code 1720 and Code 1723. However, as noted above, Si growth by CVD on other glasses could be possible at temperatures between the annealing point of the glass and its softening point, i.e., above ~600°C, which is the lowest temperature consistent with growth of Si from SiH_4.

Since it has not yet been determined with certainty what condition of viscosity of a glass surface is best for the formation of Si films of solar-cell quality, glasses remain in consideration. However, since studies of polycrystalline growth of Si on SiO_2 indicate that higher temperatures lead to increased grain size (Ref 2), early evaluation of glasses has involved those glasses which possess relatively high softening points.

Glass-ceramics are materials which have been converted from their original glassy state to polycrystalline ceramics by controlled nucleation and devitrification. Through variations in composition and heat treatment, glass-ceramics offer a wide range of grain size, crystalline orientations, and thermal expansion coefficients - from high positive values to negative values, including some that are zero over a limited temperature range. Glass-ceramics with TEC's similiar to that of Si are being sought for evaluation as substrates for solar cell structures.

The third class of substrate material of initial interest is the polycrystalline ceramic, which is available in many compositions and purities. Based on TEC values only, likely materials for study include zircon ($ZrO_2 \cdot SiO_2$), with TEC~4.9×10^{-6} per deg C (25-900°C); cordierite ($2\,MgO \cdot 2Al_2O_3 \cdot 5SiO_2$), with TEC ~$3.7 \times 10^{-6}$ per deg C (25-900°C); a number of aluminas, with TEC's $7.7\text{-}8.0 \times 10^{-6}$ per deg C (25-900°C), and mullite ($2Al_2O_3 \cdot 2SiO_2$), with TEC ~4.8×10^{-6} per deg C (40-800°C). In today's market, demand has produced "supersmooth" as-fired surfaces only on the aluminas. Further studies for producing better surfaces (without polishing) on the other ceramics are necessary; such work is in progress in the laboratories of some of the manufacturers.

Another type of substrate material considered as a substrate for Si sheet growth is a combination of two of the above classes, namely, a glass film produced upon a polycrystalline ceramic, i.e., a glazed ceramic. The typical glaze formed on a ceramic offers a surface finish better than that which can be achieved on the ceramic

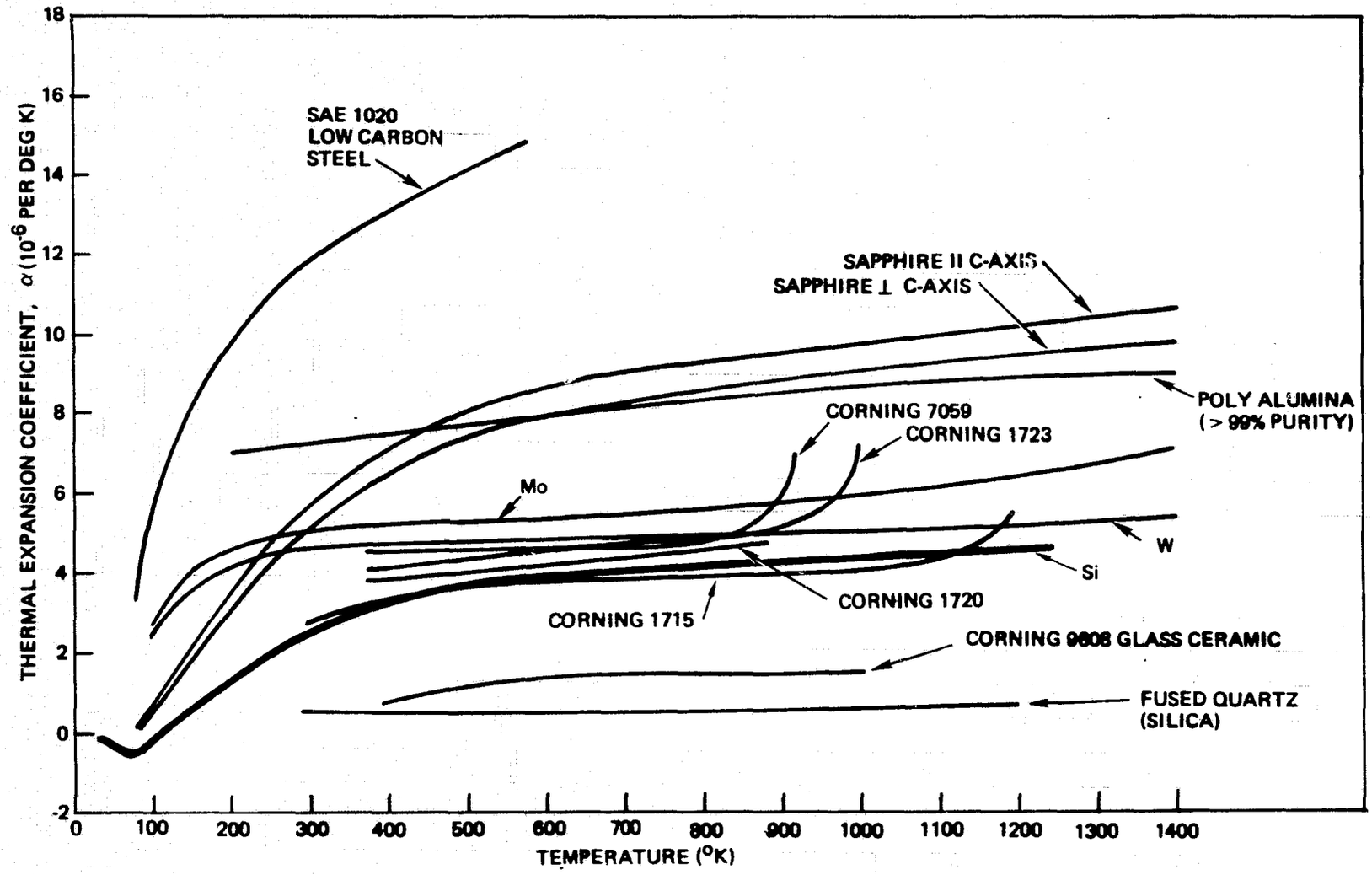

Figure 2-5. Linear Thermal Expansion Coefficients as a Function of Temperature for Si and Various Other Materials

itself (in an as-fired condition) without polishing. The glaze fills in the pores of the surface and can be used with a relatively inexpensive non-smooth substrate of purity lower than, for example, 99.5 percent alumina. Presently, however, the commercial availability of glazed ceramics is very limited, and glazes with low softening temperatures appear to be the rule. This type of composite is attractive, however, and various glazes are being considered in this program. The possibility of utilizing other types of composite substrate will also be evaluated.

Once a substrate material is identified as a candidate for experimental use in this program representative samples of it are screened for the following characteristics: physical appearance (unaided eye); thickness; surface roughness; general appearance at 100X and/or 450X magnification; and (optional) structural properties determined by such procedures as X-ray, reflection electron diffraction (RED), and scanning electron microscope (SEM) examination of the surface.

Substrates of interest are then subjected to exploratory Si CVD growth in both H_2 and He atmospheres at temperatures consistent with the reported properties of the material. For example, for free-standing glasses deposition temperatures below the softening point are used; for glazes on ceramics, higher than softening temperatures may also be used; for the high-temperature-stable ceramics, temperatures up to about 1200°C can be considered, depending upon the properties of the Si-containing compounds in the carrier gas atmosphere.

A thick ($\geq 20\mu m$) Si film usually is grown on the substrate, in the presence of a small wafer of sapphire; the latter helps in monitoring the test substrate material stability in the carrier gas and growth atmosphere, as revealed by any obvious contamination pattern in the Si growth on at least the part of the sapphire nearest the substrate. The thick Si film also helps to determine if the difference in TEC between the Si and the substrate leads to detectable bowing of the composite due to the differential stresses developed upon cooling to room temperature. The Si film also helps reveal certain nonuniformities in some of the substrates.

2.2.2 Contacts with Potential Suppliers of Substrate Materials

Prior to the start of this contract, telephone contacts were made with four potential suppliers of substrates for this program: 3M Company, Corning Glass Works, Coors Porcelain Company, and Owens-Illinois, Inc. Their initial responses led to receipt of samples of a number of commercially available and research-type candidate materials: from 3M Company (Laurens, SC) -- ASM701 (cordierite), ASM475 (zircon), ASM743 (a glazed alumina), ASM805 (sintered alumina); from Corning Glass Works (Corning, NY) -- Codes 1723, 0211, 7059, and 0317 glasses; from Coors Porcelain Company (Golden, CO) -- large-grained alumina; and from Owens-Illinois, Inc. (Toledo, OH) -- a special high-temperature glass.

Samples of most of the above substrates were used early in the contract program in exploratory Si CVD experiments using SiH_4 as the source of Si and either H_2 or He as the carrier gas. These experiments were designed to prepare samples for use in discussions during a visit to these and other potential substrate suppliers during the first month of the program.

A contract-sponsored trip to seven different potential suppliers was completed early in the first quarter. In addition to the above-listed companies, visits were made to Materials Research Corporation (MRC) (Orangeburg, NY); W. R. Grace and Co. (Columbia, MD); and Pemco-Glidden-Durkee (Baltimore, MD).

Subsequent to that trip, numerous other potential suppliers of candidate substrate materials were contacted in the following months. During the third quarter a second trip was made to some of the manufacturers who already were supplying materials, as well as to a number of potential new suppliers.

Table 2-1 lists all of the manufacturers and vendors (with locations) contacted to date regarding participation in this contract as a supplier of special or commercially-available substrate materials. Those visited on each of the two contract-sponsored trips are indicated; others have been contacted by mail or telephone or both. In each case the company's speciality is indicated, as are the types of substrate material already supplied and expected to be supplied, plus an indication of special circumstances, special materials, or other items of importance that have emerged from the contact with that company.

The response of most of the glass and ceramic manufacturers contacted for assistance in solving the substrate problem has been excellent. Both commercially-available and specially-prepared materials have been supplied in various quantities for evaluation as potential low-cost substrates (see next section). Several of the manufacturers indicated a strong interest in attempting to prepare and supply samples of non-standard glasses, glass-ceramics, ceramics, and glazes for exploratory use without charge. Others indicated the effort could not continue throughout the contract period without some specific external financial support, from the contract or otherwise. Four of the suppliers of substrate materials - Corning, 3M, Kyocera, and MRC - visited the Rockwell Electronics Research Division early in the program to discuss details of the substrate requirements.

2.2.3 Candidate Substrate Materials Obtained for Evaluation

All of the candidate substrate materials received to date from the suppliers given in Table 2-1 are listed in Tables 2-2 through 2-4. Table 2-2 lists the glasses and glass-ceramics, Table 2-3 the aluminas, and Table 2-4 the other ceramics. In each table the materials are grouped by vendor and are identified by the vendor's numbers or trade names and by the nominal purity of the material as specified by the vendor. Available data on TEC's are given, as is information about the surface finish - the latter in some cases supplied by the vendor and in some cases measured by Rockwell (see Para 2.2.5). Thicknesses of the various individual groups of substrates are also included.

2.2.4 Early Evaluation of Selected Candidate Substrate Materials

Some of the substrates on hand at the start of the contract (see Para 2.2.2) were used in preliminary CVD screening experiments early in the program. For example, Figure 2-6 shows the obvious contamination of CVD Si film growth on a single-crystal sapphire monitor wafer caused by the adjacent wafer, consisting of an ASM743 lead-borosilicate glaze on an ASM614 alumina substrate, present during Si deposition in He

Table 2-1. Manufacturers and Suppliers Contacted Regarding Substrate Substrate Materials for Use in CVD Si Growth Experiments

VENDOR (LOCATION)	PERTINENT SPECIALTY	SUBSTRATE SAMPLES		REMARKS
		SUPPLIED	MAY/WILL BE SUPPLIED	
Corning Glass Works[1,2,4] (Corning, NY)	Glasses, glass-ceramics	Corning Codes 0211; 0317; 1723; 7059; SiO_2-coated 0317; 1715 glasses	Additional 1715	Funded development program preferred for additional materials; proprietary agreements may be needed
		Corning Codes 9606; 9608; 9609 glass-ceramics	9606	O-I has requested evaluation of first
Owens-Illinois, Inc.[1,2] (Toledo, OH)	Glasses	GS-186; GS-210; GS-211; GS-213	EE-2; EE-5 glass-ceramics	O-I has requested evaluation of first 4 glasses before preparing others
3M Co. (Laurens, SC)[1,4] (St. Paul, MN)[2]	Ceramics	Cordierite; zircon; glazed alumina; aluminas of various purities, firing histories, process types	Aluminas with extended firing histories; mullite; steatite; spinel	Organizational changes shifting R&D to St. Paul, MN
Coors Porcelain Co.[1] (Golden, CO)	Ceramics	ADS96F; ADS995; Vistal (as-fired and refired)	Additional ADS995	Present Interests not oriented toward solar cell substrates; additional special materials available for purchase
Materials Research Corp.[1,4] (Orangeburg, NY)	Ceramics	Superstrate; Au-coated superstrate	Superstrates of diff. quality and purity [HiRel Hybrid (99.6 percent) ; others (96 percent)]	Initially interested, but participation decreasing
Kyocera[4] (San Diego, CA)	Ceramics	Forsterite; alumina; zircon; glazed alumina	Mullite; spinel	Trying to develop low-cost tape process for >99 percent alumina; Japan-based
Pemco-Glidden-Durkee[1] (Baltimore, MD)	Enamels, frits	Two different glazes on cordierite and alumina	—	Glazes on substrates very poor quality physically.
Morganite, Inc.[3] (Dunn, NC)	Ceramics	Recrystallized alumina; Hilox 961 (96 percent)	Mullite	England-based
Chi-Vit Corp.[2] (Cicero, IL)	Enamels, glazes	Glazed Kovar-type alloy (aluminoscilicate glass)	Glazed alumina	Alumina substrates to be supplied by Magneco Electronics

Table 2-1 (Cont)

VENDOR (LOCATION)	PERTINENT SPECIALTY	SUBSTRATE SAMPLES		REMARKS
		SUPPLIED	MAY/WILL BE SUPPLIED	
Magneco Electronics[2] (Addison, IL)	Ceramics	Alumina (96 percent)	Aluminas to Chi-Vit Corp. for glaze	Use "dry"-rolled tape process
Saxonburg Ceramics[2] (Saxonburg, PA)	Ceramics	Alumina (97.5 percent)	Mullite; cordierite	Subsidiary of Lava Crucible Refractories Co.
Plessey-Ceramics Div.[2] (Frenchtown, NJ)	Ceramics	Ceramislik; black No. 7231; tape alumina	Std. ceramics (some with Ti, Mn impurities)	No special materials to be produced for program
Ferro Corp.[2] (Independence, OH)	Frits, glazes, specialty ceramics	High-density cordierite	Glazed ceramics	Only limited commitment to program possible at present
Schott Optical Glass, Inc.[2] (Duryea, PA)	Glasses (IR, solder, optical), glass-ceramics	Glass-ceramic	Specialty glasses	Germany-based; very interested in participating
Atomics Intl.[3] (Canoga Pk, CA)	Glazes	Glazed alumina	–	Not a continuing program
Honeywell Ceramic Center[3] (Golden Valley, MN)	Ceramics	Mullite	–	Will not be actively participating
Associated Ceramics and Technology[3] (Sarver, PA)	Ceramics	–	Alumina	Very rough surfaces on present material (35-50 microinch)
Metsch Refractories[3] (Chester, WV)	Ceramics	–	Cordierite; mullite; porcelain	New matls will be supplied.
American Refractories and Crucible Corp.[3] (North Haven, CO)	Ceramics, mullite	–	–	Crucible business only
Star Porcelain Co.[3] (Trenton, NJ)	Porcelains	–	–	No substrate capability
General Electric Glass Products and Lamp Div.[2] (Cleveland, OH)	Lucalox (alumina); quartz	Quartz ribbon	–	Produce Lucalox but not as tape product; no facilities for flat glass
Ceradyne[3] (Santa Ana, CA)	Specialty ceramics	–	–	Not cost-competitive for this application

Table 2-1 (Cont)

VENDOR (LOCATION)	PERTINENT SPECIALTY	SUBSTRATE SAMPLES		REMARKS
		SUPPLIED	MAY/WILL BE SUPPLIED	
Harbison-Walker Refractories[3] (Pittsburgh, PA)	Industrial refractories	–	–	Still considering possible participation
Glass Beads Company[3] (Latrobe, PA)	Alumina	–	–	Prepare low purity (90-92 percent) alumina
Norton Company[3] (Worcester, MA)	Refractories	–	–	Present processes not compatible with substrate requirements
Du-Co Ceramics[2] (Saxonburg, PA)	Specialty steatites	–	–	Custom design and fabrication only
Wisconsin Porcelain Co[3] (Sun Prairie, WS)	Ceramics	–	–	Not interested in new project at present time
Alberox Corp.[3] (New Bedford, MA)	Ceramic-metal seals	–	–	Not interested at this time
McDanel Refractory Porcelain Co.[3] (Beaver Falls, PA)	Ceramics	–	–	Manufacture only finished ware; slip-cast tubes; no pressing facilities
Duramic Products[3] (Palesades Park, NJ)	Ceramics	–	–	Materials porous – not compatible with program requirements
W. R. Grace & Co.[1] (Columbia, MD)	Ceramics	–	–	Germany source; no commercial interest at this time

[1]Contact on first trip
[2]Contact on second trip
[3]Phone contact only
[4]Visited Rockwell

Table 2-2. Candidate Glass or Glass-Based Materials Received to Date from Various Suppliers

SUBSTRATE IDENTIFICATION	MATERIAL/TYPE	THERMAL EXPANSION COEFF (TEMP RANGE) (10^{-6} PER DEG C)	THICKNESS (mm)	STRAIN POINT (°C)	ANNEAL POINT (°C)	SOFTENING POINT (°C)
Corning 0211	Lime Borosilicate	7.4 (0–300°C)	0.25	508	550	720
0317	Alumina Soda Lime	8.7 (0–300°C)	1.52	574	622	871
1723	Aluminosilicate	5.4 (25–670°C)	0.76, 1.27	665	710	908
7059	Barium Alumino-borosilicate	4.6 (0–300°C)	0.81	587	635	842
1715	Calcium Aluminosilicate	~3.5 (0–300°C)	–	834	866	1060
Owens-Illinois GS-186	Proprietary High-temperature Glass	4.7 (0–300°C)	0.76, 1.02	–	–	982
GS-210	Proprietary High-temperature Glass	3.8 (0–300°C)	1.02	–	–	869
GS-211	Proprietary High-temperature Glass	3.6 (0–300°C)	1.02	–	–	1075
GS-213	Proprietary High-temperature Glass	2.6 (0–300°C)	1.07	–	–	1135
Atomics International (Rockwell)	Proprietary Glass (on ASM 805 Alumina)	–	0.063-0.076	–	–	830
Chi-Vit Corp.	Aluminosilicate glass (on Ni steel)	~4.5	0.15, 0.30	–	–	–
Pemco-Glidden-Durkee	Li aluminosilicate glaze (on cordierite)	~3	0.008-0.010	–	–	–
	Boron aluminosilicate glaze (on 94% Alumina)	~5.5	0.005-0.006	–	–	–
3M 743 Glaze on ASM614	Lead borosilicate (on 96% Alumina)	6.5 (40-540°C)	0.71 total	–	–	–
Kyocera GS-3	Glaze (on A473 Alumina)	~7.6	0.008/0.63	–	–	–
Corning GC9606	Magnesium aluminosilicate glass - ceramic	5.7	6.4 (as cut) 1.02, 2.04 (polished)	–	–	–
GC9608	Lithium aluminosilicate glass-ceramic	0.4	4.5	–	–	–
GC9609	Sodium aluminosilicate glass-ceramic	9.8	–	–	–	–
Schott Glass GC8559	Glass-ceramic	~2 (20-1000°C)	5.0	–	–	–

Table 2-3. Candidate Alumina Materials Received to Date from Various Suppliers

SUBSTRATE IDENTIFICATION		NOMINAL PURITY (%)	METHOD OF PREPARATION	THERMAL EXPANSION COEFF (TEMP RANGE) (10^{-6} PER DEG C)	AVERAGE SURFACE GRAIN SIZE (μm) [AV SURFACE ROUGHNESS (μm)]*	THICKNESS (mm)
Coors	ADS 96F	96	Dry press	8.1 (25–1000°C)	–	0.63
	ADS 995	99.5	Tape	7.7 (25–1000°C)	1–10 (av 1.1) [~0.35]	0.69
	Refired Large-grain Al_2O_3	99.3 (before firing)	Tape	~7.3 (25–800°C)	–	0.56
	Vistal 1	99.9 (before firing)	Dry press	8.3 (25–1200°C)	20 (1st firing)†	0.97
	2				36 (2nd firing)†	
	3				80–100 (3rd firing)†	
	4				28 (4th firing)†	
MRC Superstrate		99.6	Tape	7.3 (25–800°C)	~1.5 [~0.15]	0.63
3M	ASM 614[a]	96	Tape	7.9 (25–900°C)	[1.2–1.5]	0.63, 0.89
			Dry press	–	[2.5–3.5]	0.79, 1.09
	ASM 805[a]	99.9	Tape	7.7 (25–900°C)	<1.0 [0.1–0.2]**	0.63
	ASM 838[a]	99.5	Tape	7.7 (25–900°C)	[0.4–0.6]	0.13, 0.71
	ASM 772[a]	99.5	Tape	7.7 (25–900°C)	[0.5–1.2]	0.25, 1.02
	ASM 777	94	Tape	8.7 (25–900°C)	[1.6–2.0]	0.48
Saxonburg		97.5	Dry press	7.8 (25–900°C)	–	1.27
Morganite Recrystallized		99.8	Dry press	8.4 (20–1000°C)	–	3.12
Hilox 961		96	Dry press	8.2 (20–1000°C)	–	1.02, 2.04
Plessey	7231	92	Dry press	7.2 (25–700°C)	–	0.61
	Ceramislik	99.7	Tape	~7.7	–	0.25
Kyocera	A473	96	Tape	~7.6 (40–800°C)	–	0.63
Magneco Electronics		96	Rolled tape	~7.8 (25–900°C)	–	0.63
Comco, Inc.		96	Tape	–	–	0.63
		99.5	Tape	–	–	0.58

*Average peak-to-valley dimension

[a]Also provided in various refired conditions

†See text for discussion

**Smooth side ≤ 0.1μm; rough side ~0.25μm (average surface roughness)

Table 2-4. Candidate Miscellaneous Materials Received to Date from Various Suppliers

SUBSTRATE IDENTIFICATION	METHOD OF PREPARATION	THERMAL EXPANSION COEFF (TEMP RANGE) (10^{-6} PER DEG C)	AVERAGE SURFACE GRAIN SIZE (μm) [AV SURF ROUGHNESS (μm)]*	THICKNESS (mm)
Honeywell Mullite ($3\,Al_2O_3 - 2\,SiO_2$)	Rolled Sheet	~5.0	–	1.65 – 1.78
Kyocera Z360 Zircon ($ZrO_2 \cdot SiO_2$)	–	~4.7 (40–800°C)	–	1.02
Kyocera F1330 Forsterite ($2\,MgO \cdot SiO_2$)	–	10.5 (40–400°C)	–	1.32
3M Co. ASM475 Zircon ($ZrO_2 \cdot SiO_2$)	Dry Press	4.9 (25–900°C)	[4.0–5.0]	0.56
3M Co. ASM701 Cordierite ($2\,MgO \cdot 2\,Al_2O_3 \cdot 5\,SiO_2$)	Dry Press	3.7 (25–900°C)	[6.5–15]	1.02
Ferro FB 266M Cordierite	Dry Press	1.8 – 2.0 (25–1000°C)	–	Cylinder
Union Carbide Oriented Pyrolytic Graphite	Pyrolytic	2.8 (c) (300–1100°K)	–	0.97, 1.52

*Average peak-to-valley dimension.

carrier gas at ~825°C. Figure 2-7 shows the excessive bowing of Corning Code 7059 glass when a Si film was deposited on it in He at 700°C; the film is in tension at room temperature in this case. Additional Si deposition experiments with this glass are described in Para 2.2.7.

The deposited Si film also helped to reveal nonuniformities found in some of the substrates tested, as was evidenced by Si CVD growth on cordierite (Figure 2-8) and on large-grained alumina (Figure 2-9). Incompatability of the Si film with a glaze also manifested itself in wrinkling of the film-glaze composite after growth, as shown in Figure 2-10; the film was nominally 14 μm thick in this case and was grown in He at ~700°C, rather than at ~825°C as was the deposit shown in Figure 2-6.

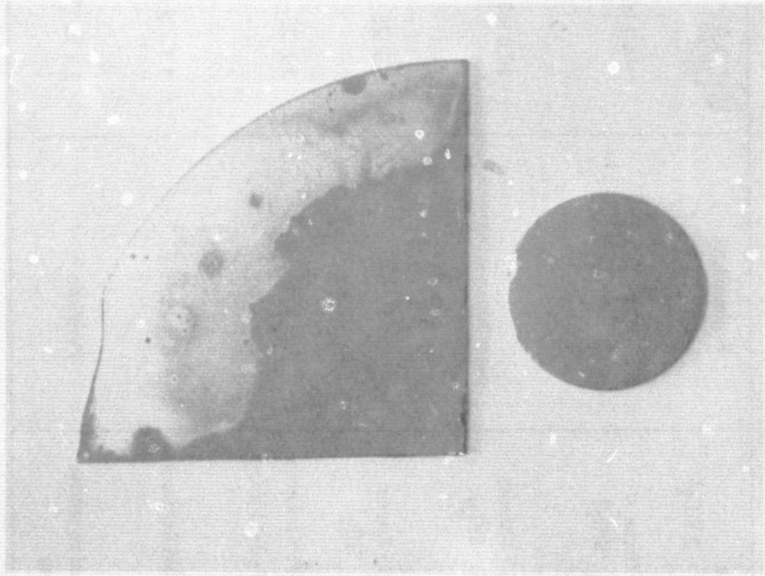

Figure 2-6. Evidence of Contamination of CVD Si Film Growth on Sapphire (Large Wafer) Caused by Nearby Glazed Alumina Substrate (Lead Borosilicate on ASM614) during Deposition in He at 827°C

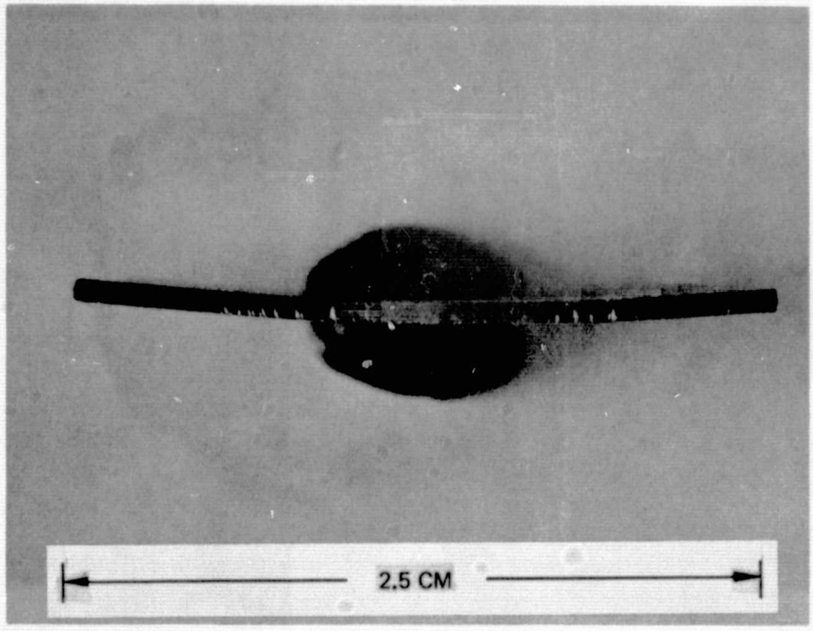

Figure 2-7. Edge View Showing Bowing of Composite of CVD Si on Code 7059 Glass after Deposition in He at 700°C. Si Film on Upper (Concave) Surface

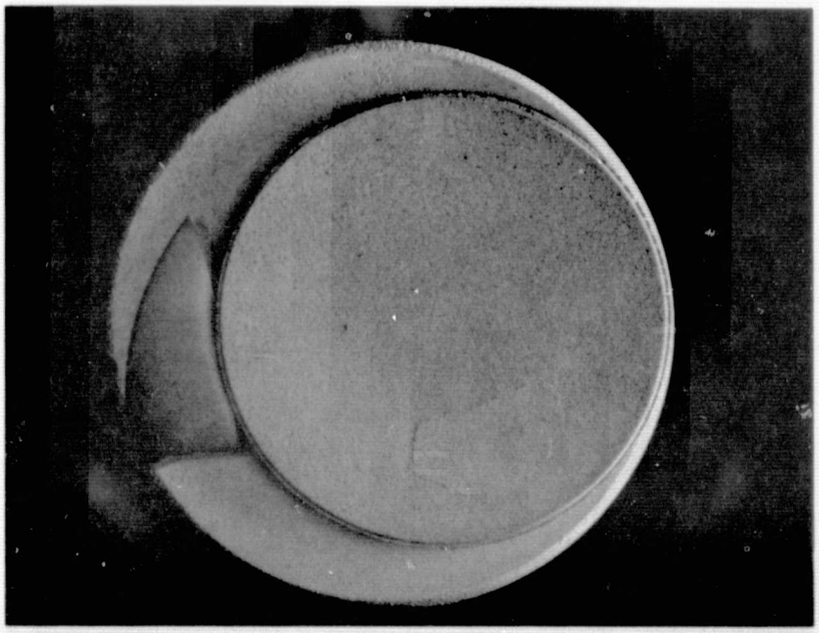

Figure 2-8. Nonuniformity in ASM701 (Cordierite) Substrate Revealed by Si CVD Film Growth in He on 3.5-cm-dia Substrate

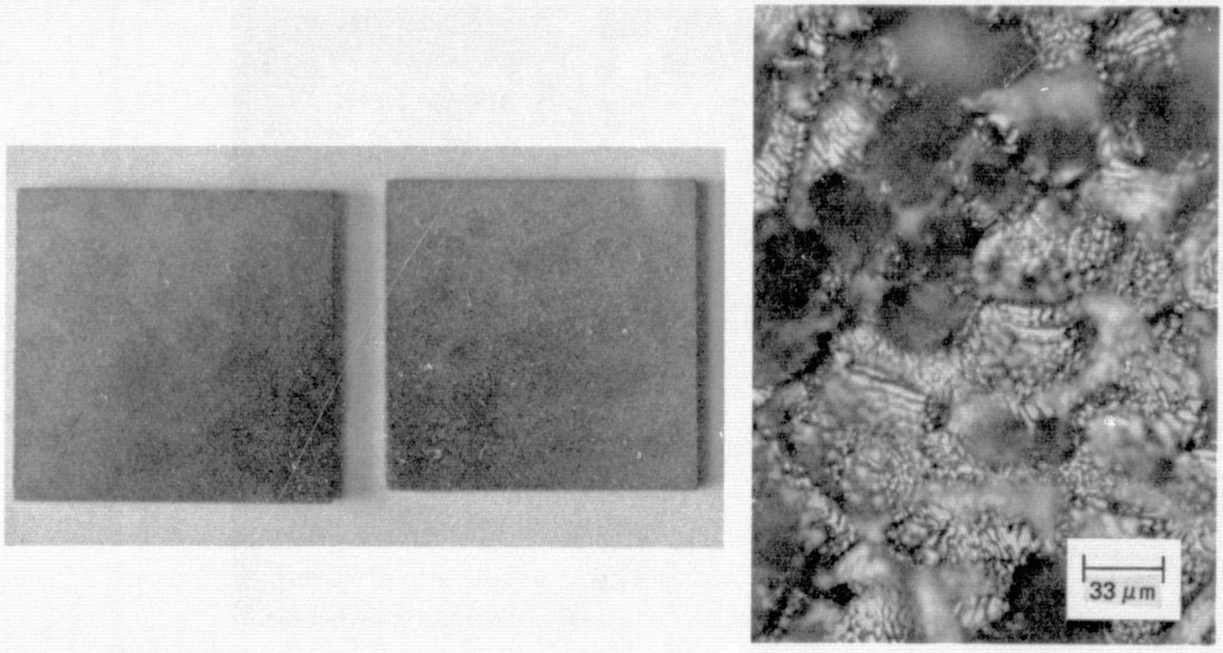

Figure 2-9. Nonuniformities in Large-grain Alumina "Tape Product" (Coors), Emphasized by Si CVD Growth. (a) Films on 12x12 mm Substrates, (b) Photomicrograph Showing Detail of Irregular Grains

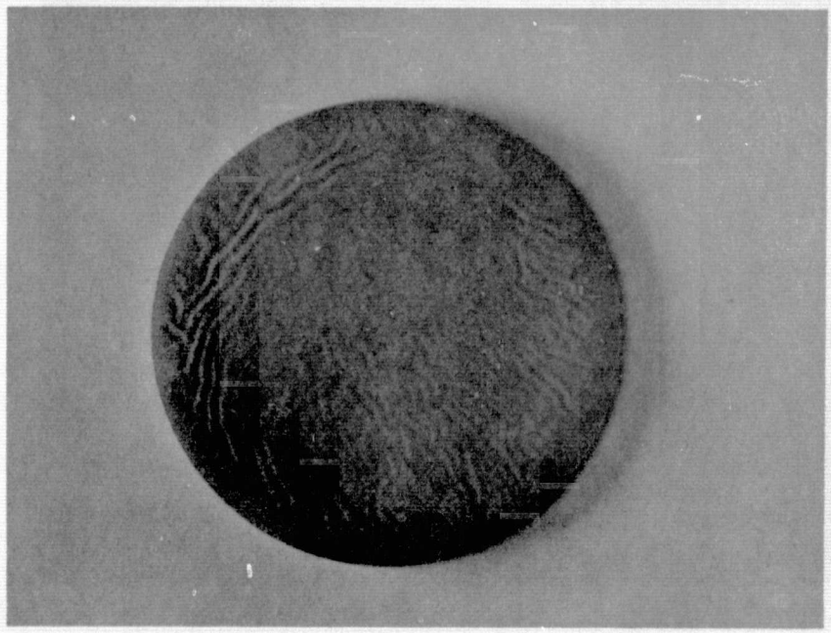

Figure 2-10. Wrinkled CVD Si Film Grown 14 μm Thick on Glazed Alumina Substrate (Lead-borosilicate Glaze 743 on ASM614) in He at 700°C

Corning Code 1723 aluminosilicate glass also failed to meet the requirements for substrate use for CVD Si, even at relatively low temperatures. This glass failed in both H_2 and He atmospheres; amorphous structural features were found on the film surface grown in H_2 at 850°C, and contamination of the companion sapphire substrate occurred during Si deposition in He at 850°C. There was even reactivity (or thermal instability) observed at 620°C in a He atmosphere. Further details of the experiments with this glass are given in Para 2.2.7.

Encouraging results, however, were obtained in the first quarter with fired polycrystalline alumina substrates, which were used for Si deposition at temperatures above 1000°C. These materials exhibit some preferred orientation in their polycrystalline structures, and the films grown on these were also preferentially oriented. The alumina substrates used first were those of the highest purity: MRC Superstrate, Coors ADS995, and 3M ASM805. The latter was found to have the best as-fired surface of the alumina substrates examined early in the program. Si grown by CVD on this material and on sapphire at 1025°C produced single-crystal growth on the sapphire and a film having reflective sheen on the alumina. No obvious form of impurity contamination in the film on the sapphire was in evidence.

Based on those preliminary results and the early availability of this and similar substrate materials received from MRC and Coors, the aluminas were selected for some of the first studies of CVD parameters in the work of Task 3 (Para 2.3), as well as for detailed characterization of the substrate materials themselves.

2.2.5 Substrate Characterization

A wide range of surface topography is represented by the three main types of substrate materials expected to be used in the contract work--namely, glasses, glass-ceramics, and polycrystalline aluminas and similar fired ceramics. The surface of a film deposited on a substrate usually has a topography directly related to that of the substrate, especially if the latter is heavily textured. In addition, if epitaxial growth occurs in the film the characteristics of its surface will also be influenced by crystallographic features resulting from the nature of the growth. In any case, it is important to know the nature and magnitude of the surface irregularities on a substrate. Optical microscopy and photomicrographs, SEM examination, and surface profilometry are among the methods used to characterize these surfaces.

The properties of several different polycrystalline aluminas, including the three mentioned above, are listed separately in Table 2-5. These are the substrates that have been used most extensively and characterized most thoroughly during the first nine months of the contract. Also included in the table are four different Vistal aluminas, which will be described further below.

SEM examination of the surfaces of the first three aluminas in the table confirmed an earlier observation that the ASM805 substrates exhibited a difference in surface smoothness on opposite sides visible to the unaided eye upon careful examination. The SEM photographs in Figure 2-11 demonstrate the difference quite clearly, with the rough side shown in Figure 2-11a and the smooth side in Figure 2-11b.

Table 2-5. Properties of Several As-fired Polycrystalline Alumina Ceramic Substrate Materials

	ASM 805 (3M) (SMOOTH) (ROUGH)	SUPERSTRATE (MRC)	ADS 995 (COORS)	ASM 805 (REFIRED) (3M) (SMOOTH) (ROUGH)	VISTAL (REFIRED) (COORS)			
					1	2	3	4
Al_2O_3 Purity (%)	99.9	99.6	99.5	99.9	99.9	99.9	99.9	99.9
Surface Crystal Size (μm) – manufacturer's specification	<1.0	~1.5	1–10 (2 av.)	– –	–	–	–	–
Surface Finish as Fired (Microin.*) – manufacturer's specification	1.0–2.0	4–5 max.	8 – 10	– –	–	–	–	–
Apparent Surface Grain Size (μm) – Meas. in SEM	0.4 0.5	0.8 – 1.0	1.1	12.5 –	20	36	80 – 100	28
Average Surface Roughness as Vertical Peak-to-valley Dimension (μm) – Meas. with Dektak	⩽0.1 ~0.25	~0.15	~0.35	⩽0.1 ~0.26	2.5	3.0	3.5	3.5
Camber† (in. per in.) – manufacturer's specification	0.003–0.004	0.003 (max.)	0.002 – 0.003	–	–	–	–	–

* Center-line average

† Measure of surface curvature of wafer, expressed as amount by which minimum separation of parallel plates through which wafer can pass under its own weight exceeds the nominal thickness, per unit length

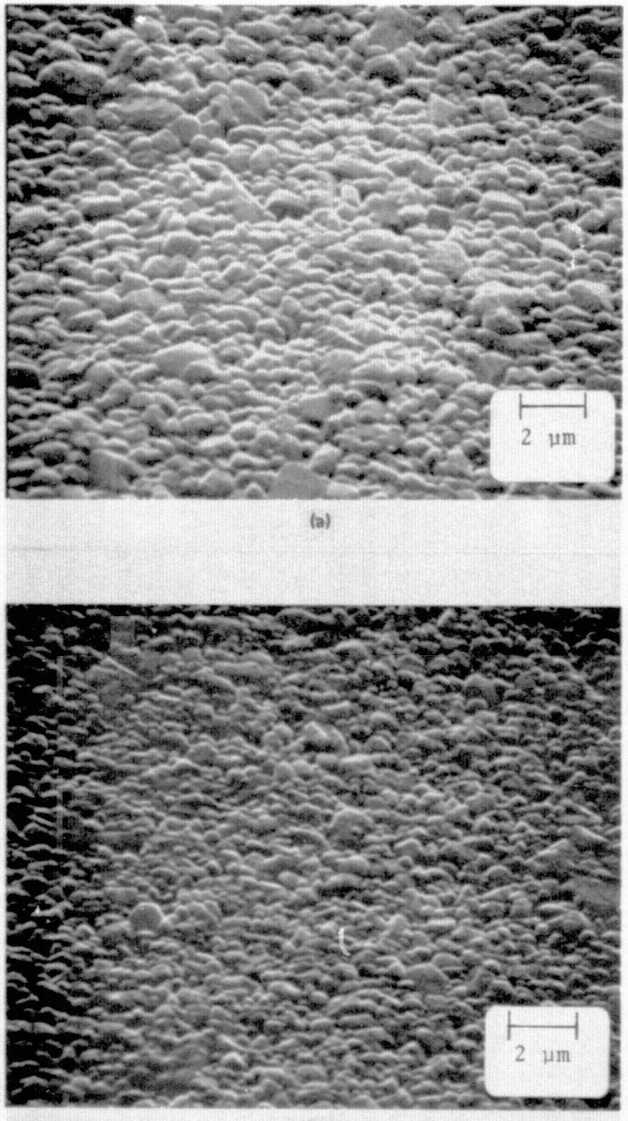

Figure 2-11. Surface Morphology of ASM805 Fired Alumina Substrate (3M Co.). (a) Rough Side, (b) Smooth Side

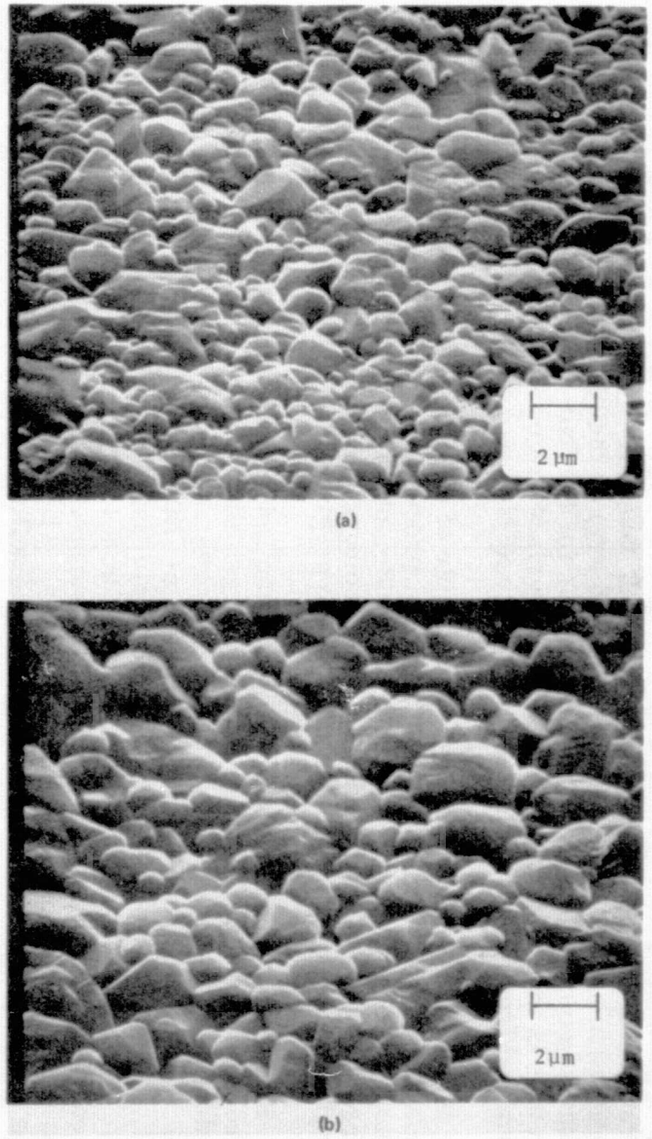

Figure 2-12. Surface Morphology of Fired Alumina Substrates. (a) MRC Superstrate, (b) ADS995 (Coors)

All three alumina substrates are microscopically rough, with three-dimensional surface features up to ~3 μm in height. Figures 2-12a and 2-12b show the MRC Superstrate and the ADS995 (Coors) surfaces, respectively, at approximately the same magnification and the same viewing angle (45 deg) as the photographs of Figure 2-11. The surface morphology is seen to be similar for the four surfaces, but the surface grain size is not. The average size of the surface grains for the three aluminas, as determined from direct measurements on the SEM photographs, is given in Table 2-5.

Included in Table 2-5 is a special sample of ASM805 that had been refired by the manufacturer beyond the normal commercial processing. This material is of interest because of the much larger apparent grain size, shown in the SEM photograph of Figure 2-13, and the changed surface morphology. Additional investigation of other refired aluminas was undertaken later in the program and is described subsequently.

Surface profilometry, employing a Sloan Dektak, was used to examine and record the surface finish on the fired polycrystalline alumina materials of interest, including those in Table 2-5. This procedure is useful for the rapid screening of substrate surfaces to provide both a qualitative overall view of the surface finish and a quantitative measure of localized surface features. The Dektak sensitivity scale and traverse rate used for a given surface must be a compromise based on the actual vertical (and horizontal) dimensions of the surface features and the ability of the probe stylus to follow the contour of these features. The probe stylus has a radius of 12.5μm, with a tracking force of 50 mg. The vertical deflection sensitivity ranges up to a maximum of 10Å per mm spacing on the recorder paper, although the highest sensitivity range found practical is 50Å per mm.

The average surface roughness of each of the aluminas in Table 2-5, as measured with the Dektak and expressed as an average vertical peak-to-valley difference, is included in the table. A large number of other as-fired polycrystalline ceramic substrates (mostly aluminas) obtained from the 3M Company was also characterized by surface profilometry in the second quarter; the results of those measurements are included in the properties that were given in Tables 2-3 and 2-4.

X-ray diffraction analysis of representative samples of three of the polycrystalline aluminas of interest produced some interesting results. Comparison of the principal low-index diffraction line intensities obtained with Cu K-alpha radiation (at 50 KV and 20 ma) for these samples (all of which consist of corundum, or polycrystalline α-alumina, which is trigonal with lattice parameters of $a_o = 4.758$Å and $c_o = 12.91$Å) with those for a standard random-oriented polycrystalline sample indicated some preferred orientation is present. Specifically, the ADS995 shows the strongest preferred orientation of the three, with a tendency for $\{10\bar{1}4\}$ and $\{11\bar{2}6\}$ planes to align parallel to the surface. The ASM805 also exhibits both $\{10\bar{1}4\}$ and $\{11\bar{2}6\}$ preferential orientation. The Superstrate appears to be the most randomly oriented of the three, although it also has some tendency for $\{11\bar{2}6\}$ planes to be parallel to the surface. X-ray analysis to determine preferred orientations in the Vistal alumina substrates has also been undertaken, but the results are not yet complete. In addition, X-ray line-broadening methods (see Para 2.5) have been applied to determination of average grain size in substrate materials, but the samples examined by this means so far have had grain sizes sufficiently large that no line broadening has been observed.

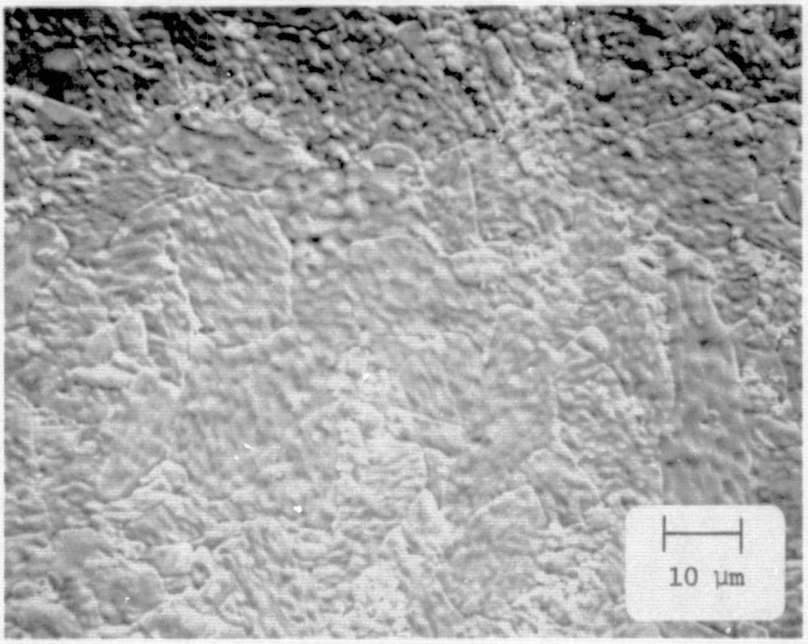

Figure 2-13. Surface Morphology of ASM805 Alumina Substrate Refired by Manufacturer (3M Co.) to Produce Grain Enlargement

Vistal alumina, four different examples of which are listed in Table 2-5, is a large-grained high purity alumina (99.9 percent) manufactured by Coors Porcelain Company. Each of the four groups of Vistal substrates has a different firing history; these substrates have been fired beyond the normal alumina processing by one, two, three, and four consecutive firings at >1800°C for six hours each. As a result, four different average grain sizes have been achieved.

The SEM photographs in Figure 2-14, which show representative areas of samples of each of the four Vistal groups in the as-fired condition, illustrate the wide range of grain sizes present in each group; grains from 5 μm to over 200 μm across can be seen. (The apparent debris on the surface--especially prominent in Figure 2-14c-- is caused by incomplete cleaning of the substrate prior to examination in the SEM.) Based on the observed surfaces of the four substrate wafers examined in the SEM it appeared that Vistal 3 had larger grains than did Vistal 4. Counts made on representative samples indicated that the average surface grain sizes listed in Table 2-5 are indeed typical of the as-fired materials. It was later learned that the segregation of smaller crystal grains to the surfaces of this type of ceramic during extended firing is a normal occurrence. Thus, a more accurate observation of true grain size is made after removal of a surface layer, by polishing or other means. This was later done for the Vistals, as they are among the substrates that have been polished to improve their surfaces for CVD Si growth. This is discussed further in Para 2.2.6.

All of the as-fired Vistal substrates exhibited a three-dimensional surface with gently rounded grains projecting less than ~10 μm in a vertical direction, as shown in

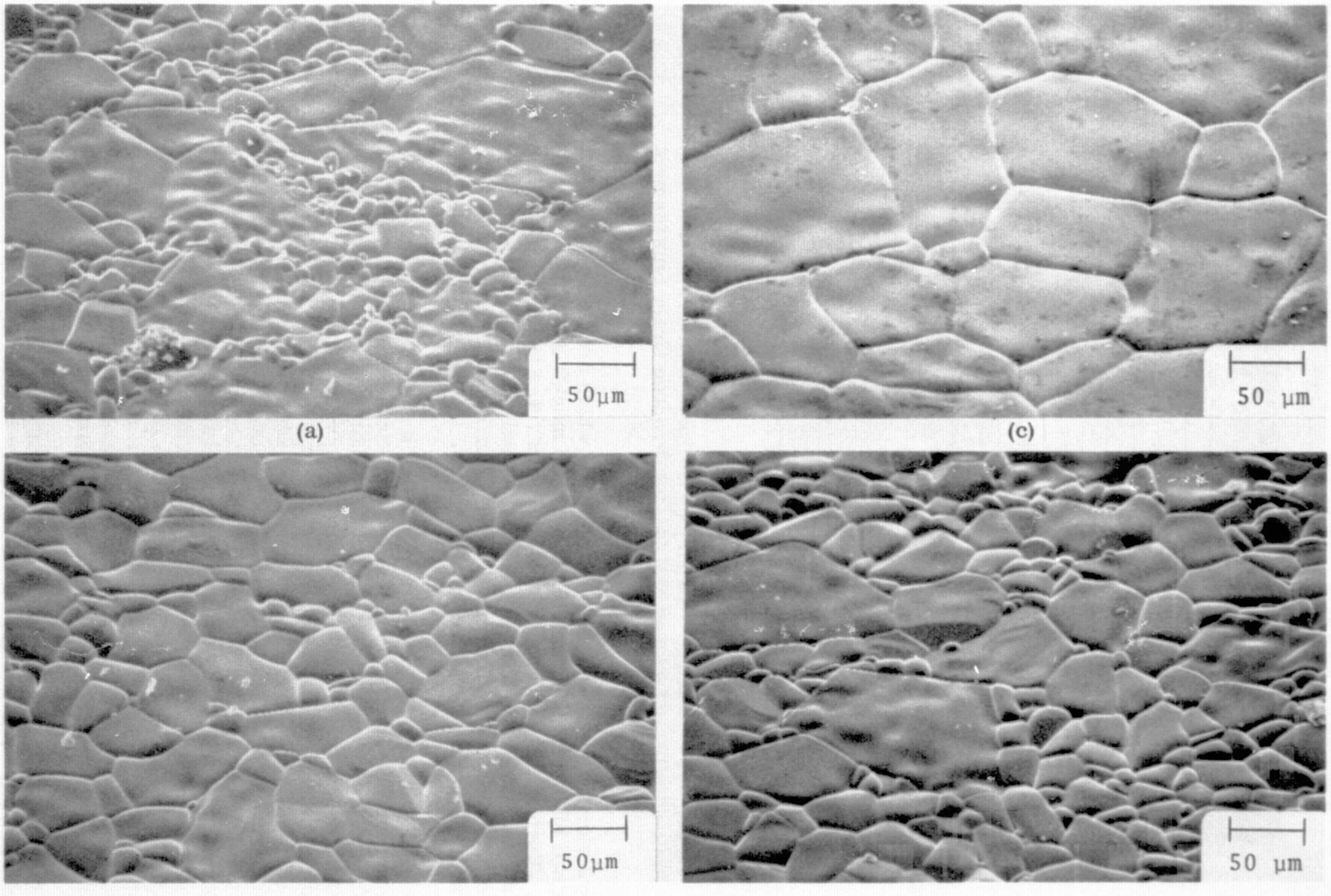

Figure 2-14. SEM Photographs of Vistal Alumina Substrates in As-fired Condition. (a) Vistal 1 (one firing at >1800°C for 6 hr); (b) Vistal 2 (two consecutive firings); (c) Vistal 3 (three consecutive firings); (d) Vistal 4 (four consecutive firings). (All photographs taken at 45 deg viewing angle with sample surface.)

Figure 2-15 for a Vistal 4 (four consecutive firings) substrate. Figure 2-15a is with the sample oriented for the standard viewing angle of 45 deg, while Figure 2-15b shows the same sample (at approximately the same magnification) viewed at a low angle of 25 deg with the sample surface, showing more clearly the height of the individual projecting crystals.

Characterization of other substrate surfaces by SEM examination has been carried out at various times in the first nine months. Recent analyses of surfaces of two aluminas from the 3M Company produced the photographs shown in Figures 2-16 and and 2-17, the former of as-manufactured ASM772 (99.5 percent purity) and the latter of ASM838 (also 99.5 percent purity). In each case the upper view is normal to the substrate surface and the bottom at a 30 deg viewing angle with the surface. Larger and more uniformly-sized grains seem to be present in as-fired ASM 772 (Figure 2-16) than in the as-fired ASM 838 (Figure 2-17a). The refiring of ASM838 appears to have led to larger grains at the substrate surface, with some size differences apparent on the two sides of the substrate (Figures 2-17b and c). Further information on the effects of firing ASM838 alumina as a function of firing history will be available for the next quarterly report.

Comparisons were also made of the uniformity of the individual grains of alumina (Al_2O_3) at the surface of some of the 96 percent (lower cost) aluminas. From Figure 2-18 it can be seen that the grains in as-fired samples of these aluminas vary considerably in size and are relatively large compared with the grains in as-fired ASM772 and ASM838 (Figures 2-16 and 2-17). The material from Kyocera appears to possess larger grains and possibly a higher degree of crystallinity than the others, although the differences in magnification in the figure can be misleading. The mullite (ASM832) also displays a very rough surface consisting of particles of many sizes.

Very little has been done to date to characterize the glass substrates considered to be candidates other than to test experimentally their physical and chemical stability in the Si CVD environment, in He as well as in H_2, and their performance as growth surfaces and mechanical supports for Si films. Some of the glasses used have as-manufactured surfaces, while others (Corning Code 1715, for example) are polished by the manufacturer before they are supplied for use in this program. Further characterization of the principal glasses of interest will be undertaken later and will be described in subsequent reports.

Corning Code 9606 glass-ceramic was recently received for evaluation as a substrate. SEM examination of its surface, which had been polished by Corning, revealed at high magnification (1200X) the presence of elongated inclusions or particles on/in the surface, as shown in Figure 2-19. This was noted subsequent to growth of Si films on the glass-ceramic, the growth habits of which are mentioned in Para 2.2.7. Discussions held with Corning personnel during the second trip to visit vendors indicated the particles may be material embedded in the surface during the polishing process and/or merely a residual contamination. An unused section of the substrate is to be returned to Corning for evaluation; another section will be evaluated further at Rockwell.

2.2.6 Substrate Surface Preparation

Because of the rough surfaces on the as-fired aluminas and on some of the other ceramic materials (Tables 2-3 and 2-4) obtained from various manufacturers, several

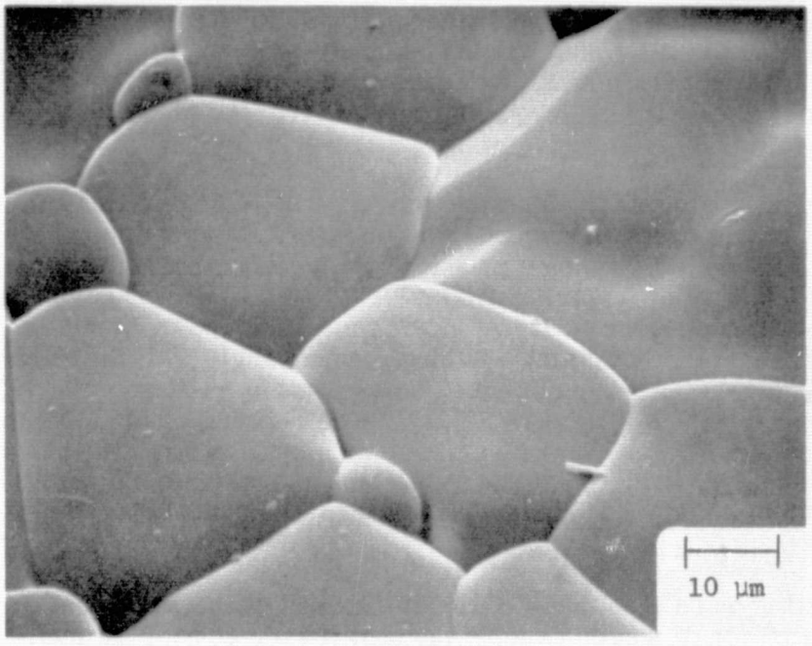

(a)

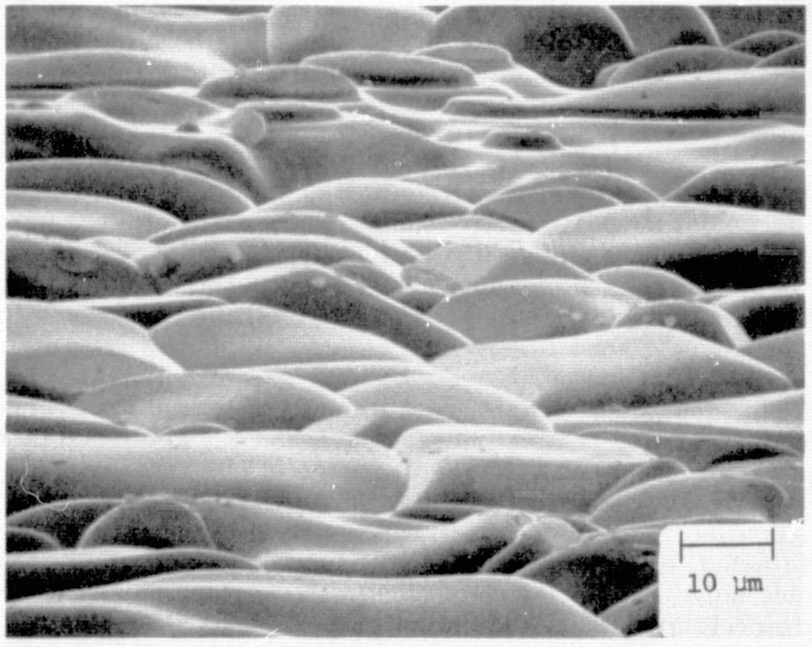

(b)

Figure 2-15. SEM Photographs of Vistal 4 (four consecutive firings) Alumina Substrate Surface in As-fired Condition. (a) Viewing Angle 45 deg; (b) Viewing Angle 25 deg with Sample Surface.

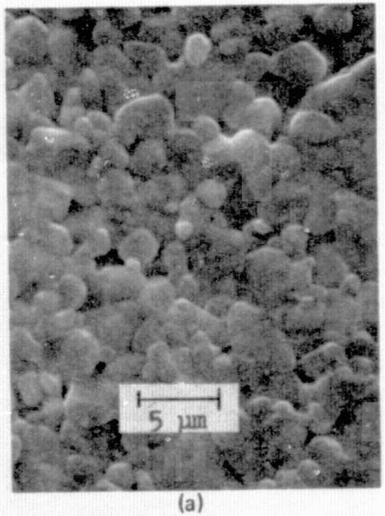

Figure 2-16. SEM Photographs of Surface of As-manufactured ASM772 Alumina (3M Co.).
a) Viewed Normal to Surface,
b) Viewed at 30 deg with Surface.

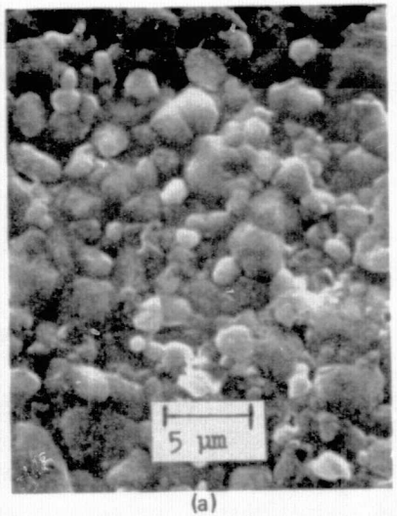

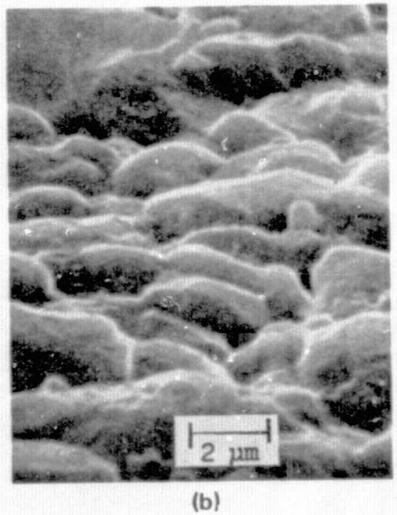

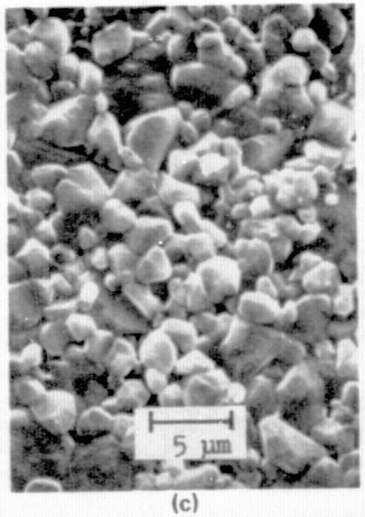

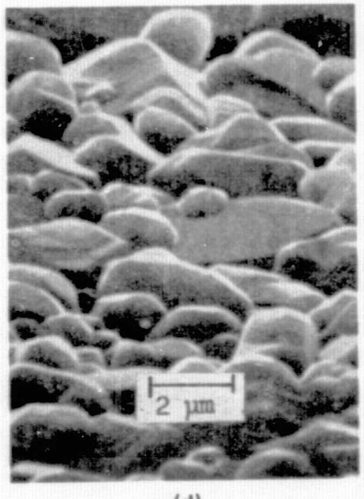

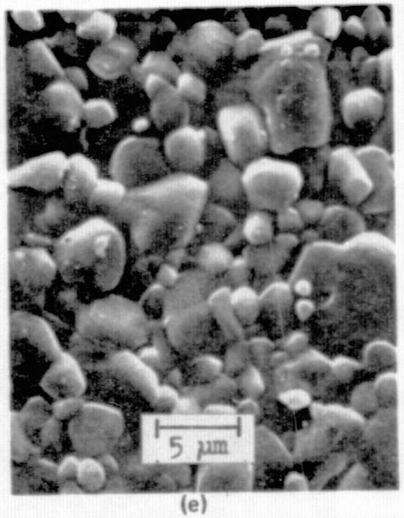

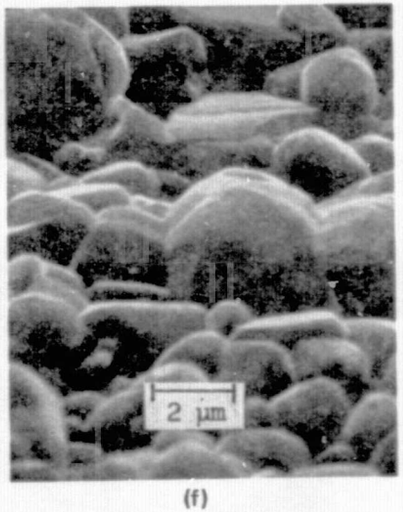

Figure 2-17. SEM Photographs of Surfaces of ASM838 Alumina (3M Co.) in As-manufactured and Refired Conditions. a) As-manufactured, Viewed Normal to Surface; b) As-manufactured, Viewed at 30 deg with Surface; c) Refired, Viewed Normal to Surface of First Side; d) Refired, Viewed at 30 deg with Surface of First Side; e) Refired, Viewed Normal to Surface of Second Side; f) Refired, Viewed at 30 deg with Surface of Second Side.

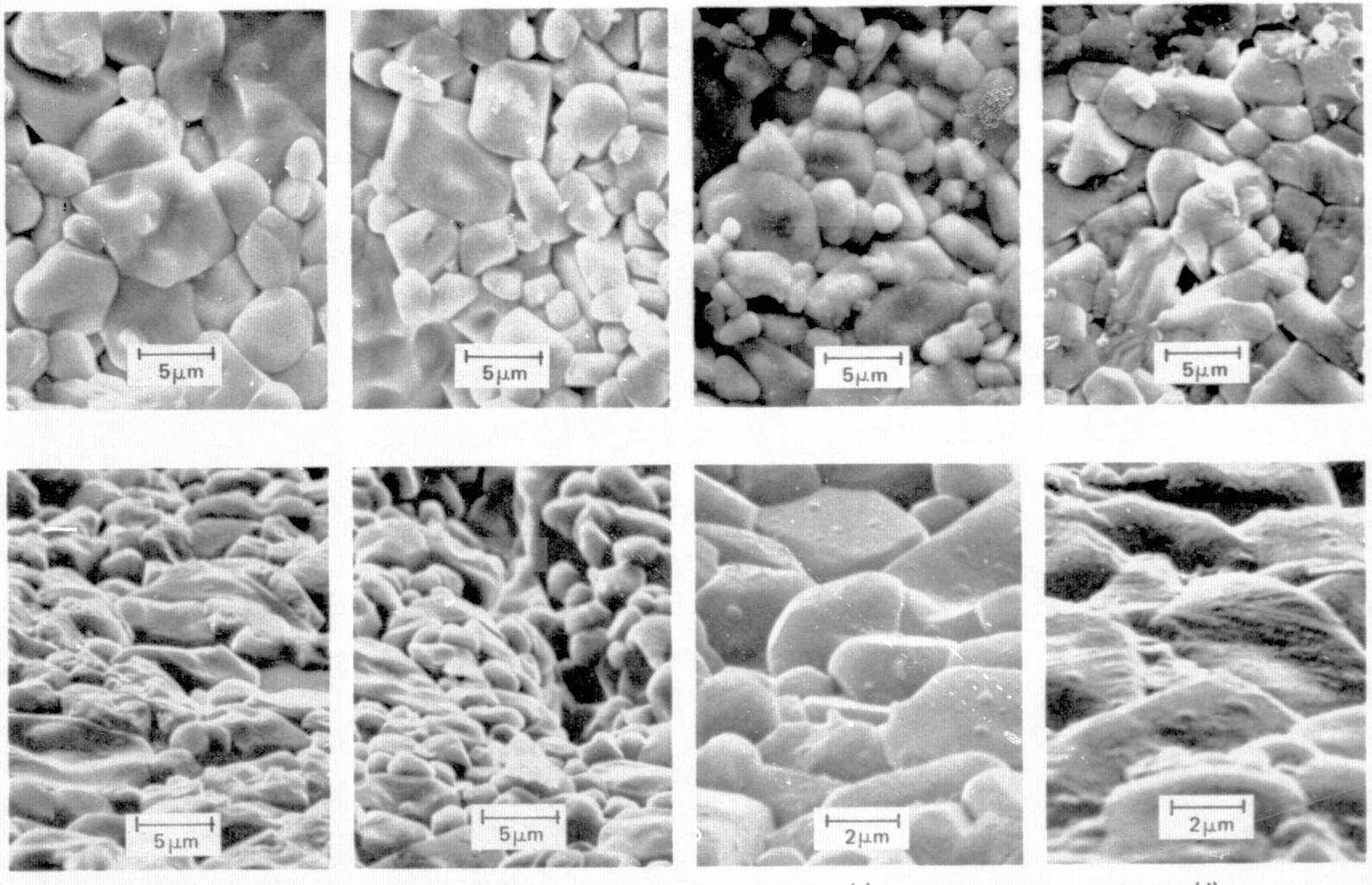

Figure 2-18. SEM Photographs of Commercial Grades of Ceramic Substrates. (a) ASM614 Alumina (3M): Top-View at Normal Incidence, Bottom-View at 30 deg to Surface; (b) S697 Alumina (Saxonburg): Top-View at Normal Incidence, Bottom-View at 30 deg to Surface; (c) A476 Alumina (Kyocera - 96%): Top-View at Normal Incidence, Bottom-View at 30 deg to Surface; (d) ASM832 Mullite (3M): Top-View at Normal incidence, Bottom-View at 30 deg to Surface.

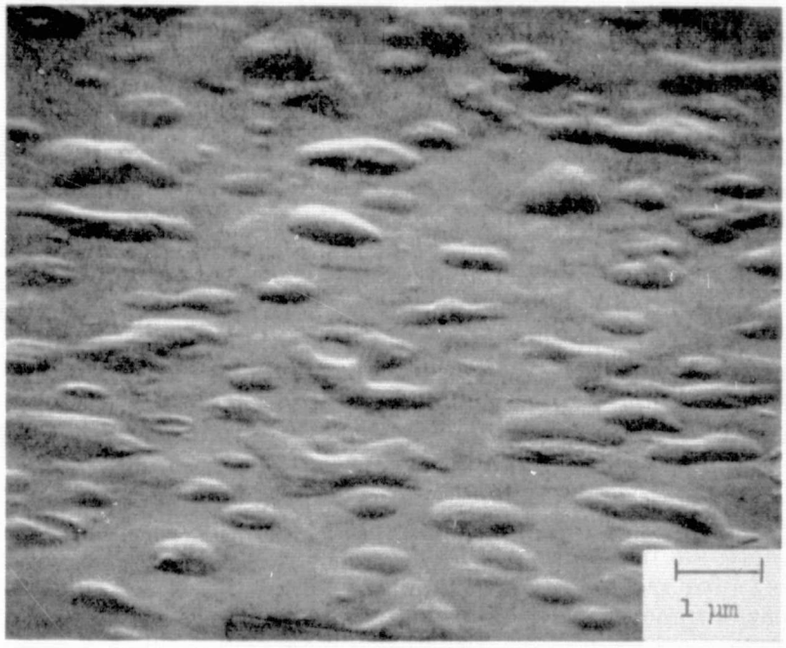

Figure 2-19. SEM Photograph of Surface of Corning Code 9606 Glass-ceramic, Showing Apparent Inclusions on/in Surface

groups of substrates from among those listed were selected for mechanical polishing. The first materials so processed were the aluminas Superstrate (MRC) and Vistal (Coors).

The purpose of this polishing procedure is twofold. First, polishing generates smooth surfaces on the substrates and thus results in smoother film surfaces, and yet retains benefits to the Si sheet nucleation and growth process that accrue from the presence of the substrate crystal grains that intersect the mechanically generated surface.

Second, simultaneous Si CVD growth experiments on polished and as-fired polycrystalline substrates are especially important. The actual growth facets of an as-fired polycrystalline substrate are not--on the average--in the same crystallographic orientations as those that are delineated in X-ray analyses for preferred orientation in the substrate materials. This is because the crystal planes so identified are referenced to the nominal surface plane of the substrate wafer as it is mounted for X-ray analysis; that is, the planes identified as preferred orientations in the substrate are parallel to the nominal wafer surface, but the growth facets are nearly all at appreciable angles to this plane. Thus, to establish correlations between substrate preferred orientations and the observed Si film habit it is necessary to grow Si on a polished surface coinciding with the nominal substrate surface.

In addition to the two aluminas mentioned above, other aluminas of different (lower) purity, zircon, mullite, and cordierite have been polished for subsequent Si

film growth experiments. Results of the sheet growth experiments on polished substrates help in the attempt to determine a reasonable balance between the increased cost of preparing substrates by this additional processing step and the expected improvement in the surface characteristics (and perhaps the internal structure) of the resulting polycrystalline Si films.

In most instances lapping has been done with Microgrit (12 μm alumina) and the polishing has been done with Syton (Monsanto). A few of the substrates were not lapped first--only polished with Syton--but the removal rate was very low. In general, approximately a 1-mil thickness of material is removed in the Syton polishing step.

One batch of Vistal substrates, including several samples of each of the four different firing histories, was lapped for 10 hr with a slurry of 5 μm SiC particles to produce a flat fine-lapped finish. Prominent irregular crevices intersecting the lapped surfaces on the four samples clearly delineated the range of grain sizes that resulted from the consecutive firings, even without any chemical etching. Surface photomicrographs of each of the four lapped surfaces are shown in Figure 2-20.

A comparison of profilometer traces for Vistal substrates in the as-fired, lapped, and polished conditions is shown in Figure 2-21 for material with one and two firings and in Figure 2-22 for material with three and four firings. In each case the horizontal scale is such that one major chart division corresponds to a distance of 0.2 mm along the sample surface. These figures show the expected improvement in surface smoothness resulting from lapping and polishing, but also clearly show the deep crevices between neighboring crystal grains in the lapped condition and the shallow but finite steps between grains in the polished condition.

The surfaces of polished Vistal substrates of each of the four groups are shown in the optical photomicrographs of Figure 2-23, made with the Nomarski interference-contrast objective on the microscope. These photographs show in strong relief the individual crystal grains in each of the four groups and illustrate clearly a progression in grain size from Vistal 1 to Vistal 4 (Figure 2-23a to 2-23d). The polished Vistal 4 substrate shows the largest average grain size and more uniform distribution of large grains.

Additional characteristics of the Vistal substrates are shown in the optical photomicrographs in Figures 2-24 and 2-25. The former shows the surface of a polished Vistal 2 (two consecutive firings) and the latter a polished Vistal 3 (three consecutive firings); in each case exactly the same region of the surface is shown at the same magnification but with three different optical conditions. Some transmitted illumination through the substrate was used in order to show interior features. In (a) of each figure the substrate surface is in focus, with the Nomarski interference-contrast objective set for maximum visibility of surface features. In (b) of each figure the color-contrast lever of the objective is shifted to use a different wavelength region of the illumination and bring out subsurface features, although the initial focus was not changed. Finally, in (c) of each figure the camera was focused on a plane just below the sample surface to delineate additional features. The procedure clearly illustrates the incidence of various voids and inclusions in this polycrystalline alumina material. The other two Vistal groups exhibited similar characteristics.

During the lapping stage it was noted that Vistal samples from the third and fourth groups appeared to have similar grain sizes, and in some regions the grains in

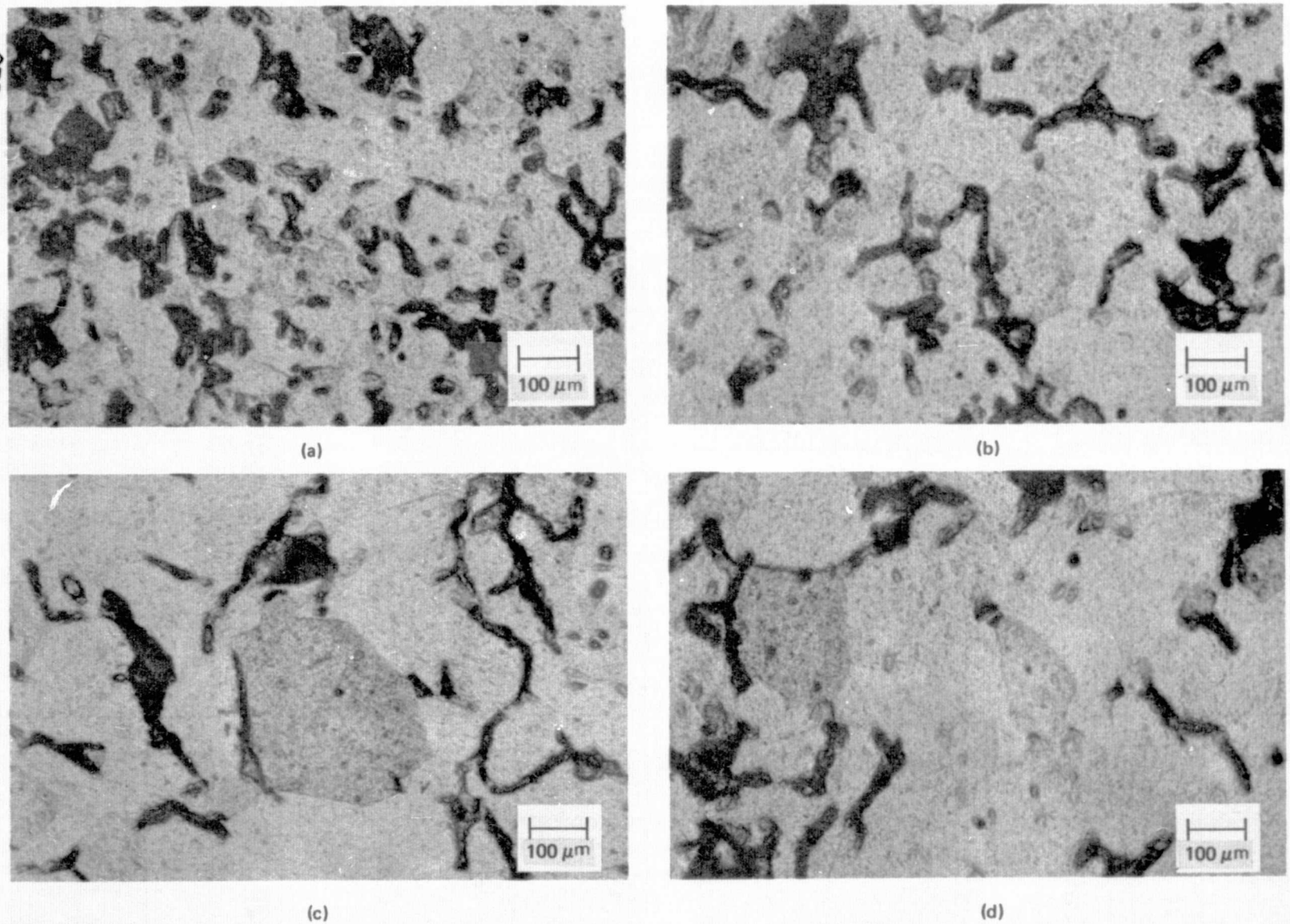

Figure 2-20. Surfaces of Four Vistal (Coors) Polycrystalline Alumina Substrates after Successive Firings Above 1800°C for 6 Hr.
(a) One, (b) Two, (c) Three, (d) Four Firings

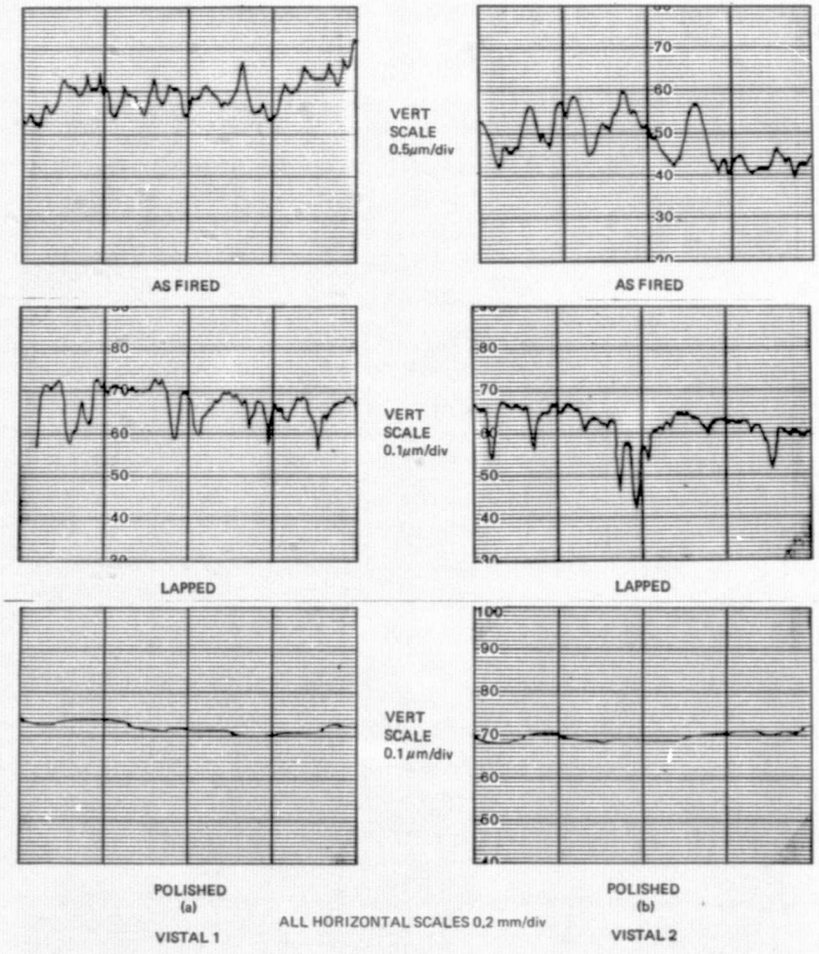

Figure 2-21. Dektak Profilometer Traces of Surfaces of Vistal Polycrystalline Alumina Substrates at Three Stages of Preparation. (a) Vistal 1 (one firing at >1800°C for 6 hr); (b) Vistal 2 (two consecutive firings).

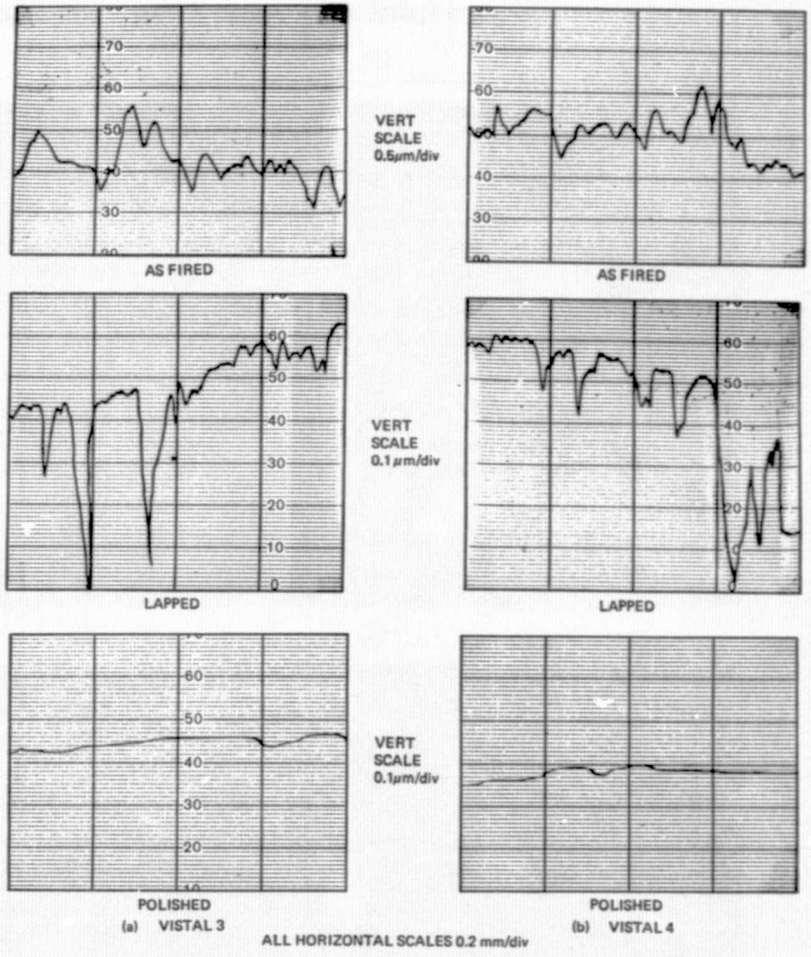

Figure 2-22. Dektak Profilometer Traces of Surfaces of Vistal Polycrystalline Alumina Substrates at Three Stages of Preparation. (a) Vistal 3 (three consecutive firings at >1800°C for 6 hr); (b) Vistal 4 (four consecutive firings).

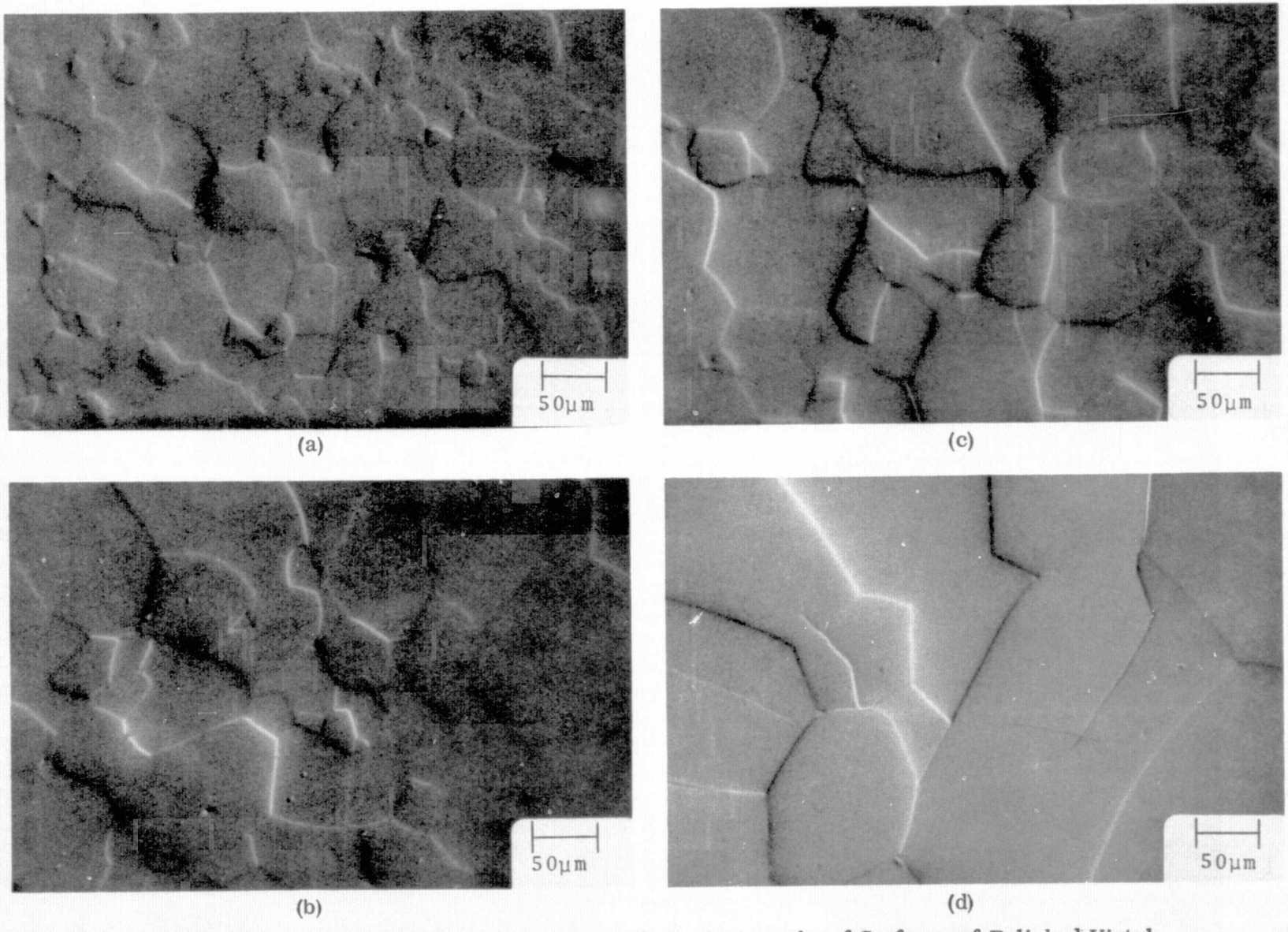

Figure 2-23. Nomarski Interference-contrast Photomicrographs of Surfaces of Polished Vistal Alumina Substrates of Four Different Firing Histories. (a) Vistal 1 (one firing at >1800°C for 6 hr); (b) Vistal 2 (two consecutive firings); (c) Vistal 3 (three consecutive firings); (d) Vistal 4 (four consecutive firings). (All photographs at normal incidence.)

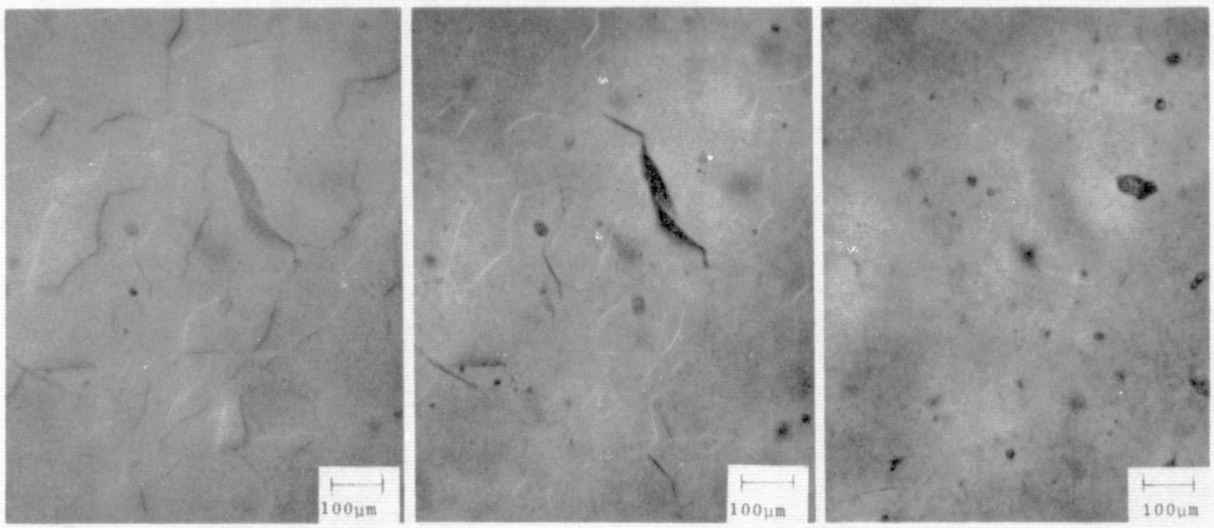

Figure 2-24. Nomarski Interference-contrast Photomicrographs of Surface of Same Region of Vistal 2 (two consecutive firings at >1800°C for 6 hr) Polycrystalline Alumina Substrate under Different Optical Conditions. (a) Surface Focus, Optimized Color Contrast; (b) Surface Focus, Changed Wavelength; (c) Subsurface Focus.

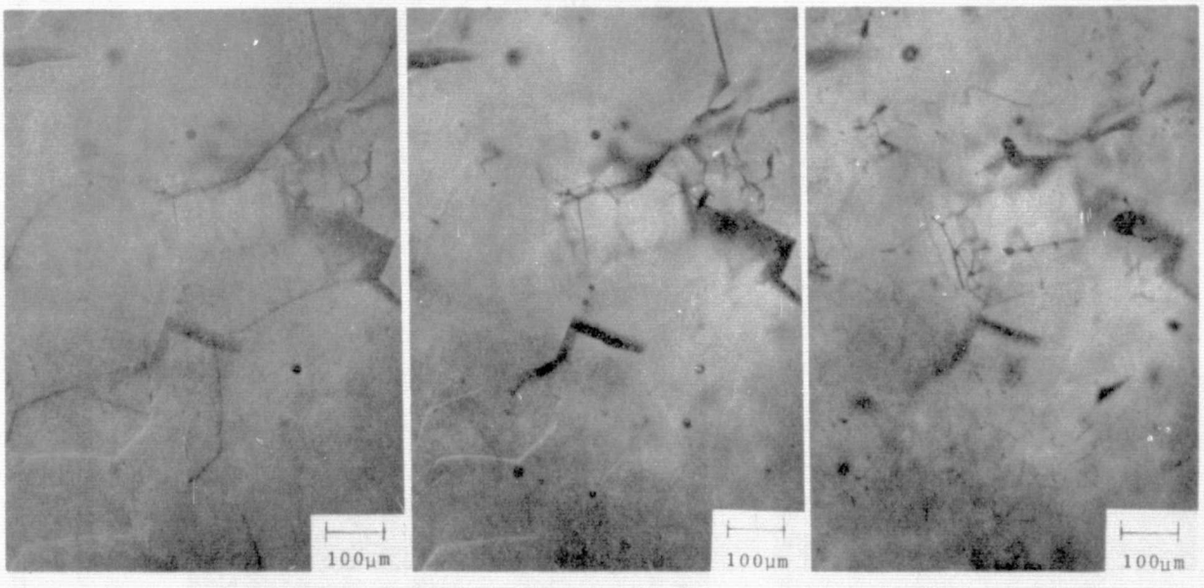

Figure 2-25. Nomarski Interference-contrast Photomicrographs of Surface of Same Region of Vistal 3 (three consecutive firings at >1800°C for 6 hr) Polycrystalline Alumina Substrate under Different Optical Conditions. (a) Surface Focus, Optimized Color Contrast; (b) Surface Focus, Changed Wavelength; (c) Subsurface Focus.

the third group appeared larger, as noted earlier. When polishing was completed, however, the photomicrographs of the surfaces of the polished substrates (Figure 2-23) clearly delineated the apparent grain boundaries at the surface. At this stage, the sample of the fourth group appeared to have significantly larger individual grains than that of the third group, as mentioned in Para 2.2.5. The average apparent grain size observed in the surfaces of the four Vistals in the polished condition, measured by SEM examination, is given in Table 2-6.

Table 2-6. Average Apparent Grain Size of Several Polished Polycrystalline Alumina Substrate Materials as Measured on Sample Surface by SEM Examination

Substrate Material	Ave Grain Size at Surface of Polished Material (μm)
Vistal 1 (Coors)	35
Vistal 2 (Coors)	74
Vistal 3 (Coors)	70
Vistal 4 (Coors)	>120
Superstrate (MRC)	~1.5

The surface of MRC Superstrate, an alumina of 99.6 percent purity that has been used in numerous Si CVD experiments to date, is shown in both the as-fired and the polished condition in Figure 2-26. Both surfaces are quite different from the corresponding surfaces on any of the Vistal aluminas. First, the apparent average grain size is considerably smaller than that of Vistal 1 (the smallest-grained of the Vistal series), averaging about 1 μm. Second, the Superstrate exhibits numerous grain boundary voids that show up especially in the polished surface (Figure 2-26b). Apart from the grain size itself, the presence of such voids makes it difficult to achieve adequate cleaning (and drying) of these substrates prior to use in deposition experiments. The average value for grain size in the polished material also is given in Table 2-6.

A total of 78 samples representing 16 different polycrystalline materials — various purity aluminas (as-fired and refired), mullite, zircon, and cordierite — was polished during the third quarter for use as substrates for Si growth. Only in the case of the highest purity aluminas (≥99.5 percent) was pitting not observed at relatively low optical magnifications in the microscope. SEM examination of the surfaces of those materials is being carried out on representative pieces of most of the samples, for reference prior to investigating the effects of different surface treatments on the nature and behavior of the substrate surface in the CVD environment.

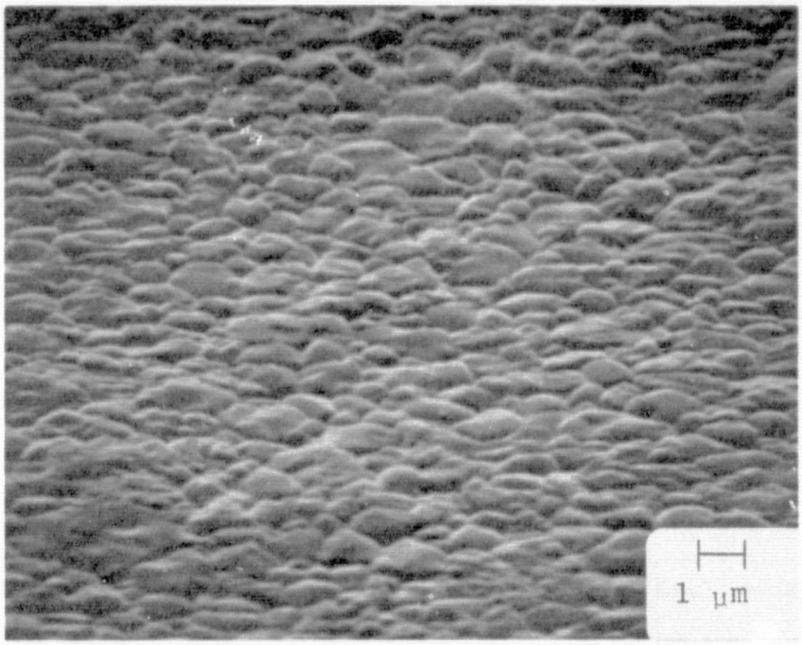

(a)

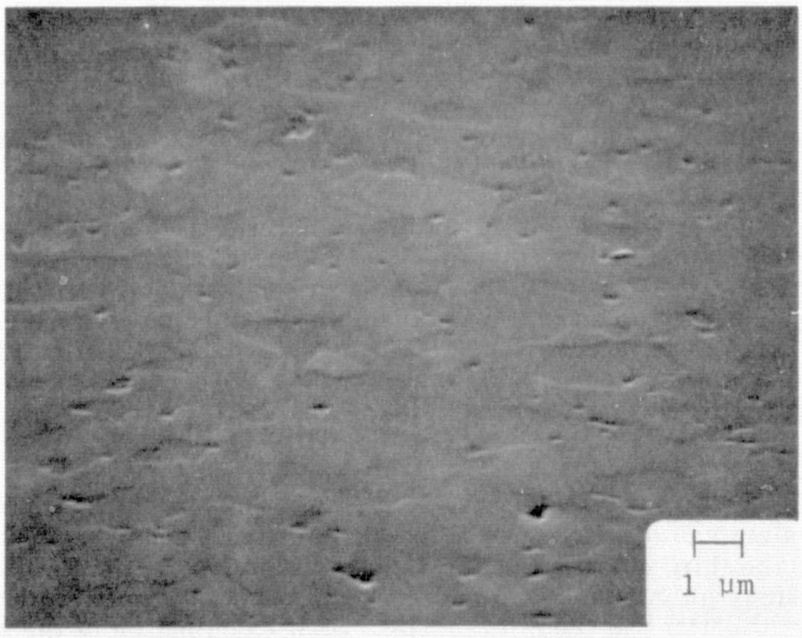

(b)

Figure 2-26. SEM Photographs of Surface of MRC Superstrate Polycrystalline Alumina Substrate, Viewed at 30 deg Angle with Sample Surface. (a) As-fired; (b) Polished.

2.2.7 Determination of Substrate Material Compatibility with Si CVD Growth Process

Initial exploratory deposition experiments with Corning Code 7059 barium aluminoborosilicate glass were done early in the first quarter, prior to the first trip to visit potential suppliers, and at that time deposition parameters were arbitrarily chosen. At a SiH_4 flow rate of 25 ccpm, a He flow of 6ℓpm, and a temperature of 700°C, a highly reflective film of Si was grown for 25 min on this glass, but considerable bowing of the film-substrate composite in a concave-upward direction occurred, as was shown in Figure 2-7, indicative of appreciable tensile stress in the film.

Based on the relative magnitudes of the TEC's for Si and 7059 glass (see Figure 2-5), bowing in the opposite direction would be expected if differential thermal contraction alone were responsible. However, the composite was observed to bow in the same direction during the growth process, prior to cooling. Thus, other causes directly related to the physical and/or chemical stability of the glass at temperatures around 700°C are probably involved.

A second similar experiment showed that the 7059 glass does not distort detectably prior to Si film deposition at 700°C. No bowing was observed in He, for example, at 600, 650, or 700°C after 30 minutes at each temperature, but concave-upward bowing was obvious after only a few minutes of Si growth at 700°C. The distortion therefore resulted from reaction of the glass surface with the SiH_4 or its products of decomposition. This incompatibility probably rules out Code 7059 glass as a simple, non-composite low-cost substrate for Si growth by SiH_4 pyrolysis.

The Corning Code 1723 aluminosilicate glass, which was specially prepared in plate form (it is normally available only in blown-ware, tubing, and rod form), was also evaluated early in the program for its compatibility with Si grown from SiH_4, in both H_2 and He atmospheres. Si grown in a H_2 carrier at 850°C (~60 deg C below the softening point) resulted in a film with "worm-like" structure, indicating probable local melting or chemical reaction of the glass, and some obvious contamination of the companion sapphire substrate. Bowing was in evidence in a convex-upward direction following deposition, prior to cooling to room temperature, for the 17-μm-thick film on the 750-μm-thick substrate. Due to differences in TEC for the two materials this bowing might be expected to increase, producing compressive stresses in the Si.

With this same glass at a growth temperature of 850°C in a He atmosphere, a Si film ~26 μm thick was produced which consisted of a mixture of large and small grains; the Si film grown simultaneously on sapphire gave evidence of having been contaminated by the neighboring glass substrate.

Si growth in He at ~620°C, which is below the strain point of the glass (665°C), produced a very reflective film on the glass, but the film grown simultaneously on the sapphire monitor wafer peeled during handling, again suggesting contamination of the Si and/or sapphire by volatile products from the glass. At high magnification, bubbles of various sizes were observed in the Si film and/or at the film-glass interface, by both optical microscope and SEM examination (Figure 2-27). These results indicate that this glass is also probably not satisfactory as a substrate for the growth of Si sheet by SiH_4 pyrolysis.

A preliminary evaluation of ASM805 as a substrate for Si CVD was made early in the program by depositing Si simultaneously on this material and on single-crystal

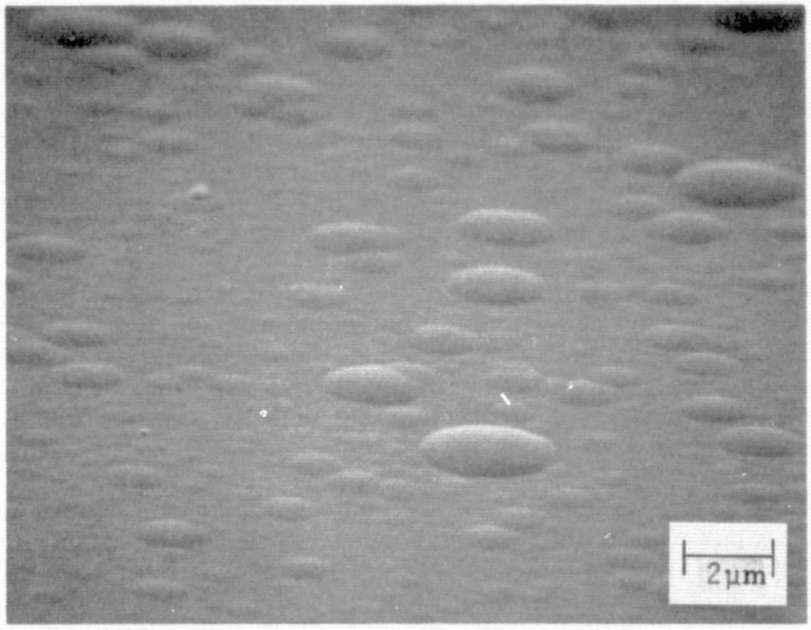

Figure 2-27. Bubbles Formed at Interface of CVD Si Film Grown on Corning Code 1723 Glass Substrate at ~650°C in He

sapphire at ~1025°C by SiH_4 pyrolysis in H_2. The evidence of some crystal faceting in the film on the alumina and the lack of any indication of gross contamination of the sapphire or its epitaxial Si film by the adjacent alumina substrate suggested further work with the fired alumina materials should be undertaken. As indicated earlier, the aluminas have become the most extensively used substrates in the program, so far.

Later in the program, during the second quarter, two Si CVD experiments using established procedures were performed with ASM805 alumina substrates to compare as-fired with refired material (see Figure 2-13) supplied by the 3M Company. The first films were grown on substrates which were cleaned only with organic solvents and H_2O rinses; the films were covered with growth whiskers, consistent with the presence of some surface contamination. Another film grown on a refired substrate which was acid-cleaned was found to be essentially free of whiskers, but the growth on the sapphire companion wafer appeared partially contaminated, indicating either the purity of the refired alumina was adversely affected by the firing process or the technique used in preparing the refired material for deposition needed improvement.

It was subsequently determined that there may have been an impurity introduced into the alumina during the refiring process by the manufacturer. The substrates were stacked for refining in a furnace with a support and cover of lower purity than the ASM805, and contamination could have occurred from the support and/or the cover. Although the refired ASM805 appeared to contain larger grain sizes (Figure 2-13), the average appearance of the Si overgrowth on the refired surface resembled that of films grown on the as-fired ASM805 material. The matter of the compatibility of refired aluminas from the 3M Company with the Si CVD growth process still is not fully

resolved. Additional sets of substrates with various firing histories have been obtained, and these are being evaluated in this regard.

Several additional candidate substrate materials have been evaluated in preliminary CVD Si growth experiments, both early in the program and recently. Relatively thin samples of zircon ($ZrO_2 \cdot SiO_2$) were received from Kyocera (Z360, Table 2-4) and the 3M Company (ASM475, Table 2-4) late in the second quarter. A preliminary evaluation of these materials was accomplished in a Si CVD experiment employing parameters known to be satisfactory for Si deposition on polycrystalline aluminas previously tested. The substrates were solvent - and acid-cleaned and subjected to a pre-deposition etch in H_2 at 1250°C in the reactor before Si growth by SiH_4 pyrolysis at ~1025°C. Whisker-like growth was obtained, as shown in the SEM photograph of Figure 2-28, indicating zircon is not as hardy as alumina in the Si CVD environment when H_2 is used. Si film deposition in He at 1025°C produced better results on these substrates, but still not good planar growth, as shown in Figure 2-29.

Mullite (see Table 2-4) was found to fare somewhat better as a substrate in a He atmosphere than in H_2 for growth of Si at ~1030°C, even through the substrate material appeared to be quite porous. The resulting Si crystallites were more regular in shape than those formed on zircon but still were non-uniform, and appeared as cucumber-like protuberances when viewed at an actuate angle to the surface, as shown in the SEM photographs in Figure 2-30.

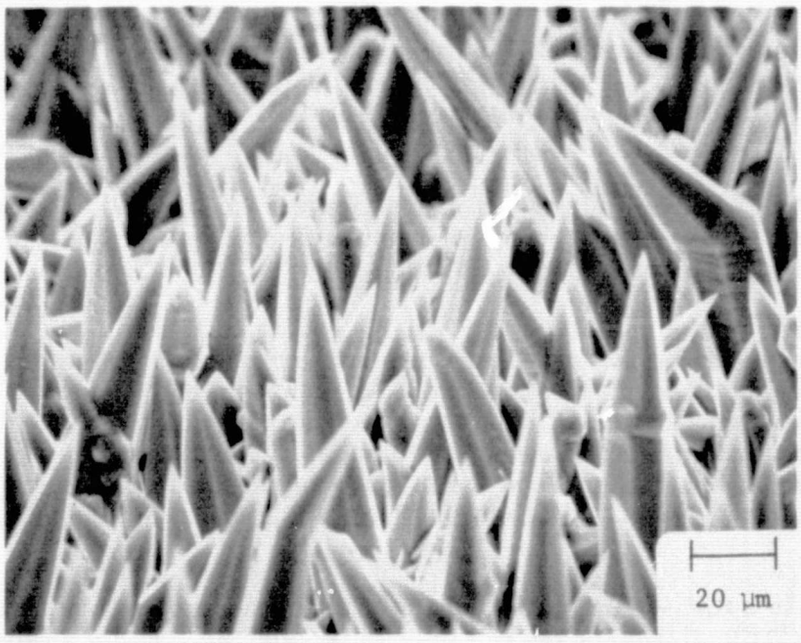

Figure 2-28. SEM Photograph of Whisker-like Deposit of Si on Zircon. Growth by SiH_4 Pyrolysis at 1025°C in H_2 Atmosphere.

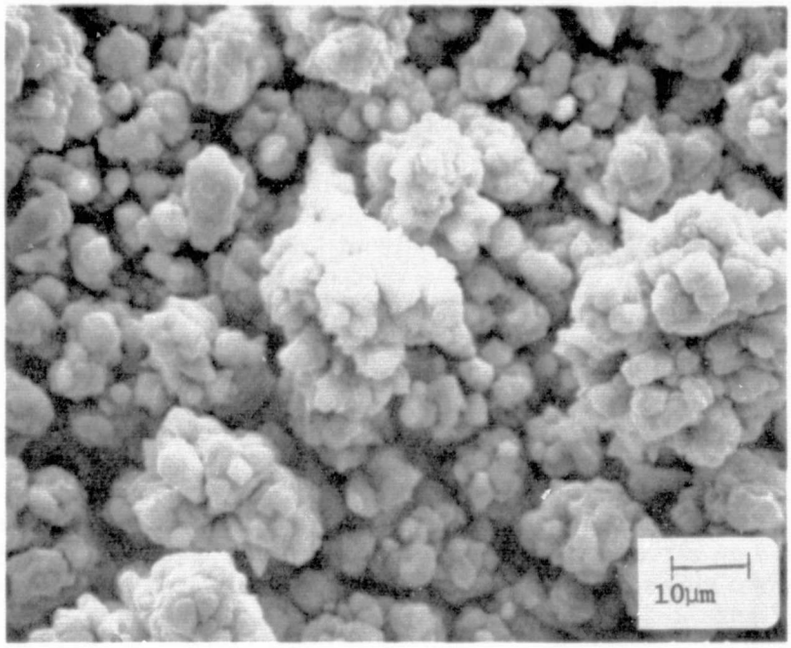

Figure 2-29. SEM Photograph at Normal Incidence of Surface of Si Film Grown on Zircon by SiH_4 Pyrolysis at 1025°C in He

These results tend to indicate that mullite is not well suited to the CVD process, primarily because of its porosity in the form available to date. There was also evidence of some discoloration in the mullite as a result of the CVD environment, probably associated with impurities in the material.

Exploratory Si CVD compatibility experiments were carried out during the second quarter with three of the glasses listed in Table 2-2: (1) Corning Code 1715, (2) Owens-Illinois GS211, and (3) Owens-Illinois GS213.

All three substrates failed the SiH_4-in-H_2 growth tests at ~850°C, evidenced by whisker-type growth on the substrate surfaces and/or major contamination of the Si film grown on the companion sapphire substrate. As an example, Figure 2-31 is an SEM photograph of the surface of the Si deposit grown on glass GS211 at ~850°C in H_2 (4 ℓpm flow rate), with a SiH_4 flow rate of 25 ccpm. In addition to the obviously defective deposit on the glass, the Si growth on the neighboring sapphire was seriously damaged by some contaminant, presumably resulting from the glass reaction with the CVD environment.

However, in a SiH_4-in-He environment at about the same temperature the Si films deposited on the three glasses appeared to be quite normal; contamination of the companion sapphire substrate did not appear to occur in any of the three cases. Consequently, additional Si deposition experiments with these substrates were carried out; results are discussed under Task 5 (Para 2.5).

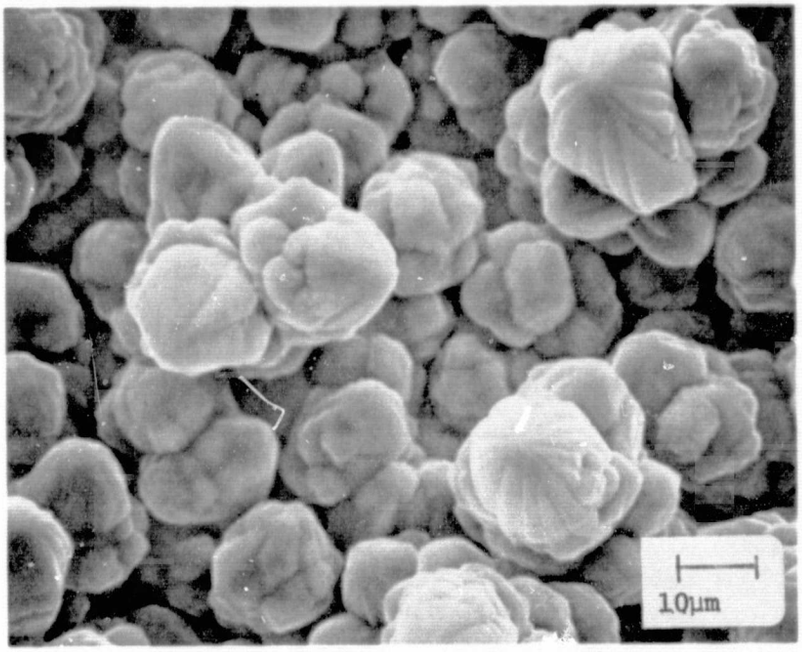

(a)

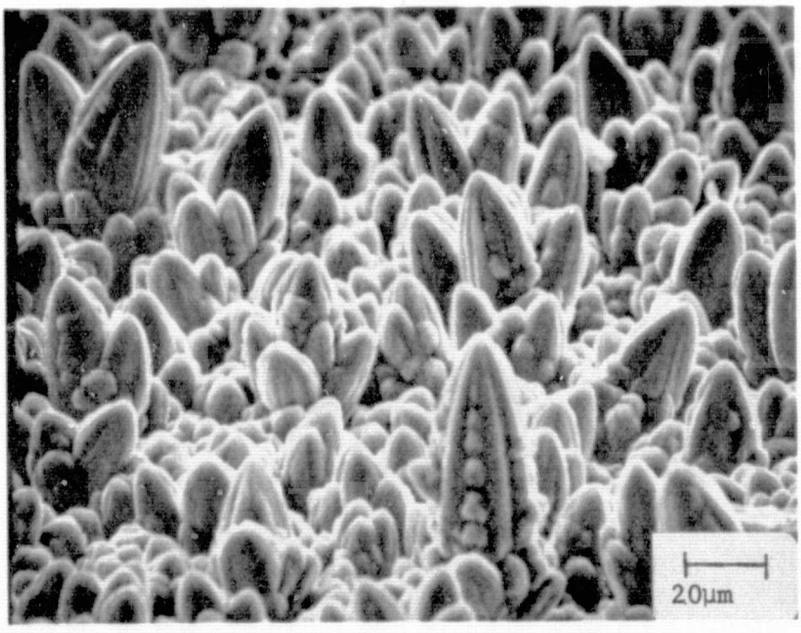

(b)

Figure 2-30. SEM Photographs of CVD Si Grown on Mullite Substrate by SiH_4 Pyrolysis in He at ~1030°C. a) Viewed at Normal Incidence, b) at 30 deg with Sample Surface.

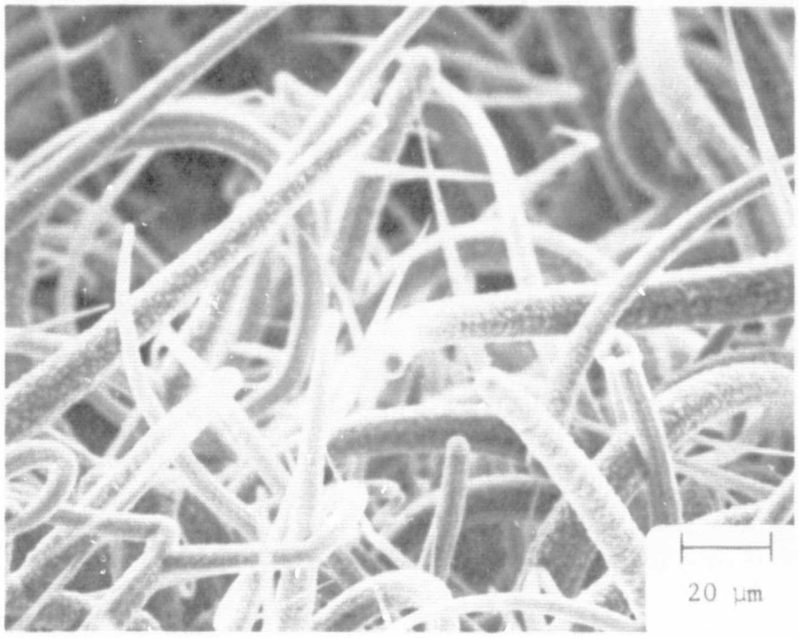

Figure 2-31. SEM Photograph of CVD Si Deposit on O-I Glass GS211 at ~850°C in H_2 Atmosphere

An exploratory Si deposition experiment was also done in the second quarter with a glazed nickel-steel supplied by Chi-Vit Corp. (see Table 2-2). The coating is an alkaline-earth aluminosilicate glass. In order to avoid contamination of the SiC-covered carbon pedestal used in the experiments with the aluminas, a pedestal of old vintage was used in direct contact with the steel base. During the heating of the pedestal and substrate, however, a part of the SiC layer separated from the carbon pedestal and sprayed the substrate with debris. Rather than abort the experiment, a Si film was grown on the glaze at ~850°C in a He atmosphere, in spite of the contamination. The film was found to be adherent to the glaze. A second experiment was recently done in which the Si film was deposited in a He atmosphere at 860°C. There was considerable wrinkling of the film near the edge of the substrate, and the composite was bowed, with the film in compression, at room temperature. During storage for several days after the deposition the highly-stressed film separated completely from the substrate and shattered into numerous small pieces.

A proprietary glass prepared by the Atomics International Division of Rockwell as a glaze on ASM805 polycrystalline alumina was tested as a substrate for Si deposition in He at ~800°C. The resulting film-substrate composite survived the deposition process and appeared satisfactory at the conclusion of the deposition. However, upon standing following removal from the reactor this film also failed under the stresses present and separated completely from the substrate, shattering into a multitude of small flakes.

Some initial screening experiments to evaluate the compatibility of Corning Code 9606 glass-ceramic, received during the third quarter, with the Si CVD environment

were conducted recently. A deposit grown in H_2 at 860°C was whisker-like (Figure 2-32), similar to the Si growth on zircon in H_2 at 1025°C. In He, the growth displayed some crystallographic order but was marked by flower-like rosette platelets emanating from the film surface, as shown in Figure 2-33. Because of the surface problem found in this substrate material (see Section 2.2.5 and Figure 2-19) further experiments have been delayed temporarily; the nonuniformity of the film shown in Figure 2-33 may be associated with this condition in some manner.

Finally, some experiments were undertaken late in the second quarter to examine the stability in the CVD process environment and the effects on the Si film properties of a metal substrate material. Among other things, such a substrate – produced on some other supporting material by a suitable deposition technique – would be of great value in achieving adequate ohmic contact to the back side of a thin-film solar cell structure. Because of its almost negligible solubility in Si at the temperatures used for Si CVD on glass substrates and its ready availability, Ti was used in the first experiments. Layers of several different thicknesses were deposited by sputtering onto Corning Code 7059 glass substrates in a separate apparatus. Si films were then grown on the Ti surfaces at ~850°C in He; Ti films ~1500Å thick were used in the first experiments. The composite samples were bowed after deposition, with the Si film in compression. It is interesting that this distortion is the opposite of that observed when Si was grown directly on 7059 glass (see Figure 2-7 and earlier in this section), indicating that the Ti layer protected the glass from the reaction in the CVD environment that produced the concave-upward bowing of the bare substrate. Thus, a metal-7059 composite may be compatible with the Si CVD process, particularly if a more suitable metal - from the standpoint of influence on the carrier lifetimes - is used.

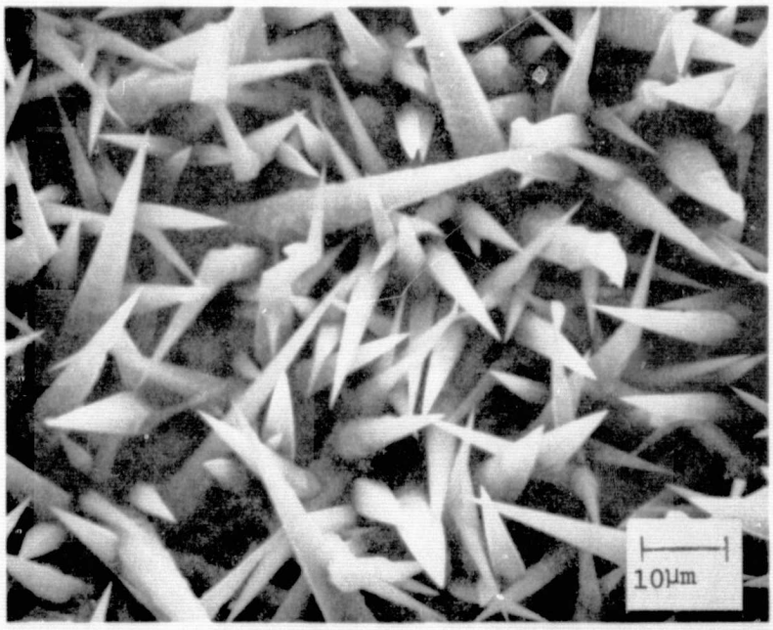

Figure 2-32. SEM Photograph of CVD Si Film Grown by SiH_4 Pyrolysis at ~860° C in H_2 on Substrate of Corning Code 9606 Glass-ceramic. (Viewed at normal incidence.)

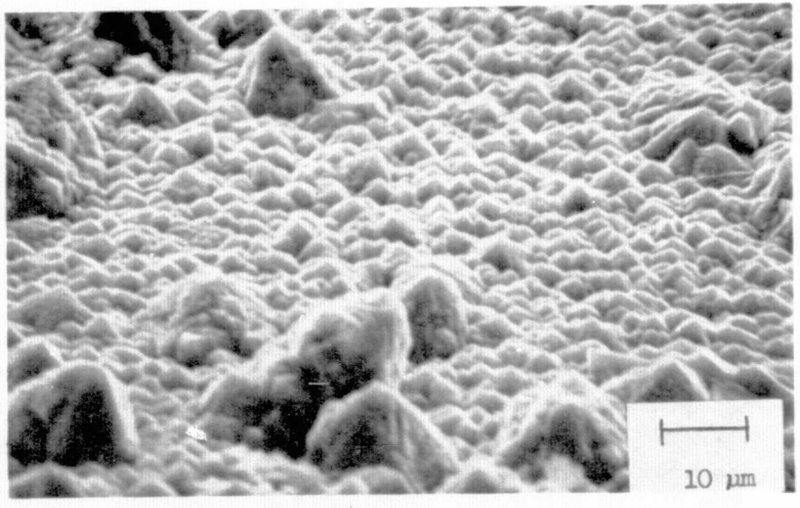

(a)

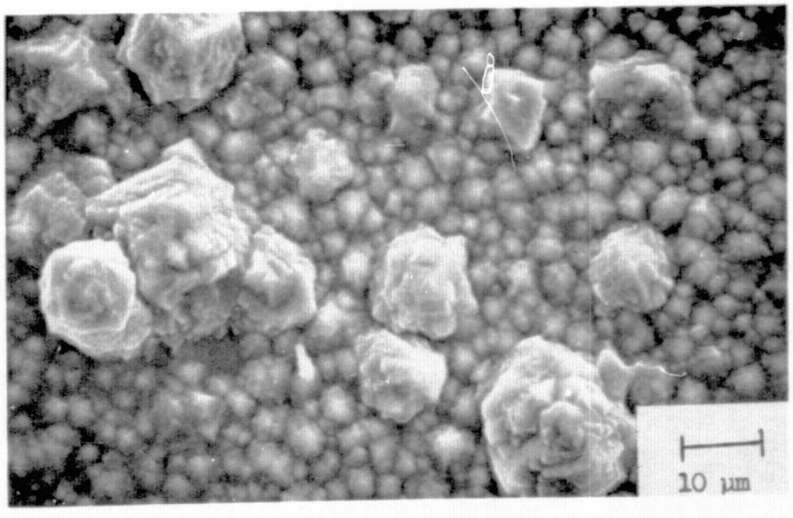

(b)

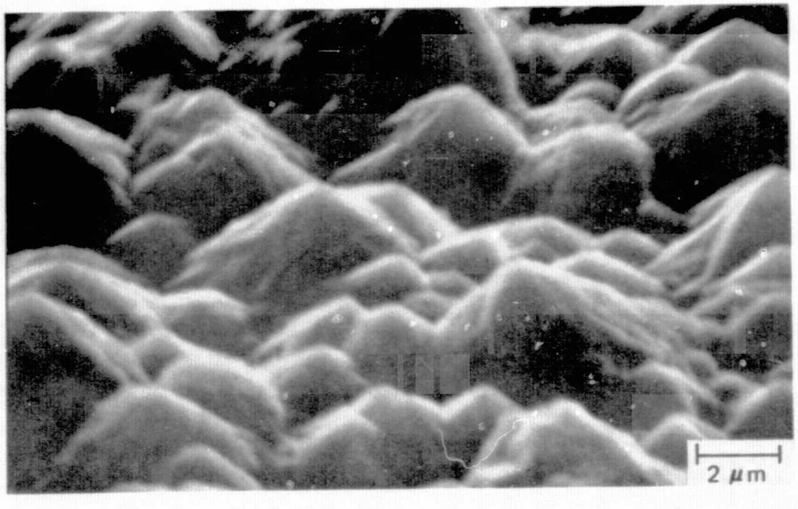

(c)

Figure 2-33. SEM Photographs of CVD Si Film Grown by SiH_4 Pyrolysis at ~840°C in He on Substrate of Corning Code 9606 Glass-ceramic.
a) and c) Viewed at 30 deg with Surface, b) Normal Incidence.

2.2.8 Substrate Costs and Related Considerations

The probable cost of a candidate substrate material produced and used in large quantities in the 1985 time frame is an important factor in determining the ultimate feasibility of that material as the support for the CVD Si sheet used in terrestrial solar arrays.

Specific 1985 cost projections for the substrate materials that have been used in the program have not been undertaken. It has even been difficult to obtain meaningful cost estimates in the present-day market for some of the candidate materials since they have been specially produced in limited experimental quantities, and often in non-standard configuration for testing in this program. However, several suppliers have provided cost figures for some of the polycrystalline aluminas of interest.

A partial compilation of these data for selected candidate aluminas is given in Table 2-7. These costs are current (or recent) and are based on quotations from the identified vendors. In most cases there is cost information for various quantities of the particular unit-size substrate, although the costs are given on a per-unit-area basis. It should be emphasized that these are not projected future costs but merely today's costs for various quantities of the materials listed. The data in this table will be augmented in later reports as additional information is made available by various vendors. For comparison purposes, costs for two different sizes of Corning Code 7059 barium-aluminoborosilicate glass are included, in each case for a single quantity range.

The table does not include such substrate materials as mullite, zircon, cordierite, or the glasses from Corning and Owens-Illinois that are being evaluated in this program. It has been difficult to obtain prices for volume purchases for mullite, zircon, and certain cordierites in the substrate configuration; further, these materials do not appear to be readily available today in the purity, density, and homogeneity that is required in a practical substrate for semiconductor CVD growth. However, these materials are believed to be potentially lower in cost than the aluminas. In addition, based on TEC values alone, they would be preferred to the aluminas for Si growth. For this reason they have been characterized as to their chemical stability in the CVD growth environment even though they are deficient in quality in their currently available forms.

Similarly, the costs associated with the most promising glasses have also been difficult to determine. The glasses with high strain points have either been prepared specially for this program or have been reprocessed from a commercial form, such as a tube or rod, into a flat substrate by non-automated techniques. Corning personnel have indicated that any glass (or glass-ceramic) found suitable for large-area solar array use can probably be produced in large volumes at costs that will meet the 1985 LCSSAP goals.

Corning Code 7059 glass, although found not to be useful in this program, has been included in Table 2-7 because it represents a high-quality glass that has been mass produced and thus provides a cost comparison. Based on the sizes and quantities shown, Corning 7059 and the 96 percent aluminas are in about the same price range. Whereas the aluminas permit film growth at high temperatures, the glasses offer

Table 2-7. Current Costs of Selected Polycrystalline Alumina Substrate Materials

SUBSTRATE IDENTIFICATION		PURITY (PERCENT)	SUBSTRATE UNIT SIZE† (IN INCHES)	APPROXIMATE COST IN $/IN^2 FOR QUANTITIES INDICATED				
				1000	10,000	50,000	100,000	250,000
Coors	ADS96F	96	2x2	0.0875	0.053	–	0.044	–
	ADS995	99.5	3-3/4x4-1/2	0.11	0.095	–	0.080	–
	Vistal (commercial)	~99.9	1/2x1/2	0.72	–	0.58	0.50	–
Magneco		96	2x2	0.062	0.052	–	0.040	0.039
			3x3	0.044	0.035	0.027	0.027	0.026
3M	ASM614	96	2x2	0.078	0.065	0.057	0.054	0.051
			3-3/4x4-1/2	0.040	0.080	0.065	0.059	0.055
	ASM772	99.5	2x2	0.117	0.098	0.085	0.080	0.076
			3-3/4x4-1/2	0.134	0.120	0.097	0.088	0.084
	ASM838	99.5	2x2	–	0.105	–	–	–
			3-3/4x4-1/2	0.143	0.127	0.104	0.094	0.089
	ASM805	99.9	2x2	0.625	0.526	0.453	0.428	0.408
			2x3	0.50	–	–	–	–
MRC	HiRel Superstrate	99.6	2x2	0.71	0.60	–	–	–
			3-3/4x4-1/2	0.52	0.48	–	–	–
			4x4	0.68	0.64	–	–	–
	Hybrid Superstrate	99.6	2x2	0.31	0.26	–	–	–
			3-3/4x4-1/2	0.22	0.18	–	–	–
			4x4	0.30	0.28	–	–	–
	Commercial	99.6	2x2	0.095	0.09	–	–	–
			3-3/4x4-1/2	0.10	0.09	–	–	–
			4x4	0.12	0.11	–	–	–
Kyocera	A476	96	2x2	–	0.046	–	–	–
Saxonburg	S697*	97	1x2	0.18	0.054	–	0.047	0.045
			2x2	0.09	0.058	–	0.050	0.048

Table 2-7. Current Costs of Selected Polycrystalline Alumina Substrate Materials (Cont)

SUBSTRATE IDENTIFICATION		PURITY (PERCENT)	SUBSTRATE UNIT SIZE† (IN INCHES)	APPROXIMATE COST IN $/IN^2 FOR QUANTITIES INDICATED				
				1000	10,000	50,000	100,000	250,000
GE	Lucalox	99.9 99.9	1 dia x 1/16 thick (disk) 1 wide x 1-8 lg. x 1/8 thick (rectangular bar)	3.95 ea. 8.35/in (<3 in); 10.45/in (>3 in)				
Insaco	Polished Vistal	99.9	1-3/8 dia x 0.030 thick	11.20 ea (up to 5 pieces)				
Corning	Code 7059 (as drawn)	Barium-aluminoborosilicate glass	12x14 (0.032 thick) 4x4 (0.032 thick)	0.037 – 0.053/in^2 (up to 10,000 pieces) 0.14 – 0.16/in^2 (up to 50,000 pieces)				

† Thickness in all cases is 0.025 in. except where indicated otherwise

* $250 setup charge; no charge if 6-week lead time is given

potentially uniform and flat surfaces for film growth and device processing. Also, the glasses can be expected to be produced in much larger sheets than can the ceramics, at least in terms of the technology now practiced for producing these materials in useful forms.

2.3 TASK 3. EXPERIMENTAL INVESTIGATION OF Si CVD PROCESS PARAMETERS

Si deposition experiments performed in the period prior to the contract start date had indicated that some of the substrates received from varous glass and ceramic manufacturers were reactive in a H_2 atmosphere at the high growth temperatures used. Major contamination was in evidence in films grown on companion pieces of single-crystal sapphire used as control wafers in those experiments. The use of an inert carrier gas such as He was thus regarded as necessary for studying Si growth phenomena on substrate materials reactive to H_2.

During the first quarter a variety of CVD experiments was carried out to establish baseline performance data for the reactor system, including temperature distributions on the sample pe stal, effects of carrier gas flow rate on temperature, effects of carrier gas flow rate on film thickness uniformity in H_2 and in He, and Si film growth rates by SiH_4 pyrolysis as a function of temperature for H_2 and for He.

2.3.1 Effect of Carrier Gas Flow Rate on Pedestal Temperature

The horizontal pedestal used in the CVD reactor system is heated by coupling of the rf field of an external coil (see Figure 2-1). The resulting temperature of the surface of this SiC-covered carbon susceptor (pedestal) is non-uniform, the areas near the periphery being hotter than the central region. The differential is greater at high temperatures (e.g., 1025°C) than at the lower end of the region of interest for this work (~600°C), and the average temperature of the pedestal for a given amount of rf power input is affected by the total gas flow rate used.

Some experiments were carried out early in the first quarter to establish the magnitude of this effect, for both H_2 and He carrier gases. The temperature of the pedestal is measured by means of an infrared radiation thermometer mounted near the chanber, in the arrangement shown schematically in Figure 2-34. Use of the radiation thermometer in position A permits measuring the temperature at any location on the pedestal surface. Corrections for the emittance of the pedestal surface and for losses associated with viewing the hot surface through the fused quartz wall of the reactor chamber are determined experimentally. Normally, during a Si CVD experiment, the pedestal temperature is monitored by viewing the vertical cylindrical surface of the rotating pedestal through one of the spaces between turns of the rf coil (position B in Figure 2-34). The corresponding temperature of the top surface of the pedestal is related to this value by a correction known from previous experimental determinations of corresponding temperatures at both locations.

To measure the effect of gas flow rate on pedestal surface temperatures the temperatures were observed for three different positions on the pedestal and at three different carrier gas flow rates in three different temperature regions, without any Si compound in the chamber and thus no deposition. In each temperature region the rf power input to the pedestal was not changed during the observations at the three flow rates; therefore, the differences in temperature at a given location on the pedestal were caused solely by the changes in gas flow rate.

Results of these measurements in terms of observed temperatures are given in Table 2-8 and Figure 2-35 for both H_2 and He carrier gases, for the 5-cm-diameter pedestal used in the vertical reactor chamber. Inspection of the data for either gas (Table 2-8) for any one of the three locations on the pedestal shows the expected effect

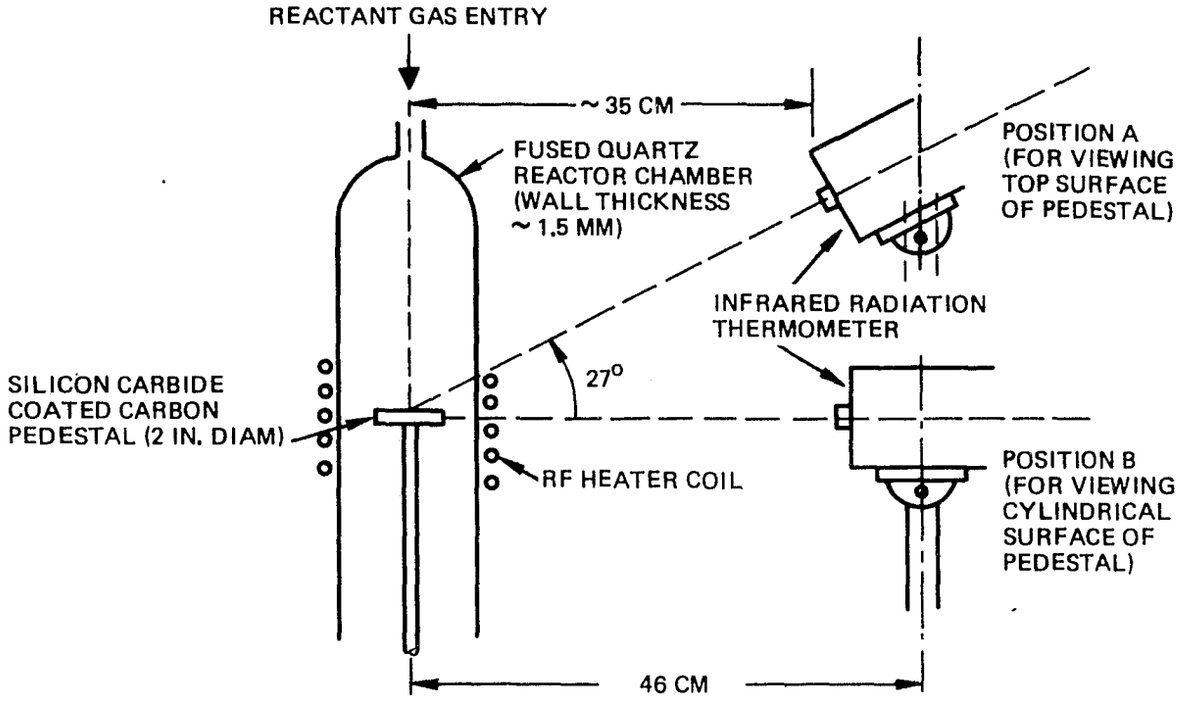

Figure 2-34. Schematic Diagram of Apparatus Arrangement for Measuring Pedestal Temperature with Infrared Radiation Thermometer ($2.0 \leq \lambda \leq 2.6\,\mu m$)

of reduced temperature (i.e, increased cooling of the pedestal) as the total gas flow rate increases. Generally, the magnitude of this cooling effect is similar for the two gases at a given location on the pedestal.

For a given gas flow rate an indication of the temperature profile on the pedestal surface can be obtained from an inspection of the three temperatures T_s, T_t, and T_c in the low-, mid-, and high-temperature regions. This temperature distribution is a consequence of the combined effects of the non-uniform heating of the pedestal/susceptor by the rf field and the several processes of heat transfer away from the pedestal, including heat conduction by the carrier gas moving past the pedestal surfaces.

The temperature difference between the center of the pedestal surface and points approximately three-fourths of the distance from the center to the edge of the top surface is given by the quantity (T_t-T_c) in Table 2-8. This difference is shown in Figure 2-35 as a function of the observed temperature T_c at the center of the pedestal surface, for the three gas flow rates used and for both gases. The results clearly show that the temperature distribution on the pedestal surface depends strongly on the magnitude of the pedestal temperature but is relatively independent of the carrier gas and the gas flow rate.

The difference between the temperature at the center of the pedestal surface -- where most substrates are placed for Si CVD experiments--and that observed on the cylindrical side of the pedestal (with the infrared thermometer in position B in Figure 2-34) follows a similar dependence on pedestal temperature, as can be verified by inspection of the values for (T_s-T_c) in Table 2-8. The difference is such that the

Table 2-8. Observed Temperatures at Three Locations on SiC-Coated Carbon Pedestal (5 cm dia) for H_2 and He Carrier Gases

Carrier Gas Flow Rate (ℓpm)	H_2 Carrier Gas Observed Pedestal Temperatures (°C)					He Carrier Gas Observed Pedestal Temperatures (°C)				
	T_s*	T_t**	T_c†	(T_s-T_c)	(T_t-T_c)	T_s*	T_t**	T_c†	(T_s-T_c)	(T_t-T_c)
4	590	586	580	10	6	590	590	583	7	7
	920	911	893	27	18	874	877	857	17	20
	1030	1019	987	43	32	1053	1042	1008	45	34
6	566††	573	568	-2	5	571	571	563	8	8
	911	899	879	33	20	872	870	850	22	20
	1024	1012	980	44	32	1026	1039	1002	24	37
8	548	549	542	6	7	555	551	544	11	7
	857††	874	854	3	20	854	862	835	19	27
	1012	1002	965	47	37	1018	1028	985	33	43

*Measured on vertical cylindrical surface or "side" of pedestal

**Measured on top pedestal surface at distance d= $\frac{3}{4}$ r from center, where r is radius

†Measured at center of top surface of pedestal

††These readings of doubtful validity

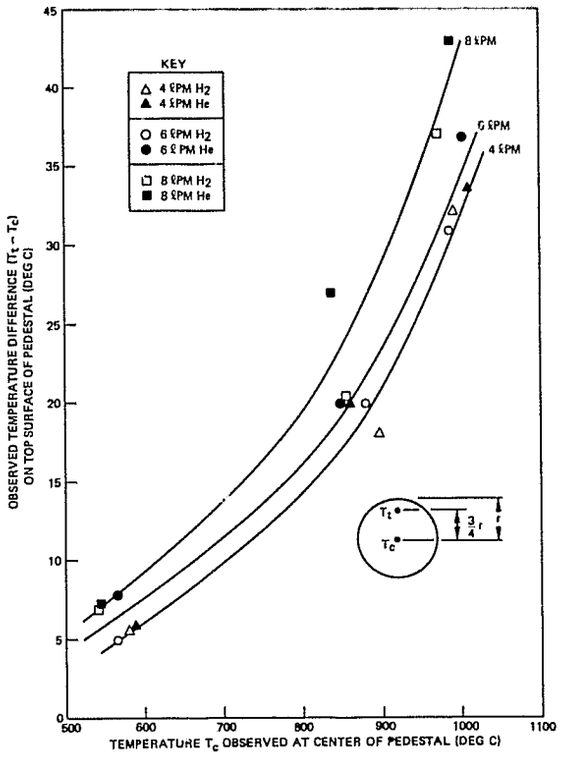

Figure 2-35. Observed Temperature Difference (T_t-T_c) on Top of rf-heated Pedestal for H_2 and He Carrier Gases at Three Different Flow Rates

temperature in the center of the pedestal surface is 8-10 deg C below that of the cylindrical side surface in the low temperature region, about 25 deg C below it in the mid-range, and 40 to 45 deg C below in the high-temperature region. Except where specifically noted, deposition temperatures given in this report are those observed on the side cylindrical surface of the pedestal.

2.3.2 Effect of Carrier Gas Flow Rate on Film Thickness Uniformity

Experiments were also undertaken early in the program to determine preferred total flow rates of H_2 and He carrier gases which would lead to acceptable Si film thickness (i.e., growth rate) uniformity across the 5-cm diameter SiC-covered carbon pedestal, over a temperature range of 600-1025°C. Total gas flows of 4, 6, and 8 ℓpm were used with pedestal temperatures of about 600, 850, and 1025°C, with SiH_4 flows of 10 ccpm for H_2 and 25 and/or 50 ccpm for He. The results are summarized in Figure 2-36.

For H_2 carrier gas, thickness/growth rate uniformity was better than 10 percent across the pedestal for most gas flow conditions. A flow rate of 4 ℓpm was selected as the preferred rate for subsequent CVD experiments using H_2 as the carrier, since it produced good growth rate uniformity (see Figure 2-36).

For He carrier gas the thickness uniformity appeared to be best for 6 ℓpm at ~1025°C. At both ~600 and ~850°C the uniformity was about the same for 6 and 8 ℓpm, as can be seen in the figure. However, a considerable variation in growth rate (as much as ~50 percent) was found across the 38-mm-diameter single-crystal sapphire substrates used for the experiments, particularly at ~1025°C.

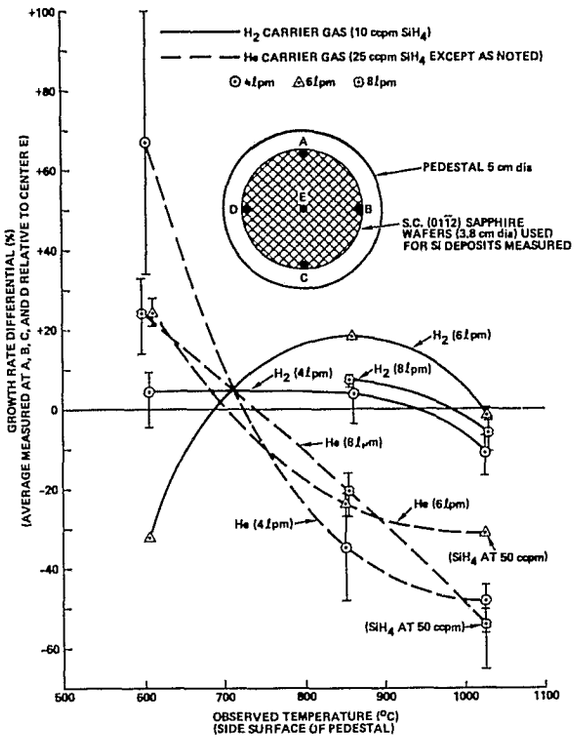

Figure 2-36 Si Film Growth Rate Variations Obtained with H_2 and He Carrier Gases for Various Flow Rates and Deposition Temperatures (Variations expressed as percent difference between growth rate at center of pedestal and average rate at several points near periphery.)

A He flow rate of 6 ℓpm was used in subsequent growth studies employing the present reactor design, with substrates to be evaluated placed at or near the center of the pedestal whenever possible.

2.3.3 Effect of Deposition Temperature on Si Film Growth Rate

Using 4 ℓpm for H_2 and 6 ℓpm for He, baseline growth rate determinations were made, with (01$\bar{1}$2)-oriented single-crystal sapphire as the substrate and a constant flow rate of SiH_4 (25 ccpm). For these experiments, a new 1000-gm tank of SiH_4 (from 3H Corporation) was used. The SiH_4 is reportedly H_2-free (less than 10 ppm); this is important in order to minimize reactions with substrates reactive with H_2. The only H_2 present when a He or inert atmosphere is used, therefore, is that generated by SiH_4 decomposition.

The results of these experiments are summarized for H_2 and for He as the carrier gas in plots of growth rate vs reciprocal absolute temperature in Figure 2-37. The temperatures used inplotting the data in these curves are corrected temperatures, representing the temperatures of the pedestal surface in regions adjoining the substrates on which Si deposition occurred. Consequently, a determination of activation energies associated with the process of Si layer growth by SiH_4 pyrolysis in H_2 and in He carrier gas atmospheres can be made.

It is clear that different mechanisms are operative in the deposition of Si by SiH_4 pyrolysis in the presence of H_2 and of He. In H_2, a rapid increase in growth rate with increasing temperature occurs for temperatures below about 900°C; above that, the rate still increases with temperature but much less rapidly. The activation energies characterizing the two regions are 1.8 and 0.14 eV, respectively. These

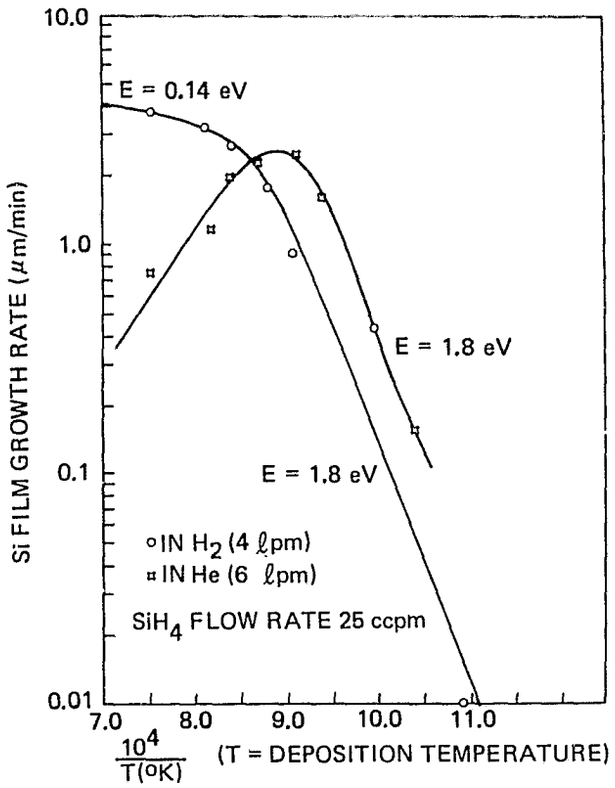

Figure 2-37. Si Film Deposition on $(01\bar{1}2)$ Sapphire Substrates as Function of Reciprocal Temperature for SiH_4 Pyrolysis in H_2 and in He

results are similar to those reported by other investigators (Refs 3, 4), who report a surface-controlled reaction for Si growth from SiH_4 below 900°C and a mass-transfer-controlled reaction in the temperature range 900-1050°C.

In He, the Si growth rate increase was also found to be rapid at low temperatures (activation energy 1.8 eV), but at about 850°C the growth rate passes through a maximum and then decreases for further increases in the deposition temperature up to at least 1050°C, the highest temperature used to date for these experiments. This maximum in the growth rate at ~850°C may be controlled by appreciable decomposition of SiH_4 caused by radiation, a finite distance away from the hot pedestal, with the formation of silicon hydride polymers $(SiH_2)_x$ which do not efficiently reach the hot pedestal for pyrolysis to form Si. Si formation from $(SiH_2)_x$ is, however, catalyzed by the presence of H_2 (Ref 5).

The differences in growth rate in H_2 and He below 850°C may be due to differences in flow characteristics in the reactor; on the other hand, the somewhat lower growth rate in H_2 in this range may be caused by H_2 adsorption on the substrate surface, thereby hindering SiH_4 adsorption and pyrolysis to Si. Previous studies at Rockwell demonstrated an increase in Si growth rate at 1025°C when additions of H_2 were made to SiH_4-He mixtures (Ref 6).

The observed difference in Si deposition rate by SiH_4 pyrolysis at temperatures above 850-900°C in H_2 and in He tends to discourage the use of He at higher temperatures because of the increased time required to obtain a given Si film thickness. Further, the film thickness uniformity across the pedestal has been much better for Si deposited

in H_2 than in He, particularly at higher temperatures. In addition, generally better looking Si films have been achieved--on substrates other than glasses--by deposition in H_2 than in He. However, for Si deposition by CVD on various glasses there is little doubt that He is the preferred carrier gas of the two, irrespective of the above disadvantages.

2.3.4 Background Impurity Doping Level in Reactor System

Early in the first quarter the electrical properties of several undoped epitaxial Si films grown on single-crystal sapphire and Si substrates were measured by both the van der Pauw and the conventional Hall bridge methods (see Task 5, Para 2.5), as a means of obtaining a measure of the background impurity doping level characteristic of the reactor system and the reactants in use at that time.

The films were grown on single-crystal $(01\bar{1}2)$-oriented polished sapphire and on high-resistivity single-crystal Si substrates, the former at temperatures of 1025 and 1100°C and the latter at 1025°C, in H_2 and in He carrier gases.

Results of these measurements indicated that the undoped films were p type, with the carrier concentrations typically $\sim 10^{15}$ cm^{-3}. This concentration level was believed to be rather high for such a system, but it was verified on several epitaxial samples during the first quarter.

After the reactor modifications were completed early in the second quarter additional measurements were made on undoped epitaxial Si films grown on sapphire substrates in H_2 and in He carrier gas, at ~1000 and ~1100°C. Two films grown in H_2 were deposited at nearly the same rate (3.3 μm/min and 3.7 μm/min), while the films grown in He were deposited at different rates (1.2 μm/min and 0.72 μm/min).

The films grown in H_2 were more uniform in thickness, consistent with earlier observations of film uniformity obtained with H_2 and with He carrier gases. However, nearly an order of magnitude difference in net carrier concentration was observed between the deposit near the center of the pedestal and that approximately halfway out toward the pedestal periphery, for either carrier gas.

The apparent background impurity doping level of $\sim 4 \times 10^{14}$ cm^{-3} indicated by these measurements (even though made on films grown on sapphire rather than on single-crystal Si substrates) is a more acceptable value than the $\sim 10^{15}$ cm^{-3} previously obtained in the first quarter. It is not known if the lower value is associated with a real reduction in the unintentional acceptor doping level in the films relative to those measured earlier or if the difference is in some way attributable to a measuring apparatus problem that was found to exist early in the second quarter and was corrected at that time.

In any case, subsequent measurements on undoped epitaxial films (on sapphire) from time to time as the program has progressed have confirmed the range $1 - 4 \times 10^{14}$ cm^{-3} as the background imperfection (impurity and/or defect) level typical of the reactor system and reactant materials now is use.

2.3.5 Si CVD on Selected Substrates

A variety of substrates has been used for Si film growth by CVD during the first nine months of the contract. These experiments are summarized in the following sections; details of the properties of the resulting films are given in Para 2.5 (Task 5).

2.3.5.1 Si CVD on Glasses

After the early exploratory experiments conducted with several of the glasses (see Para 2.2.7), there was relatively little done with Si deposition on glass substrates until well into the second quarter. At that time a series of deposition experiments was undertaken in which Si was deposited in a He atmosphere on substrates of Corning Code 1715 and Owens-Illinois GS211 and GS213 glasses.

The Si depositions on 1715 glass were done in the temperature range ~860 to ~1000°C. The He flow rate was 6 ℓpm and the SiH_4 flow rate 25 ccpm in each of the experiments. The Si film grew at a rate of ~0.6μm/min to a thickness of ~6μm in the experiment at ~860°C; ~1.4 μm/min to a thickness of ~14 μm at 914°C; ~1.0 μm/min to a thickness of ~16 μm at 955°C; and ~1.0 μm/min to a thickness of ~20 μm at 1000°C.

The films grown at the three higher temperatures each had a dull finish at the conclusion of the experiment. The film surface was heavily textured on all four samples, but the nature of the surface features was quite different in the four cases, as shown by optical microscope and SEM examination. The SEM photographs show a film surface with well-ordered crystallographically-faceted features producing good reflectivity at certain viewing angles to the normal for the 6 μm deposit prepared at a low growth rate at ~860°C (Figure 2-38). The surface texture in this case has a resemblance to those observed on Si films grown on some of the relatively fine-grained polycrystalline aluminas (see next section).

As the deposition temperature was increased, the surface texture of the deposited film was observed to change toward a coarser, more three-dimensional appearance, with numerous bulbous projections. The Si film deposited at 1000°C, for example, grew at almost a 50 percent faster growth rate than the one grown at ~860°C and was ~20 μm thick, rather than ~6 μm. SEM examination showed a much different surface texture, with little obvious faceting on the relatively tall surface features (Figure 2-39), which accounts for the dull appearance of this film. Further evidence of systematic structural differences as a function of growth temperature in the films deposited on 1715 glass in this temperature range was provided by x-ray diffraction analyses of these samples. (Both the SEM examination and the x-ray analyses are discussed under Task 5, in Para 2.5.) The observed structural differences among these films could be the result of a change in the dominant layer growth mechanism in this temperature range in He, related to the presence of the maximum in the growth rate vs temperature curve for He (Figure 2-37).

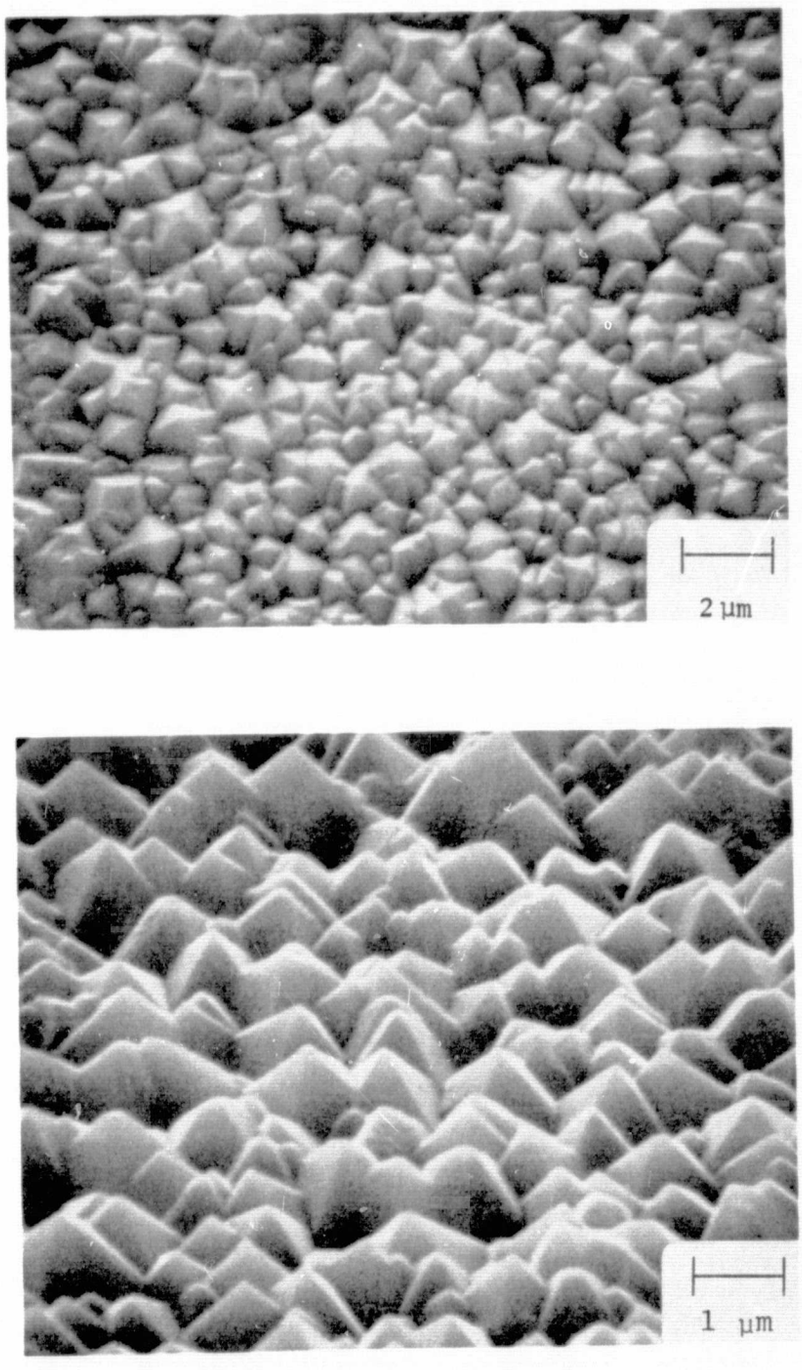

(b)

Figure 2-38. SEM Photographs of Surface of CVD Si Film Grown on Corning Code 1715 Glass by SiH_4 Pyrolysis in He at ~860°C.
a) View at Normal Incidence; b) View at 45 deg to Surface

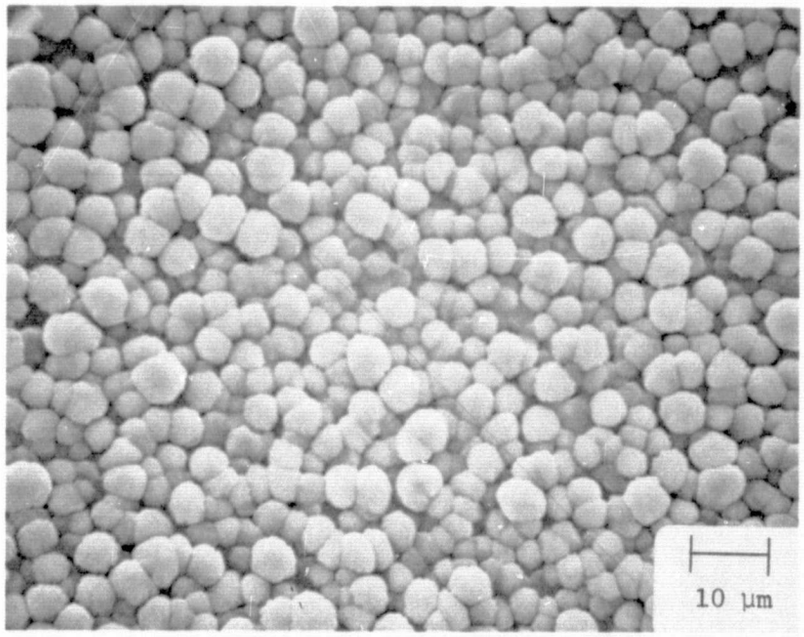

(a)

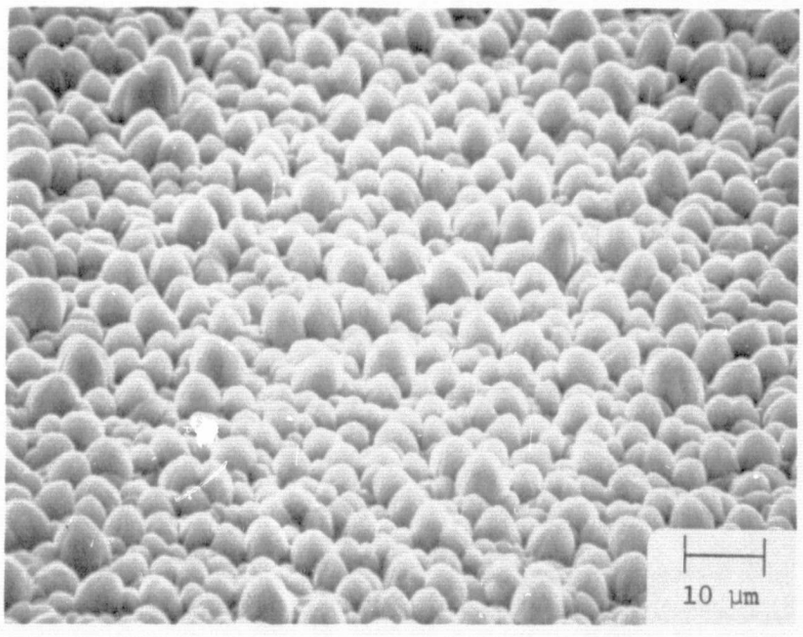

(b)

Figure 2-39. SEM Photographs of Surface of CVD Si Deposited on Corning Code 1715 Glass by SiH_4 Pyrolysis at 1000°C in He. (a) View at Normal Incidence; (b) View at 45 deg to Surface.

The experiments with Owens-Illinois glasses GS211 and GS213 were done in He carrier gas (6 ℓpm) with a SiH_4 flow rate of 25 ccpm. The film on GS211 was deposited at ~850°C at a rate of ~1.7 μm/min to a thickness of ~35 μm, while that on GS213 was deposited at 860°C at a rate of ~2 μm/min to a thickness of ~50 μm. In both cases deeply textured surfaces resulted on the Si deposit, producing a very dull appearing finish.

SEM examination of the film on GS211 indicated somewhat irregular pyramidal growth features, averaging about 4 μm across with moderate faceting (Figure 2-40). There were also what appeared to be large clusters or "chunks" of Si distributed about the surface, indicating a less orderly growth process than was observed at the same deposition temperature on Corning Code 1715 glass.

Electrical measurements on the undoped Si film on GS211 glass, reported along with the results of measurements on the Si-on-1715 samples in the Task 5 discussion, indicate a much higher conductivity than for the other undoped Si-on-glass films. The higher p-type carrier concentration ($\geq 10^{15}$ cm^{-3}) is also indicative of a high density of imperfections of some type - possibly some impurity from the glass substrate.

2.3.5.2 Si CVD on Polycrystalline Aluminas

Early in the program films of Si were grown simultaneously on as-manufactured surfaces of ASM805, ADS995, and MRC Superstrate. Temperatures of 1025 and ~1100°C and carrier gases of H_2 and He were used, to permit a comparison of film structural properties for the several sets of conditions. In each case the film deposition process was preceded by a high-temperature (1250°C) etch of the substrate in H_2. The high deposition temperatures were selected to enhance grain growth, with 1025°C considered low enough to minimize any autodoping tendency by the alumina substrates.

The results obtained in H_2 and in He were quite different. Films ~20 μm thick deposited in H_2 were found to be considerably smoother and more uniform in appearance and in surface texture than films about 6 μm thick grown in He. The thickness difference for the films grown in the two cases is simply a result of the very large difference in Si growth rate in H_2 and in He at these temperatures (cf Figure 2-37).

X-ray diffraction analysis of the three films grown in H_2 (4 ℓpm) at 1025°C with a SiH_4 flow rate of 10 ccpm indicated {110} preferred orientation was present in all three cases. The film on ASM805 had by far the strongest preferred orientation, that on MRC Superstrate was next, and the film on ADS995 was the weakest in this regard, although still preferentially oriented in the {110} plane. The set of films (comparable thickness) grown in H_2 at ~1100°C also exhibited {110} preferred orientations that were generally less pronounced than in the 1025°C group, although the relative strengths of this orientation among the three were in the same order as in the films grown at 1025°C.

SEM examination of the films grown in H_2 at 1025°C showed the film surfaces to be almost identical in appearance, as shown in Figure 2-41, with characteristic surface features having nearly the same average size (measured parallel to the interface) of ~4 μm. However, the film on ADS995 also exhibited some crystallographic faceting of the surface features that was not seen on the other two films, as shown in Figure 2-42, even though the x-ray analyses indicated it to be the least preferentially-oriented of the three films.

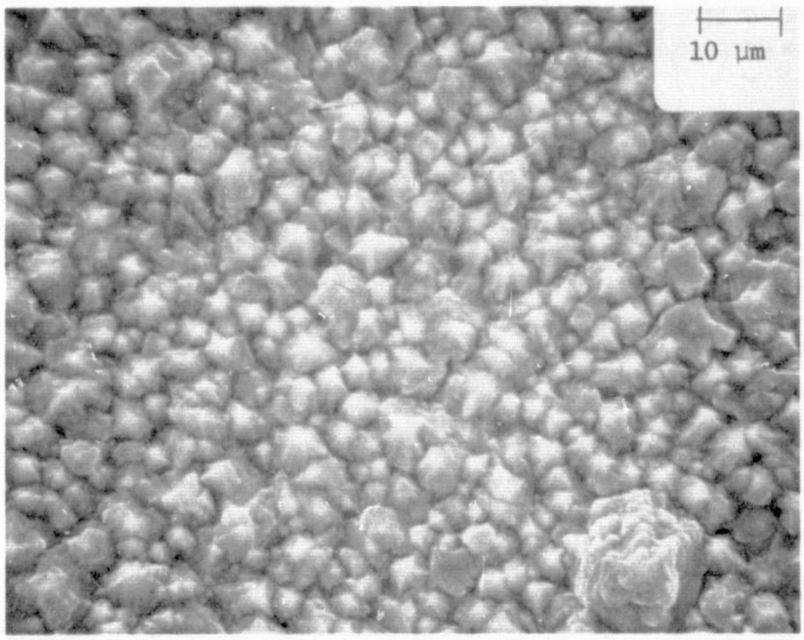

(a)

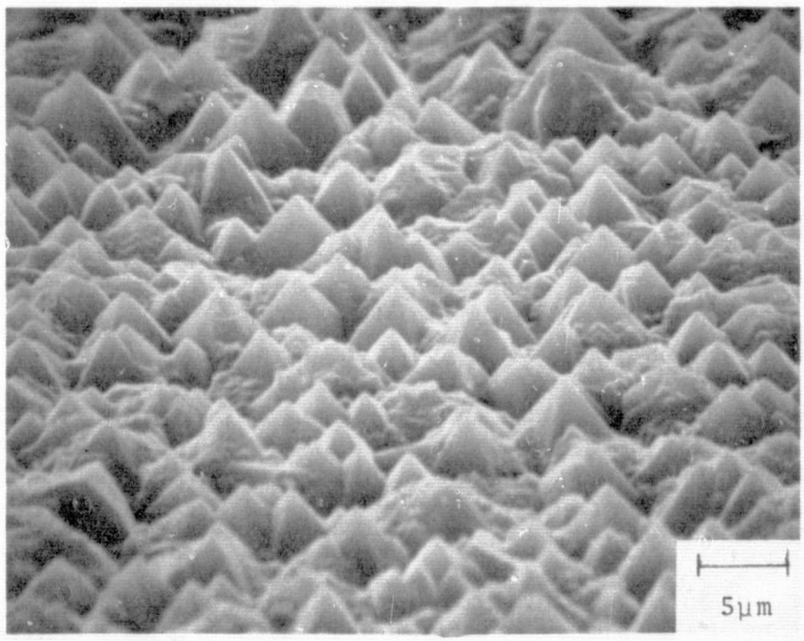

(b)

Figure 2-40. SEM Photographs of Surface of Si Film Deposited on Owens-Illinois GS211 Glass by SiH_4 Pyrolysis at ~860°C in He. (a) View at Normal Incidence; (b) View at 45 deg to Surface

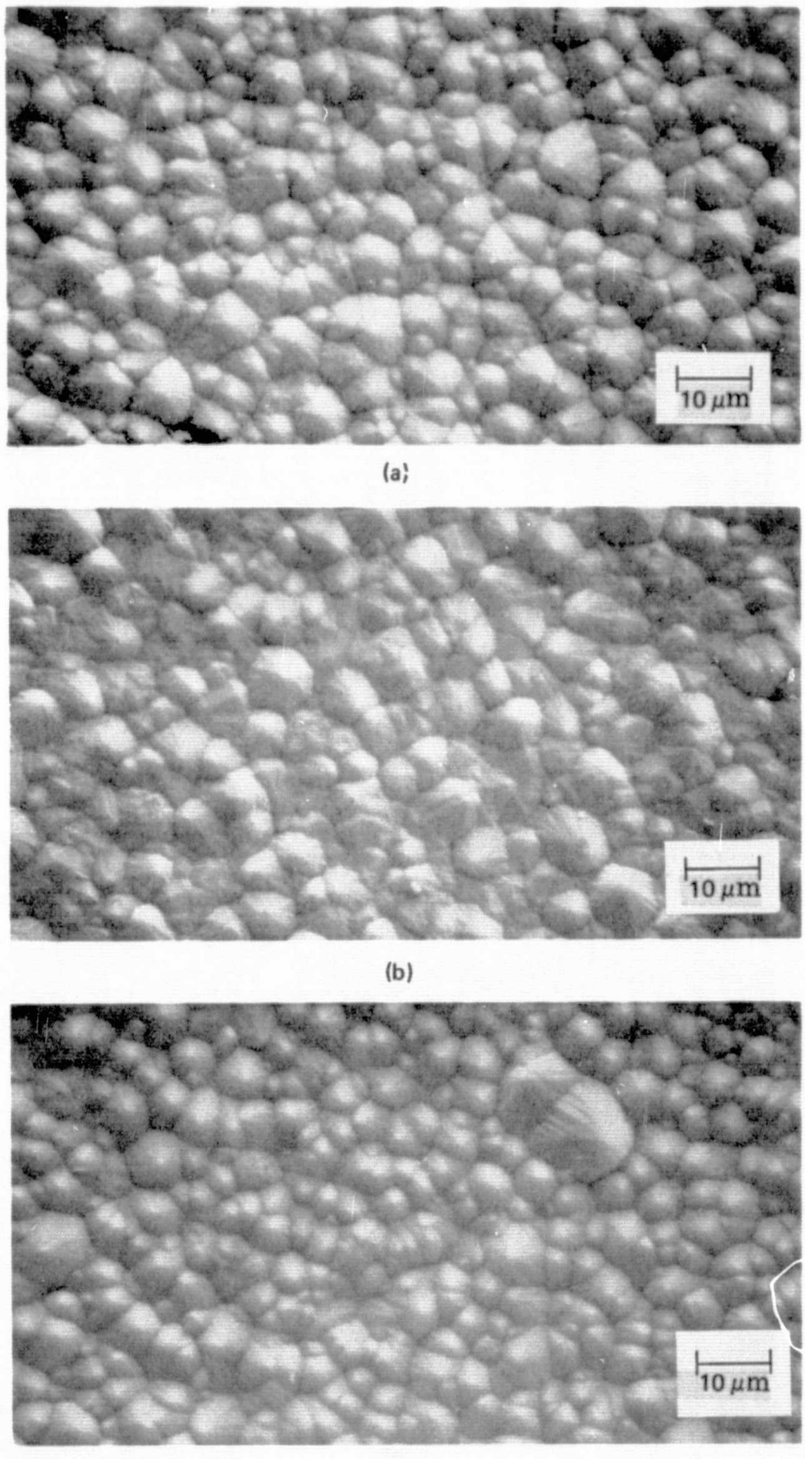

Figure 2-41. Rosette Surface Structures of CVD Si Films Grown on Fired Polycrystalline Alumina Substrates in H_2 at 1025°C by SiH_4 Pyrolysis: (a) on MRC Superstrate; (b) on ADS995 (Coors); (c) on ASM805 (3M)

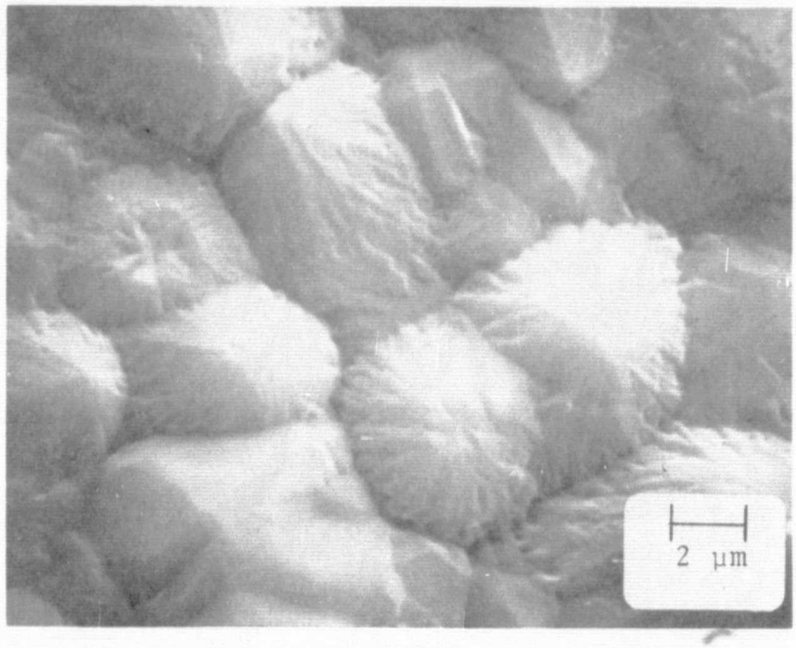

(a)

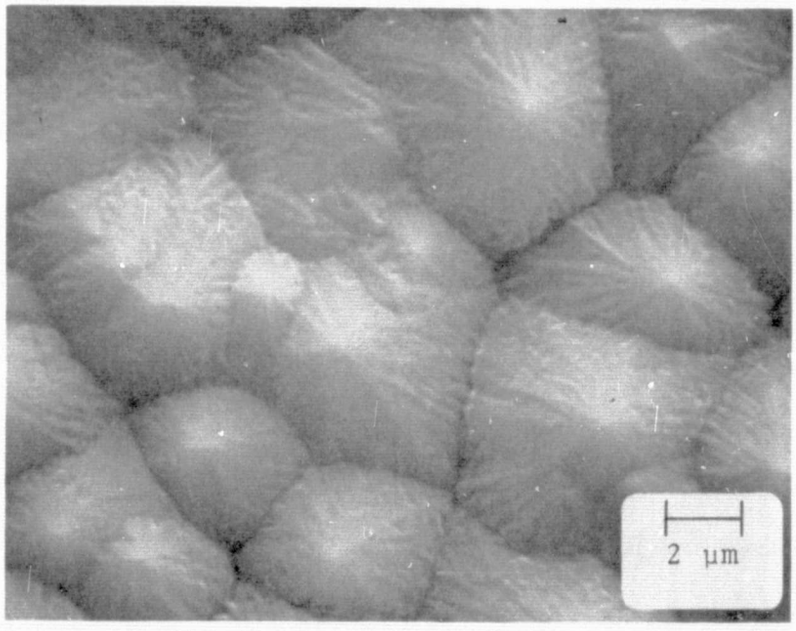

(b)

Figure 2-42. High Magnification Views of Rosette Surface Structures on CVD Si Films Grown on (a) ADS995 (Coors) and (b) ASM805 (3M), by SiH_4 Pyrolysis in H_2 at 1025°C. Note Faceting in (a).

X-ray analysis of diffraction line widths for particle-size line broadening effects indicated no such broadening in the films grown at ~1100°C but some detectable broadening in two of the films grown at ~1025°C. The film on Superstrate appeared to have an average grain size of ~0.1 μm, while that on ADS995 was the order of 0.04 μm by the x-ray analysis. The relatively small difference in deposition temperature for these two groups of films appeared to produce a detectable difference in the average grain size in two of the three cases. However, it is not clear why there is an apparent difference in the dimensions of the surface features as seen in the SEM and the average size of the crystal grains as determined by x-ray analysis.

In another early set of experiments thick Si films were grown on three as-manufactured ASM805 substrates in separate experiments at ~1025°C in H_2 (4 ℓpm); two of the films were 20-25 μm thick, one grown at ~1.6 μm/min and the other at ~3.3 μm/min, while the third film was ~40 μm thick and grown at ~3.3 μm/min. These experiments were intended to indicate what differences in film properties might be associated either with grow rate or with film thickness.

X-ray diffraction analysis of the three samples indicated a slight amount of line broadening in all three cases, consistent with the earlier observation of some line broadening for films grown on polycrystalline aluminas at ~1025°C but not at ~1100°C. However, in the earlier films the broadening was found in the Si films on ADS995 and Superstrate aluminas but not in the Si grown on ASM805. The results in all three thick films on ASM805 indicated a grain size of about 0.05 μm, similar to the earlier result on the other substrates.

The same three Si film samples were examined by SEM techniques. The surfaces of the two thinner films, which were grown at rates differing by a factor of about 2, were identical in appearance (Figure 2-43a), with surface rosette features of ~3.0 and ~2.8 μm average dimension for the films grown at ~3.3 and ~1.6μm/min, respectively. The film grown at ~3.3 μm/min to a thickness of ~40 μm had significantly larger surface features, averaging ~5.2μm (Figure 2-43b).

Evaluation of the amount of preferred orientation in the set of three films again established very strong preferred {110} orientation in all three, the amount appearing to increase with film thickness, providing confirmation of the tendency of ASM805 alumina to induce {110} Si growth. Also, the thickest film (~40 μm) gave no {100} reflection whatever, whereas in the two thinner ones the {100} reflections were relatively stronger than would be observed in a randomly-oriented sample.

During the second quarter a series of Si CVD experiments was carried out using substrates of Vistal alumina having each of four different histories of refiring beyond the normal processing used for commercial-grade Vistal. Because of the large crystal grains in these refired materials (see Para 2.2.5 and 2.2.6) it was expected that they would provide useful surfaces for study of the interdependence of Si CVD parameters as well as for preparation of polycrystalline film samples for evaluation. The Vistals have been used extensively in both the as-fired and the mechanically polished condition. As indicated earlier, simultaneous deposition on polished and as-fired substrates should not only allow establishing correlations between substrate preferred orientations and the observed Si film growth habit, but also establish the effect on the topography of the upper Si film surface of growth on a smooth polished polycrystalline surface as opposed to a rough faceted polycrystalline surface.

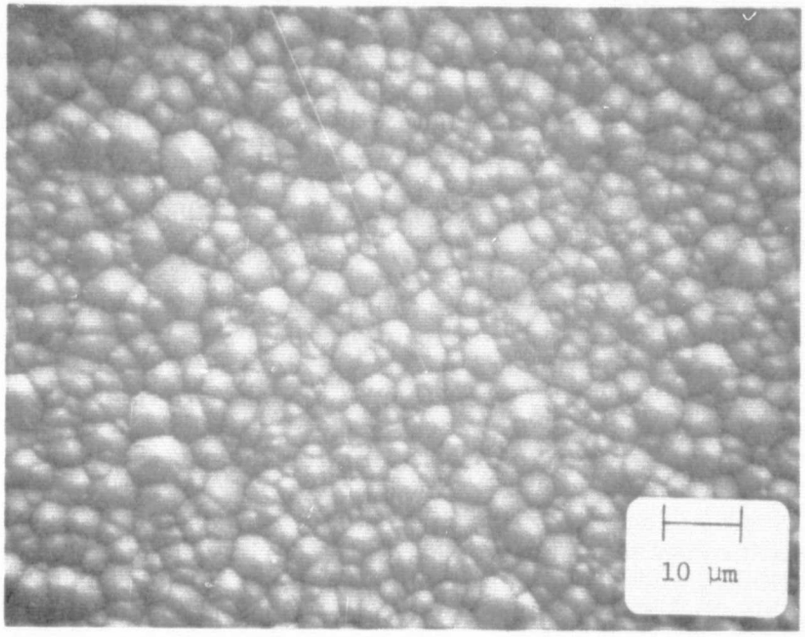

(a)

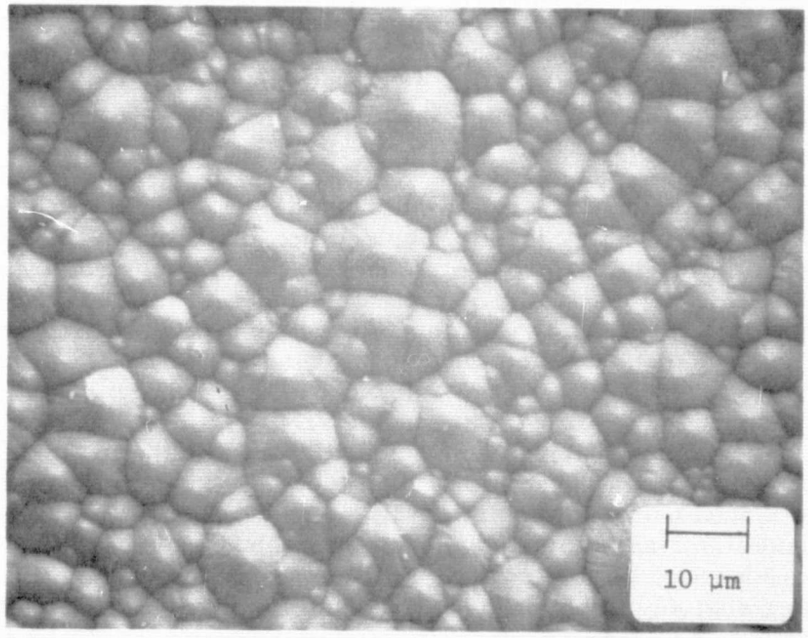

(b)

Figure 2-43. Rosette Surface Structures on CVD Si Films Grown on ASM805 Substrates in H_2 at ~1025°C at Approximately Equal Rates (>3μm/min). (a) Film Thickness ~ 20μm. (b) Film Thickness ~ 40 μm.

The large α-alumina grains of the Vistal substrates (Figures 2-14, 2-15. 2-23), both polished and as-fired, provide individual single crystals of sapphire for the growth of Si deposited by the pyrolysis of SiH_4. On the as-fired substrates these individual sapphire grains have exposed facets – presumably natural crystallographic planes – that serve as the growth surfaces for the deposited Si. The spatial (not crystallographic) orientation of these facets with respect to the plane of the nominal substrate surface is largely a consequence of the process used to form the ceramic and of any subsequent firing (annealing) procedure. Whether some of these partially-randomly oriented growth surfaces will be crystallographic planes of α-alumina that are favorable to epitaxial growth of CVD Si is a matter of chance.

For the case of the polished substrates, the surface generated by the mechanical polishing process intersects all individual α-alumina single-crystal grains lying in the surface of the substrate wafer. The plane so defined in each surface grain will have a definite crystallographic orientation in that individual α-alumina crystal; whether some of those arbitrarily-defined (by the polishing process) crystal planes will happen to be planes of sapphire that are favorable to the epitaxial growth of CVD Si is again a matter of chance, and is influenced by the spatial orientation of the surface crystals resulting from the ceramic forming process and any subsequent firing. The main distinction in the case of the polished substrate is that the polished surface can be correlated with crystallographic planes found to be preferred orientations in the polycrystalline ceramic material.

The deposition experiments with the Vistal aluminas were all done at a temperature of ~1025°C. This temperature was selected to be favorable to epitaxial growth of Si on α-alumina while keeping any autodoping effects to a minimum. H_2 was the carrier gas (4 ℓpm) and the SiH_4 flow rate was 25 ccpm. In each case, the substrates were exposed to a 15 min predeposition treatment in H_2 (4 ℓpm) at 1250°C. A growth rate of 3.0 μm/min was used.

The Si films grown in these experiments exhibited discrete regions of high reflectivity as viewed by the unaided eye, for both the polished and the as-fired samples. Closer inspection indicated that epitaxial (i.e., single-crystal) Si growth had undoubtedly occurred on many of the large individual crystal grains. Those which were oriented properly to control the growth of single-crystal Si produced the highly reflective grains or islands, in a sea of otherwise polycrystalline-appearing smaller grains.

The large grains with non-reflective Si deposits either are exposed single-crystal Si with non-reflecting planes or non-single-crystal Si which was formed because the deposition conditions (probably temperature) were not consistent with single-crystal growth on that orientation of α-alumina ($A\ell_2O_3$). For example, single-crystal Si growth on $(11\bar{2}0)$ $A\ell_2O_3$) is better at 1075-1100°C; on (0001) $A\ell_2O_3$, at 1200°C; and on $(01\bar{1}2)$ $A\ell_2O_3$, at 1025-1100°C, in the type of reactor used here.

Optical photomicrographs of a Si film 18 μm thick deposited on a polished Vistal 4 substrate are shown in Figure 2-44. They show the highly reflective epitaxial regions immersed in less favorably oriented Si, as discussed above. Figure 2-44a is at low magnification, to give an indication of the fraction of the total area of Si that consists of growth that is epitaxial or at least highly oriented. Figure 44b shows the cluster of epitaxial regions seen near the center of Figure 2-44a but at higher magnification, to illustrate the variety of oriented Si growth found in this film.

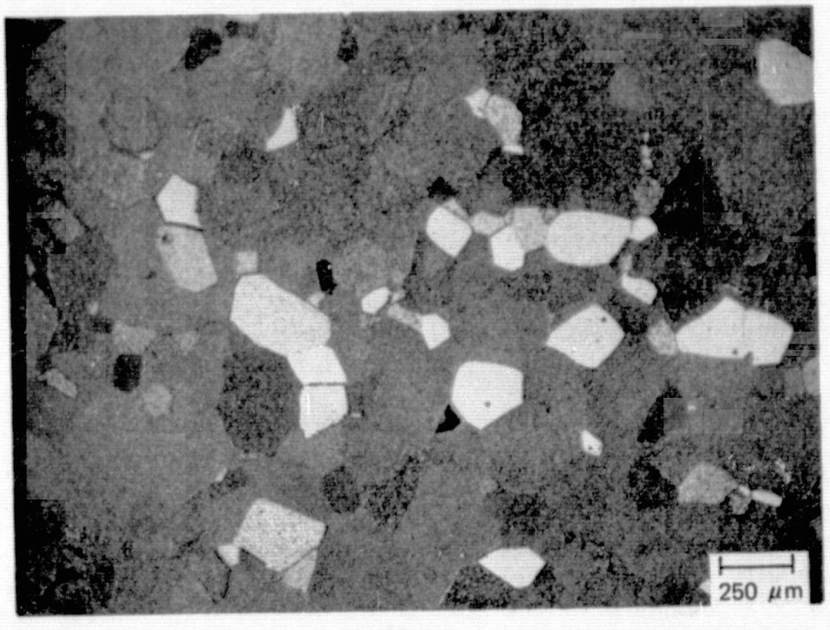

(a)

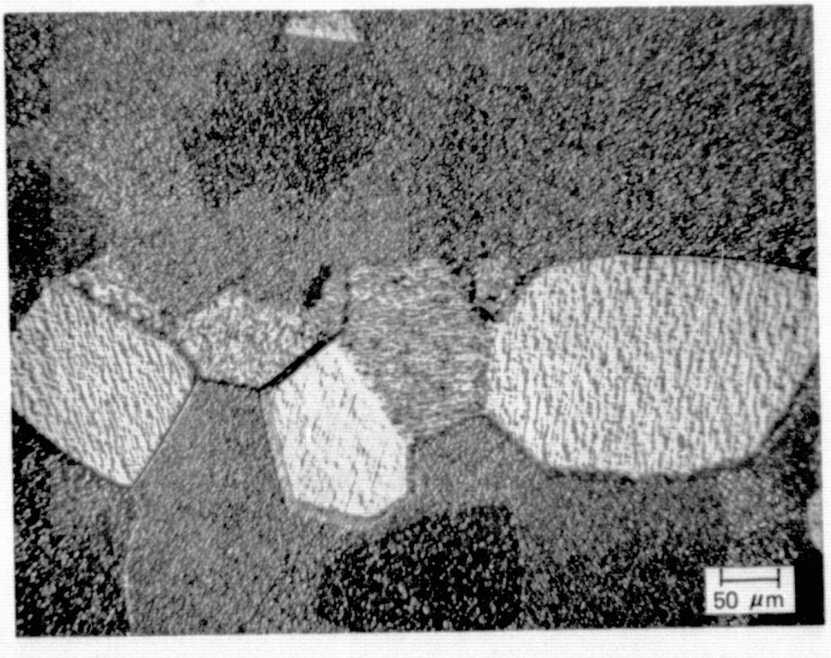

(b)

Figure 2-44. Optical Photomicrographs of CVD Si Film on Polished Vistal 4 Polycrystalline Alumina Substrate, at Two Different Magnifications

SEM-photographs of the same film deposited on polished Vistal 4 are shown in Figure 2-45. Figure 2-45a shows a region of the film surface at relatively low magnification. Several very large grains are visible in the field, although most of the film surface appears fine-grained. The large grain in the center is nearly 200 μm long in its largest dimension. Figure 2-45b shows at higher magnification the intersection of that grain with another more obviously epitaxial grain. The film replicates the large grain structure of the substrate, although the surface boundaries between grains – except for the prominent epitaxial grains – are subtle and difficult to detect in these figures.

The surface of the Si film grown simultaneously on an as-fired Vistal 4 substrate is shown in the SEM photographs in Figure 2-46, both of which were made at normal incidence. The film again replicates the grain boundary structure of the substrate; this is more readily visible in the case of the unpolished substrate involved here. Some very large grains are evident in this film, as in the film on the polished substrate. However, many of the areas outlined by what appear to be grain boundaries propagated through the film from the substrate are merely regions of relatively fine-grained polycrystalline Si growth such as is seen on other alumina substrates. This is evident in Figure 2-46b, which shows a region that appears to be epitaxial and other areas exhibiting typical polycrystalline surface features.

The results obtained with the other three groups of Vistal substrates–both polished and as-fired–were similar to those described above for Vistal 4, but with correspondly different grain sizes.

The surface roughness of the Si deposits on the Vistals was found to be considerably better on the films grown on the polished surfaces than on the unpolished surfaces. Dektak profilometer traces, shown in Figure 2-47, reveal at least a factor of 5 improvement in surface roughness for these 18 μm-thick films.

Si CVD experiments with other alumina substrates have been carried out throughout the program, for the purpose of determining preferred CVD parameters for good-quality film growth. The complexity of polycrystalline Si growth on these polycrystalline alumina surfaces is evident. The aluminas have produced the most promising results to date, although the preliminary nature of the investigations must be emphasized. The thermal expansion of alumina does lead to some obvious bowing of the Si-alumina composite when films 20-100μm thick are grown on 625-μm-thick alumina substrates. However, these materials offer a means for studying the effects of growth parameters and processes on Si film properties until an appropriate glass or other material more compatible with Si is found.

Additional details of the properties of Si films obtained on various polycrystalline aluminas are given in the discussion of Task 5, in Para 2.5.

2.3.6 Experiments Involving SiH_4-$HC\ell$ Mixtures

An investigation was begun to determine if SiH_4-$HC\ell$ mixtures could be used to enhance grain growth in polycrystalline Si films grown on low-cost substrates. Previous studies at Rockwell had demonstrated that by adding $HC\ell$ to $SiC\ell_4$ it was possible to encapsulate an amorphous SiO_2 region between two patches of bare Si with a highly twinned Si deposit, x-ray diffraction examination of which gave no evidence of polycrystalline structure (Ref 7). The $HC\ell$ added was largely responsible for inhibiting the growth of Si directly on the oxide layer while, at the same time, the Si growth extended from the two bare Si regions and joined to form a "bridge" over the SiO_2.

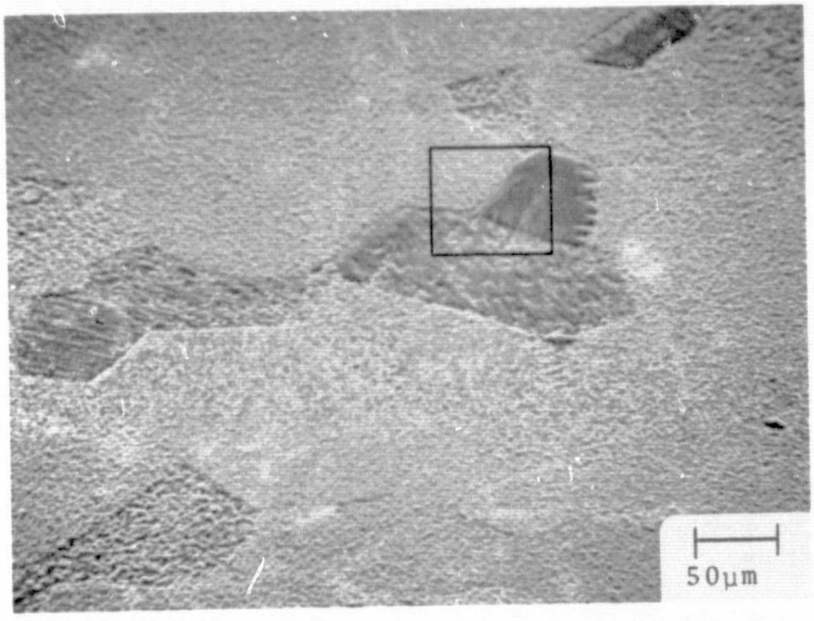

(a)

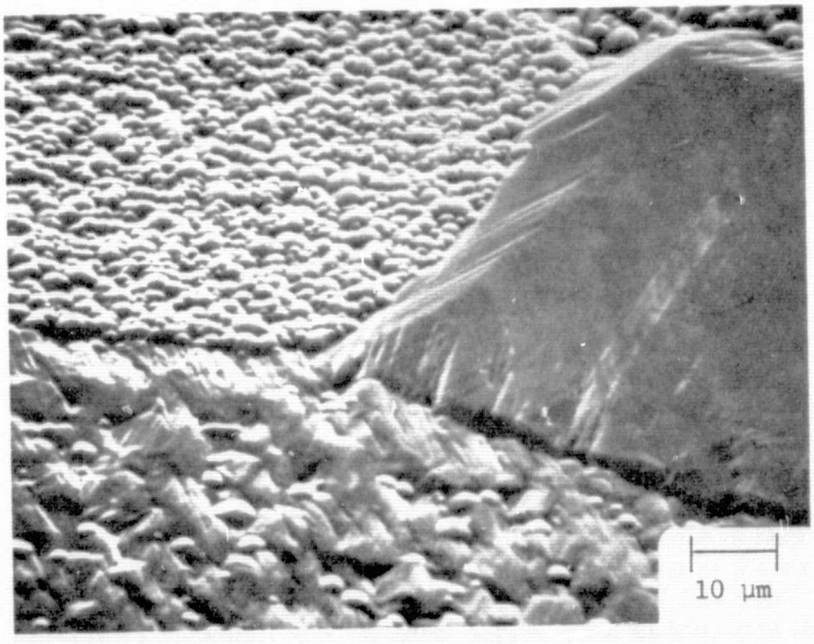

(b)

Figure 2-45. SEM Photographs of CVD Si Film of Figure 2-44, at Two Different Magnifications. (Viewing angle 45 deg with sample surface)

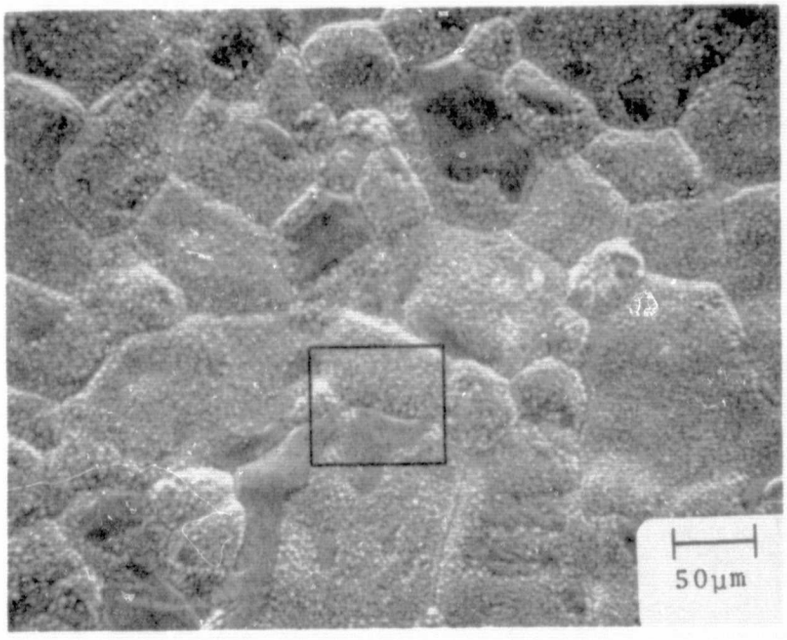

(a)

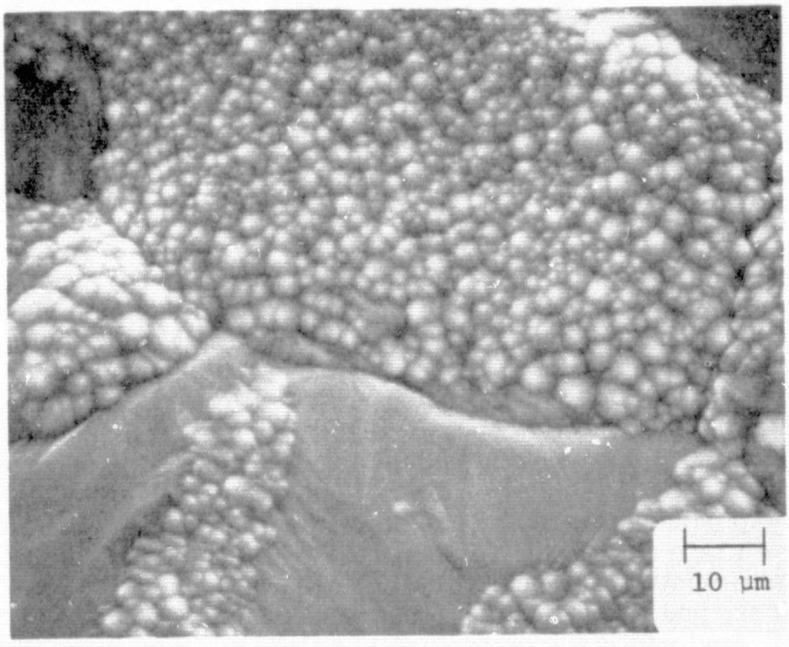

(b)

Figure 2-46. SEM Photographs of CVD Si Film on As-fired Vistal 4 Polycrystalline Alumina Substrate, at Two Different Magnifications. (Viewing at normal incidence.)

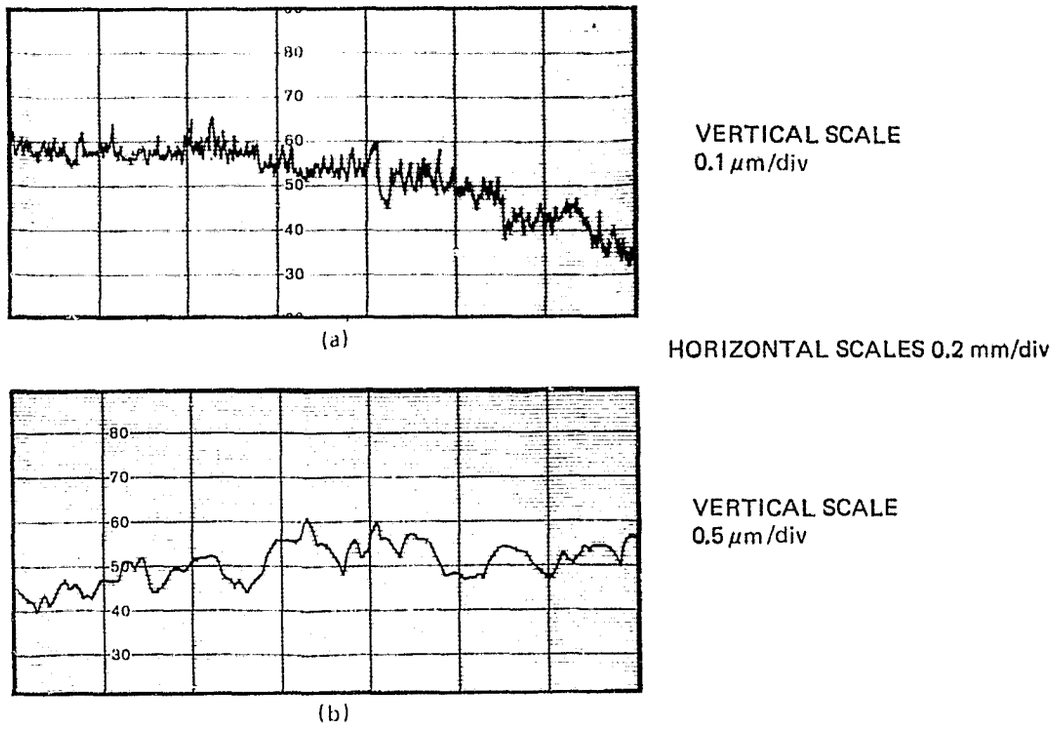

Figure 2-47. Dektak Profilometer Traces of Surfaces of CVD Si Films Deposited by SiH_4 Pyrolysis on (a) Polished Vistal 4 (four consecutive firings at ~1800°C for 6 hr) and (b) As-fired Vistal 4. (Note different vertical scales.)

In this program it is intended that the HCℓ added to the Si source will preferentially attack the smaller Si crystals formed on amorphous or polycrystalline substrates, resulting in Si growth preferentially on the larger Si crystals which survive the attack by HCℓ, thereby leading to a greater proportion of larger grains that should grow further during the continuing deposition.

Studies by Bloem (Ref 8) in a horizontal reactor have been shown that the addition of HCℓ to SiH_4 greatly enhances epitaxial Si growth rates, presumably by reduction of the gas phase nucleation rate, but this effect occurs at relatively high temperatures; at lower temperatures he found that the etching reaction predominates. Since growth from SiH_4 and etching by HCℓ proceed independently (Ref 8), reactant mixtures of SiH_4 and HCℓ at a given temperature which result in a reduced Si growth rate and preferential removal of small crystals could provide films with enhanced grain size.

The first experiments were designed to determine the effect of HCℓ additions to SiH_4 on the growth rate of Si in the vertical reactor. Sapphire substrates were used in the initial experiments to expedite film thickness (i.e., growth rate) measurements by the IR technique, and H_2 was used as the carrier gas. Additions of HCℓ to SiH_4 flows of 25 ccpm (MFC readings) were made, and Si films were grown at ~1025°C. At the first HCℓ concentration used (flow rate of 10 ccpm) a slight increase in growth rate was observed, but with progressive additions of HCℓ the growth rate gradually decreased. After several experiments it was noted that the SiH_4 MFC readout and the flow rate reading on the glass rotameter in series with the MFC did not agree. As was indicated in

Para 2.1 it was found that the MFC had become contaminated with a white powder (presumably SiO_2 produced by the entry of air and/or moisture into the system). Subsequent experiments involved reading gas flow rates on the rotameter rather than the MFC.

When this and other apparatus problems were corrected the HCℓ experiments were resumed. Figure 2-48 shows the observed dependence of Si growth rate on the concentration of HCℓ added to the SiH_4 source gas, expressed as a ratio of HCℓ flow rate to SiH_4 flow rate. The figure shows the initial data obtained in the second quarter for a SiH_4 flow rate of 25 ccpm, and also more recent data obtained with SiH_4 flow rates of 10 ccpm.

With the necessary growth rate information for the SiH_4-HCℓ system, experiments were begun to test the two-step growth process for Si deposition on low-cost substrates. Undoped Si films deposited for 12 sec simultaneously on four different substrates in H_2 at 1025°C (SiH_4 flow rate 25 ccpm) were found to cover the substrate completely in each case. In the first attempt to deposit additional Si from a SiH_4-HCℓ mixture the failure of a valve in the HCℓ line allowed excessive HCℓ concentration and resulted in an unsuccessful run. The experiment was repeated, however, with the second layer being grown from the mixture at 1025°C for 12 min, again using a relatively low HCℓ flow rate (50 ccpm). Additional two-step growth experiments were performed at a lower SiH_4 flow rate (10 ccpm) and total H_2 flow (1.5 ℓpm rather than 4 ℓpm) after it was observed that the thick films (~20 μm) exhibited large variations in thickness across the pedestal diameter when the total H_2 flow was 4 ℓpm. At a SiH_4 flow rate of 10 ccpm the Si growth rate was 1.5 μm/min; with HCℓ flowing at 200 ccpm, the net Si growth rate was slightly negative, the film grown in the first thin layer (12 sec deposition time) having almost disappeared in 13 minutes of exposure to the SiH_4-HCℓ mixture.

Double-layer films were grown at HCℓ flow rates of 25, 50, and 100 ccpm to provide HCℓ-to-SiH_4 ratios of 2.5, 5, and 10 to 1. The measured growth rate data approximately parallel the line through the earlier data obtained for a SiH_4 flow rate of 25 ccpm (Figure 2-48). Although evaluation of the films in these composite samples is not completed (see Section 2.5, Task 5) it does not appear that any extensive enlargement of average grain size has occurred with the parameters utilized to date.

However, x-ray analysis of 12-sec polycrystalline Si growths (approximately 0.5 μm thick) on substrates of as-fired ASM805 and Superstrate and polished Superstrate, grown at 1025°C in H_2(4 ℓpm) with a SiH_4 flow rate of 25 ccpm as a preliminary to the double-layer experiments, indicated completely random orientations in all three cases. The thick (20-25 μm) layer grown on such a thin layer in the presence of HCℓ had developed distinct preferred orientation in the {110} plane, and in at least one case the preferred orientation was very strong. Whether this orientation developed as a consequence of the HCℓ present or simply as a result of the CVD Si layer continuing its growth to greater thicknesses, as has been observed before, has not yet been determined. Further work with these samples and with the SiH_4-HCℓ mixture is in progress.

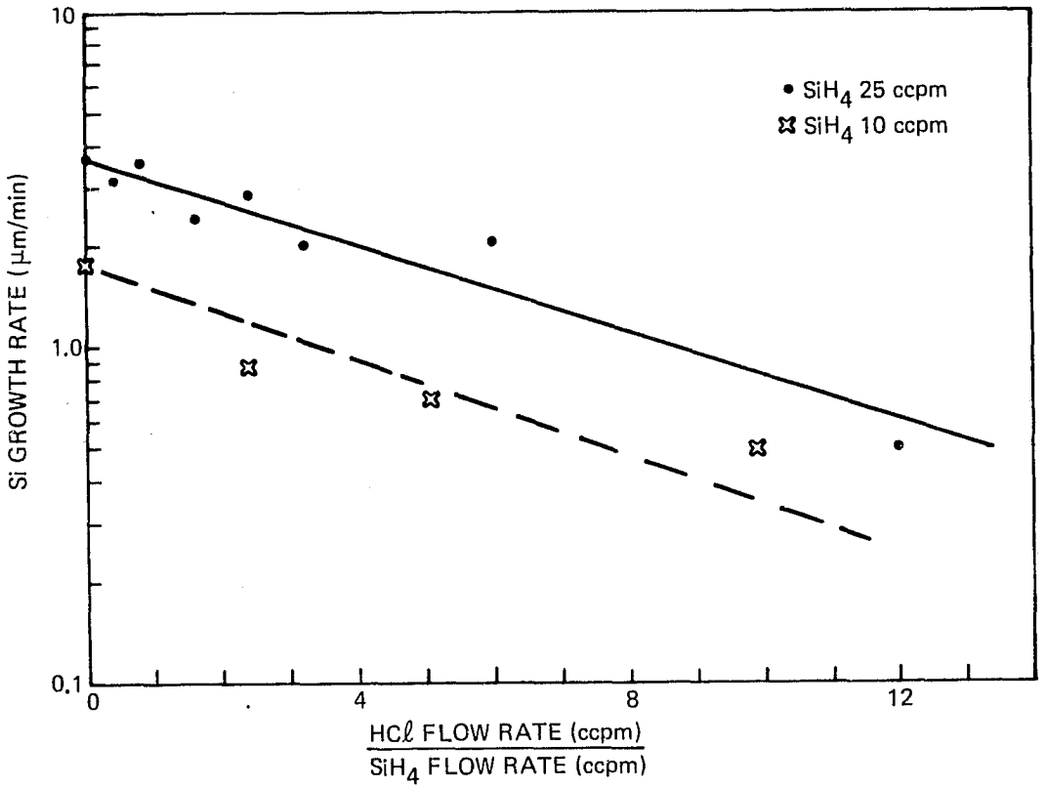

Figure 2-48. Changes in Si Growth Rate at 1025°C Caused by Additions of HCℓ to SiH_4

During the recent experiments described above it was found that the polished Superstrate wafers used — along with sapphire and Vistal substrates — as test substrates had a strong tendency to move about on the rotating sample pedestal during the initial heating in H_2. During the heating to 1250°C a yellow-orange flame was also in evidence in the H_2 burn-off box (Figures 2-1 and 2-2); both effects are associated with an outgassing of the substrate and/or volatization of impurities from the substrate. The substrate cleaning procedure used may have changed the structure of its surface. During film deposition at ~1025°C this same problem was manifested as an area of apparent contamination on neighboring substrates, thus impeding the evaluation of the two-step process by measurements of electrical and crystallographic properties.

In an attempt to clean the surfaces of the aluminas in situ before film growth, the substrates were (1) exposed to an HCℓ-H_2 mixture for 10 min at 1025°C immediately after the 15 min H_2 bake at 1250°C, then (2) reheated in H_2 at 1250°C for 21 min (the yellow-orange flame was still evident), and finally (3) exposed to Si deposition at 1025°C by the two-step growth process. The accompanying film overgrowth on sapphire was not reflective, possibly caused by HCℓ attack of the sapphire surface, and in addition some whisker growth occurred at a few regions along the edges of the Vistal and sapphire substrates and on the MRC substrate. It is apparent that cleaning procedures and their effects on substrate surfaces must be examined further and modified as necessary before proceeding with the two-step growth studies on polycrystalline alumina substrates.

2.3.7 Studies of Effects of B Doping Using B_2H_6 Source

Si layers grown by CVD can be readily doped during growth by introduction of an appropriate compound containing the doping impurity into the carrier gas stream along with the Si compound being used. In some ways the method is almost ideal for producing either n-or p-type Si sheet on a substrate, since the dopant gases are homogeneously mixed with the Si compound external to the reactor and prior to film deposition. Such n-type sources as AsH_3 and PH_3 and the p-type source B_2H_6 have been almost universally used for doping epitaxial Si films.

However, the crystallographic properties of polycrystalline films grown in different atmospheres and under different growth conditions can be expected to vary considerably with the dopant source and to affect the electrical properties of the films. For example, it has been reported that B atoms enhance the growth rate and the grain size of polycrystalline Si films, especially at higher concentrations ($>10^{18}$ cm^{-3}), whereas As tends to have the reverse effect. This favors the growth of p-type Si films for the thicker base region of a solar-cell structure, and the formation of the thin n-type front layer either by subsequent post-growth counterdoping (diffusion or ion implantation) with As or P or by sequential CVD growth of an As-doped or P-doped film.

Observations such as the above were made in experiments performed in a H_2 atmosphere, and previous studies at Rockwell have shown that much larger amounts of dopant are needed to produce a given impurity concentration in SOS films (Ref 6) grown in a He atmosphere than in a H_2 atmosphere. Also, the efficiency of the doping process changes with growth temperature and the specific growth process used. Preliminary data obtained in earlier research (Ref 6) indicate decreases in carrier concentration at high growth temperature in SOS films for a constant growth rate and constant dopant flow rate, but no definite trend was apparent over the temperature range studied (1040-1080°C). If low temperatures are to be used eventually in this program for deposition in halide-containing atmospheres, it is not evident what the doping trends will be.

It would also be expected that higher concentrations of dopants must be added in the gas phase to achieve a given effective impurity concentration in the Si as the layer becomes more polycrystalline, especially if the defects in the layer act as sinks for the impurities. The results of electrical measurements on films doped for various nominal concentrations should indicate any such effects, and such measurements are being made (see Task 5).

Thus, p-type doping experiments using B_2H_6 as the dopant source were initiated, first on high-resistivity (100)-oriented n-type Si single-crystal substrates to test the quality of the dopant source, followed by growth on sapphire and polycrystalline alumina substrates for comparative purposes.

The B source was nominally 46 ppm B_2H_6 in a He carrier in order to minimize the presence of H_2 in experiments involving an inert atmosphere. Different concentrations of B_2H_6 were introduced into the growth atmosphere, either by injecting the dopant source directly from the tank into the carrier gas stream containing SiH_4 or by using a gas proportioner, which dilutes the tank source of B_2H_6 with the carrier gas before injection into the main gas stream containing the SiH_4.

By varying the amount of proportioned gas injected, it was possible to demonstrate the growth of B-doped Si films on sapphire over a large carrier concentration range, as shown in Figure 2-49. Doping levels as high as 5×10^{19} cm^{-3} have been measured in Si films grown on sapphire and on polycrystalline aluminas. The electrical properties of various B-doped films grown to date are discussed in Para 2.5.

During the third quarter a series of doping experiments was performed in order (1) to provide samples of epitaxial CVD Si on sapphire for solar cell processing at OCLI (Task 6) for baseline reference data, and (2) to establish the relationship between added dopant concentration and measured active carrier concentration in films grown simultaneously on polycrystalline aluminas and on sapphire, especially at low B doping levels. Films 20-25 μm thick were grown with B_2H_6 flow rates as low as 0.2 ccpm to as high as 500 ccpm. The results of these experiments are described in Para 2.5 (Task 5). Just as in the case of the HCℓ experiments described in the previous section, some difficulties were encountered in the recent doping experiments with the polished MRC Superstrate substrates tending to move off the pedestal during the initial heating and/or during deposition.

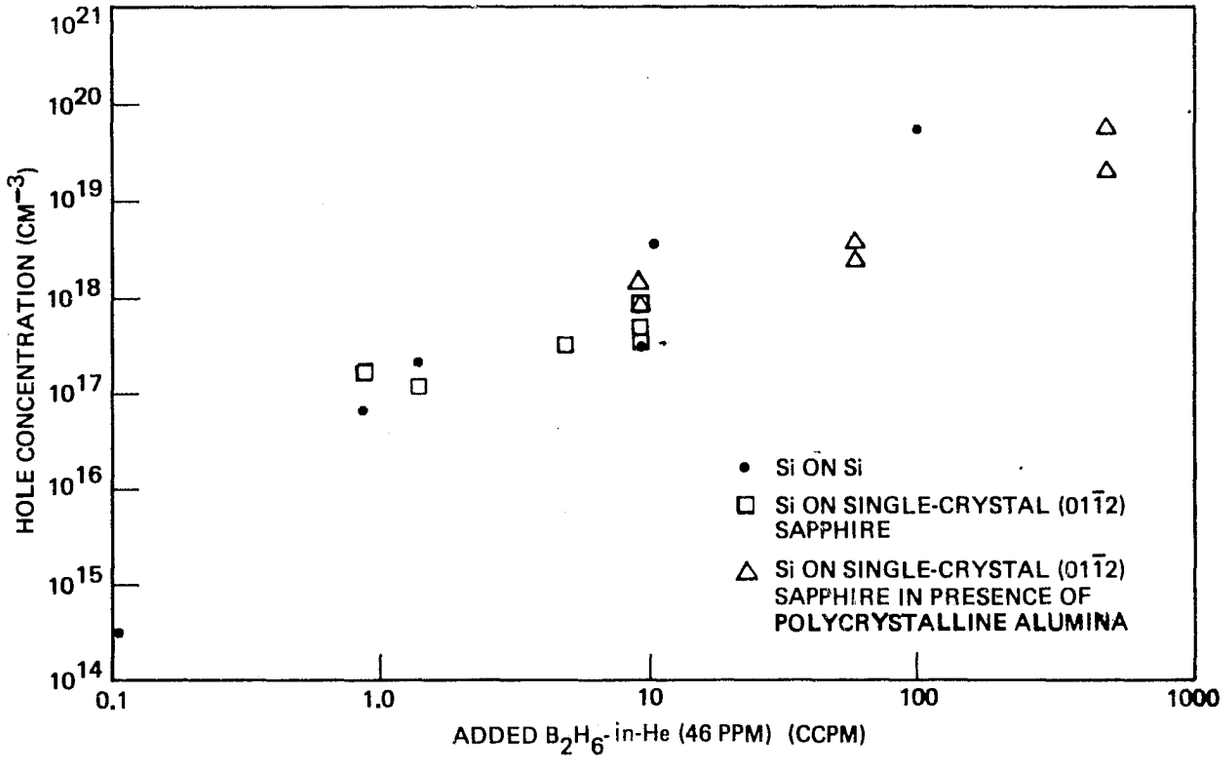

Figure 2-49. Measured Carrier Concentrations in Epitaxial CVD Si Films as a Function of B_2H_6-in-He (46 ppm) Additions.

2.4 TASK 4. PREPARATION OF Si SHEET SAMPLES

The work of Task 4 is entirely in support of the activities of Tasks 3, 5, and 6. It consists primarily of the preparation of individual samples or groups of samples of CVD Si on various substrates, utilizing established deposition procedures. These samples are mainly for use in film characterization studies (Task 5), to examine the variation in Si properties with systematic deposition parameter variations, or for use in fabrication of exploratory solar cell structures at OCLI (Task 6). Occasionally, special samples of a non-routine nature are prepared which still do not require extensive exploratory evaluation of the interdependence of CVD parameters on the resulting properties of the films; such work is also a part of this task. Any samples prepared strictly for demonstration purposes or exclusively for delivery to JPL are also considered part of this task.

Of over 165 Si CVD experiments done in the reactor system during the first nine months only about 20 utilized established or standard procedures strictly for preparation of routine samples for analysis, processing, demonstration, or delivery to JPL. All other experiments were exploratory in nature.

Ten samples, representative of various Si CVD experiments carried out on the contract prior to mid-April, were delivered to JPL on April 16, 1976, at the request of the JPL Technical Manager.

An additional four samples of CVD Si were delivered to JPL on September 14, 1976, at the request of the JPL Technical Manager.

2.5 TASK 5. EVALUATION OF Si SHEET MATERIAL PROPERTIES

During the first quarter several procedures were developed and/or applied to the characterization of Si sheet material produced by CVD on various substrates under investigation. The surfaces of the films were characterized by x-ray diffraction, reflection electron diffraction, scanning electron microscope, optical microscopy, and surface profilometric techniques. X-ray diffraction methods were used to obtain information on the amount of preferred orientation and the grain size in films deposited on polycrystalline alumina at several different temperatures. Methods of SEM analysis and classical metallography combined with etching procedures were used to provide some evidence of vertical or columnar growth in Si films on alumina. Only limited electrical measurements were made, primarily because of the emphasis on structural properties of the films and the fact that only undoped films had been prepared during the first quarter.

As the program progressed and doped films were prepared, additional techniques were utilized for film evaluation, including (1) the spreading resistance method for obtaining profiles of electrical properties (and thus impurity and/or defect concentrations) in polycrystalline Si films, and (2) measurement of minority carrier lifetime in CVD Si films on various substrates, using the pulsed C-V method in MOS structures. In addition, a comparison of van der Pauw and Hall bridge methods for measurement of charge transport properties in CVD Si films was undertaken, and a laser etching method of defining Hall bridge patterns in Si film samples was evaluated in preliminary experiments. Several of the Si film characterization procedures are outlined in the following sections.

2.5.1 Evaluation Procedures for Films

2.5.1.1 Surface Profilometry

Surface roughness and details of other topographic features of both films and substrates have been measured by surface profilometry using a Sloan Dektak. This instrument can also be used for film thickness measurement when an abrupt step from film to substrate can be formed by removal of the Si film by masking and etching procedures.

Surface profilometry has been used to examine and record the surface finish on a variety of the polycrystalline ceramic substrates of interest — both polished and as fired — and is a rapid and useful screening procedure to provide a view of the overall surface finish as well as a quantitative measure of localized surface features, such as pits, steps, etc. Similar information on the Si films deposited on various substrate surfaces has been obtained by this means. Additional details were given in Para 2.2.5.

2.5.1.2 X-ray Diffraction Analyses

To apply the techniques of x-ray diffraction line broadening to the determination of average particle or grain size in a polycrystalline specimen, such as Si films prepared under conditions that do not produce epitaxial (single-crystal) growth, it is necessary to know the diffraction line width in the absence of any grain-size broadening effects. This line width is the combined result of the true diffraction line width —which is finite because of such factors as non-perfect crystals, imperfectly collimated x-ray beams, and non-monochromatic incident radiation — and instrumental line broadening, associated with factors such as the width of the effective x-ray source in the particular diffractometer used.

It is generally considered that grain sizes in excess of ~0.1 μm do not produce any x-ray line broadening due to crystal size effects alone. Thus, the diffractometer trace obtained with a polycrystalline sample containing randomly oriented grains significantly larger than ~0.1 μm should provide a measurable reference line width free of size broadening effects, i.e., with zero grain-sizing broadening. Such a zero-broadening Si sample was prepared by grinding single-crystal (Czochralski) wafers with an agate mortar and pestle. The resulting charge was then passed through a No. 140 sieve (105 μm apertures), and this charge in turn was passed through a No. 325 sieve (44 μm apertures). The powder remaining on the latter sieve consisted of single-crystal Si particles in the size range 44-105 μm; although smaller particles would have permitted preparation of a more uniform sample for x-ray purposes, the sieved powder was adequate. Masking tape was then used as a "floor" in the sample aperture of a standard diffractometer sample holder, the tape was sprayed with Krylon, and layers of dispersed powder and Krylon were built up to form the reference sample. After drying, the sample was used to produce reference diffraction lines free of particle-size broadening.

The width of an x-ray diffraction line is usually measured as the breadth at half-maximum intensity and is expressed as an angular width, in terms of the Bragg angle. The measured breadth of a Si line exhibiting broadening due to particle-size effects is corrected for the observed zero-broadening breadth of the same Si diffraction line obtained with the reference powder sample, and the resulting value for the broadening is then used in the Scherrer formula to obtain an estimate of the particle (or grain) size.

This method has been applied in the evaluation of grain size in a variety of CVD Si films grown throughout the program to date. It has been used in conjunction with reflection electron diffraction (RED) and with inspection of the Debye rings in back-reflection Laue patterns obtained for the same samples. The latter method - that of examining the "graininess" or continuity of Debye rings in back-reflection patterns - provides a relatively rapid screening procedure for estimating grain sizes in the range down to a few microns.

A Philips Model 3181S Angle Mode Programmer System with teletypewriter output has been purchased for use with the x-ray diffractometer system employed in these studies. This equipment will be used for rapid acquisition (with printout) of diffraction line profile data by automatic angle-stepping, counting, and repeat cycling. This will facilitate examination of film samples where line broadening due to grain size is to be measured.

Another application of x-ray diffraction techniques permits the determination of preferred orientation tendencies in polycrystalline materials. The degree of preferred orientation in some of the Si films prepared in these studies has been evaluated by examination of the relative intensities of the principal low-index diffraction lines in the x-ray spectrum obtained with the diffractometer.

For example, in one of the first applications of the technique early in the program, a film grown on a single-crystal $(01\bar{1}2)$-oriented sapphire substrate in H_2 (flow rate 4 ℓpm) at ~1025°C at a growth rate of ~0.5 μm/min to a thickness of ~10 μm (but without the pre-deposition high-temperature etch) was evaluated. It and two similar films grown at lower temperatures (~600 and ~850°C) were examined for preferred orientation using Cu K-alpha radiation at 50 KV and 20 ma. Epitaxial

growth was found, as expected, in the 1025°C sample, with the {100} Si planes grown parallel to the $(01\bar{1}2)$ plane of sapphire - i.e., the surface plane. (This is a previously observed and reported epitaxial relationship.)

With both the ASTM Index line intensities and the intensities from a standard Si specimen as the comparison basis, it was found that the 600°C film was randomly oriented polycrystalline Si with very small grain sizes. The 850°C film, on the other hand, exhibited a {110} preferred orientation parallel to the interface. This sample had an average grain size several times larger than the low-temperature film but still quite small.

Careful investigation of the effects of deposition parameters - notably, temperature, growth rate, and doping species and concentrations - on the relative amounts of preferential orientation in the Si films in the principal low-index planes is required in order to select the parameters most conducive to controlled columnar-type growth of the Si sheet material on various substrates used.

As discussed in Para 2.2.5, this procedure has also been applied to the evaluation of substrate materials having polycrystalline structure, such as the fired aluminas. The polycrystalline substrate materials that are of major interest - including the glass-ceramics in which firing has produced varying amounts of crystallization and preferential orientation - are systematically examined by this method prior to carrying out extensive CVD experiments.

2.5.1.3 RED and SEM Analyses

The transmission electron microscope (AEI Model EM6) can be operated in the reflection electron diffraction (RED) mode to produce a diffraction pattern of the sample surface, from which the degree of polycrystallinity or crystal perfection can be deduced. Electrons of 100 KeV energy are directed at the sample at a glancing angle (typically 1/2 to 1 deg), producing a diffraction pattern characteristic of the crystal perfrection. Because of the glancing angle, the effective penetration depth which gives the diffraction pattern is only a few hundred angstroms.

Several of the CVD Si films have been examined by this method, used in conjunction with SEM analyses. Because RED samples only the surface region of a film it is often useful to combine the technique with x-ray diffraction studies as well, since the latter methods sample greater thicknesses; the combined evaluation sometimes permits differentiation of surface and bulk structural characteristics in thin-film samples.

Another set of three epitaxial Si films grown at three different temperatures on sapphire, similar to those mentioned above, was evaluated by RED and SEM techniques. The films were grown in H_2 (4 ℓpm) on single-crystal $(01\bar{1}2)$-oriented sapphire at ~1025, ~850, and 600°C at rates of ~2, ~0.8, and ~0.01 μm/min, respectively; final thicknesses were approximately 10, 3.8, and 0.5 μm. The high-temperature etch in H_2 was not used on the substrates prior to deposition of these films.

The 1025°C sample was shown by RED to be single-crystal (100) Si, as expected. The diffraction pattern had sharply-defined Kikuchi bands, indicative of a high-perfection single crystal with a relatively flat surface. The 600°C sample gave a weak pattern with extremely faint, broad diffraction rings, indicative of a film containing at best a small amount of extremely fine-grained polycrystalline material.

When viewed with the SEM, the 600°C sample surface was smooth and featureless at all magnifications. The 1025°C sample appeared smooth upon visual and low-power examination, but at magnifications above 1000X a number of growth defects were visible. These defects are twinned and multiply-twinned regions, commonly found in epitaxial Si films grown on both single-crystal sapphire and bulk Si substrates. As grown, the defects appeared as slight depressions with threefold symmetry. The 850°C sample has a matte black finish visible to the naked eye, suggesting an anomalous growth pattern. SEM examination revealed large whiskers and irregular growth protruding from the surface, confirming that it was indeed an anomalous sample, contaminated during growth.

Two different types of etchant were used on these samples to delineate grain boundaries and other defects. The first was a modified Sirtl etch, commonly used to delineate growth defects in bulk Si — a 5:2:1 misture of H_2O, HF, and CrO_3. Etching for 15 sec clearly delineated the growth defects in the 1025°C film, etching a deep groove between the defects and the surrounding single-crystal region. SEM examination produced striking evidence of the etching, and could have been used to determine quantitatively the defect concentration. Etching of the 600°C film did not change the surface morphology appreciably. The surface remained nearly featureless up to 24,000X magnification with the SEM.

The second etchant used on the 600°C Si-on-sapphire film was KOH:alcohol, a highly anisotropic etchant. Since the predominant Si orientation on this sapphire orientation is {100} when epitaxy occurs, it was thought this etchant might delineate individual grains by attacking the {100} -oriented planes, even though the film was largely randomly oriented. SEM examination at magnifications up to 25,000X showed that the flat surface of the film remained essentially unchanged in appearance until the entire thin Si layer had been removed, after about 30 sec of etching.

This type of SEM analysis, occasionally combined with RED examination, has been used regularly to evaluate film surface topography, internal crystal structure (including grain size) of the Si films, and characteristics of the film-substrate interfacial region.

Other operational modes of the scanning electron microscope — including electron channeling pattern generation for characterizing crystal perfection and orientation when grain sizes are sufficiently large, and the electron-beam-induced current (EBIC) mode for observing electrical characteristics such as minority carrier diffusion lengths when potential barriers are introduced — will be employed for sample evaluation as the program develops.

2.5.1.4 Electrical Measurements

Measurements of Si film resistivity, carrier concentration, and carrier mobility have been made routinely on most of the film samples, utilizing either the van der Pauw method (Ref 9) or the more accurate and conventional Hall-effect bridge method. The former method is particularly convenient as it permits measurements on a film sample of arbitrary shape without extensive processing. However, for films on insulating substrates, a bridge pattern etched in the film by photolithographic techniques is more desirable for Hall-effect and resistivity measurements. A major advantage is that a composite pattern of several Hall bridges arranged in various orientations can be etched in the layer; thus, data may be obtained on anistropy effects and/or variations in film properties with position on the film.

The van der Pauw method for measuring the electrical properties of semiconductor films was examined in earlier studies at Rockwell (Ref 6) to determine the accuracy of the technique when applied to the evaluation of Si films on sapphire. Electrical data obtained by this method were compared with those found with the standard bridge-type samples subsequently etched into each of the films. In most cases the resistivity found by the two methods differed at most by less than six percent, with the bridge method always yielding the smaller value. The carrier concentrations had a wider range of variation, with the bridge value being an average of 12 percent smaller. The largest variation occurred in the Hall mobility; the bridge values were an average of 16 percent larger than those found by the van der Pauw technique. Some comparisons of the two techniques have been made on Si films prepared in this program; these results will be enumerated in a subsequent report.

Measurements of the Hall coefficient to obtain carrier mobilities in polycrystalline films require careful interpretation. The barrier model for charge transport in polycrystalline films, as developed by Kamins (Ref 10) and later by Rai-Choudhury and Hower (Ref 11), does not provide a very good framework for application of the conventional measurements of Hall mobility. In a film in which the resistivity may be largely that due to the grain boundaries, the measured Hall effect will be mainly that associated with carrier transport in the lower resistivity regions, that is, in the interior of the crystal grains. Thus, the resistivity and Hall coefficient (i.e., carrier concentration) values that are combined to give carrier mobility may not really be representative of the same portions of the film. As a result, the calculated Hall mobility will be a somewhat artificial parameter which, although useful as a figure of merit for the film as a whole, may not have its usual rigorous significance.

The resistivity of polycrystalline Si films has occasionally been measured by simple two-terminal voltage-current methods; the agreement between results obtained by such a procedure and those from van der Pauw measurements, for example, has usually been acceptable--in one reported instance less than six percent difference (Ref 12). When large numbers of film samples are to be measured there is real advantage to this simpler technique, but four-terminal methods are generally to be preferred. For rapid evaluation of electrical properties of some of the Si films prepared in this program a conventional four-point probe is used to provide an indication of film resistivity. In most instances to date it has been found that the four-point probe data have agreed closely with resistivity values obtained by the van der Pauw or the bridge methods.

The Hall bridge pattern used for most of the measurements in the first nine months of the contract is shown in the photograph of Figure 2-50. The pattern shown is etched in single-crystal Si grown on a sapphire substrate; the sapphire was polished on one side only, accounting for the grainy background of the lapped backside of the wafer. The film in this case was 3.4 μm thick. There are several mask sizes available with this particular pattern, but the one shown is approximately 0.3 cm on a side.

The formation of sharply defined Hall bridge patterns in thick (20-50 μm) polycrystalline Si films presents several problems. Conventional photoresist and masking techniques are generally unsuitable, as the resist is degraded by the required long exposure to the etchant, and the rough polycrystalline film surface reduces the effectiveness of the resist bond to the sample surface.

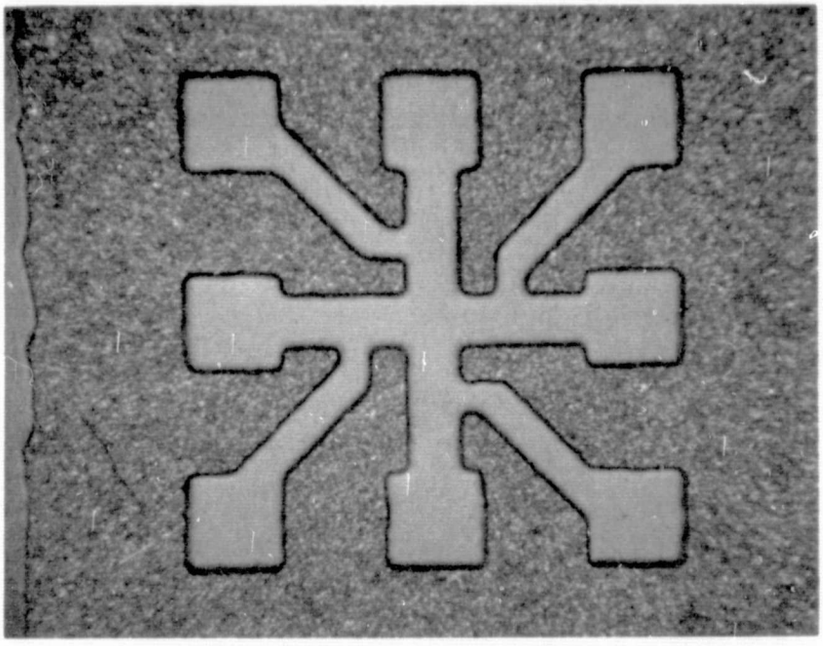

Figure 2-50. Hall-effect Bridge Pattern Photolithographically Etched in CVD Si Film on Single-crystal Sapphire Substrate. (Width of current path 310 μm, length 910 μm, pattern approximately 2.8 mm square.)

Two possible solutions have been investigated. One involves the use of the focused beam of a 5-Kw YAG laser Q-switched at 1200 pps and computer-programmed to trace the outline of a bridge pattern in the film. The beam is used either to melt a patterned groove in a protective mask, to be followed by chemical etching in the groove to isolate the bridge, or to melt/vaporize a groove in the Si film directly, in this same pattern. In the latter modification the pulsed laser beam "scribes" a channel in the film; the channel is then etched to remove any remaining Si at the bottom of the channel as well as the Si on the sidewalls of the channel that may have been damaged (or altered in its properties) by the local fusion produced by the laser beam.

The results obtained in one exploratory application of the technique are shown in Figure 2-51. In this instance a portion of a thick (~45μm) polycrystalline Si film grown on ASM805 polycrystalline alumina was laser-scribed to define the edges of a Hall bridge pattern, one corner of which is shown in the SEM photograph in Figure 2-51a. SEM examination of the film after laser-scribing the full thickness of the film showed that essentially no Si remained on the substrate at the bottom of the channel. Figure 2-51b shows a vertical view of the channel in the thick Si film, before etching. Evidence of the regularly-spaced laser-beam "strikes" can be seen in the alumina substrate surface along the channel bottom. This method is being further tested, as it appears quite promising.

The second method involves a two-step varnish-and-photoresist application, in which the desired pattern is developed in the photoresist and then transferred to the varnish, which is then used to produce the patterned region in the Si. This method appears to be satisfactory for etching layer thicknesses of at least 20 μm, but the amount of control over lateral dimensions of the pattern remains to be determined. Work on this method is continuing, also.

(a)

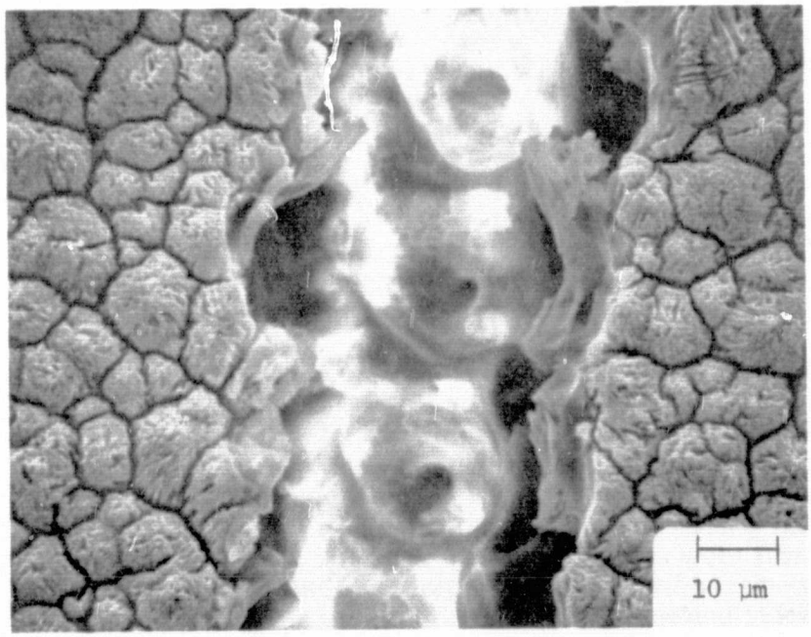

(b)

Figure 2-51. SEM Photographs of Channel Produced in Si Film by Pulsed Laser Scribing. (a) Defining the Bridge Pattern; (b) Vertical View of Channel and Exposed Polycrystalline Alumina Substrate.

The pulsed MOS C-V (or C-V-t) method for measurement of minority-carrier lifetimes in Si, which has been applied successfully to the determination of lifetimes in Si-on-sapphire epitaxial material (Refs 13, 14), provides a possible method for determination of this parameter in the polycrystalline films being prepared in this program. The C-V method is also useful for measuring the doping profile vs depth in thin samples. The technique is based on the depletion approximation, and utilizes the capacitance of a capacitor biased in the depletion condition to obtain plots of $\frac{1}{C^2}$ vs V. The slopes of these curves are expected to be proportional to the impurity concentration at the edge of the space-charge layer. However, this technique is limited by the inversion phenomenon.

The pulsed MOS C-V method, in which a short-duration voltage pulse is used to replace the steady dc reverse bias, was introduced as a means to measure the doping profile over a large distance into the Si region. As the technology of MOS devices progressed, it became much simpler and more convenient to study the pulse effect by monitoring the capacitance of an MOS capacitor as a function of time. Using this technique, it was shown that the bulk generation lifetime could be obtained. Zerbst (Ref 15) developed a technique which allowed both the generation lifetime and the surface generation velocity to be extracted from the capacitance-time decay curve.

A simplified schematic diagram of the apparatus used for C-V measurements is shown in Figure 2-52. For the C-t measurements the x-y recorder is simply replaced by a storage oscilloscope. Initial attempts to obtain a lifetime value for an undoped CVD Si film, grown in H_2 at ~1025°C to a thickness of about 3 μm, were unsuccessful early in the program. However, recently prepared samples of Si on sapphire, B-doped in the mid-10^{17} cm^{-3} range, have been processed into an array of isolated MOS structures — each surrounded by an ohmic contact region — on which the C-V-t method has been successfully applied. Minority carrier lifetimes the order of 10^{-7} sec have been measured in these 25 μm epitaxial samples. (See Para 2.6, Task 6.)

Other methods for measuring the effective minority carrier diffusion lengths — such as the EBIC mode of operation of the SEM and the photocurrent response of barrier structures under monochromatic infrared illumination — are also under consideration, and may prove more directly applicable for the polycrystalline films involved in this program.

Spreading resistance measurements have also been used in evaluating the electrical properties of both the epitaxial Si films and the polycrystalline Si films. The highly specialized spreading resistance (SR) apparatus is not available at Rockwell at the present time, but a specialty laboratory — Solecon Laboratories — that works exclusively with this analytical method is located in Costa Mesa, CA, only a short distance from the Rockwell facility in Anaheim. Rapid-response service by this experienced and highly-qualified laboratory is available, so excellent analytical assistance is readily accessible.

There was some question as to the validity of this type of measurement on polycrystalline Si material having grain sizes and other properties such as those obtained for the samples produced on this contract. A resistivity limitation of 10^3 - 10^4 ohm-cm characterizes the method and the apparatus now in use; films with effective resistivities less than that should be susceptible to spreading resistance analysis, with good spatial resolution. The significance of the absolute values of resistance obtained with the two-point SR probe is questionable in polycrystalline

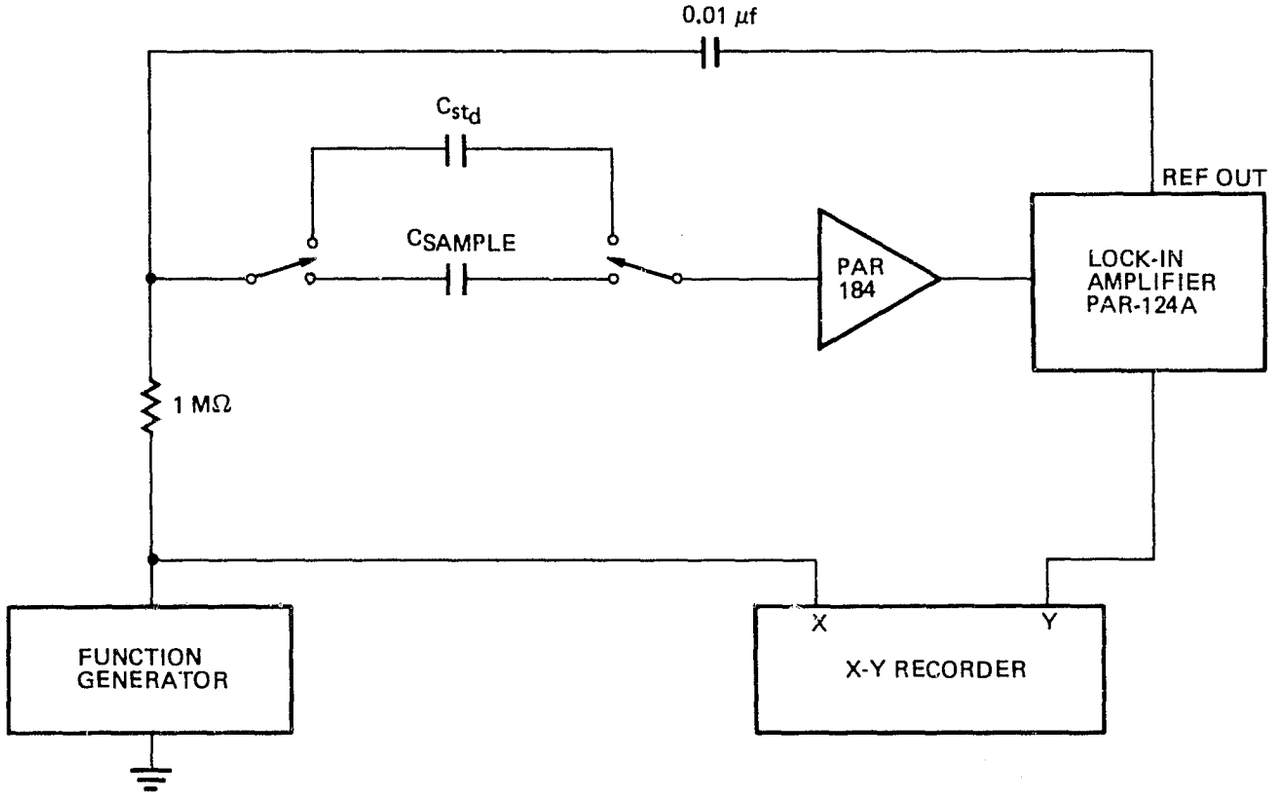

Figure 2-52. Schematic Diagram of Apparatus for MOS Capacitance-Voltage Measurements

materials. However, strong trends or any severe departures from a smooth continuous variation in resistivity as a function of depth into the layer — such as might be encountered with an impurity layer or a major change in grain size in the interior — should be revealed by the SR profile, which is obtained by making measurements on a low-angle bevel extending through the entire layer. It has been found in practice that the SR probe measurement provides data that are very consistent with the results of measurements made by the van der Pauw method or the Hall bridge method; it has also proved to be a valuable procedure for examining the variation in electrical properties in the interior of the films. (See, e.g., Para 2.5.3.)

2.5.2 Properties of CVD Si Films on Glass Substrates

A group of four undoped Si films deposited by SiH_4 pyrolysis in a He atmosphere on substrates of Corning Code 1715 glass (calcium aluminosilicate) was characterized for structural and electrical properties. The He flow rate was 6 ℓpm and the SiH_4 rate was 25 ccpm in the four depositions, carried out at temperatures of 858, 914, 955, and 1000°C. The four films are listed in Table 2-9.

The film grown at ~860°C was observed to have a dark, somewhat granular appearance due to the microscopic faceting of the surface. Examination of the specimen by SEM revealed a surface of fairly regular approximately-tetrahedral features that appeared to be ~0.9 μm in average dimension in a direction parallel to the film-substrate interface (see Table 2-9); the angular orientation of the facets was not determined.

Table 2-9. Structural Properties of CVD Si Films Grown by SiH_4 Pyrolysis in He on Corning Code 1715 Glass

DEPOS. TEMP. (°C)	AVERAGE FILM THICKNESS (μm)	DEPOSITION RATE (μm/min)	AVE. HORIZ. DIMENSION OF SURFACE FEATURES (μm)	PREFERRED CRYSTAL ORIENTATION BY X-RAY ANALYSIS*
858	5.9	0.6	0.9	VS {100}; FS {111}; A {110}
914	14	1.4	3.5	FS {100}; FS {111}; P {110}
955	16	1.0	4.0	P {100}; P {111}; FS {110}
1000	20	1.0	3.3	P {100}; P {111}; P {110}

*VS = very strong; FS = fairly strong; P = preferred, but only moderately; A = not detected.

SEM photographs of the film surface at two different magnifications, one at normal incidence and one at a 45 deg viewing angle with the sample surface, were shown in Figure 2-38 (Para 2.3.5.1). The regular faceting of the surface features is clearly visible in the normal incidence view of Figure 2-38a. The oblique view in Figure 2-38b shows the steep sides of the largely tetrahedral features. This film has external characteristics quite similar to some of the Si films obtained earlier in the program on relatively fine-grained polycrystalline alumina substrates. It is striking that such characteristics have been obtained on an amorphous substrate; these results offer considerable encouragement for continued work with this glass substrate material.

Analysis of the x-ray diffraction line profiles for this film indicated a very strong preferred {100} orientation, consistent with the external tetrahedral surface morphology observed in the SEM examination. There was also evidence of stronger {111} orientation than is characteristic of random polycrystalline Si. The {110} orientation did not appear to be detectable in this film.

The other three films on 1715 glass were also examined. X-ray diffraction analysis of these films - in terms of the relative intensities of the (111), (220), (311), and (400) lines - was carried out using both graphical analysis of the diffractometer traces and numerical results obtained from the new angle-mode programmer attachment for the diffractometer. The analyses clearly show a steady decrease in the amount of preferred {100} orientation with increasing growth temperature, although even at 1000°C this orientation is more prevalent than in a randomly oriented polycrystalline Si sample. Conversely, the {110} orientation, not preferred in the film grown at ~860°C, increases in prevalence with increasing growth temperature to 955°C, and then decreases somewhat at 1000°C.

Similar evidence of a maximum in the degree of preferred {110} orientation in this same general deposition temperature range and film thickness range was observed by Kamins and Cass (Ref 4) for CVD Si polycrystalline films deposited on thermally oxidized Si wafers. The {111} orientation, appearing as a preferred orientation in the film deposited at ~860°C, also appeared to decrease steadily with increasing deposition temperature - a result different from that found by Kamins and Cass for Si on SiO_2. (See Table 2-9.)

Examination of the same three specimens in the SEM showed surface features somewhat like those found on the film grown at ~860°C. However, the average horizontal dimension of the regular surface features was found to be 3.5, 4.0, and 3.3 μm for the films deposited on 1715 glass at 914, 955, and 1000°C, respectively (Table 2-9). It should be noted that the film grown at ~860°C was only about 6 μm thick, while the other three were two to three times as thick. If, as earlier evidence has indicated, individual grains tend to increase in horizontal dimension as the film thickness increases, then some of the difference between the observed surface-feature dimension for the 860°C film (~0.9 μm) and that of the other three films (3-4 μm) could be attributed to the thickness difference.

The difference in the surface characteristics of the films deposited at the higher temperatures is shown by the SEM photographs of the 1000°C film, which were shown in Figure 2-39 (Para 2.3.5.1). Considerably coarser surface features are evident, there are numerous tall bulbous projections, and faceting of the surface features is almost absent.

The two films deposited at the intermediate temperatures (914, 955°C) exhibited surface structures intermediate between those shown in Figures 2-38 and 2-39. The film deposited at 955°C resembled that deposited at 1000°C (Figure 2-39), while that grown at 914°C still exhibited some faceting, although not nearly as pronounced as that shown in Figure 2-38.

Electrical measurements were made on the four undoped Si films on Corning Code 1715 glass, using a Hall bridge pattern on all films and the van der Pauw method on all but the film grown at 860°C. The van der Pauw method was used first; then a Hall bridge pattern was photolithographically etched into the Si film in the center of the region in which the van der Pauw measurements were made. Resistivity in all four was high, ranging monotonically from 2.8×10^5 ohm-cm in the film grown at ~860°C down to 8.1×10^4 ohm-cm in the film grown at 1000°C. All films were p type as grown, with measured carrier concentrations in the range from 5×10^{11} to 1×10^{13} cm^{-3}. The films grown at the two intermediate temperatures (914 and 955°C) exhibited the highest carrier mobilities and the lowest carrier concentrations. Results of these measurements are given in Table 2-10.

Also included in the table are the results of electrical measurements on an undoped Si film deposited at ~860°C on Owens-Illinois glass GS211, a proprietary high-temperature glass of unspecified composition. The film was deposited in He carrier gas at a flow rate of 6 ℓpm with the SiH_4 flow rate 25 ccpm, resulting in an average thickness of ~35 μm. This undoped polycrystalline film was much more conducting than those on the Corning glass. A p-type carrier concentration $\geq 10^{15}$ cm^{-3} indicates a fairly high density of structural defects or, more likely, a significant impurity content in the film – presumably from the glass.

Table 2-10 also includes, as the last entry, the results of electrical measurements on a B-doped Si film deposited at 850°C on Corning Code 1715 glass. A high flow rate of B_2H_6-in-He was used in order to achieve a large doping concentration in the film (see Figure 2-49, Para 2.3.6).

X-ray diffraction analysis of the film grown on GS211 indicated strong {110} preferred orientation, and the {100} orientation was stronger than in a random polycrystalline Si sample but not predominant. Figure 2-40 (Para 2.3.5.1) showed SEM

Table 2-10. Electrical Properties of CVD Si Films* Grown by SiH_4 Pyrolysis† on Glass Substrates in He Carrier Gas††

SUBSTRATE	DEPOS TEMP (°C)	AVE FILM THICKNESS (μm)	METHOD OF MEAS**	RESISTIVITY (ohm-cm)	CARRIER CONC.* (cm^{-3})	CARRIER MOBILITY (cm^2/V-sec)
Corning 1715 Glass	858	5.9	HB	2.8×10^5	1.1×10^{13}	2.0
	914	14	vdP	1.3×10^5	5.8×10^{11}	82
			HB	1.1×10^5	5.0×10^{11}	111
	955	16	vdP	1.0×10^5	7.7×10^{11}	81
			HB	4.5×10^4	1.5×10^{12}	95
	1000	20	vdP	7.3×10^4	1.1×10^{13}	7.7
			HB	8.1×10^4	1.8×10^{12}	43
Owens-Illinois GS211 Glass	861	35	vdP	82.5	3.5×10^{16}	2.2
			HB	2×10^3	1.0×10^{15}	3.1
Corning 1715 Glass	850	70	vdP	0.004 xx	4×10^{19} xx	36 xx
			FPP	0.004 xx	–	–

* All films p type; all undoped except last entry

† SiH_4 flow rate 25 ccpm

†† He flow rate 6 ℓpm

** HB = Hall bridge; vdP = van der Pauw; FPP = Four point probe

xx Film doped by addition of 500 ccpm of B_2H_6-in-He to reactant stream

photographs of the surface of the film deposited on the GS211 glass. The deeply textured surface is seen to be more irregular than that found on the Si film deposited at the same temperature on Corning Code 1715 glass (Figure 2-38). The surface features have an average horizontal dimension of about 4 μm, essentially the same as the surface features observed on the three thick Si films on Corning Code 1715 glass at the higher temperatures, yet they resemble the tetrahedral morphology seen in Figure 2-38b. The large chunks of Si (or other material), referred to earlier, are quite visible in Figure 2-40a.

All of the Si-on-glass films discussed above have a general surface character similar to the rosette type of structure observed on Si films grown on polycrystalline as-fired alumina substrates and described in detail in the next section. Significantly different, however, is the greater degree of crystallographic faceting found in the films on glass and the larger angles made by these facets with respect to the nominal substrate surface plane.

2.5.3 Properties of CVD Si Films on Polycrystalline Alumina Substrates

The Si films grown on the three alumina substrates ASM805, Superstrate, and ADS995 at temperatures of 1025 and 1100°C (in H_2) early in the program and described in some detail in Para 2.3.5.2 were characterized extensively.

The average surface roughness of each of the three as-fired aluminas, as measured by the Dektak, was given in Tables 2-3 and 2-5: ASM805 (smooth), ≤ 0.1 μm; ASM805 (rough), ~0.25 μm; Superstrate, ~0.15 μm; ADS995, ~0.35 μm. Representative segments of Dektak traces for both the alumina substrate surface and the as-grown Si film on it (grown at 1025°C in 4 ℓpm H_2 and 10 ccpm SiH_4)are given for all three in Figure 2-53. The extent to which the surface roughness of the film is influenced by the topography of the substrate surface is emphasized by these traces. The apparent average peak-to-valley dimensions of the surface features on the films are ~0.7, ~1.0, and ~0.6 μm for the films on MRC Superstrate, ADS995, and ASM805 (rough side), respectively, although the latter exhibits some extreme vertical excursions. These figures are consistent with the average peak-to-valley surface roughness indicated above for the three substrate surfaces involved, as well as with the actual Dektak traces for these surfaces as shown at b, d, and f in the figure.

It was indicated in Para 2.3.5.2 that the degree of preferred orientation was different on a given substrate for the films grown at 1025°C and those grown at ~1100°C. Thus, the film on ASM805 was very strongly {110} oriented at 1025°C and less strongly oriented to those planes at 1100°C. The film on Superstrate was strongly {110} oriented at 1025°C and only moderately oriented to these planes at 1100°C, with evidence of {111} preferred orientation at 1100°C as well. The film on ADS995 was only slightly oriented preferentially to the {110} planes at 1025°C and even less so at 1100°C.

It is evident that complex growth patterns are involved in these films that are grown on substrates that themselves have complicated crystalline configurations. More detailed examination of the amount of preferential orientation of a given crystallographic plane that occurs as the growth temperature is varied throughout the range of interest would help to clarify the dominant processes involved in determining orientation tendencies. Further evidence of the complexity of these relationships is the fact that the substrate with the least detectable preferred orientation of the three – the ADS995 – is the one that appeared to support the most extensively faceted Si overgrowth (see Figure 2-42, Para 2.3.5.2).

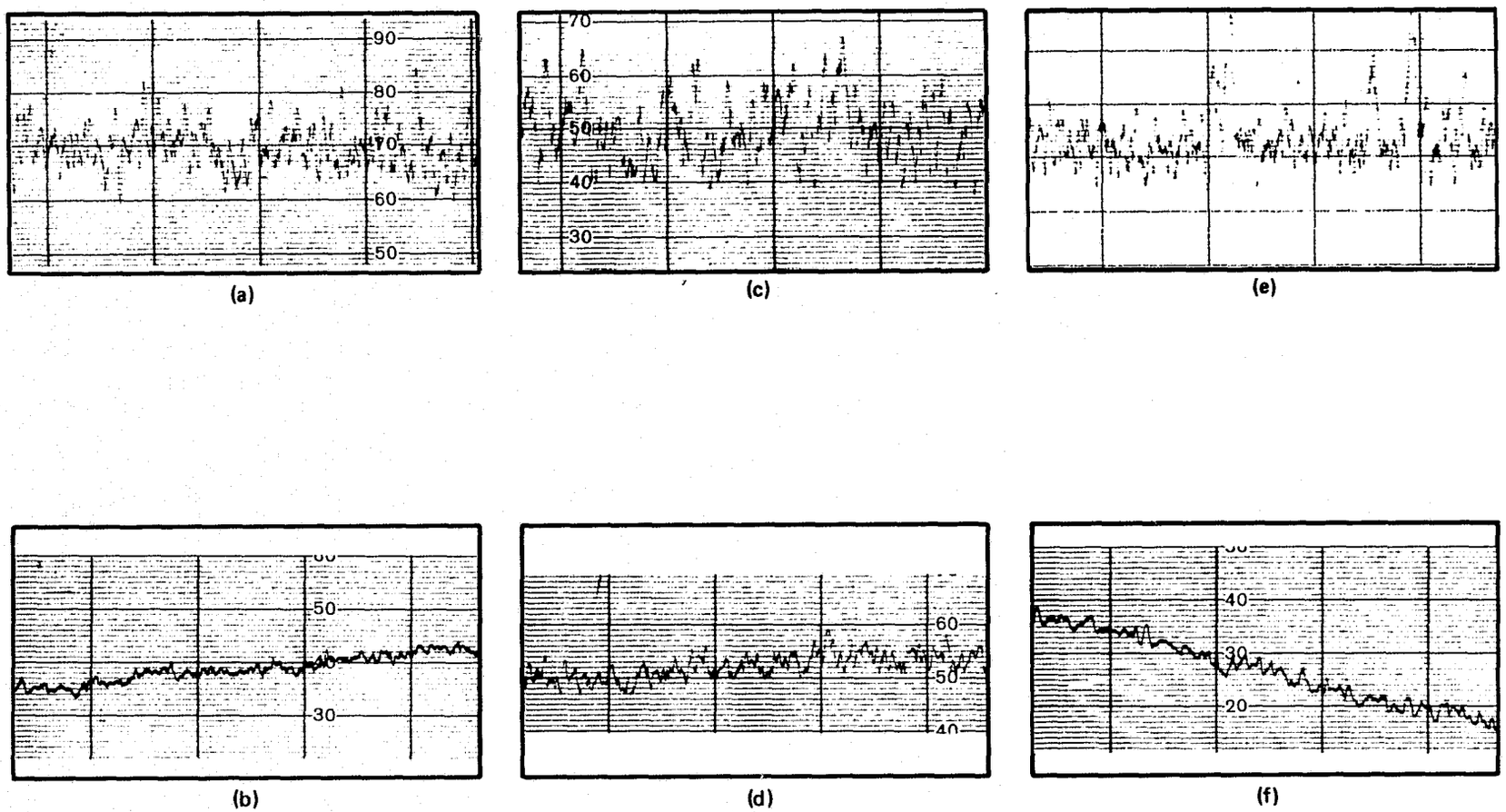

Figure 2-53. Dektak Profilometer Traces for As-Fired Surfaces of Polycrystalline Alumina Substrates and for As-Grown Surfaces of CVD Si Films (SiH_4 Pyrolysis in H_2 at 1025°C) on Each. (a) 26-μm-thick Si on (b) Superstrate (MRC); (c) 17-μm-thick Si on (d) ADS995 (Coors); (e) 27-μm-thick Si on (f) ASM805 (3M), Rough Side.

Characterization of another early set of Si films on alumina substrates – the thick films prepared at two different growth rates on ASM805 substrates at ~1025°C and described also in Para 2.3.5.2 (Figure 2-43) – produced further instructive results. Examination of broken or "cleaved" cross sections of these samples in the SEM showed peak-to-valley dimensions of the as-deposited film surfaces ranging up to 2.5 μm. Typically, however, this dimension was in the range 0.8-1.5μm for the two thinner (20-25μm) films and 1.2-1.8μm for the 40μm film.

As shown in Figure 2-54 the as-broken cross sections suggested columnar growth structure in the films, as well as some kind of transition layer in the part of the film adjoining the alumina substrate, especially in the 40μm film (Figure 2-54b).

To further elucidate the structure in these films the samples were etched for 1 min at 65°C in a 1:1 KOH-saturated H_2O:isopropyl alcohol mixture. This etch is highly anisotropic, typically etching the {100} or {110} surfaces 10 to 400 times the rate it etches {111} surfaces. After etching, the surfaces revealed the anticipated columnar structure (Figure 2-55). In addition, two other effects were visible. Certain areas exhibited faster etching to form "caves," and the top half of the film etched significantly faster than the layer adjacent to the alumina interface. This could indicate a significant difference in the average crystallographic orientation of the grains in the upper part of the polycrystalline film with respect to those nearer the alumina-film interface, with the former being more strongly {110}-oriented. It might also simply be related to a difference in the etching rate near the interface due to the effect of the nearby $A\ell_2O_3$ material.

Another portion of the same 40μm film on ASM805 was mounted for a standard metallographic cross section. Following a final step using 0.05 μm $A\ell_2O_3$ abrasive slurry on a silk polishing surface, the sample was etched in the KOH etch at 80°C for ~1 min. to delineate structural features. Figure 2-56 shows a region of this cross section after etching. The etching has delineated the vertical or columnar growth pattern and has also revealed apparent voids or "caves," most of them horizontally disposed and probably the same feature as was observed in the broken cross sections examined in the SEM. The composite photomicrograph shown in Figure 2-57 gives more detail of the region in the center of Figure 2-56, further revealing the apparent columnar growth pattern of the Si film on ASM805 alumina. Finally, examination of this metallographic cross-section sample in the SEM resulted in the photographs of Figure 2-58. These show a nearby region of the cross section at two different magnifications.

The refired ASM805 alumina substrate discussed earlier (Para 2.2.5 and Figure 2-13) was used for growth of a Si film at ~1030°C in H_2 (4 ℓpm), with a SiH_4 flow rate of 25 ccpm; the film was ~45 μm thick and grown at a rate of ~3 μm/min. It has a good typically-faceted surface with protrusions that were found, upon SEM examination, to have an average dimension of ~7 μm parallel to the film-substrate interface. This compares with surface features of <5 μm in size on films of comparable thickness grown on this alumina without the refiring. This modest but distinct enhancement of the size of the surface features on the film grown on the refired substrate was encouraging.

X-ray diffraction analysis of this film showed a very strong {110} preferred orientation, similar to that observed in Si films grown on the normally processed ASM805 substrates but much more pronounced. No evidence of {100} orientation was found in the x-ray data.

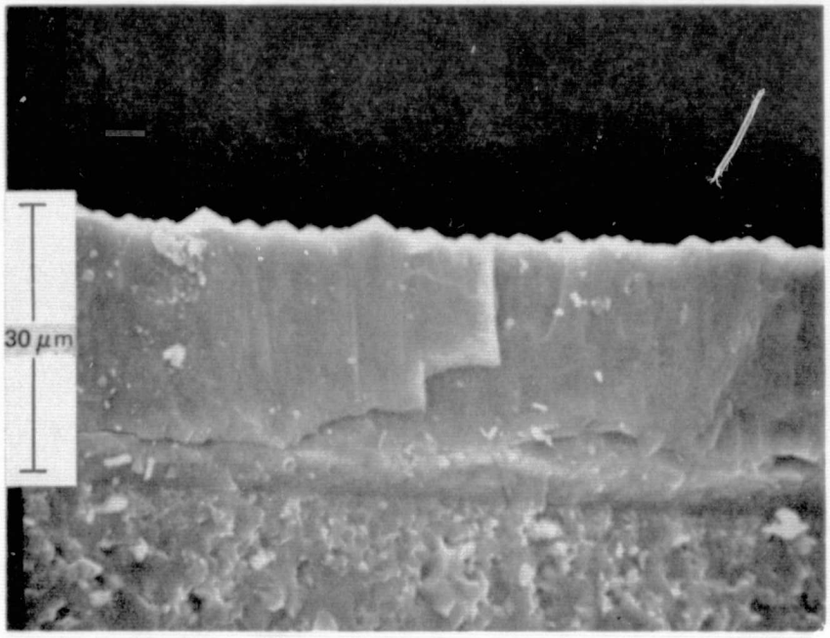

(a)

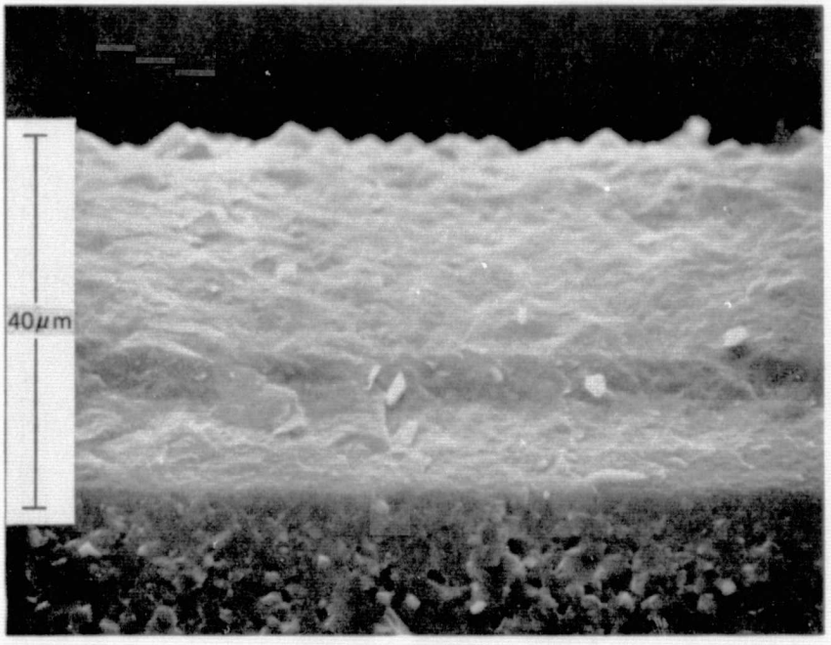

(b)

Figure 2-54. SEM Photographs of Cleaved Cross Sections of CVD Si Films Grown on ASM805 Substrates in H_2 at ~1025°C at Different Rates. (a) Rate<2μm/min, Thickness 24-30μm. (b) Rate >3μm/min, Thickness ~ 40μm.

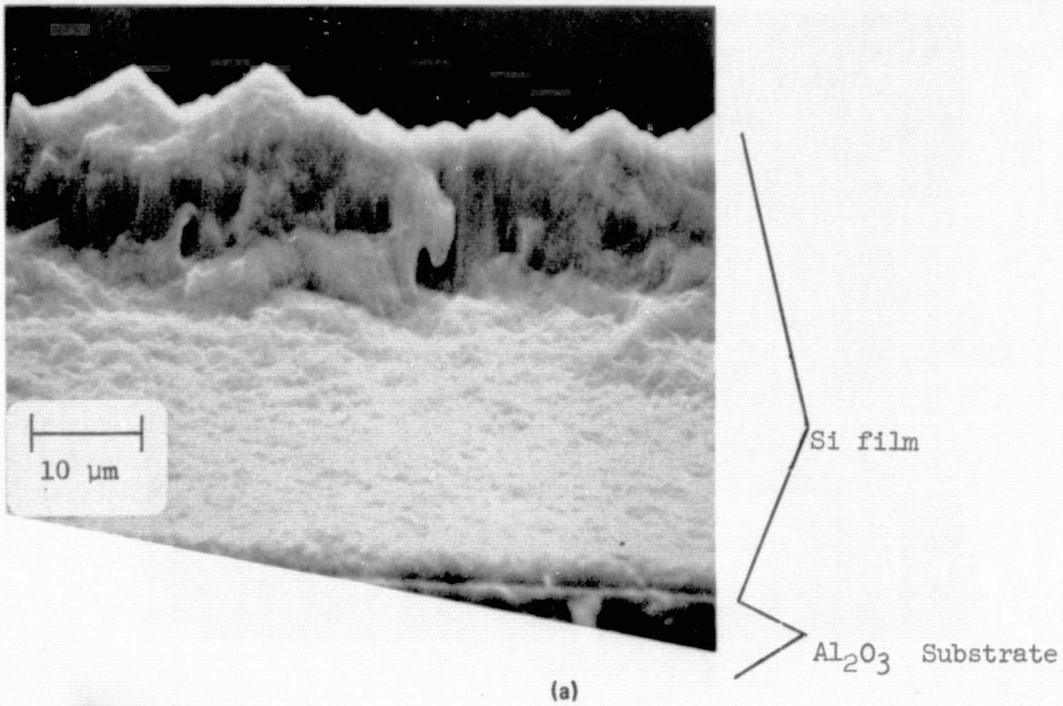

(a)

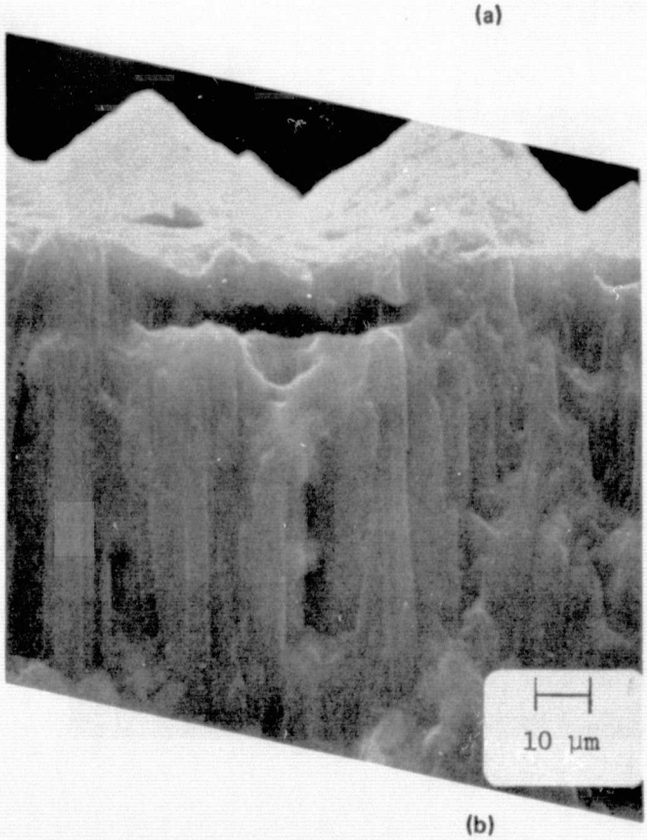

(b)

Figure 2-55. Appearance of Cleaved Cross Section of 40-μm-thick CVD Si Film of Figure 2-54(b) After KOH Etching. (a) 1500X, (b) 3000X.

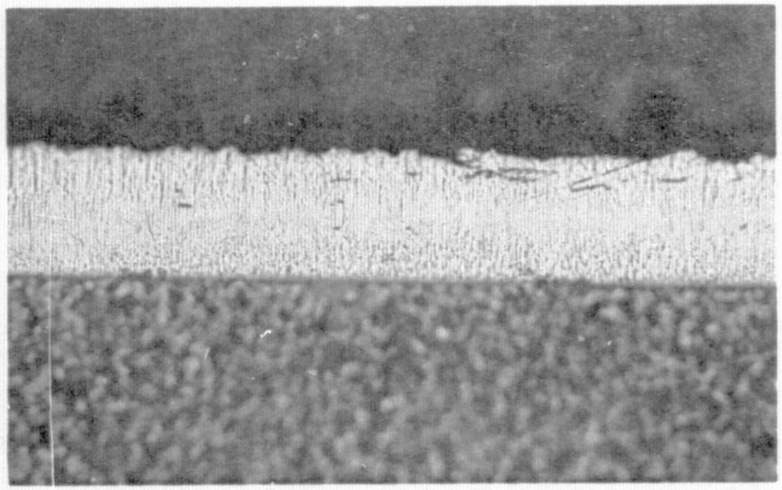

Figure 2-56. Metallographic Cross Section of 40-μm-thick CVD Si Film of Figure 2-54(b), after Polishing and KOH Etching. (Polycrystalline alumina substrate is at bottom of photomicrograph.)

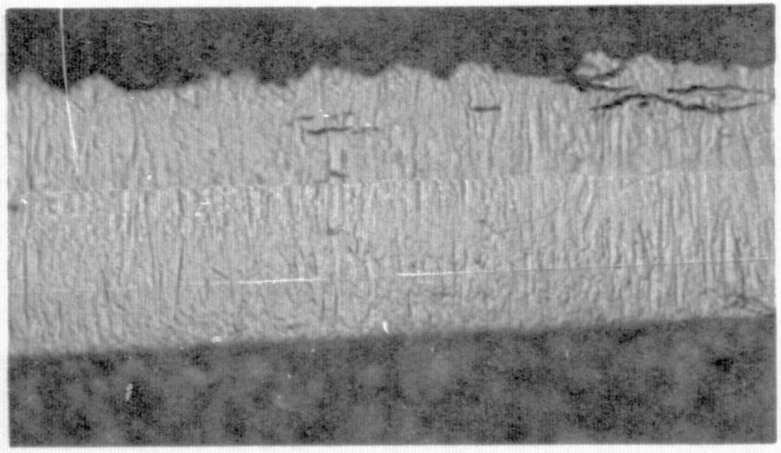

Figure 2-57. Composite Photomicrograph Showing Detail of Central Region of Figure 2-56 (40-μm-thick CVD Si Film on ASM805 Alumina)

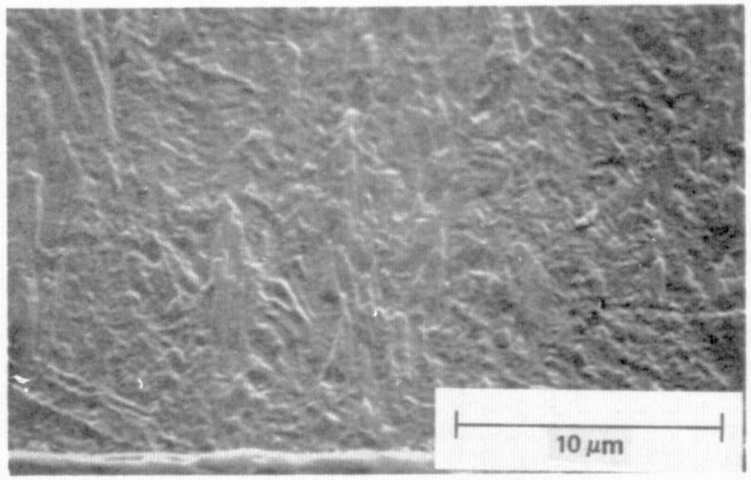

(a)

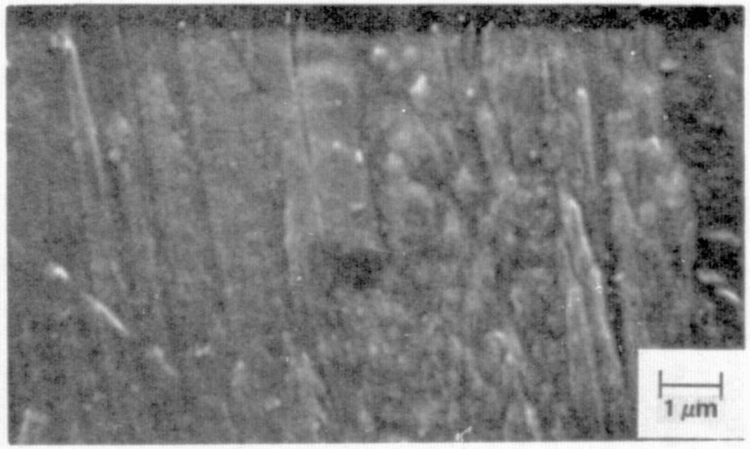

(b)

Figure 2-58. SEM Photographs of Metallographic Cross Section of Figures 2-56 and 2-57 at Two Different Magnifications. CVD Si-on-ASM805 Sample of Figure 2-54(b), Showing Apparent Columnar Growth

As a result of additional processing of this sample in preparation for electrical measurements, further information regarding grain size was obtained. Extensive etching with a modified Sirtl etch (used to produce Hall-effect bridge patterns defined by photomask techniques) produced deep trenches in the boundaries separating the three-dimensional rosette-like surface features that had been observed so clearly in SEM examination of this and other films deposited on polycrystalline alumina. The etching also resulted in some attack of the surfaces of the individual "mounds" or surface features. This is believed due to dislocations, stacking faults, or twin boundaries within the Si grains, with the etched trenches coinciding with true grain boundaries. That is, the external surface morphology appeared to accurately represent the size and shape of individual Si crystal grains in that portion of the film.

Figure 2-59 shows the surface of this Si film in the as-deposited condition as observed by SEM examination. The two photographs are at the same magnification; Figure 29a is for normal incidence and Figure 2-59b is made at a 45 deg viewing angle. The surface appearance is typical of the Si films previously grown on ASM805 alumina. Figure 2-60 shows the surface of the same Si film after the heavy etching described above, with the deep trenches around each mound clearly delineated in Figure 2-60a and the attack of the individual mounds shown distinctly in Figure 2-60b.

Efforts to define the grain boundaries in the interior of this Si layer by etching a vertical cross-section through the layer were less conclusive. Both fractured and lapped/polished sections exhibited prominent artifacts prior to etching. After etching, additional features — also believed to be artifacts — were delineated which obscured the grain boundary structure.

Spreading resistance measurements* made on this undoped sample (before etching), with appropriate corrections applied for film thickness, gave the data shown in Figure 2-61, which indicate good uniformity as a function of depth into the layer. There is evidence of a gradual decrease in net p-type carrier concentration as the film-substrate interface is approached; the approximate location of the interface for that portion of the sample measured is indicated by the vertical dashed line at ~51 μm depth. The measurements were made on a ~5-deg bevel, with a probe spacing of 30 μm and 10 μm between data points on the bevel. The ordinate scale of effective net carrier concentration is arbitrary; the automatically printed data shown are converted from the measured SR probe resistance values by a computer program for single-crystal Si, so the resulting numbers are not valid for this polycrystalline material. The trend of the data is the important thing in this figure, and the decrease in net hole concentration as the interface is approached may be indicative of a compensating donor impurity or other imperfection associated with the substrate or with the interface itself.

The undoped Si films deposited on Vistal substrates of four different firing histories (Para 2. 2. 5 and 2. 2. 6), previously discussed in Para 2. 3. 5. 2, have been extensively characterized. These films were grown at ~1025°C in H_2 (4 ℓpm) with SiH_4 flow rates of 25 ccpm; growth rates were ~3 μm/min and thicknesses 18-20 μm. In each case a pre-deposition treatment in H_2 at 1250°C for 15 min was used. Both polished and as-manufactured surfaces of all four Vistals were used in this series of depositions, always with a sapphire monitor substrate in the experiment.

*Measurements made by Solecon Laboratories, Costa Mesa, CA.

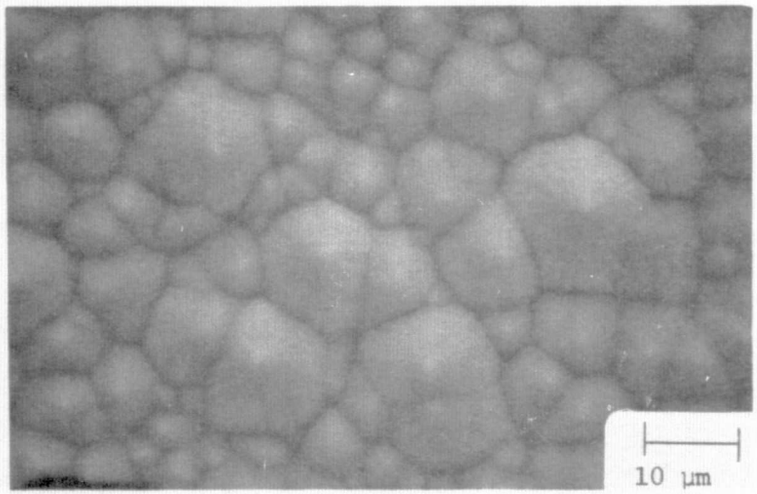

(a)

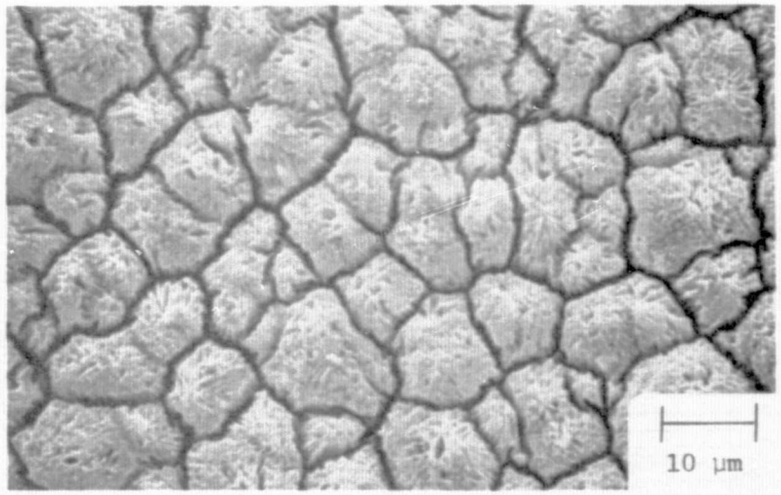

(a)

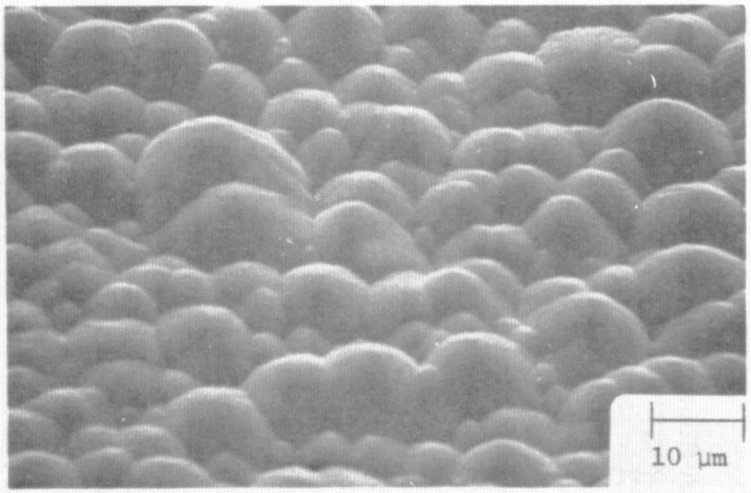

(b)

Figure 2-59. SEM Photographs of CVD Si Film on Refired ASM805 (a) at Normal Incidence and (b) at 45 deg to Sample Surface.

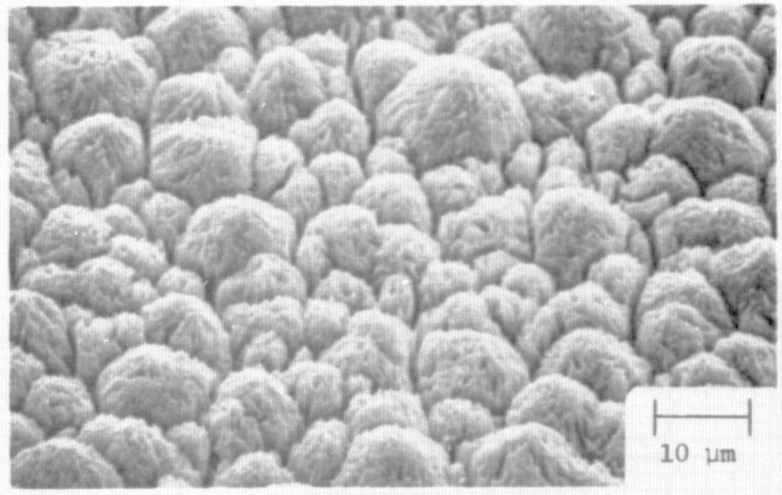

(b)

Figure 2-60. SEM Photographs of Film in Figure 2-59 after Extensive Etching in Modified Sirtl Etch.

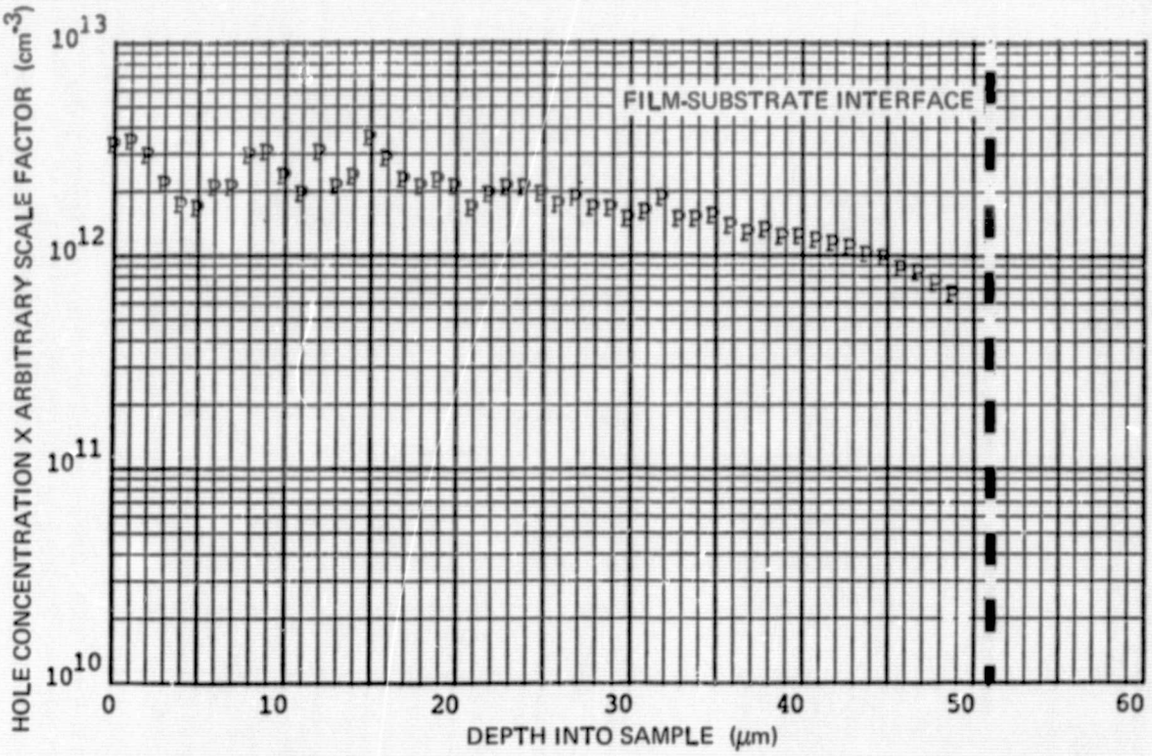

Figure 2-61. Hole Concentration (arbitrary scale factor) as Function of Depth in Si CVD Film of Figures 2-59 and 2-60, Measured by Spreading Resistance Method. (Bevel angle ~5 deg, probe spacing 30 μm, spacing between measurements 10 μm.)

The Si films grown on the polished and as-fired Vistal 4 substrates were shown in the SEM photographs of Figure 2-45 and 2-46, respectively. The film on the polished polycrystalline alumina substrate exhibited very large highly-reflective regions, prominently visible to the unaided eye, which appeared almost certainly to be epitaxial upon inspection in the optical microscope. The larger regions were typically greater than 100 μm across, with crystallographically faceted surfaces characteristic of epitaxial Si of various nominal orientations, in each case replicating in size and shape the individual substrate grain on which it had grown. Among the large epitaxial "islands" were other heavily textured regions, some of which looked like the typical fine-grained polycrystalline Si surfaces seen in earlier deposits on polycrystalline randomly-oriented alumina substrates, and others of which may also have been epitaxial (or highly oriented) regions simply tilted in an orientation such that a very rough-textured surface resulted. The overall surface texture was three-dimensional, with some of the epitaxial islands appearing to have quite different thicknesses (cf Figure 2-45b).

The film on the unpolished (as-fired) Vistal alumina substrate also exhibited very large grains — of the same dimensions as observed on the polished substrate — but many of them did not appear to be epitaxial upon inspection in the optical microscope and the SEM (Figure 2-46). Although the average dimensions of the individual growth facets on the as-fired substrate are the same as those of the polished grains on the polished substrate, the crystallographic orientations in the two cases are quite different. Thus, the structural characteristics of the Si layers in the two cases would be expected to be different, and this was, in fact, observed.

X-ray diffraction analysis of the two films on Vistal 4 alumina showed strong {110} preferred orientation in both instances, although it was very much stronger in the film grown on the polished substrate. In addition, strong {100} preferred orientation was present in the film on the polished substrate, while this reflection in the other film was only slightly greater in intensity than what would be expected for a randomly-oriented polycrystalline film. Evidence of line broadening was found in the x-ray analyses, indicating average grain sizes ~0.1 μm, apparently in conflict with the external appearance of the films. However, the numerous large epitaxial or near-epitaxial islands are evidently immersed in a sea of much smaller Si grains, so the smaller grain size obtained by x-ray analysis (which produces an average for essentially the entire Si film thickness) may not be as inaccurate as it seems at first glance.

The appearance of the Si films on the four polished Vistal substrates is shown at low magnification in the optical photomicrographs in Figure 2-62. This sequence gives a good indication of both the relative total area coverage and the size of the highly reflective individual epitaxial regions (seen as white areas in the photographs) on the four surfaces. Also clearly shown (especially in the films on Vistal 3 and 4) are other growth regions on individual substrate crystal grains which may also be epitaxial but are more heavily faceted and therefore not as reflective; these are the defined regions seen in various shades of gray in the figure. Many of these gray or black regions, of course, may be polycrystalline rather than epitaxial.

A comparison of the Si films on polished and as-fired substrates is shown for all four Vistals in the optical photomicrographs in Figure 2-63. All photographs are at the same magnification. The differences in growth characteristics on the polished and the as-fired surfaces are clearly illustrated in these photographs.

The electrical properties of the set of undoped Si films grown on Vistal substrates of four different firing histories have now been measured by both the Hall bridge and the van der Pauw methods. The results of the measurements by both methods, along with the properties of the corresponding epitaxial films grown simultaneously on single-crystal $(01\bar{1}2)$ sapphire, are given in Table 2-11. As indicated in the table, the background doping level, based on the measured properties of the epitaxial films on sapphire, continues in the low 10^{14} cm^{-3} concentration range.

The recent Hall bridge measurements confirm the previous van der Pauw results that the resistivities of the undoped polycrystalline films on Vistal substrates, whether polished or as fired, fall in the $1\text{-}4 \times 10^5$ ohm-cm range. (The Hall bridge results for the films on Vistal 1 appear of doubtful validity; no explanation for the deviation has been found.) These values are two to three orders of magnitude larger than those for the corresponding epitaxial films grown simultaneously on single-crystal sapphire substrates.

The measured carrier concentrations for the polycrystalline films are all about 10^{12} cm^{-3}, generally somewhat larger for the film on the as-fired substrate than for that on the corresponding polished substrate and consistently 1-1/2 to 2 orders of magnitude smaller in the polycrystalline films (on either type of Vistal surface) than in the corresponding companion epitaxial film (again disregarding the Hall bridge results for the polycrystalline films in experiment 94). The resulting effective Hall mobility is in the range 132-161 $cm^2/V\text{-sec}$ for the four epitaxial films. The films on Vistal tend to have mobilities smaller than those in the corresponding epitaxial films, falling in the range 10-34 $cm^2/V\text{-sec}$, with those with larger grains generally exhibiting

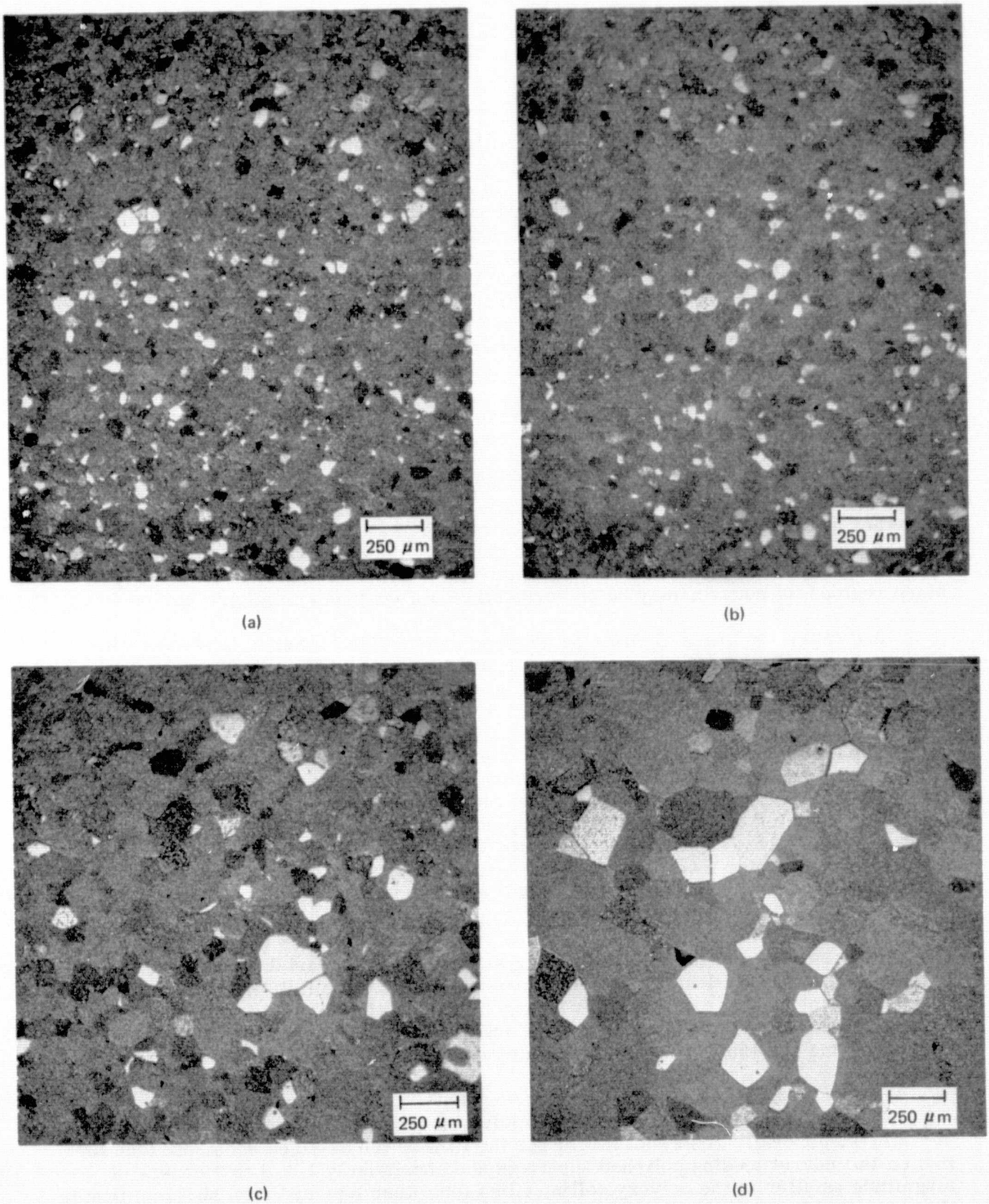

Figure 2-62. Optical Photomicrographs of CVD Si Films on Polished Substrates of (a) Vistal 1, (b) Vistal 2, (c) Vistal 3, (d) Vistal 4, at Low Magnification

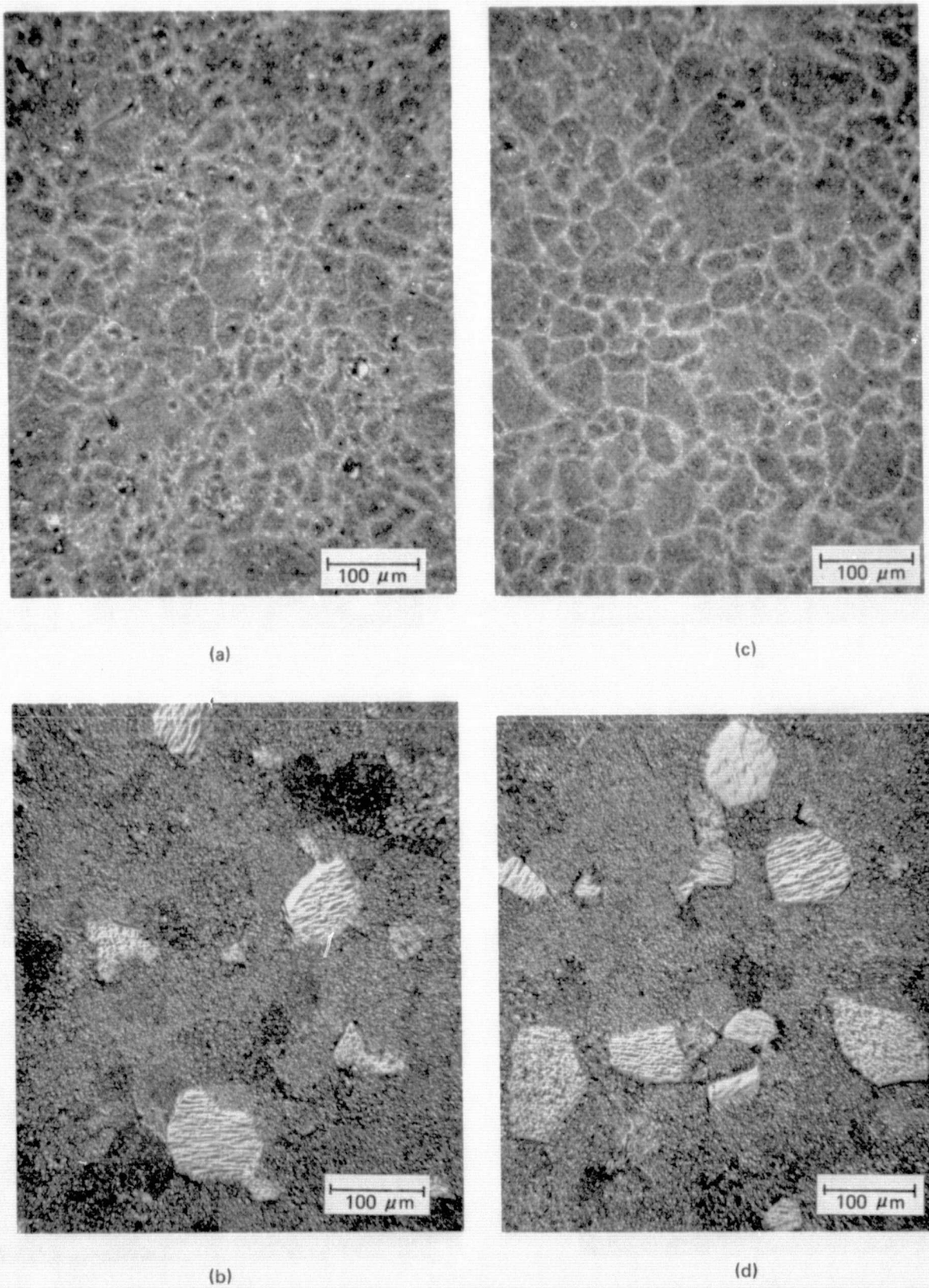

Figure 2-63. Optical Photomicrographs of Surfaces of CVD Si Films on Polycrystalline Alumina Substrates of Four Different Firing Histories: Vistal 1 (a) As-fired, (b) Polished; Vistal 2 (c) As-fired, (d) Polished; Vistal 3 (e) As-fired, (f) Polished; Vistal 4 (g) As-fired, (h) Polished.

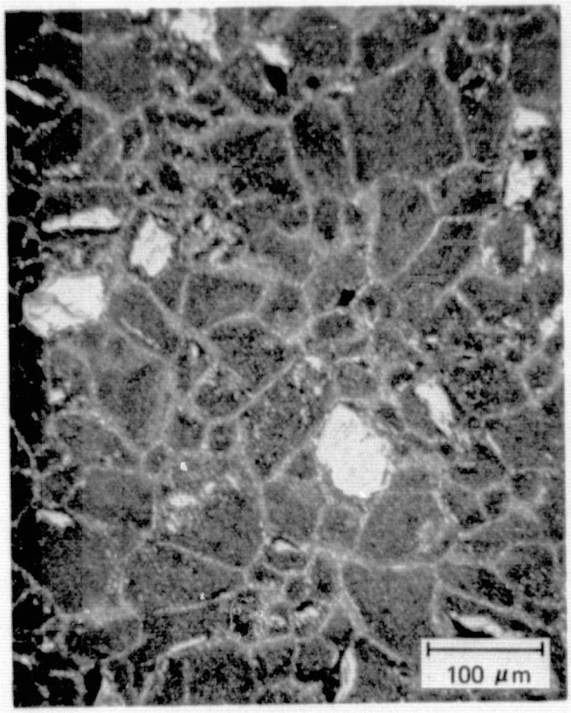

(e)

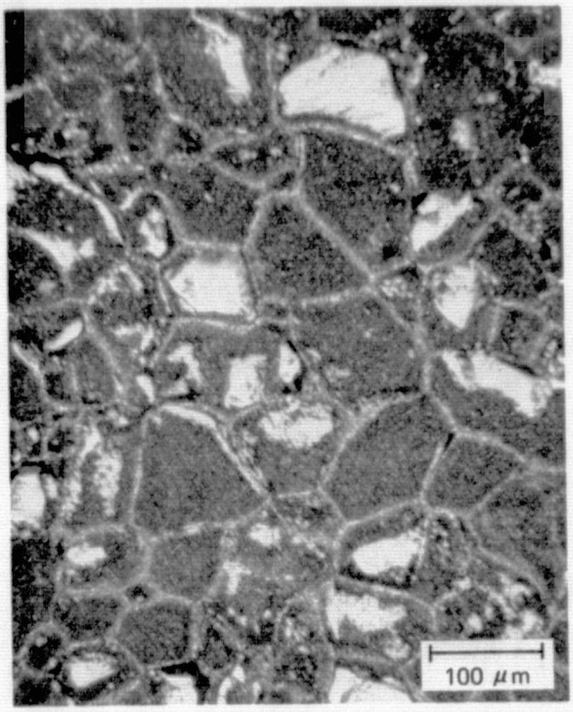

(g)

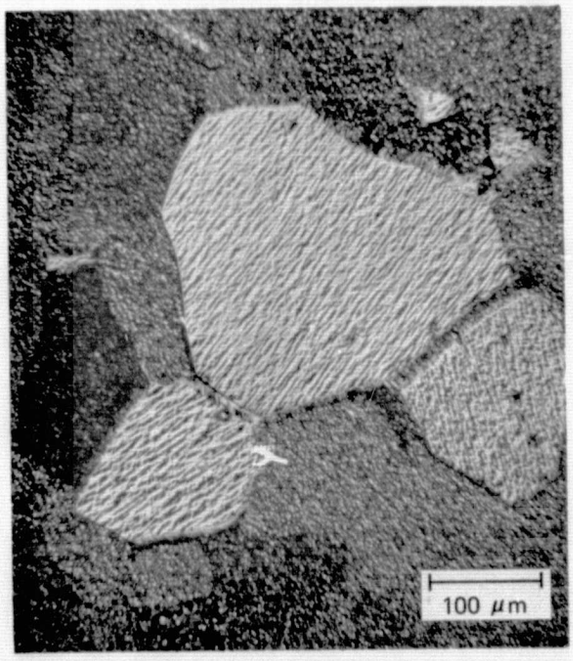

(f)

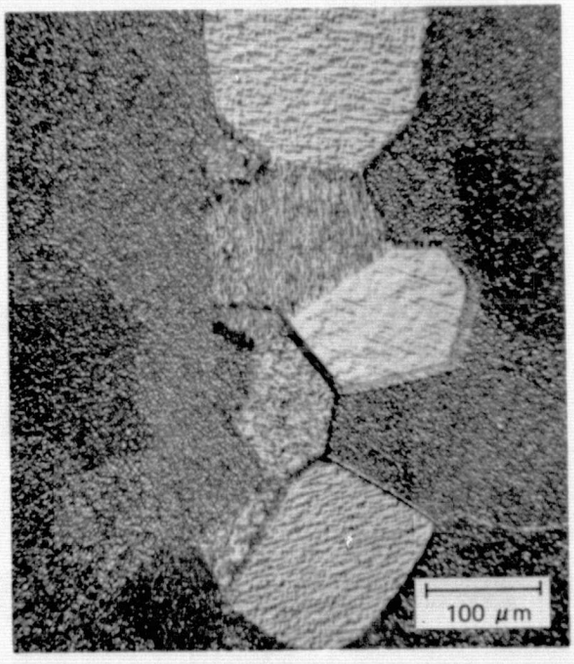

(h)

Figure 2-63. (Cont)

Table 2-11. Electrical Properties of Undoped P-type Si Films Deposited by SiH_4* Pyrolysis in H_2 (4 ℓpm) on (01$\bar{1}$2) Single-crystal Sapphire and Vistal Alumina Substrates

EXPT. NO.	DEPOS. TEMP. (°C)	SUBSTRATE		FILM THICK. (μm)	METHOD OF MEAS.†	RESIS-TIVITY (ohm-cm)	CARRIER CONC. (cm^{-3})	HALL MOBILITY (cm^2/V-sec)
		MATERIAL	SURFACE					
91	1031	Sapphire	Polished	17.3	HB	1.6×10^{2}	2.8×10^{14}	144
		Vistal 4	Polished	17.9	vdP HB	2.4×10^{4} 2.4×10^{5}	8.6×10^{13} 1.0×10^{12}	3 26
		Vistal 4	As fired	17.9	vdP HB	2.8×10^{4} 9.2×10^{4}	7.6×10^{12} 2.0×10^{12}	30 34
92	1021	Sapphire	Polished	18.1	vdP HB	1.5×10^{2} 1.4×10^{2}	5.1×10^{14} 2.8×10^{14}	81 161
		Vistal 3	Polished	17.5	vdP HB	3.5×10^{5} 3.5×10^{5}	7.3×10^{11} 7.1×10^{11}	24 25
		Vistal 3	As fired	17.0	vdP HB	3.8×10^{5} 1.6×10^{5}	9.0×10^{11} 1.7×10^{12}	18 22
93	1024	Sapphire	Polished	17.9	vdP HB	5.3×10^{3} 2.2×10^{2}	5.1×10^{13} 2.1×10^{14}	23 135
		Vistal 2	Polished	18.0	vdP HB	3.5×10^{5}	1.2×10^{12} (Bridge pattern damaged in etching)	15
		Vistal 2	As fired	18.0	vdP HB	1.2×10^{5} 1.2×10^{5}	5.0×10^{12} 3.5×10^{12}	10 15
94	1025	Sapphire	Polished	18.0	vdP HB	9.0×10^{2} 4.9×10^{2}	1.6×10^{14} 9.7×10^{13}	45 132
		Vistal 1	Polished	17.0	vdP HB	2.6×10^{5} 7.1×10^{2}**	1.2×10^{12} 3.0×10^{14}** (n-type)	20 11**
		Vistal 1	As fired	16.0	vdP HB	1.5×10^{5} 5.3×10^{3}**	3.5×10^{12} 7.2×10^{13}**	12. 16**

*SiH_4 flow rate 25 ccpm
†vdP = van der Pauw method; HB = Hall bridge method
**Validity of these Hall bridge results in doubt (cause unknown)

higher mobilities and the films on polished substrates tending to have higher mobilities than those on as-fired substrates. This is consistent with expectations, since the grain boundaries in the polycrystalline Si films would be expected to contribute an effective resistance factor separate from that associated with the intragrain doping density, and it is likely that an appreciable fraction of the acceptor centers — whatever their source in an undoped film — would become "tied-up" in the grain boundaries of the polycrystalline film. The result is a much reduced effective carrier mobility, as observed in the films on Vistal substrates.

The general similarity in electrical properties of the films on both types of Vistal surface is not surprising, especially in view of the general similarity of the external structural properties of the two films as observed in the SEM and the optical microscope. On the average, the integrated effect of the polycrystalline array comprising the film on the polished substrate might be expected to be very similar — electrically — to that of the different polycrystalline array comprising the film on the as-fired substrate.

Spreading resistance (SR) evaluation of the undoped films grown in three of these four experiments has provided some preliminary indication that an electrically-active impurity may be present in the refired Vistal substrates. The SR probe scan down a small-angle bevel through the entire film thickness for the epitaxial films grown on sapphire in experiments 92, 93, and 94 (see Table 2-11) indicated a wide-range variation in measured resistivity as a function of distance from the film-substrate interface for these undoped films. For example, the resistivity (obtained from probe SR values by applying a correction factor based on properties of {111} single-crystal Si) of the epitaxial film of experiment 92 varies gradually from ~20 ohm-cm at the surface to ~45 ohm-cm at a depth of 10 μm, and then rapidly to ~10^5 ohm-cm at the interface. The simultaneously grown polycrystalline films on polished and as-fired Vistal 3 were grossly uniform in resistivity, averaging approximately 6 x 10^4 ohm-cm to a depth of 15-16 μm and rising to ~10^5 ohm-cm at the interface. Local values varied within the range 5-8 x 10^4 ohm-cm for the film on the polished substrate and the range 4-8 x 10^4 ohm-cm for the film on the as-fired substrate. These variations were such that they may have been associated with individual (perhaps epitaxial) large grains in the film; this possibility has not been verified in the films of this experiment, however.

Similarly, the undoped epitaxial film prepared in experiment 93 (Table 2-11) was found by SR probe scan to vary continuously from 10^2 ohm-cm at the surface to 3 x 10^4 ohm-cm at the interface, while the polycrystalline film on polished Vistal 2 increases (fairly uniformly) from 4-5 x 10^4 ohm-cm at the surface to ~10^5 ohm-cm at the interface, and the film on as-fired Vistal 2 varies from ~3 x 10^4 ohm-cm at the surface to 10^5 ohm-cm at the interface. Again the traces for the polycrystalline films showed some fine structure that might be associated with individual crystal grains in the film; this effect was again more pronounced in the film grown on the as-fired substrate.

Finally, the SR probe scan in the undoped epitaxial film of experiment 94 (Table 2-11) also showed an increase in resistivity from ~45 ohm-cm at the surface to about 100 ohm-cm at a depth of 10 μm, and then a rapid increase to 4 x 10^4 ohm-cm at the interface. The simultaneously grown polycrystalline films on Vistal 1 ranged from ~5 x 10^4 ohm-cm at the surface to ~2 x 10^5 ohm-cm at the interface for the film on the polished substrate and from 2-3 x 10^4 ohm-cm at the surface to ~10^5 ohm-cm at the interface for the film on the as-fired Vistal 1. In this instance, again, the

resistivity of the film on the as-fired substrate exhibited more internal variation than did the one on the polished alumina substrate.

Although further evidence is being sought, the results described above could be associated with a compensating electrically-active donor center occurring in the deposited Si film in a concentration that increases nearer the film-substrate interface. This donor center might be a physical imperfection induced at the interface in early growth stages but is more likely a donor impurity entering the growing film from the Vistal substrate.

The SR probe was also used to identify individual crystal grains and grain boundaries in the undoped Si polycrystalline films grown on Vistal substrates in experiments 92, 93, and 94. A low-angle bevel was polished along one entire edge of one piece of the film-substrate composite, and the SR probe scan was made along nearly the entire bevel length in a line parallel to the intersection of the bevel and the top surface of the film, at a position corresponding to a depth slightly (several μm) below the original film surface. The SR probe readout trace (in terms of measured resistance in ohms) exhibited strong excursions for each of the examined films grown on Vistal substrates, and these excursions are interpreted to represent resistivity variations associated with individual crystal grains and grain boundaries. The intervals between probe readout peaks (or valleys) are largest for the films on Vistal 3 (experiment 92) and smallest for the film on Vistal 1 (experiment 94), consistent with the grain size differences observed by SEM analysis. Details of a similar application of this technique are given below, in the discussion of doped Si films on these aluminas.

One experiment undertaken in the third quarter involved the simultaneous deposition of B-doped Si films on three substrates of Vistal 3 - in the as-fired condition, lapped, and polished - along with a sapphire monitor wafer. The films were heavily doped ($\sim 2 \times 10^{19}$ cm^{-3}, by measurement of the film on sapphire) and were grown at 1028°C at rates of 2.6 to 3.5 μm/min, with thicknesses of 21 to 28 μm. X-ray diffraction analysis indicated very strong {110} preferred orientation in all three films on Vistal, consistent with earlier observations. The film on the polished Vistal 3 exhibited by far the strongest {110} orientation, with the film on the as-fired substrate next; the film on the lapped substrate was relatively much weaker in the {110} orientation, yet nonetheless highly oriented in that plane. The film on the polished substrate also exhibited a strong {100} orientation (although relatively much less than the very strong {110} orientation), whereas this plane was only slightly preferred in the film on the lapped substrate and essentially in random-orientation occurrence in the film on the as-fired substrate.

In a subsequent experiment, which involved three polished alumina substrates together with a sapphire monitor, films were grown at essentially the same temperature (1025°C) and similar growth rates (2.7 to 3.5 μm/min) to thicknesses of 22 to 28 μm. The doping level in this group was lower, however – 1.5 to 2.0 x 10^{18} cm^{-3} (van der Pauw) in the three polycrystalline films, including one on polished Vistal 3. X-ray diffraction examination of the film on Vistal 3 indicated equally strong preferred orientation of both {110} and {100} planes – quite different from the orientation habit observed in the more heavily doped (by an order of magnitude) film on Vistal 3 described above and in Table 2-12. The possible significance of this apparent difference in crystal growth characteristics with B doping level will be evaluated further.

Table 2-12. Electrical Properties of B-doped P-type Si Films Deposited Simultaneously by SiH_4* Pyrolysis at 1028°C in H_2 (4 ℓpm) on Single-crystal ($01\bar{1}2$) Sapphire and Vistal 3 Alumina Substrates

Substrate		Film Thick (μm)	Method of Meas**	Resistivity (ohm-cm)	Carrier Conc (cm^{-3})	Hall Mobility (cm^2/V-sec)
Material	Surface					
Sapphire	Polished	23	vdP	1.2×10^{-2}	1.4×10^{19}	40
			HB	1.2×10^{-2}	8.5×10^{18}	64
Vistal 3	Polished	25	vdP	1.6×10^{-2}	1.6×10^{19}	26
			HB	1.3×10^{-2}	1.2×10^{19}	42
Vistal 3	As fired	21	vdP	1.2×10^{-2}	2.1×10^{19}	25
			HB	0.9×10^{-2}	2.1×10^{19}	34
Vistal 3	Lapped	28	vdP	2.0×10^{-2}	1.2×10^{19}	25
			HB	1.6×10^{-2}	1.0×10^{19}	38

*SiH_4 flow rate 25 ccpm

**vdP = van der Pauw method; HB = Hall bridge method

The electrical properties of the films on the three Vistal substrates, obtained by both van der Pauw and Hall bridge techniques, are given in Table 2-12. Close agreement of the results for the two methods is evident. Carrier concentrations and resistivities measured in all four films are nearly the same, both tending to be only slightly larger in the polycrystalline films than in the epitaxial film. The effective Hall mobilities in the polycrystalline films are alike and about 60 percent of that in the film on sapphire, measured by either method. These measurements provide one set of data (at the high doping concentration end of the range) for correlation of electrical properties in epitaxial and polycrystalline Si films as a function of added impurity concentration. The results tend to confirm the observations of other investigators - that differences in electrical properties between epitaxial and polycrystalline films become smaller as doping levels are increased.

This same set of Si films was examined by the spreading resistance (SR) method to investigate the degree of uniformity of doping with distance from the film-substrate interface. The epitaxial film resistivity varied only slightly (and quite uniformly) throughout its thickness - from ~0.012 ohm-cm near the surface to ~0.020 near the interface. The polycrystalline films on Vistal substrates were also uniformly doped, with about the same measured resistivities as found in the epitaxial film - again only slightly higher than the latter.

It is interesting that the SR probe results in terms of resistivity for the polycrystalline films agree very closely with the results obtained directly on these films by the van der Pauw technique, despite the fact that the computer-applied correction factor used in converting the SR probe resistance readings to corresponding resistivity values is based on the properties of {111} - oriented single-crystal Si. It is

also not surprising that there is no evidence of the compensating donor at the film-substrate interface as observed in the undoped films on Vistal - presumably because of the high B doping density in these films.

The SR probe was also used successfully to identify individual crystal grains and grain boundaries in the Si film grown on the polished Vistal 3 substrate of the experiment of Table 2-12. A bevel was polished along one entire edge (~6mm long) of one quarter of the original film-substrate composite, and the SR probe scan was made along nearly the entire bevel length in a line parallel to the top of the bevel, at a position corresponding to a depth several μm below the film surface.

Optical photomicrographs were made of the entire bevel length to show the "tracks" made by the two-point SR probe (spacing between probe points 29 μm, step-distance between readings 10 μm). EBIC-mode SEM photographs were also made of the entire bevel length to delineate the large individual grains found in the Si films on this substrate material. These two sets of photographs were then assembled to make two composite views of the entire bevel length.

Figure 2-64 shows the two composite photographs aligned side-by-side, with individual crystal grains in the beveled Si film clearly visible and the tracks of the SR double-point probe (two styli 29 μm apart) evident along nearly the full length of the bevel. A scale is also mounted alongside to facilitate identification of regions in the SR readout trace, shown in Figure 2-65. This makes it possible to correlate distinct steps in the measured resistance with easily discernible crystal grain boundaries in the SEM photographs.

Some of the separate epitaxial regions/grains in this film were 100 to 200 μm across, as earlier examination by other means had shown. The measured interprobe resistance value along the entire ~5mm scan length was approximately 25 ohms and nearly constant except in the interior of large epitaxial regions, where it dropped consistently to ~20 ohms. When converted (approximately) to corresponding resistivities, the difference in the two values is quite similar to the observed difference in the resistivities of the three polycrystalline films, on the one hand, and that of the epitaxial film on sapphire grown simultaneously in this experiment, on the other.

The obvious possibilities of further analyses of this type on other polycrystalline films being explored, and the limits of resolution of the SR probe scan will be established. For example, attempts are being made to apply such a scan successively to the same region of a polycrystalline film as progressively more material is removed, to follow variations in the size and the electrical properties of individual grains with distance from the initial growth interface.

In another experiment in the third quarter three polished alumina substrates were used, along with the usual sapphire monitor wafer, for deposition of B-doped Si at a rate of ~3 μm/min at 1025°C, to permit comparison of film properties on the three high-purity aluminas of greatest interest in this program - ASM805, MRC Superstrate, and Vistal 3. Preliminary analysis of x-ray diffraction data indicates the {110} orientation to be very strongly preferred in the films on Superstrate and ASM805, and also preferred - but much less strongly - in the film on Vistal 3. The latter also exhibits equally strong {100} orientation, but this orientation appears only in random-orientation prominence in the films on Superstrate and ASM805.

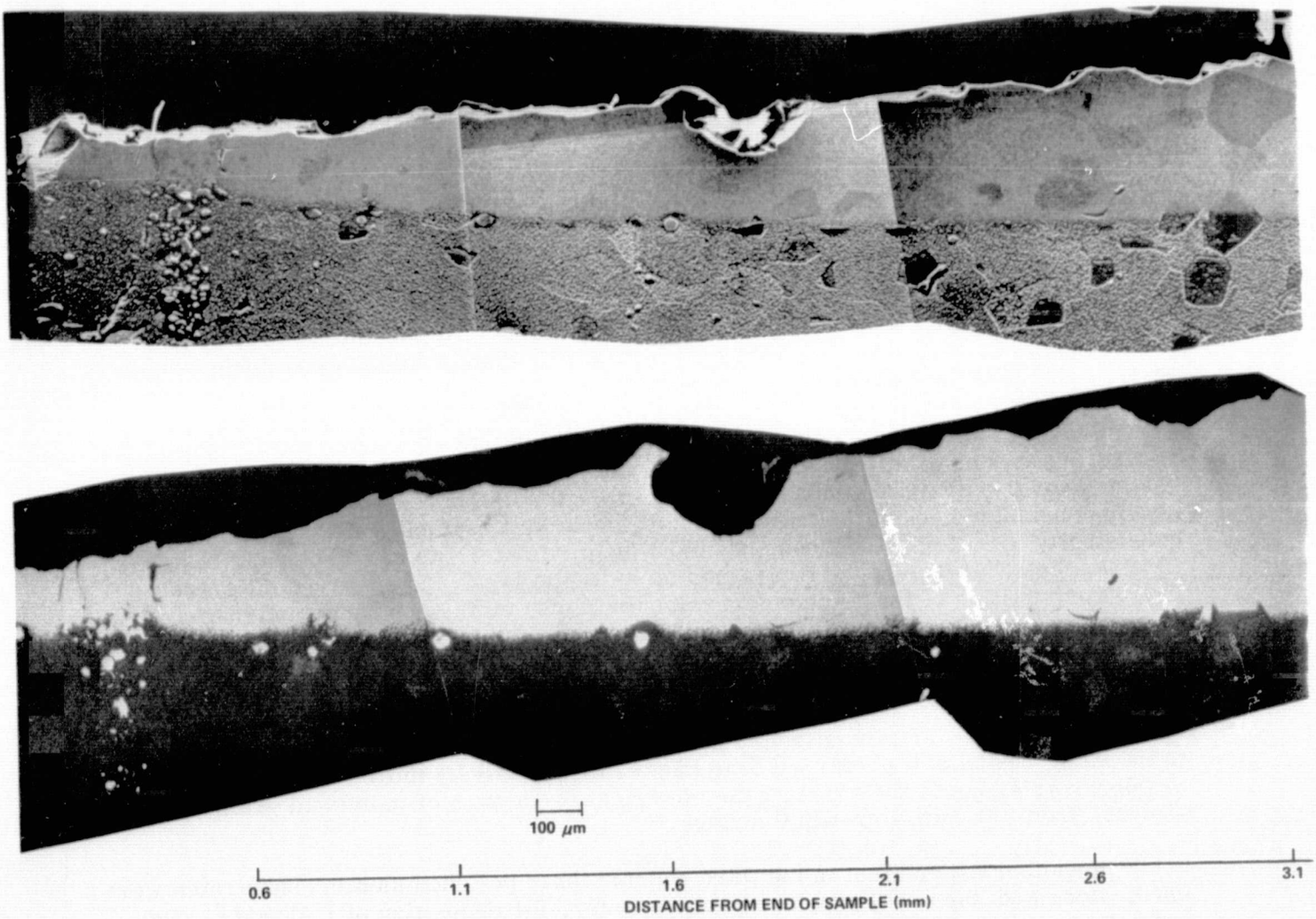

Figure 2-64. Composite Optical and SEM/EBIC Micrographs Showing Individual Grains in Doped CVD Si Film on Polished Vistal 3 and SR Probe Tracks on Bevel through Film

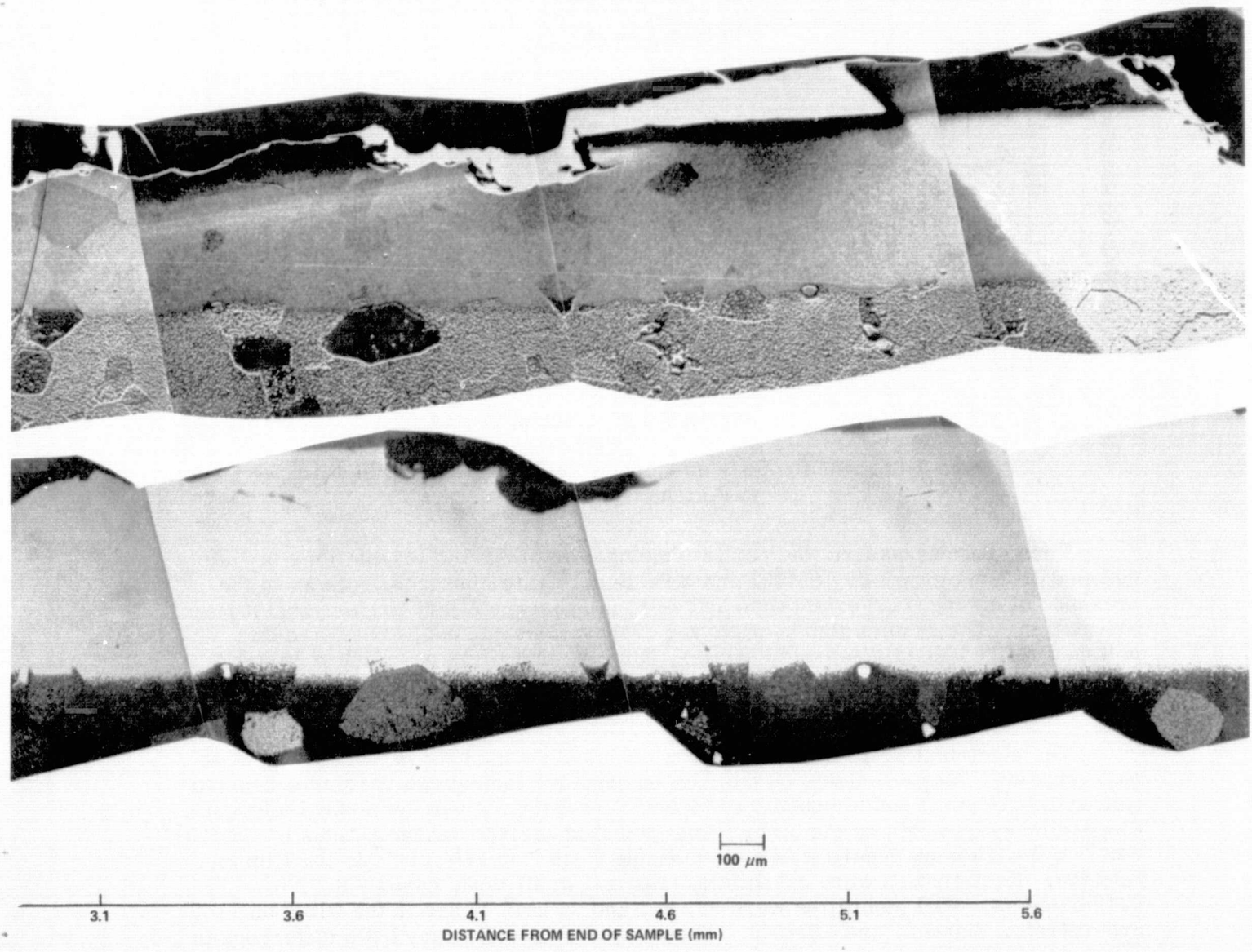

Figure 2-64. (Cont)

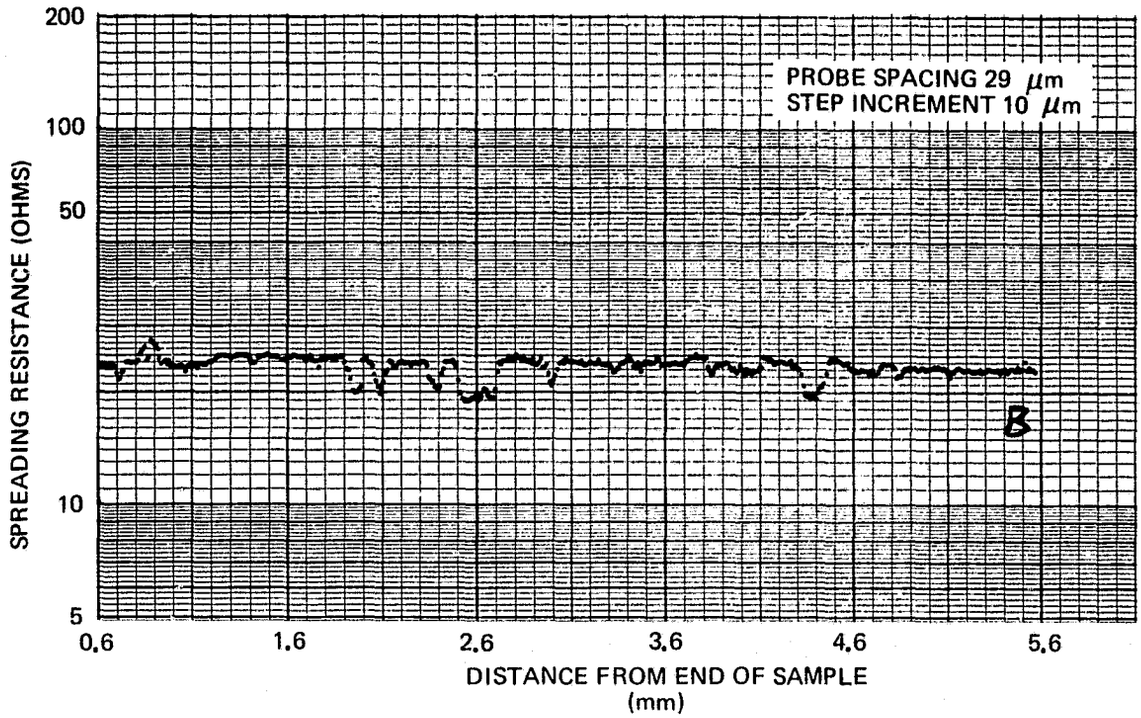

Figure 2-65. SR Probe Scan along Bevel in Doped CVD Si Film on Polished Vistal 3

These results confirm the earlier findings for preferred orientations in undoped Si films grown on ASM805 and MRC Superstrate aluminas, both as to the presence of strong {110} orientation and as to the absence of any preferred {100} orientation. The results also confirm the observations on undoped Si films on polished refired Vistals reported earlier, namely, that films on polished Vistal 4 and Vistal 3 exhibit a strong {100} orientation tendency in addition to the strong {110} preferred orientation.

The electrical properties of the three films described above were found to be quite similar. Measurements on the film on sapphire indicated a carrier concentration of 3×10^{18} cm^{-3} and a mobility of 74 $cm^2/V\text{-sec}$ (by the van der Pauw technique). Similar measurements on the other films indicated carrier concentrations of 1.5×10^{18} cm^{-3} in the films on Superstrate and on Vistal 3 and 2.0×10^{18} cm^{-3} in the film on ASM805. Resistivities were essentially identical in all three cases - 0.12 to 0.13 ohm-cm. Hall mobilities were 33, 34, and 26 $cm^2/V\text{-sec}$ in the films on Superstrate, Vistal 3, and ASM805. These results indicate very little difference in effective electrical properties in doped polycrystalline films even though in one case (Vistal 3) there is a significant distribution of large (50 to 150 μm) epitaxial grains in the layer. The validity of this preliminary observation will be carefully checked in other experiments, and the important test of fabricating solar cells in polycrystalline films grown on these same three alumina substrate materials is yet to be made.

One of the first experiments in which B-doped Si films were deposited on several alumina substrates simultaneously involved a polished and an as-fired MRC Superstrate

substrate used together with a polished $(01\bar{1}2)$-oriented sapphire for Si growth in H_2 (4 ℓpm) at 1025°C, with a SiH_4 flow rate of 10 ccpm. The flow rate of B_2H_6-in-He was sufficient to provide a moderately high doping concentration - in the 10^{17}-10^{18} cm^{-3} range.

SEM analyses of the surfaces of the polycrystalline films on the two polycrystalline alumina substrates showed very little difference in the structural characteristics. Figure 2-66 shows SEM photographs of the Si film surface on the as-fired Superstrate. Figure 2-66a is made at normal incidence and Figure 2-66b is for a viewing angle of 45 deg with the substrate surface. The surface features are essentially identical to those observed on films grown on other Superstrate surfaces earlier in the program; relatively little crystallographic faceting is discernible.

Figure 2-67 shows similar SEM photographs for the doped Si film that was deposited simultaneously on a polished MRC Superstrate surface. Careful inspection indicates there may be slightly more faceting on the surface features of the film on the polished substrate, but the difference is almost insignificant. From the SEM examination it is found that the average horizontal dimension of the surface features on the doped film grown on the polished substrate is ~2.8 μm, while that for the film on the as-fired Superstrate is ~3.0 μm, again indicating little difference.

As in other examples of films on this material, x-ray diffraction analysis of the two films indicated very strong $\{110\}$ preferred orientation in both films, although the relative line intensity was again over twice as strong in the film on the polished substrate as in the other. This time there was also evidence of slight preferred orientation of the $\{100\}$ planes (more so in the film on the polished substrate), and this is different from the random-orientation condition found for this orientation in the other Si films on this substrate material.

The results of electrical measurements on these films and on the film grown simultaneously on $(01\bar{1}2)$-oriented sapphire are shown in Table 2-13. The bridge measurements on the epitaxial film on single-crystal sapphire indicate that the flow rate of B_2H_6-in-He that was used produced a net carrier concentration of ~10^{18} cm^{-3}; the observed Hall mobility in this film was 125 cm^2/V-sec. The measurements on the two films on the polycrystalline substrates were made by the van der Pauw method, because the samples were subsequently to be sent to OCLI for solar cell fabrication and the entire sample area was to be preserved for that purpose. The resistivities of the polycrystalline Si films were nearly the same, and more than an order of magnitude larger than that of the companion film on sapphire. The measured carrier concentrations were nearly identical in the polycrystalline films and about half of the value in the single-crystal film. As a result, the effective Hall mobilities in the two films on MRC alumina were only a fraction of that found in the film on sapphire.

The fact that the electrical properties as well as the structural properties are quite similar in these films raises some question as to the real value of the extra processing - that is, the mechanical polishing - invested in the one substrate. Since there was also relatively little difference in the apparent surface roughness of the films on the polished and the as-fired substrates, even the presumed advantage of having a smoother film surface for subsequent device processing and contacting may not be valid for this particular substrate material.

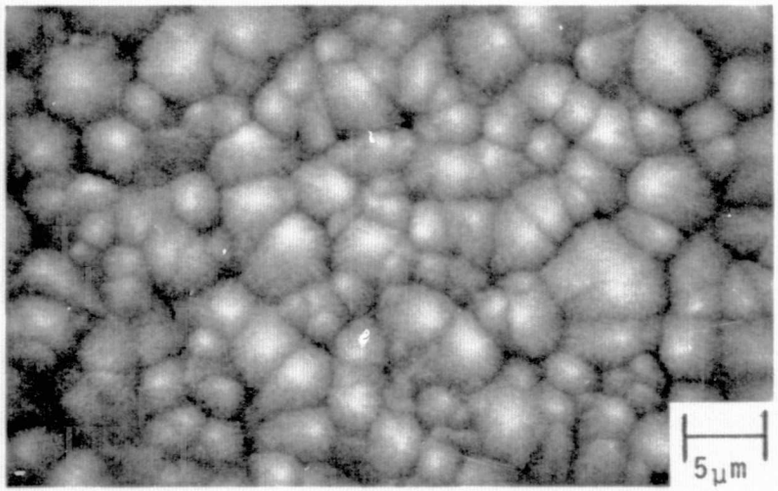

(a)

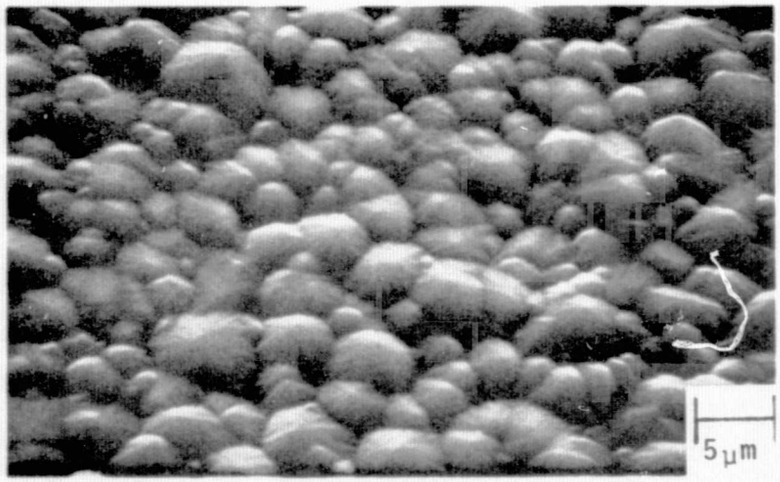

(b)

Figure 2-66. SEM Photographs of Surface of B-doped CVD Si Film Deposited by SiH_4 Pyrolysis in H_2 at 1025°C on As-fired Superstrate Alumina Substrate. a) Viewed at Normal Incidence; b) Viewed at 45 deg with Sample Surface.

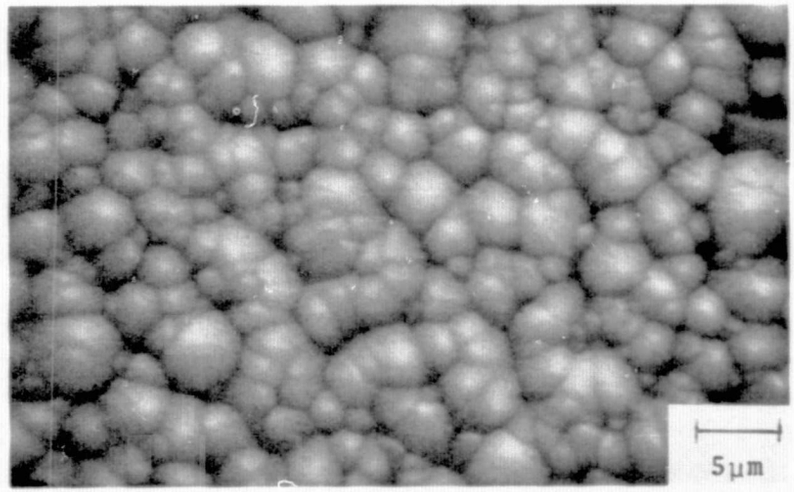

(a)

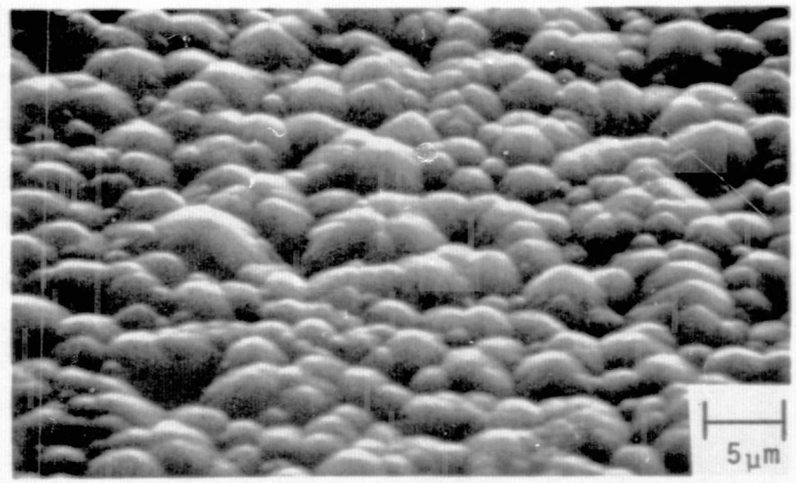

(b)

Figure 2-67. SEM Photographs of Surface of B-doped CVD Si Film Deposited by SiH_4 Pyrolysis in H_2 at 1025°C on Polished Superstrate Alumina Substrate. a) Viewed at Normal Incidence; b) Viewed at 45 deg with Sample Surface. (Film deposited simultaneously with film of Figure 2-66.)

Table 2-13. Electrical Properties of B-doped CVD Si Films Deposited by SiH_4 Pyrolysis in H_2 (4 ℓpm) Simultaneously on Single-crystal Sapphire and Polycrystalline Superstrate Alumina

SUBSTRATE MATERIAL AND SURFACE CONDITION	SiH_4 FLOW RATE (ccpm)	B_2H_6-IN-He FLOW RATE (ccpm)	DEPOS TEMP (°C)	APPROX FILM THICK (μm)	RESISTIVITY (ohm-cm)		HOLE CONCENTRATION (cm^{-3})		HALL MOBILITY (cm^2/V-sec)	
					van der Pauw	Hall Bridge	van der Pauw	Hall Bridge	van der Pauw	Hall Bridge
$(01\bar{1}2)$ sapphire (polished)	10	9.1	1025	19	0.061	0.052	1.0×10^{18}	9.5×10^{17}	102	125
MRC Superstrate alumina (as fired)	10	9.1	1025	20	0.76	–	5.0×10^{17}	–	16	–
MRC Superstrate alumina (polished)	10	9.1	1025	20	0.86	–	4.8×10^{17}	–	15	–

Another deposition experiment of the same type involved simultaneous deposition of doped Si on substrates of polished Superstrate, as-fired ASM805, and single-crystal polished $(01\bar{1}2)$ sapphire. The films were grown in H_2 (4 ℓpm) at 1033°C with a SiH_4 flow rate of 10 ccpm and a B_2H_6-in-He flow rate of 500 ccpm to produce heavy B-doping in the films.

SEM examination of the film surfaces produced the photographs shown in Figures 2-68 and 2-69. The former shows the surface of the film on the as-fired ASM805 alumina substrate, with a view at normal incidence in Figure 2-68a and at 30 deg with the film surface in Figure 2-68b. The surface features observed are very similar to those seen on Si films grown on this material earlier in the program. Little if any distinct faceting can be seen on the pyramidal features that comprise most of the surface (Figure 2-68b).

Figure 2-69 shows two views of the surface of the film on the polished MRC Superstrate alumina, at the same corresponding magnifications as those of Figures 2-68a and 2-68b. In both views there is some evidence of crystallographic faceting, as was seen on the film of Figure 2-67, also deposited on polished Superstrate. The two film surfaces again appear to be quite similar, with perhaps slightly more evidence of faceting on the film on the polished MRC substrate than on the other film. The average horizontal dimensions of the surface features observed in the SEM are ~3.0 μm for the film on the as-fired ASM805 alumina and ~3.4 μm for the film on polished Superstrate.

X-ray diffraction analysis of the two polycrystalline doped films again showed very strong {110} preferred orientation in the film on the polished Superstrate, as was the case in the experiment described above, although the effect is much greater in this film. The {100} planes again appeared as a second preferred orientation in the film on the polished Superstrate. The film on as-fired ASM805 also exhibited strong {110} preferred orientation, but the {100} planes were not detected at all. This result is similar to that found for undoped Si films deposited in H_2 on refired ASM805 at about the same temperature in a SiH_4 flow rate of 25 ccpm and, earlier in the program, on as-fired ASM805 at the same temperature and SiH_4 flow rate.

The surfaces of these Si films on the two aluminas are represented by the sections of profilometer traces shown in Figure 2-70. The trace in Figure 2-70a was obtained on the film on the polished MRC Superstrate, while that in Figure 2-70b is for the film on the as-fired ASM805 alumina. The vertical scale is the same in both instances. There is clearly less peak-to-valley excursion in the surface features of the film on the polished substrate (cf Figure 2-69) than for the film on the as-fired substrate (cf Figure 2-68).

Results of electrical measurements on the three films grown in this experiment are given in Table 2-14. Because of the high concentration of diborane introduced into the reactant gas stream in this experiment, the measured hole concentration in the epitaxial Si film grown on the single-crystal sapphire substrate was very high - about 2×10^{19} cm^{-3} as measured with the Hall bridge. The Hall mobility found for this film on sapphire was 31 $cm^2/V\text{-sec}$, a reasonable value for Si on sapphire in the 10^{19}-10^{20} cm^{-3} B doping range involved.

The characteristics of the films on the two polycrystalline aluminas were measured by the van der Pauw method. The resistivities of both films are similar

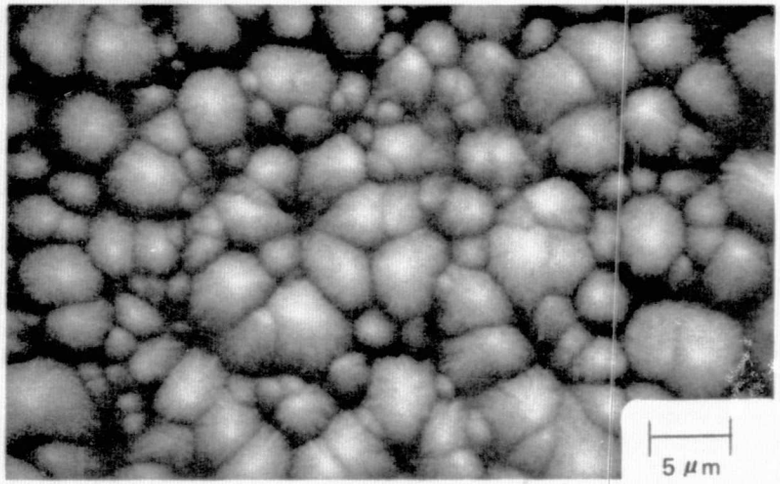

(a)

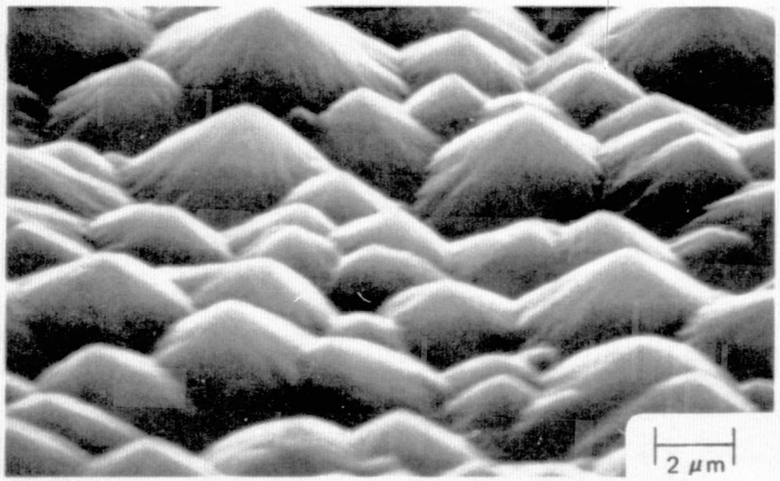

(b)

Figure 2-68. SEM Photographs of 25 μm-thick B-doped (~10^{20} cm^{-3}) Si Film on As-fired ASM805. (a) Normal to Sample Surface; (b) 30 deg to Sample Surface.

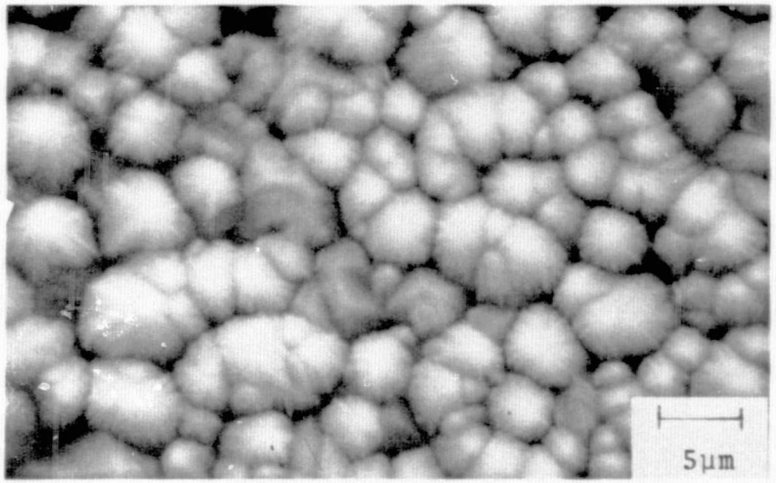

(a)

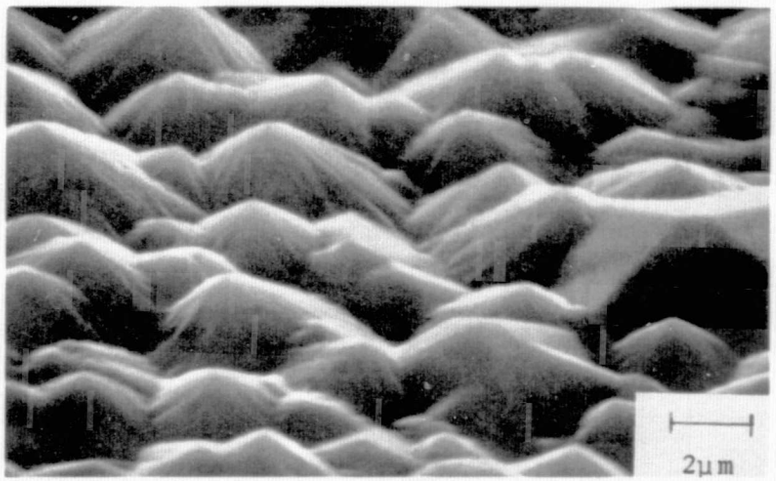

(b)

Figure 2-69. SEM Photographs of 25 μm-thick B-doped (~10^{20} cm^{-3}) Si Film on Polished MRC Superstrate. (a) Normal to Sample Surface; (b) 30 deg to Sample Surface.

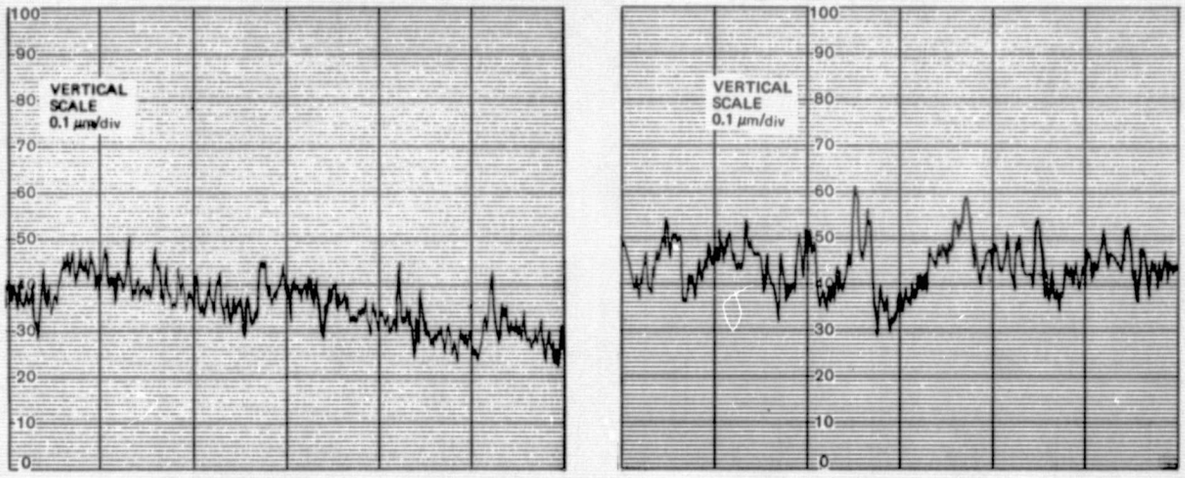

Figure 2-70. Dektak Profilometer Traces for Surfaces of B-doped CVD Si Films Grown at ~1030°C in H_2 by SiH_4 Pyrolysis, on Two Polycrystalline Alumina Substrates. (a) Polished MRC Superstrate; (b) As-fired 3M ASM805.

and are somewhat larger than the resistivity of the Si film on sapphire (measured by the van der Pauw method). The net carrier concentration measured by the van der Pauw method in these films was about $2x10^{19}$ cm^{-3} in both cases, resulting in effective Hall mobilities of about 30 cm^2/V-sec. Although there appear to be some minor inconsistencies, the results generally agree with those for heavily doped films on Vistal 3 substrates as recorded in Table 2-12.

Two separate experiments during the third quarter, there were designed to supply properly doped polycrystalline Si films on alumina substrates for experimental solar cell fabrication by OCLI, resulted in some data that give further evidence of a possible impurity escaping from the substrate during Si deposition. Si films had been grown in these experiments on as-fired ASM805 substrates at a rate of ~3μm/min by pyrolysis of SiH_4 (flow rate 25 ccpm) in H_2 (flow rate 4 ℓpm) at temperatures of 1022 and 1025°C, respectively, with B-doping from B_2H_6 flowing at rates of 75 and 10 ccpm, respectively. Measurements on the two epitaxial films on sapphire monitor wafers indicated carrier concentrations of $5.2x10^{18}$ and $9.5x10^{17}$ cm^{-3}, respectively. Measurements (by the van der Pauw method) on the plycrystalline films on as-fired ASM805 substrates indicated carrier concentrations 55 to 70 percent of the above values and resistivities of 0.085 and 0.83 ohm-cm, respectively.

Spreading resistance evaluation of these doped films was accomplished by a SR probe scan down a bevel through the entire film thickness. The scan for the more heavily doped film is shown in Figure 2-71a. The resistivity is fairly uniform at

Table 2-14. Electrical Properties of B-doped CVD Si Films Deposited by SiH_4 Pyrolysis in H_2 (4 ℓpm) Simultaneously on Single-crystal Sapphire and Polycrystalline Superstrate and ASM805 Aluminas

SUBSTRATE MATERIAL AND SURFACE CONDITION	SiH_4 FLOW RATE (ccpm)	B_2H_6-IN-He FLOW RATE (ccpm)	DEPOS TEMP (°C)	APPROX FILM THICK (μm)	RESISTIVITY (ohm-cm)		HOLE CONCENTRATION (cm^{-3})		HALL MOBILITY (cm^2/V-sec)	
					van der Pauw	Hall Bridge	van der Pauw	Hall Bridge	van der Pauw	Hall Bridge
$(01\bar{1}2)$ sapphire (polished)	10	500	1033	25	0.0050	0.012	3.3×10^{19}	1.7×10^{19}	37	31
MRC Superstrate alumina (polished)	10	500	1033	25	0.0094	–	2.0×10^{19}	–	32	–
3M ASM805 alumina (as fired)	10	500	1033	25	0.0087	–	2.4×10^{19}	–	30	–

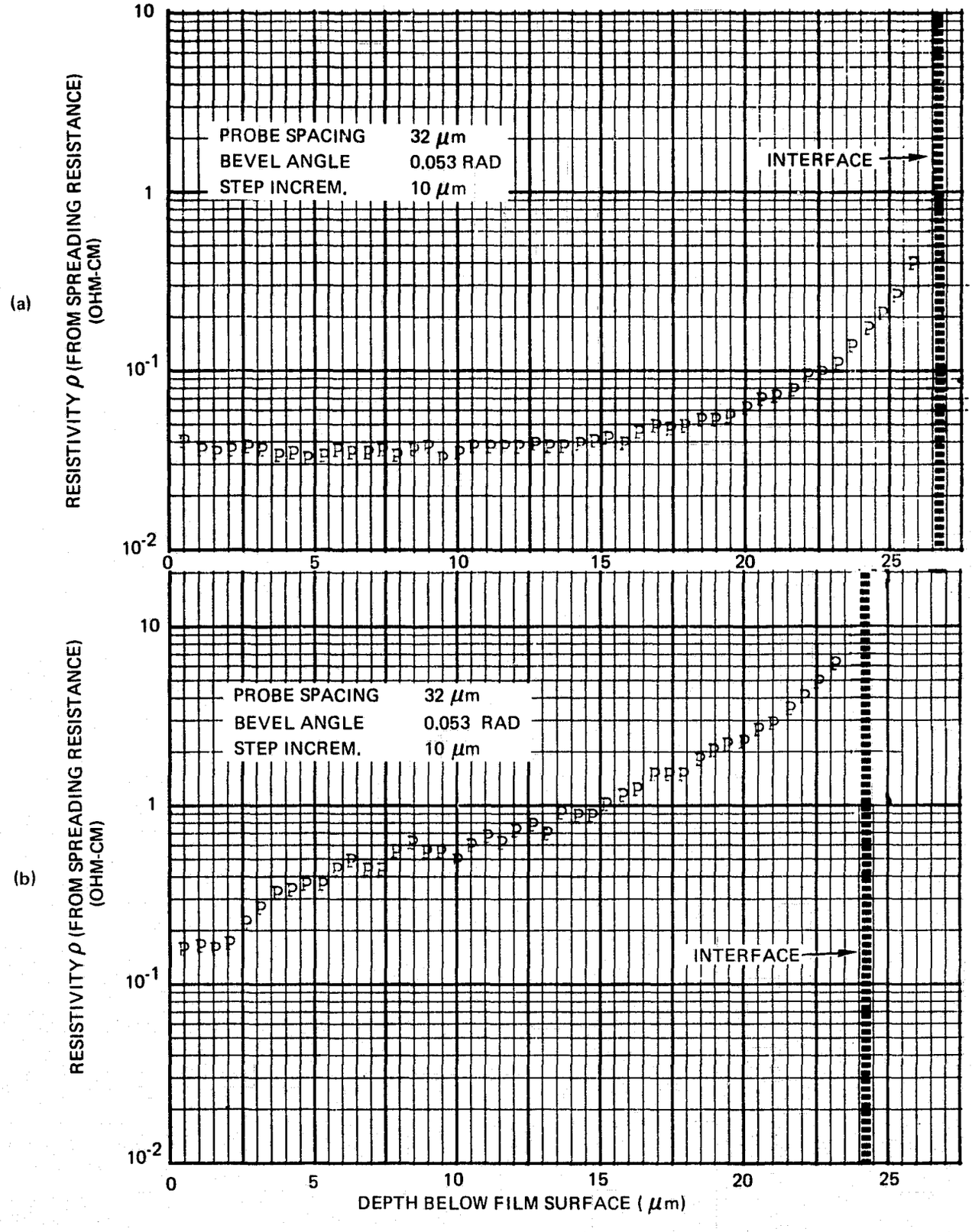

Figure 2-71. Spreading Resistance Probe Scans through Thickness of Doped CVD Si Films on As-fired ASM805 Substrates. a) p $\approx 4 \times 10^{18}$ cm^{-3}, b) p $\approx 5 \times 10^{17}$ cm^{-3} (Measured on Polycrystalline Items by van der Pauw Method)

0.035 to 0.040 ohm-cm to a depth of about 15 μm, at which point it gradually increases to a value of 0.8 to 0.9 ohm-cm at the film-substrate interface. The probe scan of the more lightly doped polycrystalline film is shown in Figure 2-71b. It shows almost no region of uniform resistivity as a function of depth, instead increasing almost continuously from about 0.15 ohm-cm at the surface to 8 to 10 ohm-cm at the interface with the alumina substrate. The observed properties in the two cases are consistent with the possible entry into the growing film of a compensating donor impurity, presumably by diffusion, from the substrate.

Additional analyses of this type will be carried out to verify these tentative conclusions, since there have been earlier indications that ASM805 may emit some type of impurity during the Si CVD process in the 1025°C range. (Slight discoloration of this substrate material has been noted in some previous deposition experiments.)

2.5.4 Properties of CVD Si Films on Other Polycrystalline Substrates

A few Si deposition experiments have been carried out during the third quarter with substrate materials other than glasses and aluminas. Most of these experiments were of an exploratory nature, to evaluate the stability of the substrate material in the Si CVD environment.

However, some of these investigations produced Si films that have been characterized by the various techniques used in this program. For example, Si films grown simultaneously on zircon Z360 (Kyocera) and zircon ASM475 (3M) in He at 1025°C were rough and irregular, as reported previously, and were found to have essentially random polycrystalline orientations.

An undoped film grown on mullite (3M Co.) at 1032°C in He (6 ℓpm) was quite rough and heavily textured; the substrate material was used in the as-fired condition and appeared to be very porous. X-ray analysis of the film indicated a moderately strong {110} preferred orientation. The polycrystalline film grown simultaneously on an as-fired ASM805 alumina substrate also had a heavily textured surface, believed to result from some adverse influence on the film growth process by impurities given off by the porous mullite during heating and Si deposition.

The film on ASM805 was very strongly oriented in the {110} plane, a preferred orientation previously observed for undoped films grown on this alumina and subsequently found also in B-doped films grown on as-fired ASM805 substrates, as indicated earlier. The latter experiments had shown the tendency for Si film growth with preferred {110} orientation to be even more pronounced on ASM805 for doped films ($\sim 4 \times 10^{18}$ and $\sim 5 \times 10^{17}$ cm^{-3}, respectively) than for undoped films. It is not clear if this is a consistently followed pattern, however.

Electrical measurements on the undoped polycrystalline films on mullite and on ASM805 alumina indicated n-type conductivity (by the Hall bridge method) and resistivities in the $2\text{-}6 \times 10^4$ ohm-cm range. Such properties could be consistent with the presence of an active donor impurity in the films, coming either from the mullite substrate or from the ASM805 alumina - the latter possibility as discussed in the preceding section.

X-ray diffraction analysis of a Si film deposited at ~850°C in He on a 1500Å-thick Ti film previously deposited on Corning Code 7059 glass by sputtering indicated

a moderate {110} preferred orientation. As previously reported, the composite was bowed, with the film in compression. Electrical measurements were not made on this film. Energy-dispersive x-ray analysis in the SEM indicated no evidence of Ti in the Si film.

The first film grown on Corning Code 9606 glass-ceramic in H_2 at 860°C exhibited whisker-like growth, but a film grown in He (6 ℓpm) at 842°C did have crystallographic order. X-ray diffraction analysis of this deposit showed a very strong {110} preferred orientation. SEM examination of the surface indicated surface features averaging ~5 μm across. Electrical measurements have not been made.

2.6 TASK 6. FABRICATION AND EVALUATION OF SOLAR CELL STRUCTURES

This contract provides for the fabrication and evaluation of experimental solar cells in CVD Si sheet on various substrates. This part of the work is provided by Optical Coating Laboratory, Inc., Photoelectronics Group, in City of Industry, CA, on a purchased-services basis.

The contract Statement of Work stipulates that the contractor shall "fabricate and evaluate solar cells with a minimum of 1 cm^2 area . . . " and that "techniques for producing solar cells from these films shall be, to the maximum extent possible, previously developed procedures." It is further stipulated that "one solar cell, on the average, shall be made per week during this program." The contract does not require delivery of samples to OCLI during the first month of the program.

With this requirement, and with the approval of the JPL Contract Technical Manager, an arrangement was developed with OCLI that provides the necessary solar cell processing and evaluation work yet still allows Rockwell personnel to concentrate on the Si CVD investigations involving various low-cost substrate materials.

2.6.1 General Sample Processing Procedure at OCLI

Although details of the handling, processing, and measurement techniques applied to any one sample at OCLI will be varied to accommodate the characteristics and/or limitations of the sample, there is a standard sequence of activities that is generally followed to whatever extent possible. Standard and near-conventional solar cell processing methods are used, to allow correlation of results with those obtained with conventional bulk single-crystal Si cells. If such procedures exhibit limiting deficiencies when applied to the Si sheet material, then the procedures are modified and/or novel processing methods are devised. It is intended that sufficiently rapid feedback of results will occur to permit timely influence of these results on subsequent CVD experiments at Rockwell.

The Si sheet samples received by OCLI are first routinely checked for thickness, conductivity type, and resistivity by standard methods. In some cases a preferential etch is applied to delineate individual crystallites in selected areas, and various surface treatments are used, if necessary, to prepare the sample for p-n junction formation. A small region of the sample is tested to determine if Schottky barriers of sufficiently good characteristics can be formed on the sheet surface to permit measurement of the minority carrier diffusion length in the as-received material; if found feasible, such measurements are made.

A junction is then formed by diffusion of phosphorus or boron, depending upon the conductivity type of the sheet sample. (In those cases where conventional diffusion temperatures are too high for the sample involved, other barrier formation methods – such as ion implantation – may have to be introduced.) Diffusion oxides are removed and open-structure ohmic contacts are applied, using conventional deposition methods. The junctions are then isolated to reduce edge-leakage, and in some cases antireflection coatings are applied to permit more accurate measurement of photovoltaic conversion efficiency.

Because of the nature of the Si sheet samples it may be determined that conventional processing techniques cannot be successfully applied. The presence of excessive numbers of grain boundaries, a high concentration of carrier lifetime "killer" impurities, uneven sheet surface morphology, irregular or specially-shaped cell configurations, temperature limitations associated with various substrate materials, and special contact configurations necessitated by the use of insulating substrate materials for the Si sheet growth may require development of alternative processing methods. These are established at the time, to meet the needs of the specific situation.

With illumination from a defined light source, such as the AM1 spectrum from a solar simulator, the conventional photovoltaic parameters I_{SC}, V_{OC}, P_{max}, CFF, and power conversion efficiency are then determined. The diffusion length of minority carriers in the completed cell structure is determined, if possible, by a photovoltaic method using a monochromatic light source. For samples in which the uniformity of photoresponse is of interest (for example, to examine effects of grain boundaries) a photocurrent scan of the surface of the sheet can be made using a small-diameter (10 μm) light spot to compare the output of various regions of the sample.

In most instances an array of small-diameter mesa diodes is formed on the junction structure by etching techniques. These diodes are evaluated separately to indicate the degree of homogeneity in the sample and correlate the electrical properties with any visible structural features (e.g., grain boundaries). Diode measurements include the photovoltaic parameters I_{SC} and V_{OC}, the dark forward diode characteristic, junction capacitance, and possibly an evaluation of trap properties.

Complete reports of all data and related observations concerning the sheet samples are supplied to Rockwell by OCLI. Technical consultation on the correlations between observed sheet properties and the details of the CVD sheet growth process takes place regularly as part of the working arrangement.

2.6.2 Si Sheet Sample Processing by OCLI

Eight samples were prepared and submitted to OCLI during the first quarter. These eight samples, with the pertinent deposition parameters and film properties, are listed in Table 2-15.

Three of the first four Si films were deposited on single-crystal $(01\bar{1}2)$-oriented sapphire substrates that were 500 μm thick. The fourth film was deposited on a multicrystalline sapphire substrate containing numerous large and elongated individual grains, with some of the grain-boundary intersections with the polished surface being nearly parallel. No attempt was made to establish the crystallographic orientations of the individual grains, although the 525-μm-thick wafer was cut with a nominal $(01\bar{1}2)$ orientation. This substrate provided a Si film with numerous relatively large single-crystal regions and numerous grain boundaries, to present a film of intermediate difficulty for the standard solar cell processing to be undertaken by OCLI.

Table 2-15. CVD Si Sheet Samples* Submitted to OCLI during First Quarter for Solar Cell Processing

Sample Designation	Substrate and (Thickness)	Observed Depos. Temp. (°C)	Carrier Gas and (Flow Rate)	SiH_4 Flow Rate (ccpm)	Film Thickness (μm)	Average Growth Rate (μm/min)	Sample Dimensions (cm) (Approximate Area in cm^2)	Film Structure and/or Surface Texture
OCLI-1	$(01\bar{1}2)$ A ℓ_2O_3† (500 μm)	605	H_2 (4 ℓpm)	10	3.5	~0.02	r≈1.9** (3.6)	Poly; Random Orientation
OCLI-2	$(01\bar{1}2)$ A ℓ_2O_3† (500 μm)	860	H_2 (4 ℓpm)	10	2.6	~0.5	r≈1.9** (3.0)	Poly; Preferred {110} Oriented
OCLI-3	$(01\bar{1}2)$ A ℓ_2O_3† (500 μm)	1032	H_2 (4 ℓpm)	5	3.0	~2.0	r≈1.9** (2.5)	Epitaxial
OCLI-4	Multicrystalline A ℓ_2O_3† (525 μm)	1025	H_2 (4 ℓpm)	10	8.6	~1.7	2.2 x 1.9 (oval) (3.3)	Epitaxial in Separate Grains
OCLI-5	$(01\bar{1}2)$ Aℓ_2O_3† (500 μm)	1030	H_2 (4ℓpm)	5	10	~2.0	r≈1.8** (2.5)	Epitaxial
OCLI-6	ASM805 Alumina (~640μm)	1025	H_2 (4 ℓpm)	25	20	~3.3	1.5 x 2.0 (3.0)	Poly: Preferred {110} Oriented; Directionally Reflective
OCLI-7	ASM805 Alumina (~640 μm)	1021	H_2 (4 ℓpm)	10	24	~1.6	1.4 x 1.9 (2.7)	Poly: Preferred {110} Oriented; Directionally Reflective
OCLI-8	ASM805 Alumina (~640 μm)	1030	H_2 (4 ℓpm)	25	40	~3.3	1.8 x 1.6 (2.9)	Poly; Preferred {110} Oriented; Directionally Reflective

* All Si films undoped.

† These substrates not subjected to high-temperature H_2 etch before deposition.

** These samples approximately 90 deg sector of circle of radius r cm.

The fifth sample sent to OCLI for processing and evaluation was another undoped epitaxial Si film grown on $(01\bar{1}2)$-oriented sapphire in H_2 at ~1025°C. This sample was to be used for double diffusion processing to produce a photovoltaic junction. The other three samples consisted of sizeable pieces of thick Si films grown on ASM805 alumina substrates in H_2 at ~1025°C, at two different growth rates to thicknesses of about 20 and 40 μm.

Results obtained on the first four samples during the first quarter were not encouraging. Considerable difficulty was encountered in processing the samples at OCLI because they were quite thin (~3 μm, except for OCLI-4) and were undoped. Both OCLI-3 and -4 were found to be slightly n-type, whereas OCLI-1 and -2 had such high resistivity that they did not permit conductivity-type detection even with a very sensitive probe. On the strength of that evidence, however, all four samples were B-diffused (1050°C for 15 min) to attempt to form a p-n junction. Mesas were formed by etching, but no evidence of any rectification or photovoltage was found in the first evaluation.

The processing of the first eight samples was completed early in the second quarter. The first four samples had been heavily stained as a result of the B diffusion (extensive cleaning did not remove the stains). However, two sets of small mesas (~0.02 cm^2) were etched into the surfaces of all four samples, in two separate procedures using different etch rates in order to control properly the amount of material removed. No photovoltage was observed under illumination, with mechanical-contact probes on the mesa tops and on the remaining Si between mesas. A very high effective resistance (~1 megohm) was observed for the mesa structures.

Regions of the diffused layers left protected in forming the first two sets of small mesas were then etched to form relatively large-area mesas (~0.8 cm^2), and contacts were vacuum-deposited on the mesas and the exposed bottom region of the Si layer. Again no photovoltage was observed on probing the mesas under illumination.

It was concluded that the undoped nature of these thin layers precluded successful formation of a diffused junction that would exhibit a photovoltage. The effective diffusion rate of the common dopants (e.g., B and P) in Si of the varied structural properties represented in this set of samples was not known at the time, and some experimentation is required to establish such information. A separate layer-doping step should probably have been undertaken (using P) before the B diffusion for junction formation was carried out. This layer doping should involve a low-surface-concentration diffusion with a low-temperature long-time distribution of the diffusant, to attempt to achieve a fairly uniform low doping level throughout the layer.

Results on the other four samples (OCLI-5, 6, 7, and 8) indicated that, at least on number 5 (Si ~10 μm thick on sapphire, grown at ~1030°C), a photovoltaic effect was observed. Sample OCLI-5 as received by OCLI tested p-type by thermal probing, so a shallow n^+ layer was formed by $POCl_3$ diffusion at 875°C for 20 min. Small mesas were formed on part of the diffused surface by masking and etching. Under illumination, and with mechanical-contact probes on the mesas and the lower region of the deposited layer, a photovoltage of ~200mV was obtained with a low photocurrent. Using a contactless rf method to measure the effective resistivity, a value of sheet resistance of ~100,000 ohms per square was obtained.

Larger mesas were formed on the remaining n^+ diffused layer, and vacuum-deposited Aℓ contacts were applied to the mesa tops and the exposed base-region p-type Si. Under tungsten-lamp illumination, with the diode reverse-biased to permit determination of the photocurrent, a current density of ~1.5 ma/cm^2 and a photovoltage of ~230mV were measured. It was estimated that a reduced internal resistance would permit a curve fill factor of ~0.5 and a conversion efficiency the order of 0.2 percent (determined by direct comparison with a conventional single-crystal cell) for a cell of the type formed here.

These first attempts to apply standard solar cell processing to some of the CVD Si films indicated that it may become necessary to develop and/or apply some specialized methods - for example, junction growth by CVD or ion implantation doping instead of, or in addition to, diffusion doping for junction formation - to these polycrystalline films in order to get an adequate indication of their suitability for solar cell fabrication.

Another six samples of CVD Si sheet were submitted to OCLI during the second quarter. These samples are listed in Table 2-16, along with their deposition parameters and other pertinent properties. All of the Si films were B-doped, with measured active carrier concentrations in the range from 10^{17} to 10^{18} cm^{-3}. Four of the samples were CVD films on single-crystal $(01\bar{1}2)$-oriented sapphire substrates and thus were epitaxial; Hall mobilities for these films were in the range from 125 to 187 cm^2/V-sec. The other two samples were polycrystalline CVD films grown on polycrystalline alumina (MRC Superstrate) substrates – one in the as-fired condition and one polished at Rockwell prior to its use as a substrate. The films on these two samples both exhibited strong {110} preferred orientation. All six Si films were in the thickness range 18 to 20 μm, and all film surfaces were in the as-grown condition.

Because all of these samples were p-type, with measured carrier concentrations in a range reasonable for base region material for Si solar cells, a standard P diffusion was carried out to form the p-n junctions. This used a $POCl_3$ source and was done at 900°C for 10 min, and included p-type 1 ohm-cm control slices of single-crystal Si. After diffusion the glass was removed and all samples probed n-type.

Using etch-resistant tape, a large mesa was etched in each sample (1:10 $HF:HNO_3$ for 30 sec), with 6 to 8 μm of Si being removed around the mesas. With moderate-intensity tungsten-lamp illumination (~100 mw/cm^2) and only mechanical-probe contacts preliminary V_{OC} readings were obtained, after which V_{OC} was also obtained for two of the cells and the control in the AMO simulator (with no attempt to control sample temperature). The open-circuit photovoltages obtained in these two preliminary measurements are shown in the first two rows of Table 2-17.

Table 2-16. B-doped CVD Si Sheet Samples Submitted to OCLI during Second Quarter for Solar Cell Processing and Measurement

SAMPLE NO.	SUBSTRATE MATERIAL AND THICKNESS (μm)	DEPOS. TEMP (°C)	CARRIER GAS AND FLOW RATE (lpm)	SiH_4 FLOW RATE (ccpm)	DOPANT GAS* FLOW RATE (ccpm)	FILM THICK-NESS (μm)	AVE. GROWTH RATE (μm/min)	FILM RESIS-TIVITY (ohm-cm)	HOLE CONCEN-TRATION (cm^{-3})	HALL MOBILITY (cm^2/V-sec)	SAMPLE DIMENSIONS (cm) AND APPROX AREA (cm^2)	FILM STRUCTURE AND/OR SURFACE TEXTURE
OCLI-9	$(01\bar{1}2)$ Al_2O_3 375	1022	H_2 4	10	0.91	18	1.8	0.26†	1.3×10^{17}†	187†	1.0 x 1.1 1.1	Epitaxial
OCLI-10	$(01\bar{1}2)$ Al_2O_3 300	1025	H_2 4	10	9.1	18	1.8	0.070†	6.1×10^{17}†	145†	1.15 x 1.0 1.15	Epitaxial
OCLI-11	$(01\bar{1}2)$ Al_2O_3 300	1023	H_2 4	10	9.1	20	1.9	0.063†	6.8×10^{17}†	146†	1.0 x 0.9 0.9	Epitaxial
OCLI-12	$(01\bar{1}2)$ Al_2O_3 300	1025	H_2 4	10	9.1	19	1.9	0.052†	9.5×10^{17}†	125†	1.0 x 0.95 0.95	Epitaxial
OCLI-13	MRC Superstrate alumina (as fired) 700	1025	H_2 4	10	9.1	20	2.0	0.76**	5.0×10^{17}**	16**	1.3 x 1.2 1.6	Poly; preferred {110} oriented
OCLI-14	MRC Superstrate alumina (polished) 675	1025	H_2 4	10	9.1	20	2.0	0.86**	4.8×10^{17}**	15**	1.4 x 1.4 2.0	Poly; preferred {110} oriented

*Films B-doped from B_2H_6-in-He (46 ppm)
†Measured by Hall bridge method
**Measured by van der Pauw method

Table 2-17. Photovoltaic Properties of Solar Cell Structures** in Si Sheet Samples OCLI-9, 10, 11, 12, 13, and 14

MEASUREMENT/PROPERTY	SAMPLE							REMARKS
	Control† (1 ohm-cm s.c. Si)	OCLI-9	OCLI-10	OCLI-11	OCLI-12	OCLI-13	OCLI-14	
1. V_{oc} (mV) (~100 mw/cm^2 W Lamp)	490	283	355	347	278	48	43	Mechanical probe contacts
2. V_{oc} (mV) (AMO Solar Simulator)	535	NM*	440	NM*	NM*	80	NM*	Mechanical probe contacts; no temp. control
3. V_{oc} (mV) (AMO Solar Simulator)	560	290	415	340	270	43	40	Ti-Ag contacts; no temp. control; contacts evidently poorly bonded
4. I_{sc} (ma)	11.8	0.87	3.85	0.8	2.6	0.4	0.34	
5. CFF	–	Concave	0.30	Concave	0.25	0.25	0.25	
6. V_{oc} (mV) (~100 mw/cm^2 W Lamp)	523	260	342	175	119	26	23	New contacts
7. I_{sc} (ma)	6.2	0.23	0.56	0.28	0.36	0.022	0.020	
8. V_{oc} (mV) (~100 mw/cm^2 W Lamp)	525	280	230	110	78	32	25	After annealing at 550°C for 5 min.
9. I_{sc} (ma)	6.6	1.04	0.67	0.60	0.56	0.79	0.86	
10. V_{oc} (mV) (~130 mw/cm^2 W Lamp)	570	345	360	236	125	82	77	As above
11. I_{sc} (ma)	21.6	6.9	3.7	3.9	3.9	5.8	3.4	
12. V_{oc} (mV) (AM1 Solar Simulator)	525	325	340	230	NM*	62	65	As above
13. I_{sc} (ma)	23	2.9	1.6	2.0	NM*	0.8	0.75	
14. L_e (μm)	100	~2	~1	~1	~1	~2	~1	Estimates based on control sample and photocurrent responses

** None of the structures was anti-reflection coated.
† Nominal efficiency 10 percent
* NM = Not measured

Simple stripe or U-shaped Ti-Ag contacts were then applied to the mesa tops and to the exposed base Si and the responses were obtained in the AMO simulator, again without temperature control. The results are given in the third, fourth, and fifth rows of Table 2-17. Since it appeared that the contacts were not properly adherent they were removed and reapplied. The responses to the moderate tungsten-lamp illumination obtained with the new contacts are given in rows 6 and 7 of Table 2-17; essentially no improvement was observed. Since all of the Si sheet samples exhibited high dark reverse leakage currents the mesas were all re-masked and re-etched; again no improvement was observed.

Because of the poor curve shapes obtained (row 5, Table 2-17), the samples were heat-treated at 550°C for 5 min to attempt to reduce contact series resistances. Again responses were measured, with the results given in rows 8-13, inclusive, in Table 2-17.

On the basis of the known minority carrier diffusion length in the control sample (~100 μm) and the photocurrent responses given in the table, estimates of the diffusion lengths in the Si sheet samples were made, and these are listed in row 14 of Table 2-17.

Sample OCLI-10 had the best curve shape of the sheet samples in this group. The estimated AM1 efficiency for this cell is ~0.5 percent; this would increase to ~0.65 percent if an AR coating were applied. (None of the samples was AR-coated.)

Additional attempts to reprocess samples OCLI-9 and 14 – including complete removal of the contacts and the diffused layer on the mesa, and rediffusion and recontacting – were ineffective in producing any improvement in performance. Similarly, attempts to determine the junction depth in OCLI-12, which had exhibited very poor performance, by bevel-and-stain techniques were unsuccessful.

The variation in V_{OC} in the Si sheet cells on sapphire can perhaps be correlated with the variation in the base material doping concentration (see Table 2-16). The greatly reduced V_{OC} values for the small-grained polycrystalline cells (OCLI-13 and -14) on MRC Superstrate alumina substrates are probably related to factors such as the high reverse saturation current density in the junctions formed in polycrystalline material, not an unexpected result.

During the third quarter of the program ten more samples were delivered to OCLI for processing and evaluation. These are listed in Table 2-18 with their deposition parameters and relevant properties. Six of them were doped epitaxial samples on single-crystal sapphire, to provide Si sheet material for processing into solar cell structures that would exhibit photovoltaic performance that might be considered to represent an upper limit that could be expected from any similarly processed polycrystalline Si sheet material on low-cost substrates. The other four samples consisted of three B-doped and one undoped polycrystalline Si films grown on polycrystalline alumina substrates; two of them were deposited on polished MRC Superstrate and two on as-fired ASM805 (3M Co.). It was expected that the generally larger samples in these two groups (five were delivered on each of two dates) would facilitate the handling and processing at OCLI and generally provide more information of value to the program.

Figure 2-18. B-doped CVD Si Sheet Samples Submitted to OCLI During Third Quarter for Solar Cell Processing and Measurement

SAMPLE NO.	SUBSTRATE MATERIAL AND THICKNESS (μm)	DEPOS TEMP (°C)	CARRIER GAS AND FLOW RATE (lpm)	SiH_4 FLOW RATE (ccpm)	DOPANT GAS* FLOW RATE (ccpm)	FILM THICK-NESS (μm)	AVE. GROWTH RATE (μm/min)	FILM RESIS-TIVITY (ohm-cm)	HOLE CONCEN-TRATION (cm^{-3})	HALL MOBILITY (cm^2/V-sec)	SAMPLE DIMENSIONS (cm) AND APPROX AREA (cm^2)	FILM STRUCTURE AND/OR SURFACE TEXTURE
OCLI-15	MRC Superstrate alumina (polished) 700	1031	H_2 4	10	None	33	1.6	2.8×10^{5} **	5.5×10^{11}**	41**	1.2x1.1 1.3	Poly: preferred {110} oriented
OCLI-16	3M ASM805 alumina (as fired) 700	1022	H_2 4	25	75	25	3.1	0.04†	3.2×10^{18}†	47†	1.8x1.7 3.1	Poly; preferred {110} oriented
OCLI-17	3M ASM805 alumina (as fired) 625	1025	H_2 4	25	10	25	3.2	0.5†	5.8×10^{17}†	22†	1.7x1.7 2.9	Poly; preferred {110} oriented
OCLI-18	$(01\bar{1}2)A\ell_2O_3$ 575	1023	H_2 4	25	10	25	3.2	0.08**	6.6×10^{17}**	114**	3.[illegible]x2.4 7.4	Epitaxial
OCLI-19	$(01\bar{1}2)A\ell_2O_3$ 500	1022	H_2 4	25	5	26	3.2	0.1**	5×10^{17}**	125**	2.5x2.2 5.5	Epitaxial
OCLI-20	$(01\bar{1}2)A\ell_2O_3$ 550	1024	H_2 4	25	10	20††	2.5	NM***	$\sim10^{17}$††	NM***	2.3x2.0 4.6	Epitaxial
OCLI-21	$(01\bar{1}2)A\ell_2O_3$ 550	1027	H_2 4	25	10	20††	2.5	NM***	$\sim10^{17}$††	NM***	3.4x1.1 3.7	Epitaxial
OCLI-22	$(01\bar{1}2)A\ell_2O_3$ 500	1030	H_2 4	25	10	20††	2.5	NM***	$\sim10^{17}$††	NM***	2.5x1.7 4.2	Epitaxial
OCLI-23	$(01\bar{1}2)A\ell_2O_3$ 375	1024	H_2 4	25	10	20††	2.5	NM***	$\sim10^{17}$††	NM***	1.5x1.0 1.5	Epitaxial
OCLI-24	MRC Superstrate alumina (polished) 700	1030	H_2 4	25	1.96	20††	2.5	NM***	$>10^{16}$††	NM***	1.5x0.9 1.3	Poly; preferred {110} oriented

*Films B-doped from B_2H_6-in-He (46 ppm)

†Measured by Hall bridge method

**Measured by van der Pauw method

††Estimate from CVD parameters

***NM = Not measured

The processing of these two groups of samples was not complete at the time of preparation of this report, but some preliminary results have been obtained. Samples OCLI-18 and 19 were processed first, along with the usual high-lifetime single-crystal Si control sample. Both sheet samples were etched lightly (1:6:10 HF:HNO_3: CH_3COOH for 20 sec) before processing, to remove any shallow damaged layer and/or surface contamination. They were then P-diffused at 900°C for 14 min, using a $POCl_3$ source. The resulting glass was removed after diffusion by immersion in HF; the samples were found then to be n-type by probe test.

Etch-resistant tape was then used to permit etching a large digitated mesa covering about half the area of each sample; about 5 μm of Si was removed by the etching (1:10 HF:HNO_3 for 25 sec), resulting in p-type material in all regions among the mesa fingers. The junctions were thus less than 4 to 5 μm deep, at most. The samples were then cleaned and Ti-Ag was deposited by vacuum deposition over the total sample area; no post-deposition heat treatment was used. Wax masking was used to remove the metal from the edges of the mesas, leaving two interdigitated contacts - one for the mesa top and one for the p-type Si in the base region. No AR coating was applied at that stage of the processing.

The two epitaxial sheet samples and the single-crystal control all were then tested in the AMO solar simulator. Results of these measurements are given in rows 1 through 5 in the left half of Table 2-19. The open-circuit photovoltages of the Si sheet cells compare reasonably well with that of the control sample, but the short-circuit current densities and the maximum power per unit area delivered to the load are quite low for the sheet cells relative to the single-crystal control cell. It is interesting to note, however, that the curve fill-factor is very low and about equal for all three cells. The fact that the Ti-Ag contacts were not heat treated for any of the three cells is believed to be the main cause of this. The power conversion efficiency is low for both of the Si sheet cells, but it is also quite low for the control cell. This indicates that the front-contact arrangement is far from satisfactory for the control cell and that there may be other aspects of the processing that should be modified to obtain improved cell performance in the sheet samples as well as the single-crystal control material. It should be emphasized that the control cells have deliberately been subjected to the same processing as that experienced by the sheet samples, to provide the best comparison basis.

Measurements were also made of the photocurrent density in tungsten-lamp illumination alone and xenon-lamp illumination alone, and these results are given in rows 6 and 7 of the table. The results show that the response at longer wavelengths (i.e., >0.6 μm) in the sheet cells is especially poor; that at shorter wavelengths is relatively better, as would be expected.

The three samples were then exposed to monochromatic illumination ($\lambda \approx 0.92$ μm) from an LED, with the junction back-biased in order to get a measure of the generated photocurrent due to the illumination over the arbitrary area of the light spot used. The results so obtained are entered in row 8 of Table 2-19. On the basis of an assumed minority carrier diffusion length of ~100 μm in the single-crystal control sample, the diffusion lengths in the two sheet samples would probably be about 3μm, as shown in row 9 of the table. This result was verified for numerous locations over the surface of each of the sheet cells, thus indicating uniformity of this characteristic.

Table 2-19. Preliminary Measurements of Photovoltaic Properties of Solar Cell Structures in Si Sheet Samples OCLI - 17, 18, 19, 20, 21
(Blank spaces represent measurements not yet made)

MEASUREMENT/PROPERTY	SAMPLE							REMARKS
	Control No. 1 (2 ohm-cm s.c. Si)	OCLI-18	OCLI-19	Control No. 2 (2 ohm-cm s.c. Si)	OCLI-17	OCLI-20	OCLI-21	
Active cell area (cm^2)	1.5	2.54	2.68	2.35	1.6	2.8	2.25	
Uncoated samples								
1 V_{oc} (mV) (AMO Solar Simulator)	490	400	360	470	56	350	420	No control of sample temp; Ti-Ag contacts not heat treated; I_{sc} partly limited by readout series resistance.
2 I_{sc} (ma/cm^2)	16	6.1	7.8	14.5	-	-	-	
3 Load power delivered (mw/cm^2)	2.25	0.82	0.81	1.55	-	-	-	
4 CFF	0.29	0.33	0.29	0.23	-	-	-	
5 Power conversion efficiency (%)	1.6	0.6	0.6	1.1	-	-	-	Based on 140 mw/cm^2 insolation
6 I_{sc} (ma/cm^2) (W Lamp alone)	12	2.4	3.0	12.1	-	-	-	Illumination mainly at $\lambda > 0.6\mu m$
7 I_{sc} (ma/cm^2)(Xe Lamp alone)	7.3	3.9	4.8	-	-	-	-	Illumination mainly at $\lambda < 0.6\mu m$
8 I_g (ma) (LED at $\lambda = 0.92\mu m$)	0.8	0.06	0.06	0.85	-	0.12	0.07	Junction back-biased; area is that of light spot.
9 L_e (μm)	~100 (est)	~3	~3	~100 (est)	≤1	~4	~2	Estimates based on control sample and photocurrent responses.
Samples coated with SiO								
10 V_{oc}(mV) (AMO Solar Simulator)	-	415	450	-	70	375	445	As in rows 1 - 4.
11 I_{sc} (ma/cm^2)	-	8.3	12.2	-	0.69	3.12	8.62	
12 Load power delivered (mw/cm^2)	-	1.8	2.35	-	-	0.26	1.47	
13 CFF	-	0.52	0.43	-	-	0.23	0.38	
14 Power conversion efficiency (%)	-	1.3	1.7	-	-	0.2	1.1	As in row 5
15 I_{sc} (ma/cm^2) (W Lamp alone)	-	3.5	4.3	-	-	-	3.4	As in row 6

The two sheet samples were then coated with SiO to reduce reflection losses, and the performance in the AMO solar simulator was again determined. The results are given in rows 10 through 14 of Table 2-19. The improved performance of both cells is striking; in particular, the improved curve fill-factor of OCLI-18 and the increased power conversion efficiency of both cells tend to indicate that the proper modifications in contact design and overall processing would produce even further improvements in performance. However, the photocurrent generation indicated by the response to the tungsten lamp (row 15, Table 2-19) still corresponds to a short diffusion length, as suggested above.

Processing of two samples from the second group of five (OCLI-20 and 21) together with OCLI-17 from the first group has also begun. The latter is a polycrystalline Si film B-doped to $\sim 6 \times 10^{17}$ cm^{-3} and grown on as-fired ASM805 alumina, while OCLI-20 and -21 are both epitaxial films on single-crystal $(01\bar{1}2)$ sapphire, each doped to the low 10^{17} cm^{-3} range. One of these three samples (OCLI-20) had been used in a preliminary test at OCLI designed to investigate if the sapphire substrates in any way could alter the lifetime properties of good quality single-crystal high-lifetime Si during a heating cycle to ~1020°C by being in contact with it. For this purpose, OCLI-20 was in contact with a Si control wafer at 1020°C for about 10 min (the experiment failed to reveal any pronounced effect), but otherwise was used as delivered.

These three samples plus another 2 ohm-cm control wafer were etched lightly, as before; OCLI-17 was extensively darkened by the etching - at least in part due to its already heavily faceted and textured surface. The samples were P-diffused (from $POCl_3$) at 900°C for only seven minutes (compared with 14 min for the other three samples), to produce a junction at about 0.7 the depth generated in the other set. After removal of the glass all four samples were n-type.

Tape masking was again used to produce a finger-type mesa, and interdigitated Ti-Ag contacts were applied to the Si sheet cells but with finer lines than in the previous set of samples. The control cell of this group had a backside contact this time instead of two interdigitated front-surface contacts.

The four samples were then exposed to the AMO solar simulator illumination, with the results shown in rows 1 through 5 in the right half of Table 2-19. The open-circuit photovoltages of OCLI-20 and 21 were in the same range as those of OCLI-18 and 19, and poor curve shapes were again observed indicating high series resistance – probably at the contacts. The polycrystalline Si sheet cell (OCLI-17) exhibited a V_{oc} value only about 15 percent of those found for the epitaxial Si cells (OCLI-18, 19, 20, 21). Other parameters were not determined for the uncoated cells under AMO illumination.

The four samples were then exposed to the LED illumination ($\lambda \approx 0.9$ μm) to observe the generated photocurrent response. The results are given in row 8 of the table. A first-quality single-crystal Si cell with long diffusion length generates ~2.2 ma under this same illumination. Again on the basis of the observed photoresponses for the sheet samples, it appears that minority carrier diffusion lengths in the epitaxial samples are in the 2 to 4 μm range, as shown in the table. The effective diffusion length in the polycrystalline sample is difficult to estimate, but it probably does not exceed ~1 μm.

The Si sheet cells were then coated with SiO to reduce reflection losses, and the AMO responses were again determined (rows 10 through 14, right half of table). The improvement in V_{OC} was similar to that found for OCLI-18 and 19. The curve shapes were still poor, although again it should be noted that the single-crystal control cell (No. 2) - which was not coated - also had a poor curve fill-factor. The tungsten-lamp response of OCLI-21 after coating (row 15) again confirmed the long-wavelength response deficiency associated with short diffusion lengths.

On the basis of these preliminary measurements it appears unlikely that Si sheet cell efficiencies better than about two percent can be expected, even if series resistance problems are solved so that curve fill factors are better. The apparently low diffusion lengths (short lifetimes) are the most likely cause of this limitation. This problem is well known in Si-on-sapphire, of course, and it should be noted that none of the recognized precautions for reducing the effects of lifetime killers in Si-on-sapphire - such as the use of a heavily-doped adjoining getter layer (in this case a p^+ layer under the p-type grown layer) - was used in preparing the Si sheet samples discussed above. As was indicated earlier (Section 2.5.1.4), recent measurements by the C-V-t method on similar B-doped epitaxial Si films on sapphire, also without the gettering underlayer, have indicated lifetimes of about 10^{-7} sec, corresponding to calculated minority carrier diffusion lengths (using assumed carrier mobility values for the films in question) in excess of 10 μm. This apparent discrepancy raises several questions which will be the subject of study in the coming quarter, both in terms of the basic properties of the films and in terms of the effects of the OCLI solar cell processing on these basic properties.

If the limitations on minority carrier lifetime (and diffusion length) in the epitaxial films are found to constitute limitations on the performance of solar cell structures fabricated in the same materials, then any available corrective measures must be taken before it can be considered that a realistic upper limit on Si sheet cell performance has been established. As for the performance of the solar cell structures in the polycrystalline films processed to date, it is probably being limited by other drastic shortcomings in the film properties that have not yet been fully identified. Additional polycrystalline film samples on alumina and glass substrates that will be processed at OCLI in the coming quarter will help to establish these limitations and the possible causes.

3. CONCLUSIONS AND RECOMMENDATIONS

Although the work of Task 1 was completed in the second quarter, problems with the mass flow controllers - especially the one in the SiH_4 line - have persisted. The controllers in this application are definitely not maintenance-free; it has been determined that both the controller and the nearby flow valve in the SiH_4 line will be periodically disassembled and cleaned as routine preventive maintenance, to avoid the SiO_2 powder contamination problem encountered on several occasions to date. In addition, the glass rotameters will be left in the gas lines in series with the mass flow controllers, both as flow "on" indicators and as substitutes for the controller whenever needed.

The cooperation and assistance received from many of the suppliers contacted relative to the substrate requirements (Task 2) have continued to be excellent. Additional candidate substrate materials have recently been received and more are still expected from several of the manufacturers (see Table 2-1). However, several of the substrate vendors that have very willingly supplied substrate materials in limited quantities without charge for experimental evaluation on this program are now beginning to take the view that further supplies will have to be purchased, and any significant development activities will have to be supported by sources other than their own company funds. This position is certainly reasonable, and it requires that the situation be factored into planning for expenditures and experimental work, as well, for the remainder of the program.

The alumina substrates, both single-crystal (sapphire) and polycrystalline, continue to be the most available and hardy substrates for baseline film growth experiments and for evaluation of the effects of changes in growth parameters on film properties. However, there appears to be little indication or belief--on the part of manufacturers and/or suppliers--that the costs per unit area of high-purity polycrystalline aluminas are likely to be reduced to sufficiently low levels to meet the requirements of the LCSSAP, even in the very large quantities envisioned for future production for the project. Further, the work of the past quarter has indicated that there may be troublesome impurity problems in several of the structurally most attractive aluminas. There is also some evidence that the differences in the significant (for solar cells) properties of the polycrystalline Si films deposited on several of the principal polycrystalline aluminas of interest may not be large, and may be relatively independent of the surface condition (i.e., polished or as fired), although additional data on this point are required. There is no question, however, about the value of the aluminas (especially those with large crystal grains) in studies of Si CVD growth parameters and – especially – mechanisms of film nucleation, island growth, and orientation.

There is need for the emphasis to shift from polycrystalline alumina substrates to glass substrates in the coming quarter, perhaps "passing through" the lower-cost (i.e., lower purity) aluminas on the way. It is hoped that additional special glasses, with properties closely matched to those required for Si film deposition by CVD, can be obtained for experimental evaluation. Additionally, attempts are being made to obtain suitable glass-ceramic samples for evaluation.

Especially for glass substrates, it will be necessary to use deposition temperatures lower than those employed for the aluminas, and with most of the glasses a He (or other inert) carrier gas is also necessary. This will require developing the appropriate CVD parameters for suitable growth rates and growth uniformity in this temperature range, and doping techniques and parameters for this environment will also have to be established.

The experiments with SiH_4-$HC\ell$ mixtures in Task 3, intended to lead to development of a two-step growth process involving $HC\ell$ etching effects and thus to enhanced grain sizes in the Si films under otherwise similar conditions, have not been carried sufficiently far to permit proper evaluation of the technique. These experiments should be continued and - irrespective of the outcome of the investigations - other two-step processes for increasing grain sizes should also be explored, as originally planned. In particular, the use of two different Si source compounds in sequence - such as SiH_4 and $SiH_2C\ell_2$ - should be investigated; the nature of the $HC\ell$ release at the surface by this reaction is quite different (in its chemical kinetics) from that involved in the direct $HC\ell$ addition experiments now in progress. The effects on in situ annealing at various stages of growth - especially in the early post-nucleation stage when island coalescence is playing a dominant role in development of the layer - should also be examined. These measures should be investigated with accelerated vigor, as should the nucleation experiments in which the details of island formation and growth on both polycrystalline surfaces (such as alumina) and amorphous surfaces (such as glass) will be studied. Such investigations could provide the knowledge needed to control the early stages of growth sufficiently to obtain large individual grains even on unfavorable substrates.

The results obtained to date in fabricating solar cell structures in both epitaxial Si films on sapphire and polycrystalline films on low-cost substrates have indicated that additional measures should probably be taken in preparing the films for such processing. In particular, the use of a heavily doped gettering layer beneath the principal base region (usually p-type), would improve the minority carrier properties (esp. diffusion length) in the epitaxial layers processed into baseline reference cells, and might also produce distinct improvements in cells fabricated in polycrystalline films. Also, because of impurity diffusion characteristics peculiar to polycrystalline Si films it may not be possible to obtain an accurate measure of the best photovoltaic performance of solar cell structures in the CVD Si sheet material unless processing methods other than diffusion--such as in situ growth of the p-n junctions in the CVD reactor--are applied. This possibility should be explored experimentally as soon as possible.

The methods being used for film characterization in Task 5 - optical microscopy, scanning electron microscopy, x-ray diffractometry, surface profilometry, spreading resistance measurements, Hall coefficient (and resistivity) measurements, minority carrier lifetime measurements by the pulsed-MOS (C-V-t) method - will be continued. The complex nature of the mechanisms of charge transport in polycrystalline Si films requires that careful consideration be given both to the types of measurements made and the interpretation of these measurements. Attention should soon be given to developing an improved model of conduction in polycrystalline films to fit the data being obtained. When the properties of the Si films have improved sufficiently, additional techniques--such as Schottky-barrier methods for determination of impurity

distributions, EBIC-mode analysis with the SEM to investigate properties of individual crystal grains and the intervening grain boundaries, and surface photovoltage measurements to obtain effective minority carrier diffusion length values--will be applied to give more complete understanding of the Si sheet properties.

Finally, it is clearly important to increase the rate of sample delivery to OCLI in Task 6, for fabrication and evaluation of solar cell structures. Such a change will correspondingly increase the amount of information generated by that task and - if the data feedback is accomplished according to plan - also the timeliness of the results, thus increasing the value of the work to the other tasks of the program.

4. PLANS FOR NEXT SIX MONTHS

The planned work for the next six months will follow the Updated Technical Program Plan given in Appendix B of this report. The planned work, summarized by task, is as follows:

TASK 1

The work of this task was completed during the second quarter.

TASK 2

1. Continue experimental evaluation and screening of candidate substrate materials by structural analyses and by Si CVD experiments, with major emphasis on glasses

2. Conduct experimental evaluation of lower purity (lower cost) polycrystalline alumina substrates

3. Continue to investigate effects of various substrate surface treatments, including metal deposits, on resulting film properties

4. Identify most promising substrate material(s).

TASK 3

1. Continue deposition experiments to identify preferred substrate materials and CVD parameters for each

2. Continue examination of two-step deposition process employing HCℓ as means for improving properties (esp., grain size) in polycrystalline Si films

3. Investigate effects of in situ and post-growth annealing on Si film properties

4. Conduct experiments to determine conditions for producing doped p-type films in He carrier gas on glass substrates

5. Continue simultaneous Si growth experiments on polycrystalline and/or amorphous substrates and single-crystal sapphire to compare electrical properties of doped films in the two cases

6. Continue investigation of effects of identity of dopant impurity on Si film growth phenomena and on Si film properties

7. Conduct experiments with partial-coverage deposits of Si on selected substrate(s) to examine incubation phenomena and film nucleation processes.

TASK 4

1. Prepare samples of doped epitaxial Si on single-crystal substrates for processing into baseline solar cell structures

2. Prepare samples of appropriately doped CVD Si films on selected polycrystalline and amorphous substrates for fabrication of experimental solar cell structures

3. Prepare various CVD Si samples for evaluation, demonstration, and for delivery to JPL.

TASK 5.

1. Continue analyses of Si film and substrate structural properties by surface profilometry, x-ray diffraction, metallographic sectioning, reflection electron diffraction, and scanning electron microscopy techniques

2. Continue application of x-ray diffraction methods for determination of preferred orientation and grain size in polycrystalline CVD Si films on various substrates

3. Continue determination of film electrical properties by van der Pauw and Hall bridge measurements, and compare results at various doping levels

4. Extend and/or develop model for electrical properties of polycrystalline Si films

5. Continue use of spreading resistance measurements to determine carrier concentration profiles and locate structural inhomogeneities (esp. grain boundaries) in polycrystalline Si films on various substrates

6. Investigate and apply methods for measurement of minority carrier diffusion lengths/lifetimes in CVD Si films - including pulsed C-V method in MOS structures, EBIC-mode analysis of barriers in SEM, surface photovoltage measurements

7. Investigate applicability of x-ray topographic methods and electron channeling pattern studies (in SEM) for orientation determination in selected polycrystalline Si film samples.

TASK 6

1. Prepare and submit additional samples of CVD Si sheet to OCLI for solar cell processing and evaluation, emphasizing doped films on glass and polycrystalline alumina and/or other ceramic substrates.

5. NEW TECHNOLOGY

No reportable items of new technology have been identified during the conduct of the first three quarters of work on this contract, which is the period covered by this report.

6. REFERENCES

1. E. Rasmanis, The Electrochemical Society, Spring Meeting, Pittsburgh, April 1963, Paper No. 72.

2. See, e.g., Y.S. Chiang, The Electrochemical Society, Spring Meeting, Chicago, May 1973, Paper No. 119; also, P. Rai-Choudhury and P.L. Hower, J. Electrochem. Soc. 120, 1761 (1973).

3. S. Horiuchi, Solid-State Electron. 18, 1111 (1975).

4. T.I. Kamins and T.R. Cass, Thin Solid Films 16, 147 (1973).

5. See, e.g., Y.S. Chiang and D. Richman, Met. Trans. 2, 743 (1971); also see Ref 6, Section 3.

6. R.P. Ruth, A.J. Hughes, J.L. Kenty, H.M. Manasevit, D. Medellin, A.C. Thorsen, Y.T. Chan, C.R. Viswanathan, and M.A. Ring, "Fundamental Studies of Semiconductor Heteroepitaxy," Final Report, August 1973, ARPA Order No. 1585, Contract DAAH01-70-C-1311. (Prepared by Rockwell International, Electronics Group, Research and Technology Division, Anaheim, Ca., for USAMICOM, Redstone Arsenal, AL).

7. H.M. Manasevit, Arnold Miller, F.L. Morritz, and D.H. Forbes, AIME Meeting, Chicago, Oct. 1966.

8. J. Bloem, J. Crystal Growth 18, 70 (1973).

9. L.J. van der Pauw, Philips Res. Repts. 13, (1958).

10. T.I. Kamins, J. Appl. Phys. 42, 4357 (1971).

11. P. Rai-Choudhury and P.L. Hower, J. Electrochem. Soc. 120, 1761 (1973); originally given as Paper 240, Fall Meeting of The Electrochemical Society, Miami Beach, October 1972.

12. J.D. Joseph and T.I. Kamins, Solid-State Electron. 15, 355 (1972).

13. D.K. Schroder and P. Rai-Choudhury, Appl. Phys. Lett. 22, 455 (1973).

14. Denis J. McGreivy and C.R. Viswanathan, Appl. Phys. Lett. 25, 505 (1974).

15. M. Zerbst, Z. angew. Phys. 22, 30 (1966).

APPENDIX A. MANPOWER AND FUNDING EXPENDITURES

This report covers the first nine months of the contract. Through the eighth month of the contract (that is, through August 28, 1976) a cumulative total of 4108 engineering and support manhours and a cumulative total of $130,506 (excluding fee and commitments) were expended.

For the ninth month of the contract (August 29 through October 2, 1976) a total of 403 engineering and support manhours and a total of $16,350 (excluding fee and commitments) were expended.

The cumulative manpower expenditure total through October 2, 1976, is thus 4511 manhours, and the cumulative cost total (excluding fee and commitments) through that date is $146,856.

APPENDIX B. UPDATED TECHNICAL PROGRAM PLAN

The Initial Technical Program Plan was approved by the JPL Technical Manager on February 4, 1976.

An Updated Technical Program Plan, revised to show changes in the date of completion of reactor modifications and the date of the design review for Task 1, was included in the Monthly Technical Progress Report for April, 1976. That revised plan was approved by the JPL Technical Manager on May 17, 1976.

A further updating of the plan, including a suggested change in schedule for Technical Goal No. 4 of Task 5, was shown in Quarterly Report No. 2 and in the Monthly Technical Progress Report for July, 1976.

Additional changes in the Technical Program Plan, involving changes in several Technical Goals, were discussed with and tentatively approved by the JPL Technical Manager at the Bimonthly Program Review Meeting at the Rockwell Anaheim facility on August 12, 1976. These changes were approved by the JPL Technical Manager on September 2 and September 21, 1976.

The Updated Technical Program Plan shown here includes those approved changes, and is also updated to show the achieved technical goals (filled-in triangles) through October 2, 1976, and the actual manpower and funding expenditures through that same date.

CHEMICAL VAPOR DEPOSITION GROWTH
SILICON SHEET GROWTH DEVELOPMENT

JPL CONTRACT NO. 954372

TASK 2: LARGE AREA SILICON SHEET
JPL/ERDA LOW COST SILICON SOLAR ARRAY PROJECT

UPDATED TECHNICAL PROGRAM PLAN

(Note: Numbered technical goals are listed at end of each task)

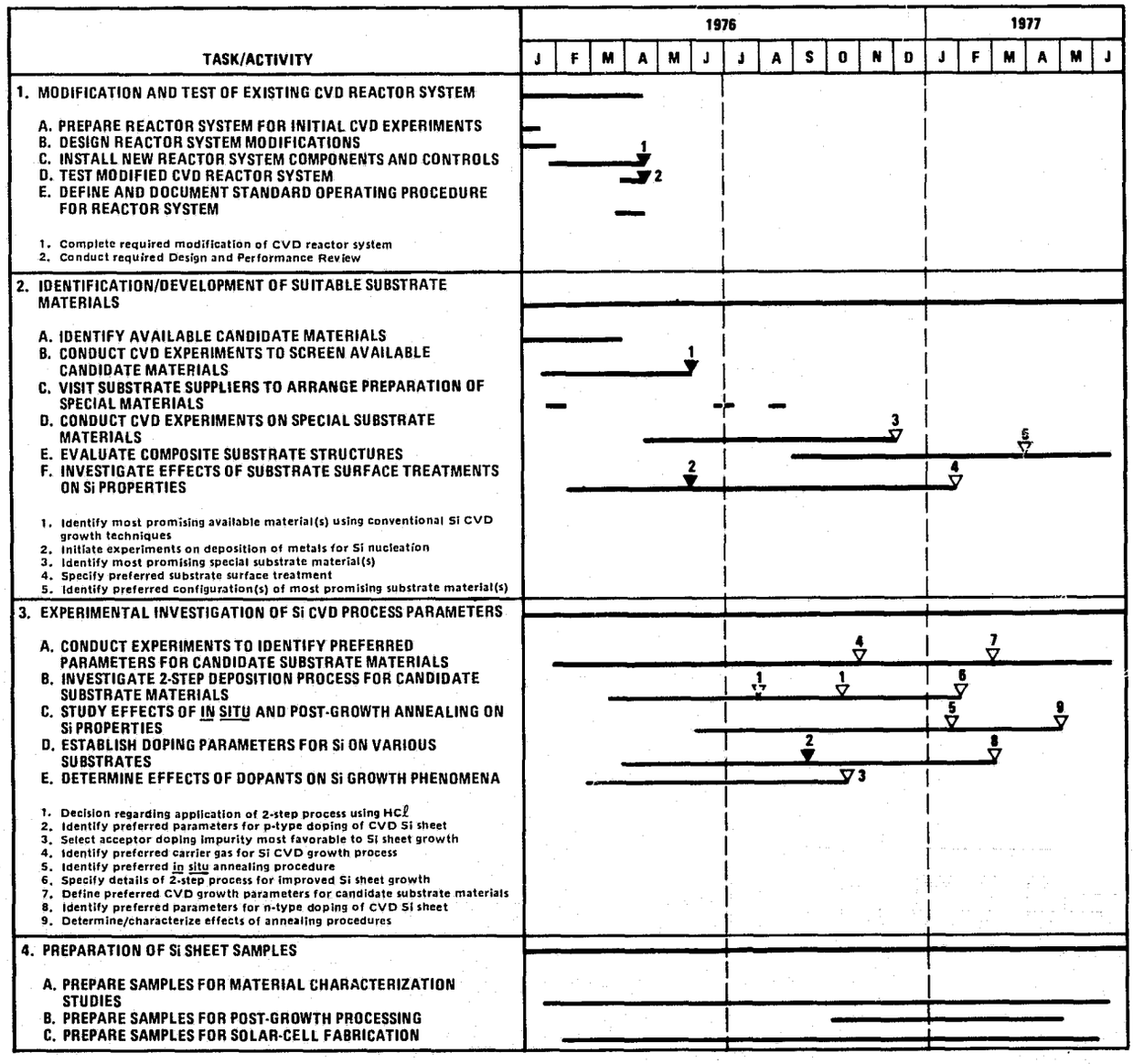

UPDATED TECHNICAL PROGRAM PLAN (Cont)

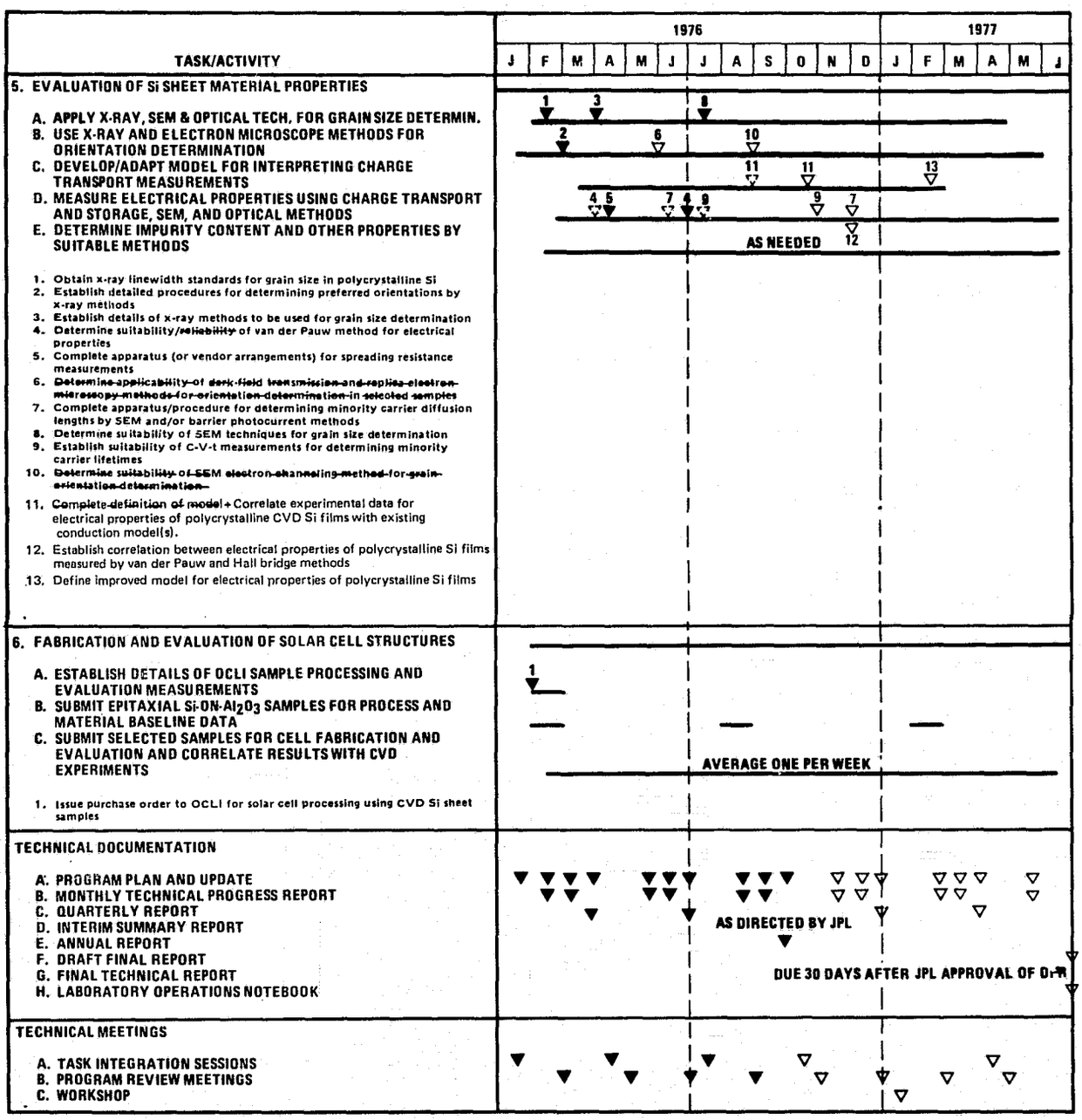

CHEMICAL VAPOR DEPOSITION GROWTH
SILICON SHEET GROWTH DEVELOPMENT

JPL CONTRACT NO. 954372

TASK 2: LARGE AREA SILICON SHEET
JPL/ERDA LOW COST SILICON SOLAR ARRAY PROJECT

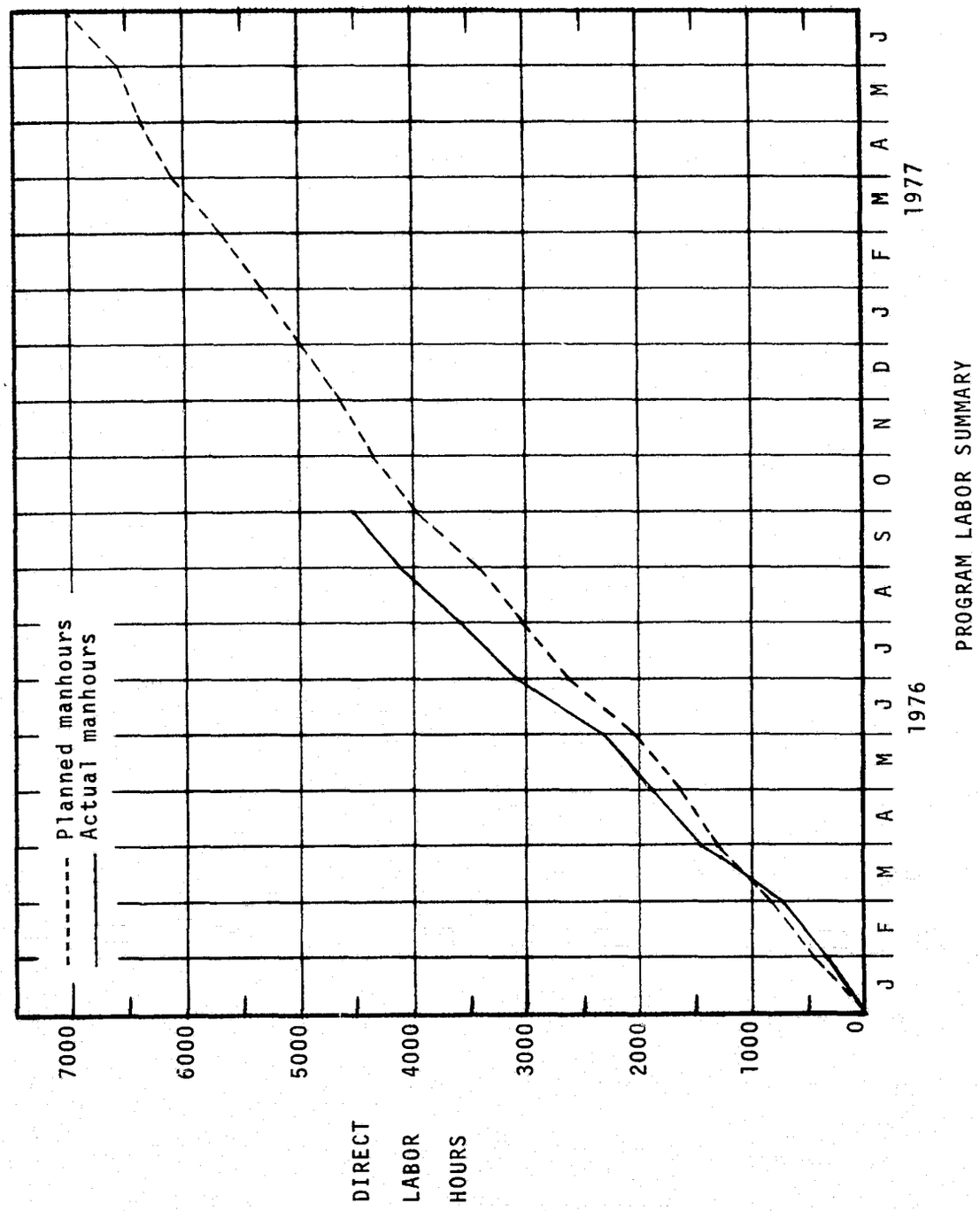

CHEMICAL VAPOR DEPOSITION GROWTH
SILICON SHEET GROWTH DEVELOPMENT

JPL CONTRACT NO. 954372

TASK 2: LARGE AREA SILICON SHEET
JPL/ERDA LOW COST SILICON SOLAR ARRAY PROJECT

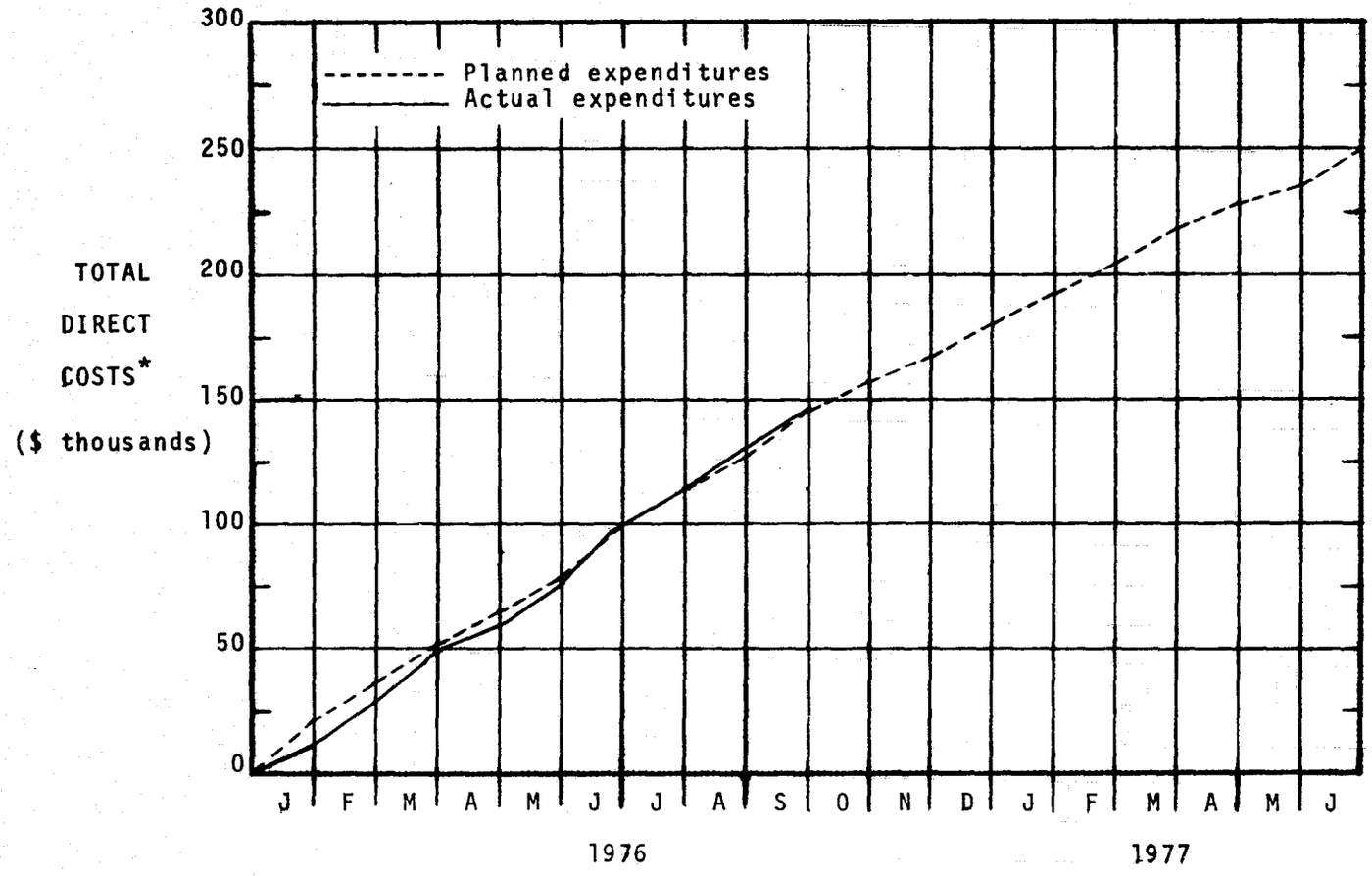

PROGRAM COST SUMMARY

*excluding fee